Synthesis of Bottlebrush Polymers Using the Grafting-Through and Transfer-To Methods

Scott Charles Radzinski

Dissertation submitted to the faculty of the Virginia Polytechnic Institute and State University in partial fulfillment of the requirements for the degree of

Doctor of Philosophy

In

Chemistry

John B. Matson, Chair

Timothy E. Long

Harry Gibson

Guoliang Liu

March 23rd 2017

Blacksburg, VA

Keywords: Comb polymer, Controlled radical polymerization, Z-RAFT

Abstract: Synthesis of Bottlebrush Polymers Using the Grafting-Through and Transfer-To Methods

Scott Radzinski

Bottlebrush polymers are interesting topologies that have become increasingly relevant in various applications including rheology modifiers, super-soft elastomers, photonic crystals, anti-fouling coatings, the in vivo delivery of therapeutic agents, and as promising substrates in lithographic printing. These macromolecules are comprised of numerous polymeric side-chains densely grafted to a polymer backbone. The densely grafted nature of bottlebrush polymers results in steric repulsion between neighboring polymer chains, forcing these macromolecules to adopt a chain-extended conformation. Although these remarkable macromolecules have a many different applications, the transformative potential of the bottlebrush polymer topology has not been realized because the synthesis of high molecular weight bottlebrush polymers is challenging. This dissertation focusses on improving the synthesis of these large macromolecules using the grafting-through strategy in the first section and the transfer-to strategy in the second section.

For the first time the effect of anchor group chemistry—the configuration of atoms linking the polymer to a polymerizable norbornene— was studied on the kinetics of ring-opening metathesis polymerization (ROMP) of macromonomers (MMs) initiated by Grubbs 3rd generation catalyst. A variance in the rate of propagation of >4-fold between similar MMs with different anchor groups was observed. This phenomenon was conserved across all MMs tested, regardless of

solvent, molecular weight (MW), or repeat unit identity. Experimental and computational studies indicated that the rate differences likely resulted from a combination of varying steric demands and electronic structure among the different anchor groups. This new insight will allow others to achieve high MM conversion and prepare pure, high MW bottlebrush polymers by ROMP grafting-through.

The second section of this dissertation deals with a little studied bottlebrush synthesis technique called the transfer-to method. This method is a hybrid of the grafting-from and grafting-to approaches in which the growing polymer side chains detach from the backbone, propagate freely in solution, and then reattach to the backbone in a chain transfer step. Several parameters were investigated to determine optimal conditions for this process. This study provides for the first time a guide to use the transfer-to method to produce high purity bottlebrush polymers with controllable backbone and side chain length.

General **Abstract: Synthesis of Bottlebrush Polymers Using the Grafting-Through and Transfer-To Methods**

Scott Radzinski

Bottlebrush polymers are interesting topologies that have become increasingly relevant in various applications including super-soft elastomers and drug delivery agents. These macromolecules are comprised of numerous polymeric side-chains densely grafted to a polymer backbone. The densely grafted nature of bottlebrush polymers results in steric repulsion between neighboring polymer chains, forcing these macromolecules to adopt a chain-extended or worm like conformation. Although these remarkable macromolecules have a many different applications, the transformative potential of the bottlebrush polymer topology has not been realized because the synthesis of large bottlebrush polymers is challenging. This dissertation focusses on improving the synthesis of these big macromolecules using the grafting-through strategy in the first section and the transfer-to strategy in the second section.

For the first time the effect of anchor group chemistry—the configuration of atoms linking the polymer to a polymerizable norbornene—was studied on bottlebrush synthesis. A variance in how fast the polymerization took between similar MMs with different anchor groups was observed. Experimental and computational studies indicated that the differences likely resulted from a combination of varying steric demands and electronic structure among the different anchor groups. This new insight will allow others to achieve high MM conversion and prepare pure, high MW bottlebrush polymers by ROMP grafting-through.

The second section of this dissertation deals with a little studied bottlebrush synthesis technique called the transfer-to method. This method is a hybrid of two well-known methods, grafting-from and grafting-to approaches, in which the growing polymer side chains detach from the backbone, polymerize freely in solution, and then reattach to the backbone in a chain transfer step. Several parameters were investigated to determine optimal conditions for this process. This study provides for the first time a guide to use the transfer-to method to produce high purity bottlebrush polymers with controllable sizes.

Dedication

This dissertation is dedicated to my son Brogan Scott Radzinski

Acknowledgments

I would like to first thank my advisor Dr. John Matson for his continued support throughout my career at Virginia Tech. He has taught me immensely and helped me grow into the scientist I am today. I would also like to thank my committee members Dr. Gibson, Dr. Long, Dr. Turner, and Dr. Liu for guidance.

A special thanks goes to my beautiful wife Christine for her patience throughout my academic career. Without her support none of this would have been possible and now she looks forward to me getting a "real" job.

Thank you to fellow graduate student Jeff Foster for wonderful collaborations and keeping me sane during this endeavor. To my colleagues in the Matson lab thank you for constant laughs and breaking the GPC so I always have something to fix in the lab.

To my family that has supported me during my time here, thank you very much; I could not have done this without your support. Lastly, to all my friends that have helped me and supported me along the way, thank you.

Table of Contents

Attribution

Several colleagues and coworkers aided in the writing and research behind several of the chapters of this dissertation. A brief description of their background and their contributions are included here.

Chapter 2: Scott Radzinski (graduate student, Department of Chemistry, Virginia Tech) synthesized and characterized polymers in this chapter. Jeff Foster (graduate student, Department of Chemistry, Virginia Tech) contributed to the synthesis and characterization of polymers. John Matson (Ph.D., Department of Chemistry, and Macromolecules Innovation Institute (MII) at Virginia Tech) is the advisor and committee chair. Professor Matson provided guidance, writing, and editing of this chapter.

Chapter 3: Scott Radzinski (graduate student, Department of Chemistry, Virginia Tech) synthesized and characterized polymers in this chapter. Jeff Foster (graduate student, Department of Chemistry, Virginia Tech) contributed to the characterization of polymers. John Matson (Ph.D., Department of Chemistry, and MII at Virginia Tech) is the advisor and committee chair. Professor Matson provided guidance, writing, and editing of this chapter.

Chapter 4: Scott Radzinski (graduate student, Department of Chemistry, Virginia Tech) contributed in writing of the review. Jeff Foster (graduate student, Department of Chemistry, Virginia Tech) contributed to the writing of this review. John Matson (Ph.D., Department of Chemistry, and MII at Virginia Tech) is the advisor and committee chair. Professor Matson provided guidance, writing, and editing of this chapter.

Chapter 5: Scott Radzinski (graduate student, Department of Chemistry, Virginia Tech) synthesized and characterized polymers in this chapter. Jeff Foster (graduate student, Department of Chemistry, Virginia Tech) contributed to the synthesis and characterization of polymers. John

Matson (Ph.D., Department of Chemistry, and MII at Virginia Tech) is the advisor and committee chair. Professor Matson provided guidance, writing, and editing of this chapter.

Chapter 6: Scott Radzinski (graduate student, Department of Chemistry, Virginia Tech) synthesized and characterized polymers in this chapter. Jeff Foster (graduate student, Department of Chemistry, Virginia Tech) contributed to the synthesis and characterization of polymers. Sally Lewis (Virginia Tech) and Matthew Slutzker (Virginia Tech) were all undergraduate researchers that contributed to the synthesis of the polymers discussed in this chapter. John Matson (Ph.D., Department of Chemistry, and MII at Virginia Tech) is the advisor and committee chair. Professor Matson provided guidance, writing, and editing of this chapter.

Chapter 7: Scott Radzinski (graduate student, Department of Chemistry, Virginia Tech) synthesized and characterized polymers in this chapter. Jeff Foster (graduate student, Department of Chemistry, Virginia Tech) contributed to the synthesis and characterization of polymers. Sally Lewis (Virginia Tech) and Eric French (Virginia Tech) were all undergraduate researchers that contributed to the synthesis of the polymers discussed in this chapter. John Matson (Ph.D., Department of Chemistry, and MII at Virginia Tech) is the advisor and committee chair. Professor Matson provided guidance, writing, and editing of this chapter.

Section I: Synthesis of Bottlebrush Polymers Using Grafting-Through.

Chapter 1: Introduction to Bottlebrush Polymers

Bottlebrush polymers are large macromolecules with densely grafted polymeric side chains. When the bottlebrush polymer has a high grafting density and the side chain polymers are large enough, the macromolecule will adopt a cylindrical shape due to the steric repulsion of the side chains Bottlebrush polymers are becoming increasingly relevant in polymer applications due to newer methods that can lead to simpler synthesis of these unique polymers. The ability to control both the length and monomers added to the backbone and the side chains will give rise to bottlebrush polymers with specific architectures that can be tuned both in length and width of the bottlebrush for various applications. (Figure 1.1).

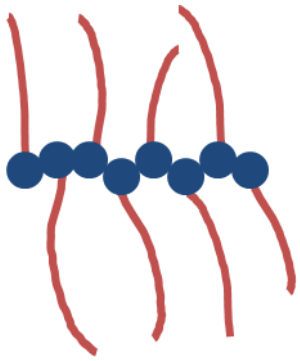

Figure 1.1: Illustration of a bottlebrush polymer, where the blue balls represents the backbone and the red lines represent the pendent sidechains.

Bottlebrush polymers with a cylindrical shape have applications as emulsifiers and can be building blocks for nanostructured materials. Living and pseudo-living polymerizations are great methods to synthesize bottlebrush polymers and allow for controllable and well-defined backbone and side chains.

1.1 Polymerization Techniques in Bottlebrush Synthesis

Various polymerization methods can be employed to synthesize bottlebrush copolymers, with the most popular being living or pseudo living systems, such as reversible-deactivation radical polymerization (RDRP) techniques. RDRP techniques differ from free radical polymerizations (FRP) in which there are higher rates of chain termination and chain transfer reactions in FRP that lead to broad molecular weight distributions and low chain end functionality, both of which are important to suppress for the synthesis of bottlebrush polymers. The RDRP techniques rely on an equilibrium between a dormant state and an active propagating radical state (Scheme 1.1). The key to this concept is to have the equilibrium lie primarily to the left and only have a small concentration of propagating radical in solution that reduces the termination and chain transfer pathways.[1]

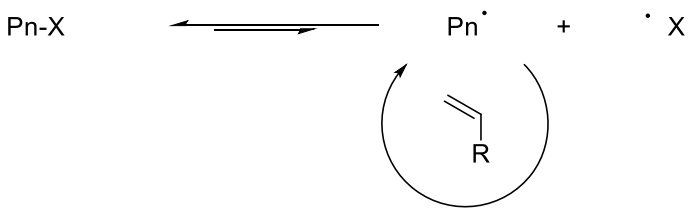

Scheme 1.1: Generalized Controlled Radical polymerization equilibrium.

Several popular RDRP techniques are nitroxide mediated polymerization (NMP), reversible addition fragmentation chain transfer polymerization (RAFT), and atom transfer radical polymerization (ATRP). These three techniques are all based on the RDRP equilibrium but use different reactive groups and conditions to achieve control. The control of these polymerizations allows for control of molecular weight that leads to well defined structures and high chain end functionality.

Reversible Addition-Fragmentation Chain Transfer Polymerization

RAFT was developed in 1998 by Thang et al. and gains control over the polymerization by the use of chain transfer agents (CTA) such as dithiocarbonates and trithiocarbamates.[2] These chain transfer agents work by reversibly trapping the propagating radical, thus reducing the concentration of the propagating radical in solution. The polymerization is initiated by a radical initiator to form a propagating polymer chain, (Scheme 1.2A).

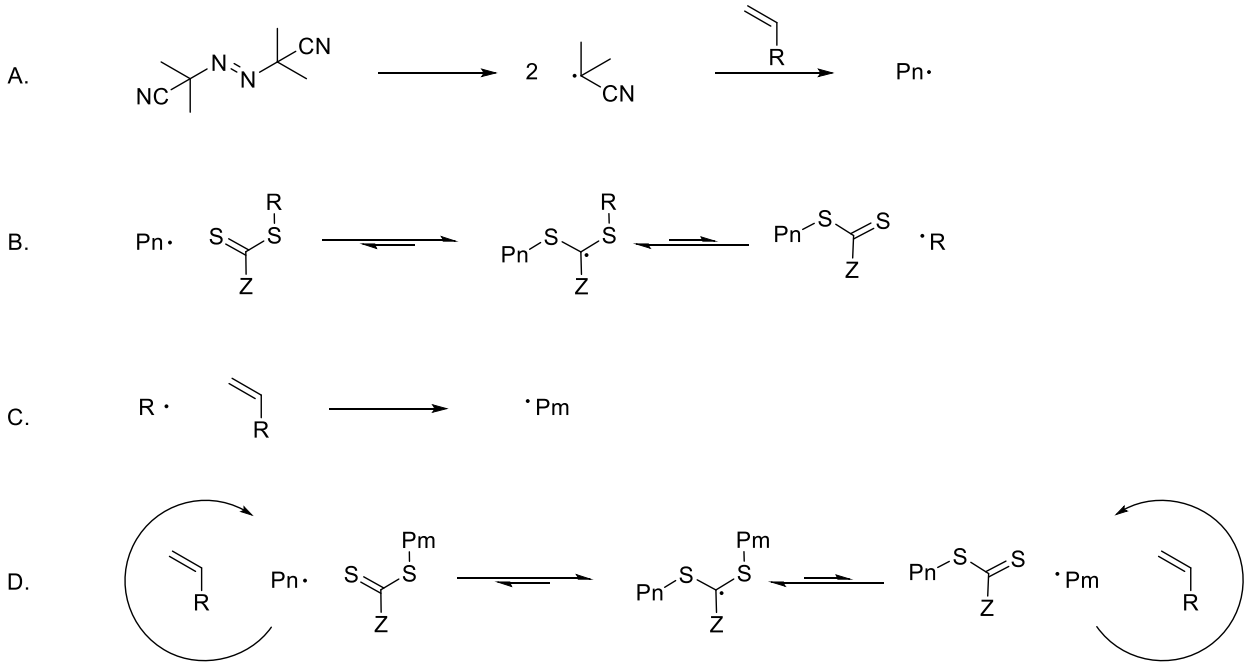

Scheme 1.2: RAFT polymerization mechanism. A) Initiation, B) Pre-equilibrium, C) Reinitiation, D) RAFT Main equilibrium.

The propagating radical can be trapped by the CTA to form an adduct radical in the pre-equilibrium step in which only one side of the CTA has a polymer chain (Scheme 1.2b). The R group on the CTA can dissociate to form a radical that can initiate another polymer chain (Scheme 1.2C). The CTA can trap this radical forming the RAFT main equilibrium (Scheme 1.2D). The RAFT main equilibrium gains control of the polymerization by limiting the

concentration of propagating radicals, therby reducing the termination pathways. A disadvantage to RAFT is that the chain transfer agents are specific to certain groups of monomers and can be expensive. However, many syntheses have been developed to synthesize many different CTA's in very few steps, opening the door for RAFT to become a more important and widely used technique.[3]

Atom Transfer Radical Polymerization

Atom transfer radical polymerization (ATRP) was developed in the 1990's by Matyjaszewski et al.[4,5] ATRP exploits the homolytic cleavage of a carbon-halogen bond catalyzed by a metal ligand complex, typically of copper, to form the oxidized metal and a propagating radical. This radical will initiate the polymerization and create the propagating radical, which can be reversibly trapped by the oxidized metal. Like other RDRP techniques the equilibrium favors the reactants, or the dormant state, to produce the low concentration of radicals that reduces the rate of termination and chain transfer (Scheme 1.3).

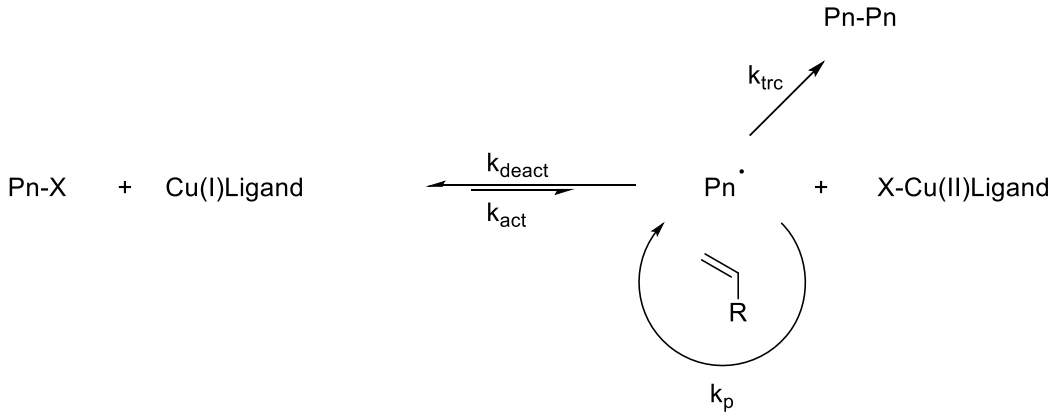

Scheme 1.3: Atom Transfer Radical polymerization equilibrium.

ATRP traditionally requires equimolar amounts of metal/ligand complex to brominated species that can make the polymers synthesized by this technique difficult to purify and become

biocompatible. In recent years ATRP methods using low levels of catalyst have been developed by Matyjaszewski et al., with the most popular being activators regenerated by electron transfer (ARGET),[6] and initiators for continuous activator regeneration (ICAR).[7] During ATRP a small amount of propagating radicals undergo termination reactions that produce the oxidized metal that cannot catalyze this polymerization. This is dealt with in normal ATRP by having a large quantity of metal catalyst. In reduced metal ATRP, the termination is dealt with by the addition of some type of reducing agent, (Scheme 1.4). These reducing agents reduce the metal back to its active form that can mediate the polymerization. ARGET uses reducing agents such as ascorbic acid, tin(II) ethyl hexanoate, or glucose, while ICAR uses an organic radical as the reducing agent to regenerate the metal catalyst, the first used being AIBN. The advantage to using ARGET or ICAR is the reduction in catalyst loading, leading to systems that do not need to be purified, as well as reducing the cost of the polymerization.

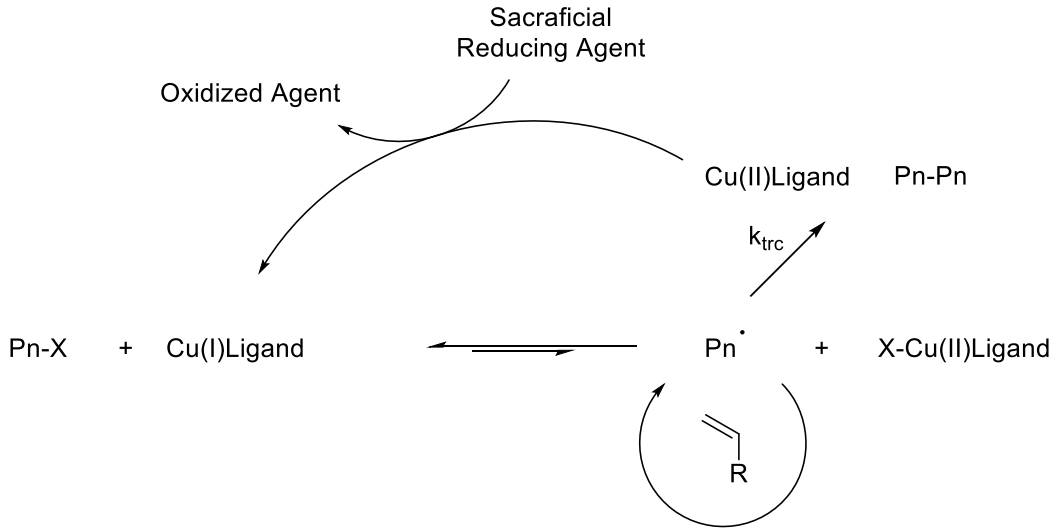

Scheme 1.4: ARGET and ICAR ATRP.

Ring Opening Metathesis Polymerization

Ring opening metathesis polymerization (ROMP) is another chain growth polymerization technique that can give well defined structures. ROMP typically uses a ruthenium or molybdenum catalyst, which reacts with strained cyclic olefins.[8] The ROMP mechanism involves a metal catalyst that reacts with a strained cyclic olefin to form a metallocyclobutane ring, (Scheme 1.5).[8] This is further reacted to open the ring and regenerate the carbene that can undergo further reactions to form the polymer.

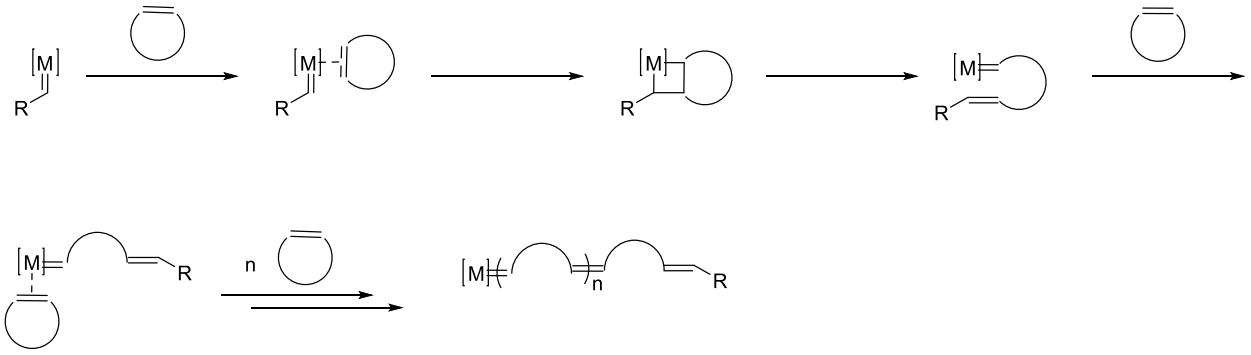

Scheme 1.5: ROMP mechanism.

Grubbs and coworkers have developed several different catalysts for ROMP, with Grubbs I, II, and III being the most important, (Figure 1.2). All of these catalysts can tolerate many different functional groups and solvents, and can be used in the presence of oxygen. Grubbs I was first synthesized in 1995 and shows high affinity towards olefins;[9] however, reaction times with Grubbs I can be long compared to Grubbs II due to slow rates of propagation. Replacing one of the phosphine ligands with an N-heterocyclic carbene produces Grubbs II (Figure 1.2-2). Grubbs second generation is an improvement over the first generation due to higher rate of reaction for metathesis reactions. However, the rate of initiation is on the same time scale as rate of propagation meaning there is a loss of control over the polymerization because not all of the chains will initiate at the same time. To combat this, a modified Grubbs II or living catalyst was developed by ligand exchange to place pyridines on the ruthenium.[10] The pyridine ligands

disassociate quickly, thus increasing the rate of initiation for ROMP that will create a living polymerization (Figure 1.2).[11]

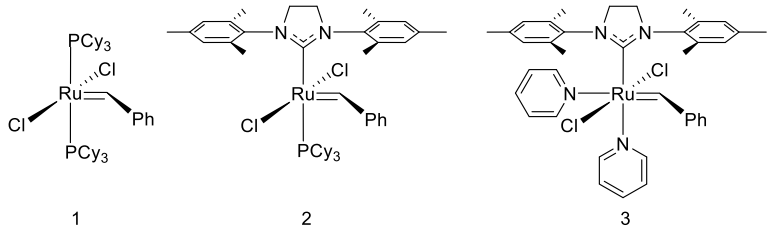

Figure 1.2: Grubbs catalysts typically used for ROMP, Grubbs' First Generation (1), Grubbs' second generation (2), and Grubbs' third generation (3).

1.2 Bottlebrush Polymer Synthesis Techniques

There are four synthetic techniques to synthesize bottlebrush polymers, which include grafting-from, grafting-to, transfer-to, and grafting-through. These techniques give bottlebrush polymers with varying grafting densities along the backbone.[12] As the density of the grafts increase the bottle brush polymer will begin to extend from a random coil to an extended chain formation, which will adopt a cylindrical shape from the steric repulsion of the side chains.[13]

Grafting-From

Grafting-from involves synthesizing polymer chains with pendent groups that can initiate other polymerizations or be modified to produce an initiation site for further polymerizations, (Figure 1.3).

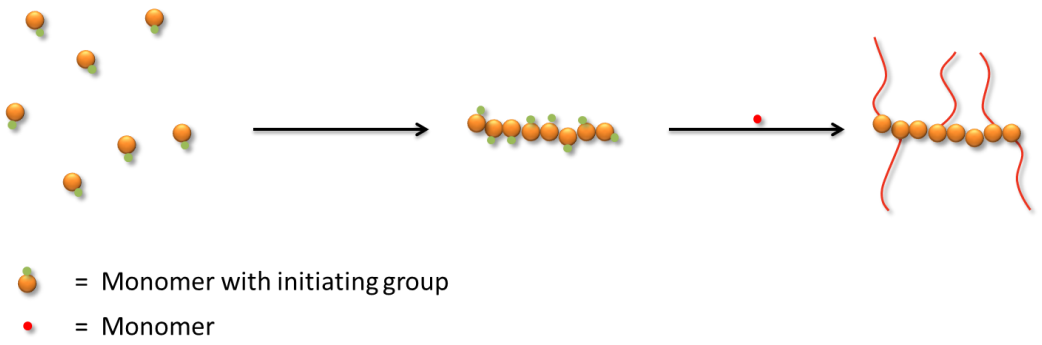

Figure 1.3: Grafting-From bottlebrush synthesis.

This method to produce bottlebrush polymers will not create a perfectly grafted polymer due to incomplete initiation from the backbone. Also, due to steric factors the degree of branching and the length of the side chains will be lower in comparison to other methods. This arises from the side chains beginning to fold over each other and blocking reactive sites. In the cases of radical processes loop formations may occur.

Matyjaszewski et al. has demonstrated that ATRP can be used to synthesize bottlebrush polymers by the grafting-from technique (Scheme 1.6). [14-17]

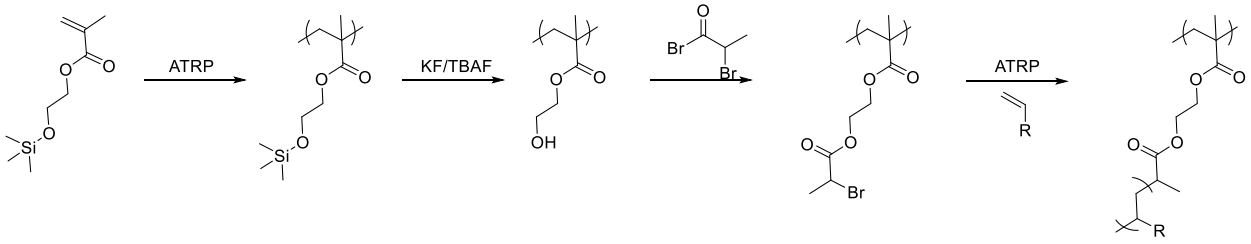

Scheme 1.6: Synthesis of bottlebrush polymers by and ATRP/ATRP approach.

The 2-(trimethylsilyoxy) group on the side chain of the polymer is then deprotected to form the alcohol, which can react to form an initiator for ATRP. From this basic scheme several different bottlebrush polymers have been made. A bottlebrush polymer with block copolymers off the side chains has been reported, with the first block comprised of poly *n*-butyl methacrylate and

the second block of styrene.[14] To show that the side chain polymerization reactions were exhibiting living character, the chains were cleaved from the backbone by acid hydrolysis and a size exclusion chromatography (SEC) analysis was run. The SEC trace showed a polymer with a low dispersity (Đ) (below 1.2) meaning the polymers grafting off the backbone were grown in a controlled manner. An extension of this method is growth of a second block from the ends of the side chain polymers of a methacrylate modified with a fluorescent molecule, fluorescein.[17]

A ROMP/ROMP bottlebrush synthesis made by the grafting-through technique has been reported by Kiessling.[18] Like other systems that use the grafting-from technique, post polymerization modifications are required to generate an initiator site. In this case, a norbornene with a pedant maleimide group was polymerized to form the backbone polymer. The maleimide then underwent a Diels-Alder cycloaddition to form a new norbornene, (Scheme 1.7).

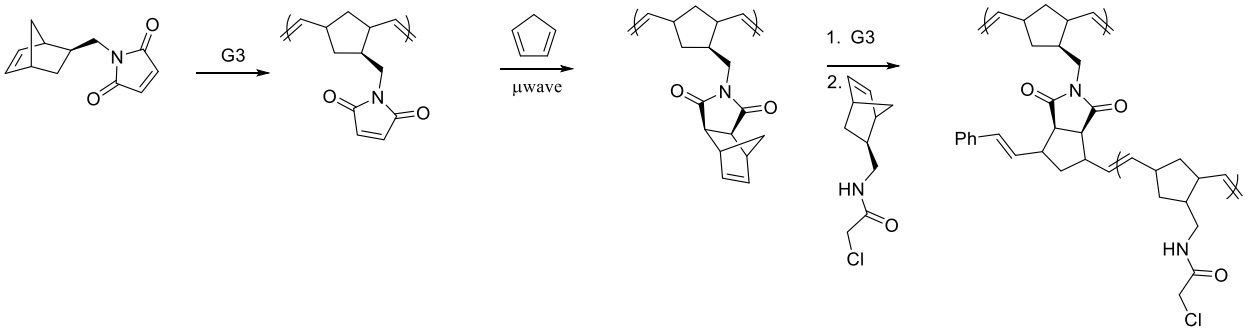

Scheme 1.7: A ROMP/ROMP synthesis of bottlebrush polymers.[18]

In order for polymer chains to be grown from the backbone of the polymer the ruthenium catalyst must be attached. This is done by first reacting the polymer backbone with the catalyst, and then once a color change is observed, norbornene monomer is added to form the bottlebrush polymer.

Grafting-From using Combined Polymerization Techniques

The combination of various polymerization methods can be a powerful tool in the synthesis of bottlebrush polymers because many of these do not need the post polymerization modifications that the other systems need. One example that uses ROMP, ATRP, and ring opening polymerization (ROP) shows the wide variety of combinations that are possible for the synthesis of bottlebrush polymers (Scheme 1.8).[19] The backbone of the polymer was synthesized by consecutive ROMP of two different norbornene monomers, one monomer having an alcohol at the end of a short PLA block and the other having an α-bromo ester functional group that can initiate ATRP. The resulting block polymer then undergoes ATRP and ROP in two steps to form the bottlebrush polymer. This strategy affords a bottlebrush polymer with two different side chain polymers in blocks producing a bottlebrush copolymer. These unique polymers form self-assembled structures that are much larger than the linear analogs, which may be useful in photonic and nanofluidics applications.

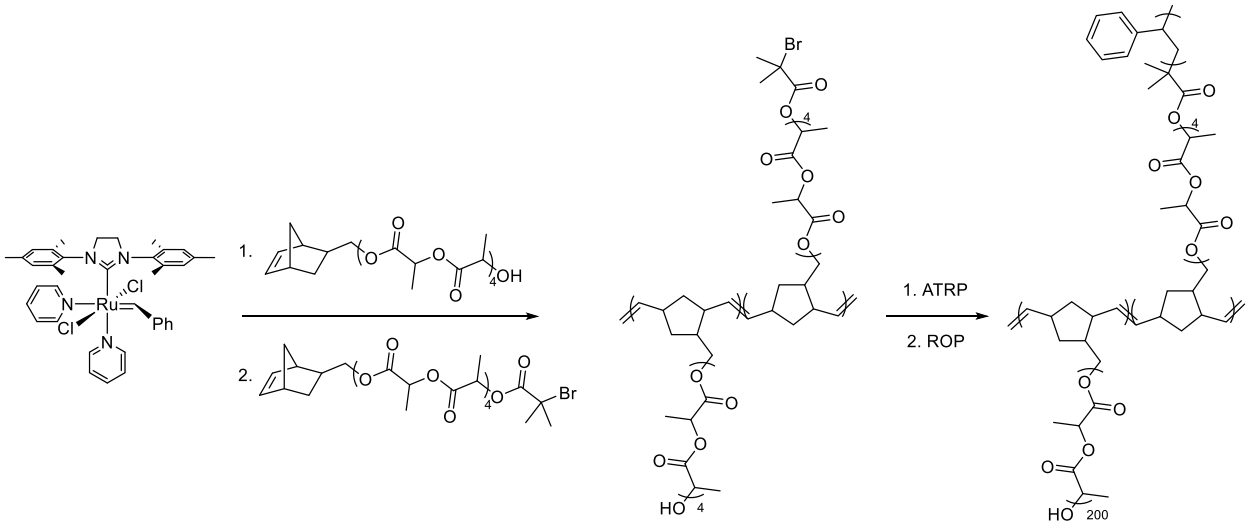

Scheme 1.8: The combination of ROMP, ATRP, and ROP was used to form a bottlebrush polymer from the grafting-from technique.[19]

Grafting-To

Grafting-to is a technique for synthesizing bottlebrush polymers whereby the backbone of the polymer is synthesized with reactive groups attached. In addition another polymer is synthesized to produce a polymer with a reactive group on the chain end. The backbone with reactive side chains and the polymer with reactive end groups are coupled to form the bottlebrush polymer, (Figure 1.4).

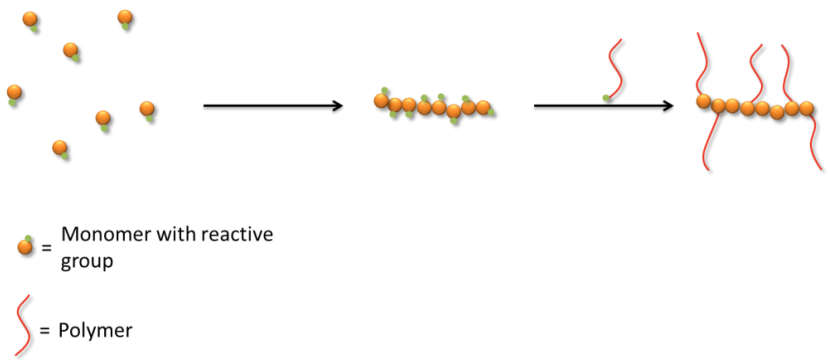

Figure 1.4: Grafting-to for the synthesis of bottlebrush polymers.

The grafting-to technique allows for complete characterization of both the backbone and the sides chains prior to the synthesis of the bottlebrush polymer. This control can allow for the development of well-defined structures. This method gained popularity with the development of click reactions to attach the polymer side chain to the polymer backbone. An example where azide alkyne click reactions to form the bottlebrush polymer is shown by Matyjaszewski et al. where a mixture of methyl methacrylate and glycidyl methacrylate (GMA) was polymerized via ATRP to form the backbone of the bottlebrush polymer, a post polymerization reaction was then

used to place a azide along the backbone. An alkyne terminated polyethyleneglycol was reacted by click chemistry to form the bottlebrush polymer, (Scheme 1.9).[20]

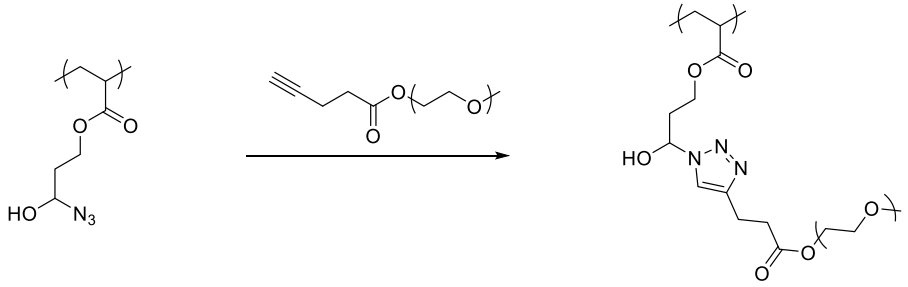

Scheme 1.9:Grafting-to by click chemistry.[20]

The epoxide ring was transformed to an azide by a reaction with sodium azide. This route to bottlebrush polymers gives moderate grafting density depending on how many GMA units are reacted and how many of the grafts can click onto the backbone, reaching approximately 60% conversion.

Both grafting-from and grafting-to are post polymerization modifications on the backbone assembly; these modifications are subject to neighboring group effects and the steric effects of reactions on polymers. Since these will affect the grafting density, grafting-from and grafting-to will not produce perfectly grafted bottlebrush polymers.

Transfer-To

The transfer-to technique is a unique hybrid between grafting-from and grafting-to, where the propagating polymer sidechains grown in solution and then transfer back to the backbone to form the bottlebrush polymer. This technique is discussed in detail in section two of this dissertation.

Grafting-Through

The grafting-through technique yields bottlebrush polymers with a polymer side chain on every repeat unit of the backbone. This is done by first synthesizing a macromonomer, which is a polymer chain with a reactive group on the end that can be reacted to form the bottlebrush polymer (Figure 1.5).

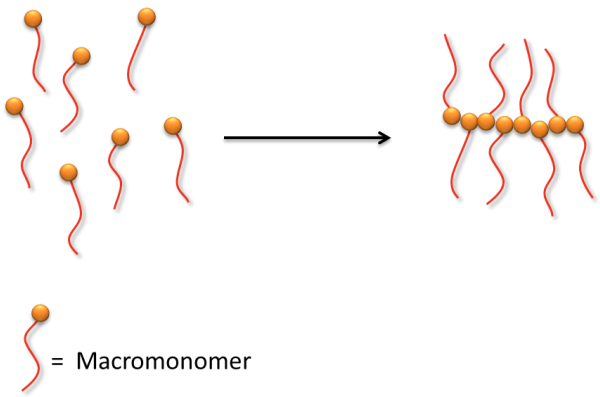

Figure 1.5: Grafting-through approach to bottlebrush synthesis.

In order for the grafting-through technique to be used, a very reactive system must be used to overcome the sterics of reacting the functional end. Bowden has shown several examples of ROMP based systems and has compared the grafting-from and the grafting-through approach to bottlebrush synthesis. Using the same monomer but different routes, two different bottlebrush polymers were made (Scheme 1.10).[13]

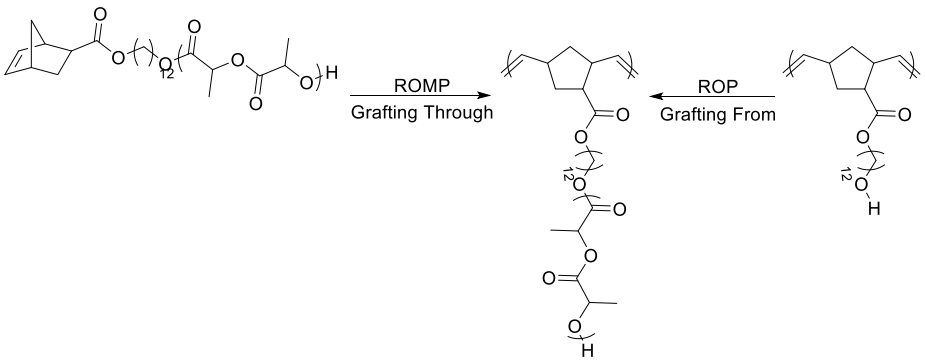

Scheme 1.10: Two different pathways to form a bottlebrush polymer, with one being grafting-from and the other grafting-through.

A norbornene with alcohol functionality was used for both syntheses. The grafting-from approach used ROMP first and then ROP was performed to create the bottlebrush polymer. The grafting-through approach had the opposite order of polymerizations; the ROP was performed first to create a macromonomer and then the norbornene was polymerized through to create the bottlebrush polymer. The main differences between the two techniques are the length of the backbone and the side chains. It was found that using the grafting-from approach allowed for longer backbone and longer side chains. When the grafting-through approach was used there was a limit on how large the macromonomer could be. As the side chains increases, the bottlebrush synthesis becomes more uncontrolled and achieves a lower degree of polymerization. The paper, however, had no discussion on grafting density. The grafting-through technique should produce a much higher grafting density than the grafting-from approach, because performing reactions on polymers can be difficult due to factors previously discussed.

1.3 Unique Bottlebrush Polymers

The synthesis of interesting shapes using a grafting-through technique has been shown by the Wooley lab where dumbbell type topologies were synthesized.[21] The shape arises from the sequential reaction of monomers of different molecular weights. A norbornene functionalized alcohol was employed for ROP to form various molecular weights of PLA with a metathesis active chain end. Using the living ROMP catalyst, Grubbs 3, the macromonomers that were synthesized can be reacted to 100% conversion while keeping the living nature of the polymerization. The livingness of the polymerization is very important to this synthesis, in that

the macromonomers need to be added one after another to form the interesting shape of the bottlebrush polymer. A larger molecular weight norbornene functionalized PLA is reacted to form the first block of the bottlebrush polymer. Next a smaller molecular weight norbornene at three equivalents is added to form the bar of the dumbbell and last the same molecular weight PLA as the first block is added to form the final ball of the dumbbell bottlebrush polymer (Scheme 1.11).

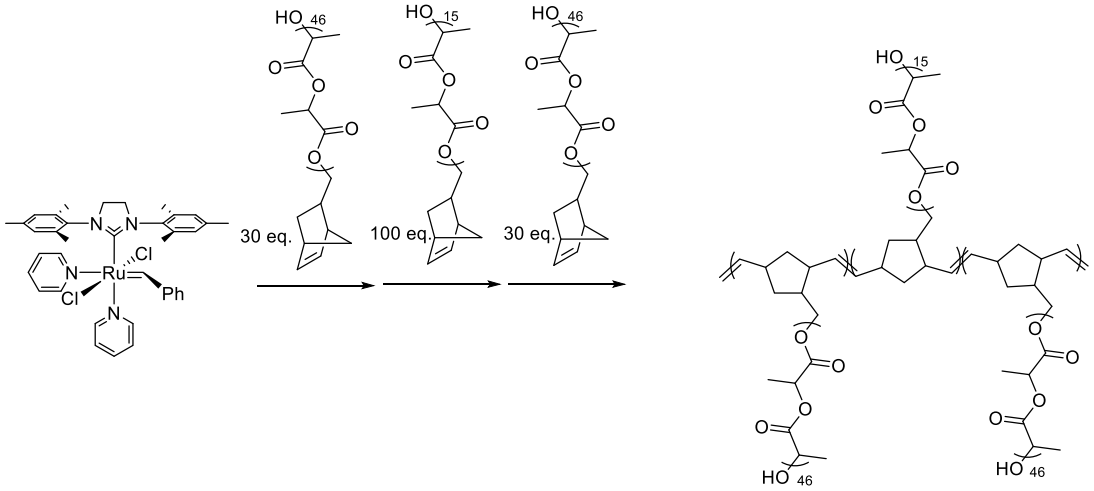

Scheme 1.11: The synthesis of a dumbbell shape utilizing ROMP as the polymerization technique.

The dumbbell bottlebrush polymer was imaged by AFM showing that the larger molecular weight blocks manifests ball like structures bridged by a smaller molecular weight "bar". The ability to synthesize the interesting shapes may better mimic large biomolecules and also give rise to interesting morphologies (Figure 1.6).

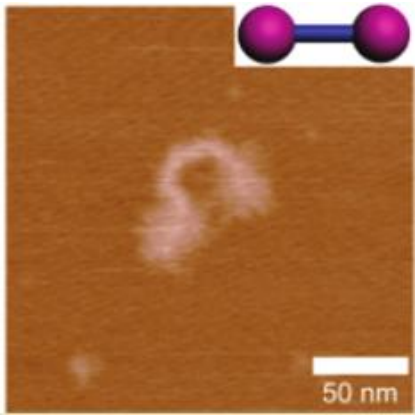

Figure 1.6:Image of the dumbbell bottlebrush from tapping mode AFM.[21]

The synthesis of gradient bottlebrush polymers, where the bottlebrush polymer initially has no side chain polymers then gradually forms into a bottlebrush polymer having densely grafted polymer side chains, has been shown.[15] The gradient polymer is created by starting the polymerization with only MMA then slowly adding in a functionalized monomer until only the functionalized monomer is being polymerized. This creates a gradient of functionalized sites along the backbone that can undergo transformations to form the polymer side chains. These polymer chains create the gradient bottlebrush polymer that is asymmetric in shape.

Amphiphilic bottlebrush copolymers have been prepared from polymers functionalized with norbornene that were then grafted through.[22] Two different macromonomers were synthesized by RAFT, consisting of a norbornene functionalized with a chain transfer agent where the first block was polystyrene and the second block was poly *tert*-butyl methacrylate. Upon acid hydrolysis, the *tert*-butyl methacrylate block formed methacrylic acid. These macromolecules then formed amphiphilic bottlebrush copolymer that self-assembled into supramolecular spherical micelles, (Figure 1.7).

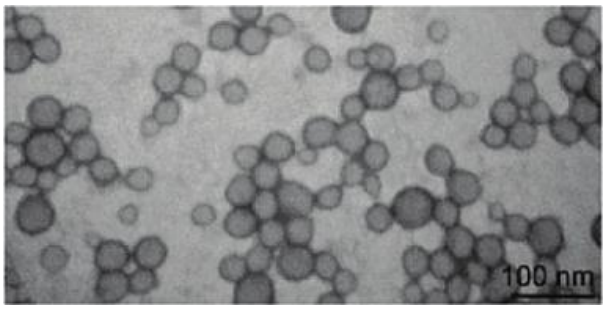

Figure 1.7: TEM image of spherical micelles.[22]

Amphiphilic diblock bottlebrush polymers have been synthesized by the grafting-through technique by reacting two different macromonomers, sequentially. Another route has been used by first synthesizing an amphiphilic macromonomer with a functional group at the junction.[23] The amphiphilic macromonomer is composed of norbornene functionalized with a PEO as the hydrophobic block and PLA and the hydrophilic block. When the macromonomer is polymerized via ROMP, the resulting diblock bottlebrush polymer will have two distinct regions on either side of the bottlebrush polymer, resulting in differing properties from the traditional block bottlebrush polymer (Scheme 1.12).

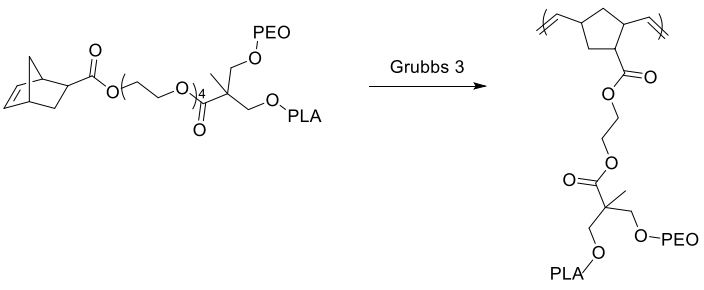

Scheme 1.12: Synthesis of amphphilic diblock bottlebrush polymers

Miniemulsions were made with the diblock bottlebrush polymer with oil in water and were monitored over time to test the stability of the system. Over a span of 25 days the miniemulsions were examined by dynamic light scattering (DLS) to probe their size and stability. With an average diameter approximately 220 nm or 260 nm depending on the lengths of the polymer side

chains, the DLS shows that the emulsions are quite stable in that no change in size over time was observed. Bottlebrush polymers were used in the synthesis of nanotubes using a grafting-from approach; a diblock or triblock copolymer backbone was synthesized with GMA and ethylene oxide methacrylate (PEOMA). The PGMA block was used as a macroinitiator for PLA to form grafts off the center of the polymer backbone (Scheme 1.13). The ends of the PLA side chains were then reacted with an acid chloride functionalized chain transfer agent to form a site where RAFT polymerization occurs. A mixture of 3-buteneylstyrene and styrene was then polymerized to form a block copolymer side chain.

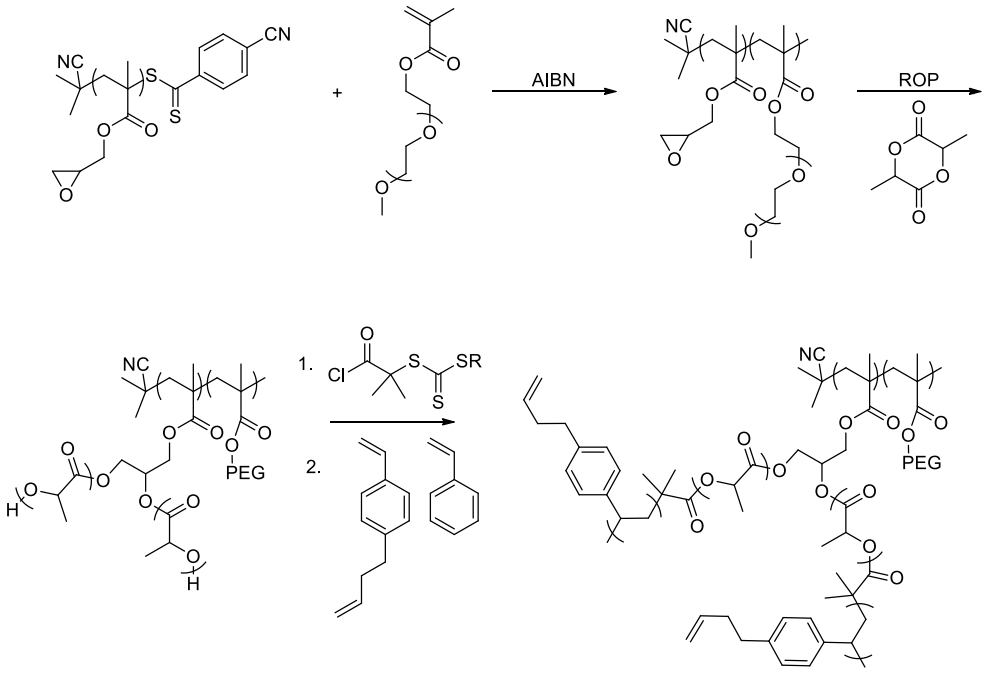

Scheme 1.13: Synthesis of a bottlebrush polymer towards nanotubes.

The bottlebrush polymer was synthesized with high grafting density, which caused the polymer to adopt a cylindrical shape. With the polymer in the cylindrical shape the 3-buteneylstyrene block was subjected to olefin metathesis to form an outer crosslinked shell. The crosslinked bottlebrush polymer was hydrolyzed to degrade the PEOMA block of the backbone and the PLA side chains of the bottlebrush. The only polymer left was the crosslinked outer shell with the

center no longer intact. To confirm that a nanotube has been synthesized instead of the bottlebrush collapsing on itself, SEC and AFM were performed before and after the degradation. The SEC before and after the degradation yielded a similar apparent molecular weight and the AFM showed both cylinders before and after the degradation. TEM showed that the inner core of the cylinders was less dense than the outer shell, further proving that nanotubes were synthesized (Figure 1.8).

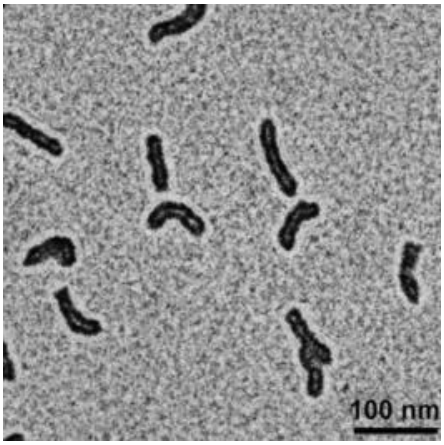

Figure 1.8:TEM of a nanotube.[24]

This method was further studied by creating nanotubes with reversible crosslinks that would dissociate under certain conditions.[25] Nanotubes can be synthesized to contain charged groups either on the inside[26] of the nanotube or the outside.[27] The nanotubes with charged groups on the inside wall of the nanotube were synthesized similarly to other nanotubes with the addition of a poly *tert*-butyl acrylate as the first block off the backbone. The acid hydrolysis the *tert*-butyl acrylate groups transforms them to polyacrylic acid. These groups could be deprotonated to form an anionic core that can be used for separations of various cations. The nanotubes with anionic groups on the outside of the tubes were synthesized in a similar way except the *tert*-butyl

acrylate was the outer block of the side chains that create a nanotube that can be used for biological applications.

A diblock bottlebrush polymer using the grafting-from technique was synthesized by Rzayev and the morphological features were investigated.[28] It was shown that a high percentage of the polymer adopts a lamellar morphology, which was attributed to the stretched out backbone and the small amount of entanglements in the polymers. When the blocks were asymmetric, meaning the blocks were of different lengths, no ordered morphology was seen from the rigid backbone. A different asymmetric diblock bottlebrush polymer was synthesized in a similar manner except the two blocks were of different lengths.[29] This synthetic strategy produces a bottlebrush polymer with one long polystyrene chain and the other block a shorter PLA chain (Figure 1.9).

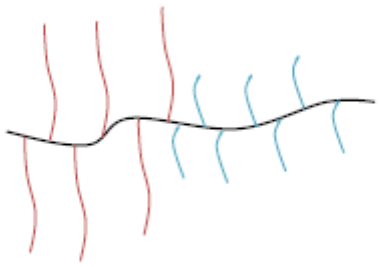

Figure 1.9: Representation of the diblock bottlebrush where there are long polystyrene chains (red) and the shorter PLA chains (blue)

The bottlebrush adopts a cylindrical morphology from the asymmetric shape. This is the first report of non-lamellar morphology of a diblock bottlebrush polymer. The smaller PLA chains that form the cylinders can be degraded away to from channels through the material. The ability

to create different sized cylinders may have implications in water purification by allowing only water to go through the polymer.

This dissertation concentrated on the synthesis of bottlebrush polymers using primarily two methods: grafting-through and transfer-to. Section 1 of this thesis is devoted to investigating the grafting-through technique of bottlebrush synthesis using ROMP. Based off of the results in Chapter 2 we were then able to employ ROMP grafting-through using a one-pot technique that is discussed in Chapter 3. Chapters 4-7 explore the little studied technique call transfer-to, a hybrid between grafting-from and grafting-to. Here a novel CTA was synthesized and underwent this mechanism of bottlebrush synthesis. Various parameters were studied and optimal conditions are found to produce bottlebrush polymers that are well defined by the transfer-to technique.

1.4 References:

(1) Matyjaszewski, K. *Current Opinion in Solid State and Materials Science* **1996**, *1*, 769.

(2) Chiefari, J.; Chong, Y. K.; Ercole, F.; Krstina, J.; Jeffery, J.; Le, T. P. T.; Mayadunne, R. T. A.; Meijs, G. F.; Moad, C. L.; Moad, G.; Rizzardo, E.; Thang, S. H. *Macromolecules* **1998**, *31*, 5559.

(3) Skey, J.; O'Reilly, R. K. *Chemical Communications* **2008**, 4183.

(4) Wang, J.-S.; Matyjaszewski, K. *Macromolecules* **1995**, *28*, 7572.

(5) Wang, J.-S.; Matyjaszewski, K. *Macromolecules* **1995**, *28*, 7901.

(6) Jakubowski, W.; Min, K.; Matyjaszewski, K. *Macromolecules* **2005**, *39*, 39.

(7) Mueller, L.; Jakubowski, W.; Tang, W.; Matyjaszewski, K. *Macromolecules* **2007**, *40*, 6464.

(8) Trnka, T. M.; Grubbs, R. H. *Accounts of Chemical Research* **2000**, *34*, 18.

(9) Schwab, P.; France, M. B.; Ziller, J. W.; Grubbs, R. H. *Angewandte Chemie International Edition in English* **1995**, *34*, 2039.

(10) Love, J. A.; Morgan, J. P.; Trnka, T. M.; Grubbs, R. H. *Angewandte Chemie International Edition* **2002**, *41*, 4035.

(11) Choi, T.-L.; Grubbs, R. H. *Angewandte Chemie* **2003**, *115*, 1785.

(12) Xie, M.; Dang, J.; Han, H.; Wang, W.; Liu, J.; He, X.; Zhang, Y. *Macromolecules* **2008**, *41*, 9004.

(13) Jha, S.; Dutta, S.; Bowden, N. B. *Macromolecules* **2004**, *37*, 4365.

(14) Börner, H. G.; Beers, K.; Matyjaszewski, K.; Sheiko, S. S.; Möller, M. *Macromolecules* **2001**, *34*, 4375.

(15) Börner, H. G.; Duran, D.; Matyjaszewski, K.; da Silva, M.; Sheiko, S. S. *Macromolecules* **2002**, *35*, 3387.

(16) Boyce, J. R.; Shirvanyants, D.; Sheiko, S. S.; Ivanov, D. A.; Qin, S.; Börner, H.; Matyjaszewski, K. *Langmuir* **2004**, *20*, 6005.

(17) Nese, A.; Lebedeva, N. V.; Sherwood, G.; Averick, S.; Li, Y.; Gao, H.; Peteanu, L.; Sheiko, S. S.; Matyjaszewski, K. *Macromolecules* **2011**, *44*, 5905.

(18) Allen, M. J.; Wangkanont, K.; Raines, R. T.; Kiessling, L. L. *Macromolecules* **2009**, *42*, 4023.

(19) Runge, M. B.; Dutta, S.; Bowden, N. B. *Macromolecules* **2005**, *39*, 498.

(20) Tsarevsky, N. V.; Bencherif, S. A.; Matyjaszewski, K. *Macromolecules* **2007**, *40*, 4439.

(21) Li, A.; Li, Z.; Zhang, S.; Sun, G.; Policarpio, D. M.; Wooley, K. L. *ACS Macro Letters* **2011**, *1*, 241.

(22) Li, Z.; Ma, J.; Cheng, C.; Zhang, K.; Wooley, K. L. *Macromolecules* **2010**, *43*, 1182.

(23) Li, Y.; Zou, J.; Das, B. P.; Tsianou, M.; Cheng, C. *Macromolecules* **2012**, *45*, 4623.

(24) Huang, K.; Rzayev, J. *Journal of the American Chemical Society* **2009**, *131*, 6880.

(25) Huang, K.; Johnson, M.; Rzayev, J. *ACS Macro Letters* **2012**, *1*, 892.

(26) Huang, K.; Rzayev, J. *Journal of the American Chemical Society* **2011**, *133*, 16726.

(27) Huang, K.; Jacobs, A.; Rzayev, J. *Biomacromolecules* **2011**, *12*, 2327.

(28) Rzayev, J. *Macromolecules* **2009**, *42*, 2135.

(29) Bolton, J.; Bailey, T. S.; Rzayev, J. *Nano Letters* **2011**, *11*, 998.

(30) Li, A.; Ma, J.; Wooley, K. L. *Macromolecules* **2009**, *42*, 5433.

Chapter 2: Bottlebrush Polymer Synthesis by Ring-Opening Metathesis Polymerization: The Significance of the Anchor Group

2.1 Authors

Scott C. Radzinski, Jeffrey C. Foster, Robert C. Chapleski, Jr., Diego Troya, John B. Matson

Department of Chemistry and Macromolecules Innovation Institute, Virginia Tech, Blacksburg, Virginia 24061, United States

2.2 Abstract:

Control over bottlebrush polymer synthesis by ring-opening metathesis polymerization (ROMP) of macromonomers (MMs) is highly dependent on the competition between the kinetics of the polymerization and the lifetime of the catalyst. We evaluated the effect of anchor group chemistry—the configuration of atoms linking the polymer to a polymerizable norbornene—on the kinetics of ROMP of polystyrene and poly(lactic acid) MMs initiated by (H2IMes)(pyr)$_2$(Cl)$_2$Ru=CHPh (Grubbs 3rd generation catalyst). We observed a variance in the rate of propagation of >4-fold between similar MMs with different anchor groups. This phenomenon was conserved across all MMs tested, regardless of solvent, molecular weight (MW), or repeat unit identity. The observed >4-fold difference in propagation rate had a dramatic effect on the maximum obtainable backbone DP, with slower propagating MMs reducing the maximum bottlebrush MW by an order of magnitude (from ~106 to ~105 Da). A chelation mechanism was initially proposed to explain the observed anchor group effect, but experimental and computational studies indicated that the rate differences likely resulted from a combination of varying steric demands and electronic structure among the different anchor

groups. The addition of trifluoroacetic acid to the ROMP reaction substantially increased the propagation rate for all anchor groups tested, likely due to scavenging of the pyridine ligands. Based on these data, rational selection of the anchor group is critical to achieve high MM conversion and to prepare pure, high MW bottlebrush polymers by ROMP grafting-through.

2.3 Introduction

The study of bottlebrush polymers has gained momentum in recent years due to the unique architecture and physical properties of this polymer topology.[1,2] Comprised of numerous polymeric side-chains densely grafted to a polymer backbone, the highly branched nature of bottlebrush polymers results in steric repulsion between neighboring polymer chains, forcing these macromolecules to adopt a chain-extended conformation.[3,4] Bottlebrush polymers differ from their linear analogs in their size, shape-persistence, cylindrical nanostructure, and their inability to interact through chain entanglement—properties that are highly dependent on the molecular weight (MW) of the pendant side-chains as well as the backbone degree of polymerization (DP).[5,6] Consequently, bottlebrush polymers have become increasingly relevant in applications such as rheology modifiers,[7] super-soft elastomers,[8] photonic crystals,[9] anti-fouling coatings,[10] the in vivo delivery of therapeutic agents,[11,12] and as promising substrates in lithographic printing.[13,14]

Despite recent progress, bottlebrush polymers with controllable MWs, high side-chain and backbone DPs, narrow molecular weight distributions, and uniform grafting densities remain challenging synthetic targets. There are a number of approaches toward the synthesis of these macromolecules, and each has its advantages and shortcomings. The grafting-through approach involves the polymerization of macromonomers (MMs) (polymers that contain a polymerizable chain end) to form a “perfectly grafted” bottlebrush polymer. Bottlebrush polymers prepared

using this technique possess polymeric side-chains of known and uniform MW, as MMs are synthesized prior to the grafting step. Additionally, grafting-through allows for 100% grafting density, unlike other methods.[15] However, this technique is often limited to low DPs for the bottlebrush polymer backbone due to the relatively low concentration of polymerizable end groups and steric congestion around the propagating site caused by the interaction of two polymeric species.[16]

Many reports on the grafting-through strategy employ ring-opening metathesis polymerization (ROMP) of MMs containing norbornene end groups.[17-26] During ROMP grafting-through, highly active olefin metathesis catalysts mediate the polymerization of MMs functionalized with strained terminal norbornenes to afford narrow dispersity bottlebrush polymers with a great degree of control over backbone and side-chain MW.[27] However, while some very high MW bottlebrush polymers have been prepared by ROMP grafting-through,[28-30] low backbone DPs or side-chain MWs are more commonly reported. In fact, some reports indicate that an inherent backbone DP ceiling exists for specific MMs under their tested conditions.[31-33] Intuitively, the maximum DP that is obtainable in ROMP grafting-through is limited by (among other factors): (1) the rate of propagation of the polymerization; (2) the limited lifetime of the active catalytic species (a form of termination in ROMP). Therefore, complete conversion of MM to bottlebrush polymer can be obtained with rapidly propagating MMs, while incomplete conversions result from MMs that propagate slowly, such that the timescale of the polymerization exceeds the lifetime of the catalyst. Incomplete conversion as the result of catalyst deactivation is particularly problematic in grafting-through syntheses of bottlebrush polymers using ROMP because it leads to a broadening of the molecular weight distribution and contaminates the bottlebrush polymer sample with residual MM impurities that can be difficult to remove.

Scheme 2.1. Typical synthesis of a bottlebrush polymer by ROMP grafting-through

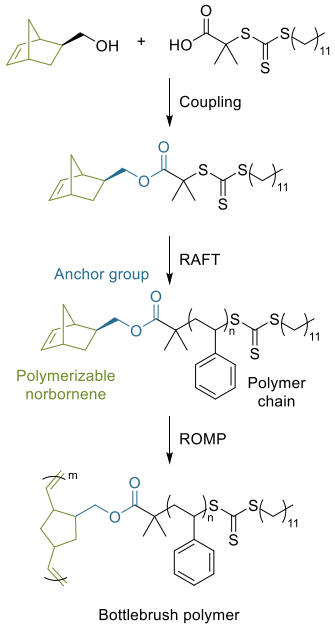

In our laboratory we have often observed widely different MM conversions and ultimate molecular weights despite employing the same ROMP catalyst, the same solvent, the same type of repeat unit in the MM, and MMs of similar MWs. Similar discrepancies appear throughout the literature. Considering these puzzling results, we sought to understand why some MMs undergo ROMP quickly to high conversion and high DP while nearly identical MMs undergo relatively slower propagation, achieve a lower maximum conversion, and have a lower backbone DP as a result. The three-dimensional shape of bottlebrush polymers (i.e., cylindrical or globular) depends largely on the backbone DP and ultimately determines their possible applications.5,30,34 Therefore, measuring and controlling the factors that affect the rate of MM polymerization (and correspondingly, the molecular weight of the bottlebrush polymer) will enable access to a wider variety of well-defined bottlebrush polymers via the grafting-through approach.

MMs functionalized with a norbornene derivative on their chain terminus are commonly prepared by esterification or imidization of norbornene carboxylic acid,[29] norbornenol,[18] or norbornene anhydride,[27] derivatives (Scheme 2.1). These reactions represent convenient routes to attach the polymer unit to the polymerizable functionality and are ubiquitous to ROMP grafting-through regardless of the method of MM synthesis. Ultimately, these reactions leave a carbonyl near the Ru center in the propagating alkylidene species. The proximity of a carbonyl to the metal center influences the activity of the ruthenium carbene complex, as stable Ru chelates may sequester the catalyst in an unproductive form.[35-37] In particular, a significant retardation in the rate of propagation during ROMP of small molecule norbornene monomers using $(PCy_3)_2(Cl)_2Ru{=}CHPh$ (Grubbs' 1st generation catalyst) has been demonstrated through a proposed chelation interaction between the carbonyl oxygen atom of the ring-opened monomers and the metal center.[38] In our efforts to prepare bottlebrush polymers by ROMP grafting-through using olefin metathesis catalyst $(H_2IMes)(pyr)_2(Cl)_2Ru{=}CHPh$ (G3), we have noticed a similar variance in the rate of propagation dependent on the chemical structure of the anchor group—the atoms connecting the polymer side-chain to the polymerizable group. We imagined that the anchor group might be a leading cause for the observed variability in bottlebrush polymer synthesis by ROMP. Based on reported results, as well as our own observations, we initially hypothesized that an interaction between the carbonyl oxygen in the anchor group and the Ru center in the propagating alkylidene could compete with the binding of an incoming MM, thereby decreasing the rate of propagation. In this contribution, we investigate the effect of the anchor group on the rate of propagation, the MM conversion, and the maximum obtainable DP during ROMP grafting-through polymerization.

2.4 Results and Discussion

To investigate the proposed anchor group effect, we prepared polystyrene MMs with 3 different moieties anchoring the polymer unit to the polymerizable norbornene chain end. MMs are named following the general scheme XP_y where X = anchor group 1, 2, or 3 (Figure 2.1A); P = monomer repeat unit, styrene (S) or lactide (L); and y = number average molecular weight (M_n) of the MM (therefore, $3S_{3k}$ indicates anchor group 3 (imide), with an attached polystyrene chain of 3 kDa). These anchor groups were chosen because they are widely used and provide varying degrees of proximity of the ester or imide carbonyl to the Ru center, with the norbornene imide- and norbornene carboxylic acid-derived groups placing the carbonyl in position to chelate the metal center via the formation of a 6-membered ring. Stelzer and coworkers observed a retardation effect due to the existence of 6-membered ring chelates in similarly functionalized monomers.38 Therefore, we theorized that MMs of the type $1P_y$, whose carbonyl group cannot chelate to the Ru center via formation of a 6-memberd ring, should propagate more rapidly than MMs of type $2P_y$ and $3P_y$, which can chelate via a 6-membered ring. Additionally, MMs of types $1P_y$ and $2P_y$ are monosubstituted with respect to the norbornene ring system, leading to the formation of two possible regioisomers for the propagating alkylidene. In the case of MM $2P_y$, only one of the two regioisomers would have the potential for 6-membered chelate formation. Based on these qualifications, we envisioned that MMs prepared using the selected anchor groups would follow the trend of propagation rate 1 > 2 > 3.

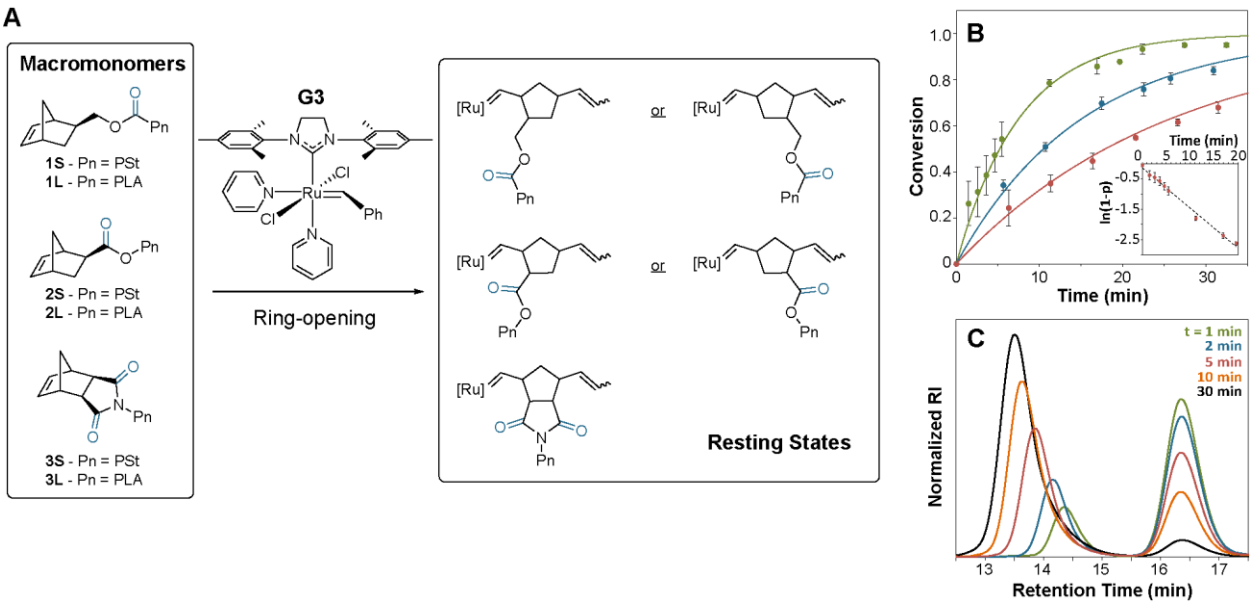

Figure 2.1. A) Structures of propagating alkylidenes for various MMs highlighting i) the potential for chelation between the carbonyl oxygen of the anchor group and the Ru center, and ii) regioisomers that are unlikely to form chelates. B) Kinetic analyses of ROMP of MMs with different end groups: representative kinetic plot of in situ NMR experiments using polystyrene MMs of Mn ~5,000 Da with an [MM]/[G3] ratio of 100 at 50 mg/mL (green circles = $1S_{5k}$, blue circles = $2S_{5k}$, red circles = $3S_{5k}$). Solid lines represent fits of each dataset generated using experimentally determined k_p values based on the equation $p=1-e^{\wedge((-k\_pt))}$. B, inset) Representative log plot for in situ NMR kinetic analysis of MM $1S_{5k}$. C) Representative SEC traces of the kinetic study of MM $1S_{3k}$.The peaks at longer retention times (ca. 16.5 min) correspond to residual MM.

Macromonomer Synthesis

Polystyrene MMs of number average MW (Mn) ~3 kDa were synthesized by reversible addition–fragmentation chain transfer (RAFT) polymerization using three different norbornene

functionalized chain transfer agents (CTAs) containing the anchor groups shown in Figure 2.1A. Low AIBN loadings (0.01 equiv relative to CTA) were employed during RAFT polymerization to avoid radical reactions involving the norbornene olefins, to reduce the proportion of initiator-derived chains, and to limit the incidence of termination by coupling, which would result in polymers functionalized with norbornene groups on both chain ends.[26,39-41] Despite our efforts, ROMP of $1S_{3k}$ at different [MM]/[G3] ratios revealed the presence of ~5% of initiator-derived chains, as grafting-through using this MM reached a maximum conversion of 95% regardless of the targeted DP (Figure 2S39), with quantitative consumption of norbornene olefin. In addition, to establish whether the proposed anchor group effect is consistent across other MMs of varying repeat unit structure and MW, a series of higher MW polystyrene MMs (~5 kDa) were synthesized by increasing the [S]/[CTA] ratio. Three poly(lactic acid) (PLA) MMs (~4 kDa) were also prepared via DBU-catalyzed ring-opening polymerization (ROP) of $_{D,L}$-lactide using three different norbornene alcohols as initiators in accordance with a previously reported procedure.[42] ^{1}H NMR spectroscopy and size exclusion chromatography (SEC) were employed to characterize the resulting MMs. In all cases, the MMs possessed narrow molecular weight distributions, low dispersities (Đ), and M_n values consistent with conversions determined by ^{1}H NMR spectroscopy (Table 2S1).

^{1}H NMR Kinetic Analysis

Our principal kinetic analysis of ROMP grafting-through of MMs containing anchor groups 1, 2, and 3 was conducted using in situ ^{1}H NMR spectroscopy by monitoring the disappearance of the resonance corresponding to the olefin protons of the terminal norbornene relative to protons from the side-chain repeat units of the MMs, which remain constant (Figure 2S11). Conversions determined using this method were averaged over multiple runs and utilized to calculate

propagation rate constants and half-lives. ROMP mediated by catalyst G3 can be considered as pseudo-first-order; therefore, first-order kinetic analysis was applied. As is evident in Table 2.1 and Figure 2.1B, a substantial dependence of the rate of MM consumption on the anchor group was observed, with k_p values differing by a factor of 7 across MMs 1-3S_{3k}. The rate of propagation of the MMs followed the trend based on their anchor groups of 1 > 2 > 3,

Kinetic analysis of polystyrene MMs of MW ~5 kDa with anchor groups 1, 2, and 3 revealed the same trend in propagation rates. Consistent with literature reports, an overall decrease in k_p was observed upon increasing the MM size, likely resulting from increased steric congestion surrounding the propagating catalyst.[31,32,43] The terminal conversions achieved during ROMPs of these MMs were also reduced compared to the 3 kDa set. For example, $3S_{3k}$ reached a conversion of 91% after 1 h while $3S_{5k}$ only attained 80% conversion in the same time. The kinetics of ROMP of PLA MMs (1-3L_{4k}) exhibited the same dependence on the anchor group, with kp trending as 1 > 2 > 3. These data indicate that this trend in anchor groups is likely to be broadly conserved, regardless of MM size or the type of repeat unit.

Table 2.1. Summary of ROMP kinetic analysis of MMs.

	Measured by NMR			Measured by SEC[h]					
MM Name	k_p (10^{-3} s^{-1})[a]	$t_{1/2}$ (s)[b]	%conv[c]	k_p (10^{-3} * s^{-1})[d]	$t_{1/2}$ (s)[b]	%conv[e]	BB M_n, (kDa)[f]	BB $M_{n,expected}$ (kDa)[g]	BB Đ[f]
1S$_{3k}$	11 ± 2	68 ± 20	>99	8.0	87	95	280	280	1.01
2S$_{3k}$	3.3 ± 0.3	210 ± 20	98	3.6	190	89	260	280	1.01
3S$_{3k}$	1.6 ± 0.2	450 ± 80	91	1.6	430	87	250	260	1.03
1S$_{5k}$	2.9 ± 0.4	250 ± 40	>99	2.5	280	94	470	520	1.10
2S$_{5k}$	1.1 ± 0.1	620 ± 70	92	0.95	730	82	480	510	1.15
3S$_{5k}$	0.64 ± 0.07	1100 ± 100	80	0.61	1100	69	400	500	1.32
1L$_{4k}$	8.1 ± 0.7	87 ± 9	>99	6.9	99	96	530	420	1.01
2L$_{4k}$	5.1 ± 0.4	140 ± 10	>99	4.5	160	95	530	460	1.01
3L$_{4k}$	1.7 ± 0.3	420 ± 70	>99	1.2	560	88	390	400	1.29

Polymerizations were conducted in CHCl3 (or CDCl3) with [MM]/[G3] = 100 at [MM] = 50 mg/mL at rt. [a]Calculated from conversions from ^{1}H NMR spectroscopy using first-order kinetic analysis. [b]Calculated using t1/2 = ln(2)/k_p. [c]Measured by monitoring olefin consumption using 1H NMR spectroscopy. [d]Determined using conversions measured by SEC. [e]Measured using SEC by comparing the relative integrations of the bottlebrush and MM peaks in the RI trace (95% represents full conversion for MMs 1-3S_{3k} due to the existence of initiator-derived chains; see Figure 2S39). [f]Measured by SEC using absolute MW determined by light scattering. [g]Determined using the formula $M_{n,expected}$ = M_n, MM * conv * ([MM]/[G3]). [h]These data represent the conversion and MW achieved after 24 h.

SEC Kinetic Analysis

A similar kinetic investigation was conducted using an SEC-based method. The sampling procedure included taking aliquots of the reaction mixture and injecting them into a solution containing ethyl vinyl ether (EVE) to terminate the polymerization at each time point. Conversions were determined via SEC by comparing the relative integrations of the MM and bottlebrush polymer peaks in the refractive index (RI) traces. Similar to our ^{1}H NMR spectroscopic analysis, propagation rate constants and half-lives were calculated from these conversions employing pseudo-first-order kinetic analysis. The same trend in the relative rates of propagation observed during the in situ NMR experiments, 1 > 2 > 3, was also clear in the SEC experiments, with half-lives differing by a factor of 4-6 for the different anchor groups across each series. ROMPs of MMs 1-3S_{3k} in CH_2Cl_2 and THF, common solvents for Ru-catalyzed metathesis, also conformed to the aforementioned trend and gave rates similar to those measured in CDCl3 (Table 2S2).

In addition to half-life data, the SEC kinetic studies gave information regarding the control of the polymerization through evaluation of the shape and Đ of the bottlebrush polymer molecular weight distributions. M_n and Đ values were compared for the bottlebrush polymers after 24 h of ROMP grafting-through polymerization. The consequences of the observed difference in rate for different anchor groups are exemplified by these data. When the rate of propagation is slow during ROMP of MMs, in this case as the result of the anchor group effect, a broadening of the molecular weight distribution and a more pronounced disagreement between measured and theoretical M_n is observed. Further, both the conversion of the polymerization and the DP obtained during ROMP of MMs decrease as a function of decreasing propagation rate. This effect is most apparent for larger MMs, as is the case with $3S_{5k}$. Here, the conversion obtained

after 24 h decreased by 25% compared to $1S_{5k}$, with the only notable difference in the two MMs being the chemical structure of the anchor group. Incomplete conversion within the window of catalyst lifetime leads to undesired termination (as evidenced by the substantial tailing observed in the bottlebrush molecular weight distributions of MMs $3S_{5k}$ and $3L_{4k}$ in particular as well as in deviations from linearity in their first-order kinetic plots); thus, control over the polymerization is eroded. Additionally, incomplete conversion leads to bottlebrush polymer samples that are contaminated with linear MM impurities.

Origin of the Anchor Group Effect

In an effort to understand the chemical origin of the observed rate differences among anchor groups, we next explored the possibility of modifying the rate of propagation of MMs 1-$3S_{3k}$ through the use of additives. A number of compounds have been employed during Ru-catalyzed cross-metathesis or ROMP to improve reaction rates, increase yields, or influence product stereochemistry. For example, Lewis acids have been used to coordinate with functional groups that interfere with catalyst turnover.[44,45] In particular, titanium (IV) tetraisopropoxide (TTIP) has been shown to destabilize six- and seven-membered ring chelates that form between Ru-based metathesis catalysts and carbonyl-containing substrates.[46] We chose to evaluate the effect of TTIP on the process of bottlebrush formation to disrupt the potential chelation interactions proposed between the MMs and the Ru center. In addition to this action, TTIP can scavenge pyridine; therefore, the effect of addition of trifluoroacetic acid (TFA) in the ROMP of MMs 1-$3S_{3k}$ was also studied for comparison.

ROMP kinetics of MMs 1-$3S_{3k}$ were reevaluated in the presence of TTIP (2 or 100 equiv with respect to G3) or TFA (2 equiv with respect to G3) in $CDCl_3$. For these experiments, MMs and additives were dissolved in a solution of $CDCl_3$, and the polymerizations were initiated via

addition of a solution of G3. Aliquots of the reaction mixtures were removed at various time points and quenched with EVE, and then analyzed by SEC. The results of this study are summarized in Table 2.2. In all cases, the previously observed trend in k_p of MMs 1-3S_{3k} was maintained. Addition of TTIP to the polymerizations, regardless of the amount added, had no appreciable effect on the kinetics of the polymerizations. If chelation between the anchor group and the Ru catalyst were the cause of the observed differences in rates, addition of TTIP would have been expected to enhance the rates of propagation of MMs $2S_{3k}$ and $3S_{3k}$. Interestingly, addition of 2 equiv of TFA had an effect on the k_p of all MMs, enhancing the rate dramatically in the case of $1S_{3k}$ and moderately for $2S_{3k}$ and $3S_{3k}$.

Table 2.2. Evaluation of additives on ROMP of MMs 1S3k-3S3k.

	Additive k_p (10^{-3} * s^{-1})[a]			
MM	None	TTIP (2 equiv)	TTIP (100 equiv)	TFA (2 equiv)
$1S_{3k}$	8.0	6.3	6.1	>60
$2S_{3k}$	3.6	3.7	3.2	7.9
$3S_{3k}$	1.6	1.0	0.9	5.8

Polymerizations were conducted in $CHCl_3$ with [MM]/[G3] = 100 at [MM] = 50 mg/mL. [a]Determined from MM conversions using SEC.

These results contradicted our initial hypothesis of anchor group carbonyl chelation, as TFA is unlikely to disrupt these types of interactions. Instead, it ostensibly acts as a scavenger of pyridine. Pyridine concentration affects the equilibrium between the dormant and active catalyst species, and seems to play a critical role in the ROMP of MMs.[47,48]

To further investigate the chelation process, we performed density-functional theory (DFT) calculations of the resting states of the alkylidene Ru catalyst for all three anchor groups after ring-opening of a single monomer unit in the chelated and nonchelated forms (Figure 2S40, Table 2S3). The DFT calculations revealed that there is not a large driving force for chelation in any of the monomers. Even though chelated species occurring via formation of 6-membered rings are possible, the calculated ΔGchelation values are between zero and -5 kcal/mol. Moreover, stable chelated species were not found for one of regioisomers of both MM $1S_{3k}$ and MM $2S_{3k}$, as they involve formation of larger rings. We note that the formation of a chelated species from the unchelated isomer involves a rotation around a Ru=C-C-C dihedral angle of the alkylidene, which might incur an energetic penalty. In effect, potential energy surface scans of this coordinate indicate that the chelation process is activated, involving barriers of ~5 kcal/mol. Both the relatively low exoergicity of the chelation process and the presence of barriers for chelation obtained from the DFT calculations further dispute the chelation hypothesis.

Instead of resulting from a possible chelation process, we propose that the differences in k_p between MMs 1-3P_y derive from at least two considerations. First, the capability of MMs $1P_y$ and $2P_y$ to form regioisomers in which the anchor group is placed away from the Ru center may be the primary cause of the difference in k_p between MMs $1P_y$/$2P_y$ and MM $3P_y$. Second, the electronic structure of the monomer likely plays a role in the overall reaction rate. A key step in the ROMP mechanism is the addition of the monomer to the alkylidene Ru catalyst. Since species with a higher-energy HOMO exhibit greater reactivity in addition reactions, monomers with anchor groups that raise the HOMO energy might result in a larger overall polymerization rate. DFT calculations of small molecule analogues of MMs 1-3P_y (Figure 2S41) indeed revealed that the HOMO stability of the monomers (MM $1P_y$ < MM $2P_y$ < MM $3P_y$) is inversely

correlated with the measured kp values (MM $3P_y$ < MM $2P_y$ < MM $1P_y$). The fact that monomers with higher HOMO energies result in faster polymerization rates lends support to the idea that the anchor groups can modulate the reaction rate by influencing the electronic structure of the monomer.

Consequences of Anchor Group Choice

The backbone DP and the purity of the polymer sample are critical parameters to consider when designing chemical syntheses to prepare bottlebrush polymers. Indeed, the ultimate 3-dimensional shape (i.e., globular vs. cylindrical) and physical properties depend on the fine-tuning of these parameters, with most applications targeting bottlebrush polymers with high DPs and purity. It is clear that anchor group chemistry affects the kinetics of ROMP of MMs. However, the >4 fold difference in k_p may not fully convey the importance of the configuration of the handful of atoms that connect the polymer chain to the norbornene.

To underscore the importance of the differences in the kinetics of reaction between MMs observed here, we targeted high backbone DPs for polymerizations using the fastest and slowest propagating anchor groups. For these experiments, ROMP of $1L_{4k}$ and $3L_{4k}$ was conducted at increasing [MM]/[G3] ratios (50-1000) under our optimized conditions (50 mg/mL, $CHCl_3$, 24 h), and the resulting bottlebrush polymers were analyzed by SEC (Figure 2.2B). As shown in Figure 2.2C, the conversion of the polymerization remained relatively constant throughout the [MM]/[G3] series for MM $1L_{4k}$. In stark contrast, the conversion of MM $3L_{4k}$ decreased rapidly with increasing [MM]/[G3]. A plot of M_n vs. [MM]/[G3] (Figure 2.2D) illustrates the concept of a backbone DP ceiling for a set of experimental conditions, with ROMP of $3L_{4k}$ limited to a DP of ~100 repeat units regardless of the targeted [MM]/[G3]. However, using $1L_{4k}$ it was possible to synthesize a bottlebrush polymer with a M_n in excess of 3000 kDa (Figure 2.2B)—

approximately an order of magnitude larger than the bottlebrush polymer prepared using an MM of nearly identical M_n with the same repeat unit. It should be further emphasized that this broad discrepancy in obtainable DP arises entirely from the chemical structure of the anchor group (Figure 2.2A shows SEC traces of MMs $1L_{4k}$ and $3L_{4k}$ to exemplify the similarity of the MM molecular weight distributions), and that this phenomenon primarily originates from the kinetics of polymerization.

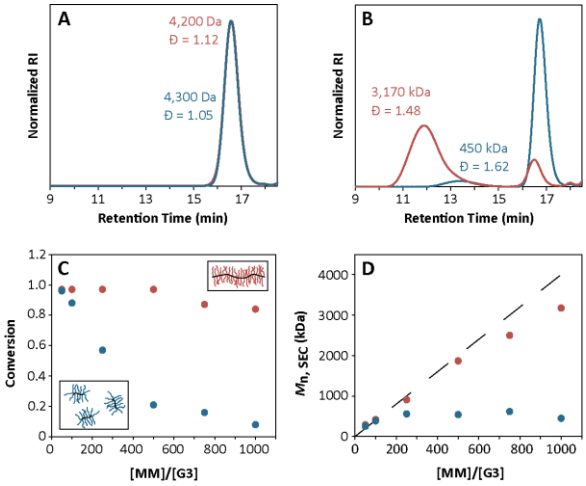

Figure 2.2. ROMP grafting-through with increasing [MM]/[G3] ratios for MMs $1L_{4k}$ (red) and $3L_{4k}$ (blue). A) SEC traces of both MMs. B) SEC traces (RI detector) of bottlebrush polymers resulting from ROMP of both MMs at [MM]/[G3] = 1000. C) Conversion (as measured by SEC) vs [MM]/[G3] for both MMs. D) M_n (as measured by SEC) as a function of [MM]/[G3] for both MMs.

2.5 Conclusions

Our kinetic analyses of ROMP grafting-through support our hypothesis that the anchor group has a large effect on polymerization kinetics and the ultimate MW of the bottlebrush polymer. The observed trend (kp of anchor group 1 > 2 > 3) was conserved for polystyrene MMs of different MWs as well as for PLA MMs. We initially proposed a chelation mechanism to explain the

observed differences in propagation rate. However, experimental and computational studies showed that this phenomenon more likely originates from a combination of steric effects and differences in monomer electronic structure. Addition of TFA to polymerizations of MMs 1-3S_{3k} enhanced the rate of propagation, demonstrating the critical role of pyridine concentration in the ROMP of MMs. Importantly, the >4 fold difference in the propagation rates between the three different anchor groups had a dramatic effect when targeting high bottlebrush backbone DPs. Bottlebrush polymers with MWs >3000 kDa could be prepared from $1L_{4k}$. However, using $3L_{4k}$, the maximum obtainable MW was nearly an order of magnitude lower (~450 kDa) and corresponded with a relatively broad molecular weight distribution and low conversion. Given that the properties of these complex macromolecules depend on factors such as the backbone DP and the purity of the polymer sample, rational selection of the anchor group is a critical factor when designing synthetic strategies for preparing bottlebrush polymers. We expect that this anchor group effect may also be important for polymerization of other challenging monomers, such as those with peptides, sugars, dendrimers, or other bulky groups.

Acknowledgements

This work was supported by the Army Research Office (W911NF-14-1-0322) and the American Chemical Society Petroleum Research Fund (54884-DNI7). We thank Materia for catalyst. We acknowledge Advanced Research Computing at Virgina Tech for providing computational resources and technical support that have contributed to the results reported within this paper.

2.6 References

(1) Sheiko, S. S.; Sumerlin, B. S.; Matyjaszewski, K. *Prog. Polym. Sci.* **2008**, 33, 759.

(2) Rzayev, J. *ACS Macro Lett*. **2012**, *1*, 1146.

(3) Grigoriadis, C.; Nese, A.; Matyjaszewski, K.; Pakula, T.; Butt, H.-J.; Floudas, G. *Macromol. Chem. Phys*. **2012**, *213*, 1311.

(4) Pietrasik, J.; Sumerlin, B. S.; Lee, H.-i.; Gil, R. R.; Matyjaszewski, K. *Polymer* **2007**, *48*, 496.

(5) Pesek, S. L.; Li, X.; Hammouda, B.; Hong, K.; Verduzco, R. *Macromolecules* **2013**, *46*, 6998.

(6) Tsukahara, Y.; Namba, S.-i.; Iwasa, J.; Nakano, Y.; Kaeriyama, K.; Takahashi, M. *Macromolecules* **2001**, *34*, 2624.

(7) Celli, J. P.; Turner, B. S.; Afdhal, N. H.; Ewoldt, R. H.; McKinley, G. H.; Bansil, R.; Erramilli, S. *Biomacromolecules* **2007**, *8*, 1580.

(8) Neugebauer, D.; Zhang, Y.; Pakula, T.; Sheiko, S. S.; Matyjaszewski, K. *Macromolecules* **2003**, *36*, 6746.

(9) Sveinbjörnsson, B. R.; Weitekamp, R. A.; Miyake, G. M.; Xia, Y.; Atwater, H. A.; Grubbs, R. H. *PNAS* **2012**, *109*, 14332.

(10) Krishnan, S.; Weinman, C. J.; Ober, C. K. *J. Mater. Chem*. **2008**, *18*, 3405.

(11) Johnson, J. A.; Lu, Y. Y.; Burts, A. O.; Lim, Y.-H.; Finn, M. G.; Koberstein, J. T.; Turro, N. J.; Tirrell, D. A.; Grubbs, R. H. *J. Am. Chem. Soc*. **2010**, *133*, 559.

(12) Yu, Y.; Chen, C.-K.; Law, W.-C.; Mok, J.; Zou, J.; Prasad, P. N.; Cheng, C. *Mol. Pharm.* **2013**, *10*, 867.

(13) Sun, G.; Cho, S.; Clark, C.; Verkhoturov, S. V.; Eller, M. J.; Li, A.; Pavía-Jiménez, A.; Schweikert, E. A.; Thackeray, J. W.; Trefonas, P.; Wooley, K. L. *J. Am. Chem. Soc.* **2013**, *135*, 4203.

(14) Hong, S. W.; Gu, W.; Huh, J.; Sveinbjornsson, B. R.; Jeong, G.; Grubbs, R. H.; Russell, T. P. *ACS Nano*, **2013**, *7*, 9684.

(15) Verduzco, R.; Li, X.; Pesek, S. L.; Stein, G. E. Chem. *Soc. Rev*. **2015**.

(16) Breunig, S.; Héroguez, V.; Gnanou, Y.; Fontanille, M. *Macromol. Symp.* **1995**, *95*, 151.

(17) Li, Y.; Themistou, E.; Zou, J.; Das, B. P.; Tsianou, M.; Cheng, C. *ACS Macro Lett.* **2011**, *1*, 52.

(18) Li, Z.; Ma, J.; Cheng, C.; Zhang, K.; Wooley, K. L. *Macromolecules* **2010**, *43*, 1182.

(19) Li, A.; Ma, J.; Sun, G.; Li, Z.; Cho, S.; Clark, C.; Wooley, K. L. *J. Polym. Sci., Part A: Polym. Chem.* **2012**, *50*, 1681.

(20) Kim, K. O.; Choi, T.-L. *Macromolecules* **2013**, *46*, 5905.

(21) Engler, A. C.; Chan, J. M. W.; Fukushima, K.; Coady, D. J.; Yang, Y. Y.; Hedrick, J. L. *ACS Macro Lett*. **2013**, *2*, 332.

(22) Li, C.; Gunari, N.; Fischer, K.; Janshoff, A.; Schmidt, M. *Angew. Chem., Int. Ed.* **2004**, *43*, 1101.

(23) Hilf, S.; Kilbinger, A. F. M. *Macromol. Rapid Commun.* **2007**, *28*, 1225.

(24) Foster, J. C.; Radzinski, S. C.; Lewis, S. E.; Slutzker, M. B.; Matson, J. B. *Polymer* **2015**, *79*, 205.

(25) Radzinski, S. C.; Foster, J. C.; Matson, J. B. *Polym. Chem*. **2015**, *6*, 5643.

(26) Teo, Y. C.; Xia, Y. *Macromolecules* **2015**, *48*, 5656.

(27) Xia, Y.; Kornfield, J. A.; Grubbs, R. H. *Macromolecules* **2009**, *42*, 3761.

(28) Li, Z.; Zhang, K.; Ma, J.; Cheng, C.; Wooley, K. L. *J. Poly. Sci. Part A: Polym. Chem.* **2009**, *47*, 5557.

(29) Jha, S.; Dutta, S.; Bowden, N. B. *Macromolecules* **2004**, *37*, 4365.

(30) Dalsin, S. J.; Hillmyer, M. A.; Bates, F. S. *ACS Macro Lett.* **2014**, *3*, 423.

(31) Feast, W. J.; Gibson, V. C.; Johnson, A. F.; Khosravi, E.; Mohsin, M. A. *J. Mol. Catal. A: Chem.* **1997**, *115*, 37.

(32) Morandi, G.; Mantovani, G.; Montembault, V.; Haddleton, D. M.; Fontaine, L. *New J. Chem.* **2007**, *31*, 1826.

(33) Cho, H. Y.; Krys, P.; Szcześniak, K.; Schroeder, H.; Park, S.; Jurga, S.; Buback, M.; Matyjaszewski, K. *Macromolecules* **2015**, *48*, 6385.

(34) Müllner, M.; Dodds, S. J.; Nguyen, T.-H.; Senyschyn, D.; Porter, C. J. H.; Boyd, B. J.; Caruso, F. *ACS Nano* **2015**, *9*, 1294.

(35) Fürstner, A.; Thiel, O. R.; Lehmann, C. W. *Organometallics* **2002**, *21*, 331.

(36) Fürstner, A.; Langemann, K. *J. Org. Chem.* **1996**, *61*, 3942.

(37) Fu, G. C.; Grubbs, R. H. *J. Am. Chem. Soc.* **1992**, *114*, 7324.

(38) Slugovc, C.; Demel, S.; Riegler, S.; Hobisch, J.; Stelzer, F. *Macromol. Rapid Commun.* **2004**, *25*, 475.

(39) Gody, G.; Maschmeyer, T.; Zetterlund, P. B.; Perrier, S. *Nat. Commun*. **2013**, *4*, 2505.

(40) Keddie, D. *J. Chem. Soc. Rev.* **2014**, *43*, 496.

(41) Vandenbergh, J.; Junkers, T. *Macromolecules* **2014**, *47*, 5051.

(42) Radzinski, S. C.; Foster, J. C.; Matson, J. B. *Macromol. Rapid Commun*. **2016**, *37*, 616.

(43) Rizmi, A. C. M.; Khosravi, E.; Feast, W. J.; Mohsin, M. A.; Johnson, A. F. *Polymer* **1998**, *39*, 6605.

(44) Aitken, B. S.; Lee, M.; Hunley, M. T.; Gibson, H. W.; Wagener, K. B. *Macromolecules* **2010**, *43*, 1699.

(45) Simocko, C.; Wagener, K. B. *Organometallics* **2013**, *32*, 2513.

(46) Ghosh, A. K.; Cappiello, J.; Shin, D. *Tett. Lett.* **1998**, *39*, 4651.

(47) Simons, R.; Guntari, S. N.; Goh, T. K.; Qiao, G. G.; Bateman, S. A. *J. Poly. Sci. Part A: Polym. Chem.* **2012**, *50*, 89.

(48) Slugovc, C. *Macromol. Rapid Commun.* **2004**, *25*, 1283.

2.7 Appendix

All reagents were obtained from commercial vendors and used as received unless otherwise stated. 2,2′-Azobis(2-methylpropionitrile) (AIBN) was recrystallized from MeOH and dried under vacuum prior to use. D,L-Lactide was recrystallized from toluene (3x), dried in a vacuum oven, and stored in a desiccator. Styrene was freed of radical inhibitor via passage down a small column of basic alumina. **CTA1** was prepared according to a literature procedure.[1] NMR spectra were measured on Agilent 400 MHz or Bruker 500 MHz spectrometers. ^{1}H and ^{13}C NMR chemical shifts are reported in ppm relative to internal solvent resonances. Yields refer to chromatographically and spectroscopically pure compounds unless otherwise stated. Size exclusion chromatography (SEC) was carried out in THF at 1 mL min^{-1} at 30 °C on two Agilent PLgel 10 μm MIXED-B columns connected in series with a Wyatt Dawn Heleos 2 light scattering detector and a Wyatt Optilab Rex refractive index detector. No calibration standards were used, and dn/dc values were obtained by assuming 100% mass elution from the columns. High-resolution mass spectra were taken on an Agilent Technologies 6230 TOF LC/MS mass spectrometer.

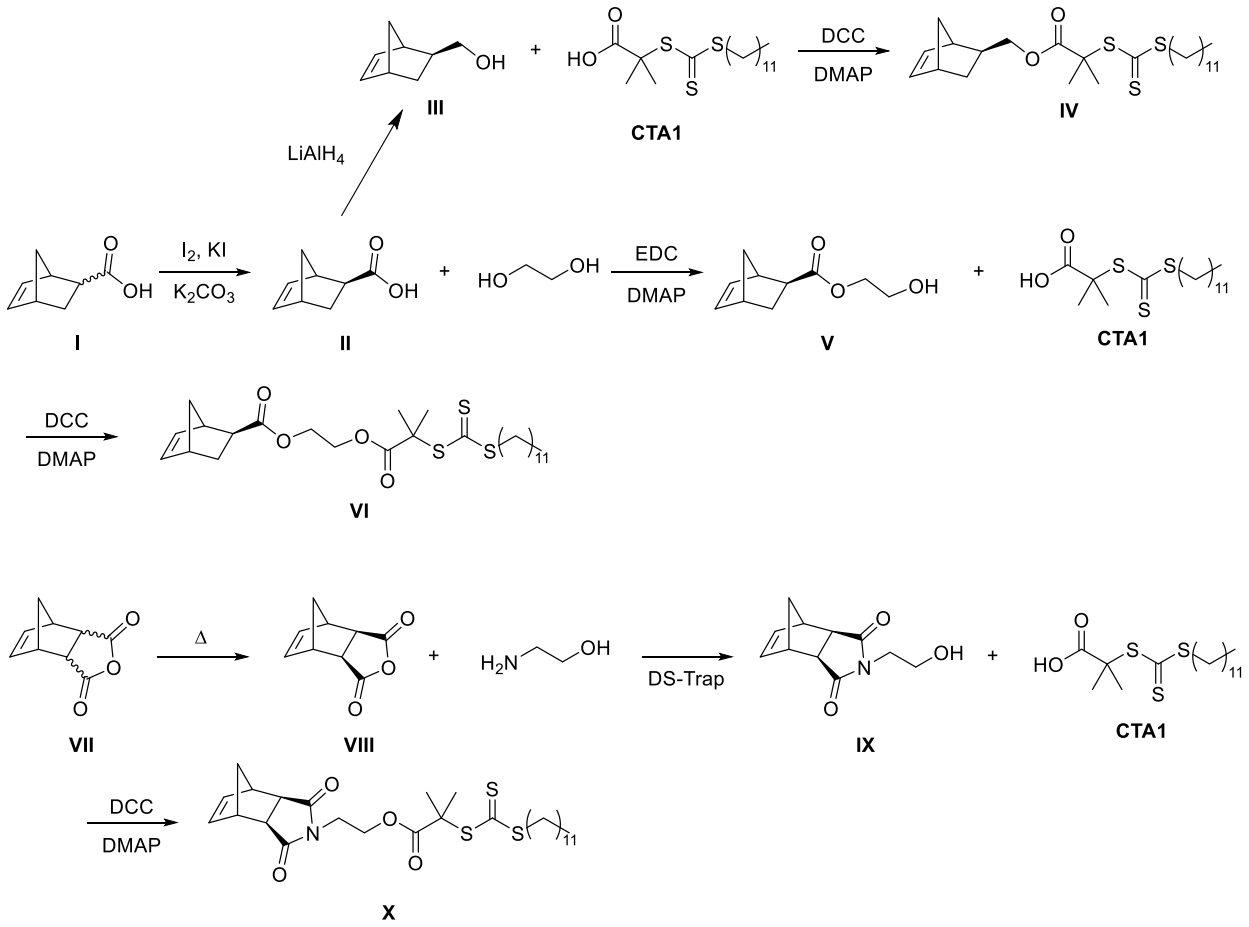

Exo-5-norbornene-2-carboxylic acid (II)

Exo-5-norbornene-2-carboxylic acid was prepared according to a previously reported procedure.[2] ^{1}H NMR ($CDCl_3$): δ 1.40 (m, 2H), 1.54 (d, J = 8 Hz, 1H), 1.95 (m, 1H), 2.27 (m, 1H), 2.94 (s, 1H), 3.11 (s, 1H), 6.14 (m, 2H). ^{13}C NMR ($CDCl_3$): δ 182.8, 138.3, 135.9, 46.9, 46.5, 43.3, 41.8, 30.5.

Exo-5-norbornene-2-methanol (III)

Exo-5-norbornene-2-methanol was prepared according to a previously reported procedure.[2] ^{1}H NMR (CDCl3): δ 6.08 (m, 2H), 3.70 (m, 1H), 3.54 (m, 1H), 2.82 (s, 1H), 2.74 (s, 1H), 1.64 (m,

1H), 1.30 (m, 3H), 1.12 (m, 1H). ^{13}C NMR ($CDCl_3$): δ 136.9, 136.6, 67.7, 45.1, 43.4, 42.0, 41.6, 29.6.

Compound IV

Compound **III** (0.50 g, 4.03 mmol), **CTA1** (1.60 g, 4.39 mmol), DMAP (0.05 g, 0.41 mmol), and DCM (20 mL) were added to a 100 mL RBF. DCC (0.910 g, 4.42 mmol) was added to the flask in one portion and the reaction mixture was stirred at rt for 10 hours. The solids were filtered off and the crude product was purified using column chromatography with 25% hexanes in CH_2Cl_2 as the mobile phase. The product was recovered as a yellow oil that crystallized upon standing (1.30 g, 68% yield). ^1H NMR ($CDCl_3$): δ 0.88 (t, J = 8 Hz, 3H), 1.25 (m, 20H), 1.31 (m, 3H), 1.70 (s, 6H), 2.66 (s, 1H), 2.82 (s, 1H), 3.27 (td, J = 1.6, 8 Hz, 2H), 3.95 (t, J = 8 Hz, 1H), 4.22 (dd, J = 8, 4 Hz, 1H), 6.07 (m, 2H). ^{13}C NMR ($CDCl_3$): δ 221.6, 173.2, 137.0, 136.5, 70.2, 56.2, 45.1, 43.8, 41.8, 37.9, 37.0, 32.1, 29.8, 29.7, 29.6, 29.5, 29.3, 29.1, 28.1, 25.6, 25.6, 22.9, 14.3. HR-MS: $[M + H]^+$ calculated 471.2420; found 471.2424.

Compound V

Ethylene glycol (1.93 g, 31.0 mmol) was dissolved in 10 mL of CH_2Cl_2 in a round bottom flask equipped with a stir bar. Meanwhile, a second flask was charged with compound **II** (1.43 g, 10.4 mmol), EDC (1.98 g, 10.4 mmol), DMAP (0.13 g, 1.06 mmol), and 50 mL of CH_2Cl_2. This second solution was stirred until the solids had completely dissolved (~5 min). The activated acid solution was added dropwise to the flask containing ethylene glycol via addition funnel with vigorous stirring. The reaction mixture was stirred at rt for 12 h. The reaction mixture was then transferred to a separatory funnel, washed with H_2O (2 x 50 mL and brine (50 mL), dried over

Na_2SO_4, and rotovapped. The crude product was further purified on a silica column, eluting with 93:7 CH_2Cl_2/MeOH to give the pure product as a colorless oil (0.83 g, 44% yield). ^{1}H NMR ($CDCl_3$): δ 1.37 (m, 2H), 1.51 (d, 1H), 1.91 (m, 1H), 2.25 (m, 1H), 2.91 (s, 1H), 3.04 (s, 1H), 3.82 (m, 2H), 4.21 (m, 2H), 6.11 (m, 2H). ^{13}C NMR ($CDCl_3$): δ 176.8, 138.2, 135.8, 66.2, 61.4, 46.8, 46.4, 43.2, 41.8, 30.6. HR-MS: $[M + H]^+$ calculated 183.1016; found 183.1015.

Compound VI

A round bottom flask was charged with **CTA1** (395 mg, 1.08 mmol), compound **V** (197 mg, 1.08 mmol), DMAP (13.0 mg, 0.11 mmol), and 10 mL of CH_2Cl_2. To the flask was added DCC (244 mg, 1.18 mmol) in one portion. The reaction mixture was stirred at rt for 2 h. The precipitated solids were then filtered, and the filtrate was dry-loaded onto a silica column. The product was collected by eluting with 3:1 hexanes/CH_2Cl_2 and was recovered as a yellow oil that crystallized upon standing (460 mg, 80% yield). ^{1}H NMR ($CDCl_3$): δ 0.88 (t, J = 8 Hz, 3H), 1.25-1.37 (m, 20H), 1.52 (d, J = 8 Hz, 1H), 1.65 (t, J = 8 Hz, 2H), 1.69 (s, 6H), 1.92 (m, 1H), 2.22 (m, 1H), 2.92 (s, 1H), 3.04 (s, 1H), 3.25 (t, J = 8 Hz, 2H), 4.30 (m, 4H), 6.12 (m, 2H). ^{13}C NMR ($CDCl_3$): δ 221.5, 176.1, 173.0, 138.2, 135.9, 63.8, 62.0, 56.0, 46.8, 46.6, 43.2, 41.8, 37.1, 32.1, 30.5, 29.8, 29.7, 29.6, 29.5, 29.3, 29.1, 28.0, 25.4, 22.8, 14.3. HR-MS: $[M + H]^+$ calculated 529.2474; found 529.2468.

Compound VIII

Norbornene anhydride was prepared according to a previously procedure.[3] ^{1}H NMR ($CDCl_3$): δ 1.44 (m, 1H), 1.65 (m, 1H), 3.00 (d, J = 1.2 Hz, 2H), 3.45 (m, 2H), 6.33 (t, J = 4 Hz, 2H), 9.20 (bs, 1H). ^{13}C NMR ($CDCl_3$): δ 179.0, 137.8, 49.3, 45.2, 43.0.

Compound IX

A round bottom flask was charged with compound **VIII** (2.00 g, 12.2 mmol), ethanolamine (0.78 mL, 12.8 mmol), and 30 mL of toluene. The flask was affixed with a Dean-Stark trap and condenser. The reaction mixture was heated at reflux for 16 h. The toluene was removed by rotovapping. The resulting solids were redissolved in EtOAc (~50 mL) with heating and this solution was transferred to a separatory funnel. The organic solution was washed with 1N HCl (2 x 50 mL) and brine (30 mL), dried over Na_2SO_4, and rotovapped to give the pure product as a white solid (2.26 g, 90% yield). ^{1}H NMR ($CDCl_3$): δ 1.33 (d, J = 8 Hz, 1H), 1.49 (m, 1H), 2.45 (s, 1H, OH), 2.69 (s, 2H), 3.25 (s, 2H), 3.67 (m ,2H), 3.74 (m, 2H), 6.27 (s, 1H). ^{13}C NMR ($CDCl_3$): δ 178.7, 137.8, 59.9, 47.9, 45.2, 42.8, 41.2. HR-MS: $[M + H]^+$ calculated 208.0968; found 208.0968.

Compound X

A round bottom flask was charged with **CTA1** (400 mg, 1.09 mmol), compound **IX** (227 mg, 1.09 mmol), DMAP (13.0 mg, 0.11 mmol), and 10 mL of CH_2Cl_2. To the flask was added DCC (246 mg, 1.19 mmol) in one portion. The reaction mixture was stirred at rt for 2 h. The precipitated solids were then filtered, and the filtrate was dry-loaded onto a silica column. The product was collected by eluting with 3:1 hexanes/EtOAc and was recovered as a yellow solid (453 mg, 75% yield). ^{1}H NMR ($CDCl_3$): δ 0.87 (t, J = 8 Hz, 3H), 1.2-1.4 (m, 20H), 1.51 (d, J = 8 Hz, 2H), 1.56-1.68 (m, 7H), 2.69 (s, 2H), 3.23 (t, J = 8 Hz, 2H), 3.27 (s, 2H), 3.77 (t, J = 4 Hz, 2H), 4.26 (t, J = 4 Hz, 2H), 6.28 (t, J = 1.8 Hz, 2H). ^{13}C NMR ($CDCl_3$): 221.7, 177.8, 172.8, 137.9, 62.4, 56.0, 48.0, 45.4, 43.0, 37.5, 37.2, 32.1, 29.8, 29.8, 29.7, 29.6, 29.5, 29.2, 29.1, 27.9, 25.3, 22.8, 14.3. HR-MS: $[M + NH_4]^+$ calculated 571.2692; found 571.2693.

Synthesis of Polystyrene MMs

A typical polymerization procedure of styrene is as follows: to an oven-dried Schlenk tube equipped with a magnetic stir bar was added CTA (**IV**, **VI**, or **X**), AIBN, and styrene such that [M]/[CTA]/[AIBN] = 100:1:0.01 when targeting 3 kDa or 200:1:0.01 when targeting 5 kDa. This mixture was diluted with THF to a final [monomer] of 50% v/v. The reaction mixture was deoxygenated by three freeze-pump-thaw cycles. The Schlenk tube was then backfilled with N_2 and submerged in an oil bath maintained at 80 °C. The polymerization was terminated after ca. 24 h by submerging the tube into liquid N_2 and exposing the reaction mixture to air. The resulting polystyrene was purified via precipitation from MeOH (3x).

Synthesis of PLA MMs

A typical polymerization procedure of D,L-lactide is as follows: to a flame-dried Schlenk tube equipped with a magnetic stir bar under N_2 atmosphere was added D,L-lactide and initiator at [M]/[I] = 40, and freshly distilled CH_2Cl_2 such that the final concentration of monomer was 10% w/v. This mixture was stirred for ~20 min until the solids had completely dissolved. 1,8-Diazabicyclo[5.4.0]undec-7-ene (DBU) (0.1 equiv to initiator) was then added rapidly under N_2 flow to initiate the polymerization. The polymerization was terminated after ca. 20 min by adding 1 drop of acetic acid to the reaction mixture. The resulting PLA was purified via precipitation from cold MeOH.

***In Situ* NMR Kinetic Experiments**

MM (25 mg) was dissolved in 0.4 mL of $CDCl_3$ in a vial. This solution was transferred to an NMR tube. A ^1H NMR spectrum was collected for the t = 0 time point. **G3** (0.1 equiv to MM)

was dissolved in 1 mL of $CDCl_3$ in a second vial. 0.1 mL of the **G3** solution (to achieve 0.01 equiv to MM) was then added rapidly to the NMR tube to make the final concentration of MM = 50 mg/mL. The tube was capped and inverted to facilitate mixing. ^1H NMR spectra were then collected at various time points. Conversion was calculated via relative integration of the norbornene olefin peak to a polystyrene or PLA resonance that was assumed to not change during MM polymerization (Figure 2S11). Kinetic parameters were obtained from a plot of ln(1 - p) vs. time.

SEC Kinetic Experiments

MM (20 mg) was dissolved in 0.4 mL of $CDCl_3$ in a vial equipped with a stir bar. **G3** (0.1 equiv to MM) was dissolved in 1 mL of $CDCl_3$ in a second vial. 0.1 mL of the **G3** solution (to achieve 0.01 equiv to MM) was then added rapidly to the first vial to make the final concentration of MM = 50 mg/mL. At various time points, 20 uL aliquots were removed from the polymerization mixture and were injected into a vial containing a solution of EVE (a few drops) in THF. These samples were analyzed by SEC. Conversion was calculated via relative integration of the bottlebrush peak to the macromonomer peak. A maximum conversion of 95% was assumed for polystyrene MMs due to the presence of ca. 5 mol% of initiator-derived chains. Kinetic parameters were obtained from a plot of ln(0.95 - p) vs. time for polystyrene MMs or ln(1 – p) vs. time for PLA MMs.

TTIP Additive Experiments

MM (20 mg, 5 kDa) was dissolved in 0.4 mL of a solution of TTIP (1 equiv to MM) in $CDCl_3$ in a vial equipped with a stir bar. **G3** (0.2 mg, 0.05 equiv to MM) was dissolved in 1 mL of $CDCl_3$

in a second vial. 0.1 mL of the **G3** solution (to achieve 0.005 equiv to MM) was then added rapidly to the first vial to make the final concentration of MM = 50 mg/mL. At various time points, 20 uL aliquots were removed from the polymerization mixture and were injected into a vial containing a solution of EVE (a few drops) in THF. These samples were analyzed by SEC. Conversion was calculated via relative integration of the bottlebrush peak to the macromonomer peak. A maximum conversion of 95% was assumed for polystyrene MMs due to the presence of ca. 5 mol% of initiator-derived chains. Kinetic parameters were obtained from a plot of ln(0.95 - p) vs. time.

Macromonomer Characterization:

Table 2S1. MMs used in this study.

MM Name	**% conv.**[a]	**M_n**[b] **(Da)**	**$M_{n,\ theo.}$**[c] **(Da)**	**$M_{n,\ NMR}$ (Da)**[d]	**Đ**[b]
$1S_{3k}$	30	2800	3100	2700	1.02
$2S_{3k}$	30	2800	3000	3000	1.01
$3S_{3k}$	28	2600	2900	2800	1.03
$1S_{5k}$	26	5200	5500	4800	1.01
$2S_{5k}$	25	5200	5200	4700	1.03
$3S_{5k}$	24	5000	5000	5700	1.06
$1L_{4k}$	99	4200	4000	3700	1.12
$2L_{4k}$	99	4600	4000	3600	1.05
$3L_{4k}$	99	4300	4000	3600	1.05

[a]Determined by [1]H NMR spectroscopy. [b]Measured by SEC using absolute MW determined by light scattering. [c]Calculated from conversions determined using [1]H NMR spectroscopy. [d]Calculated using [1]H NMR spectroscopy via end group analysis.

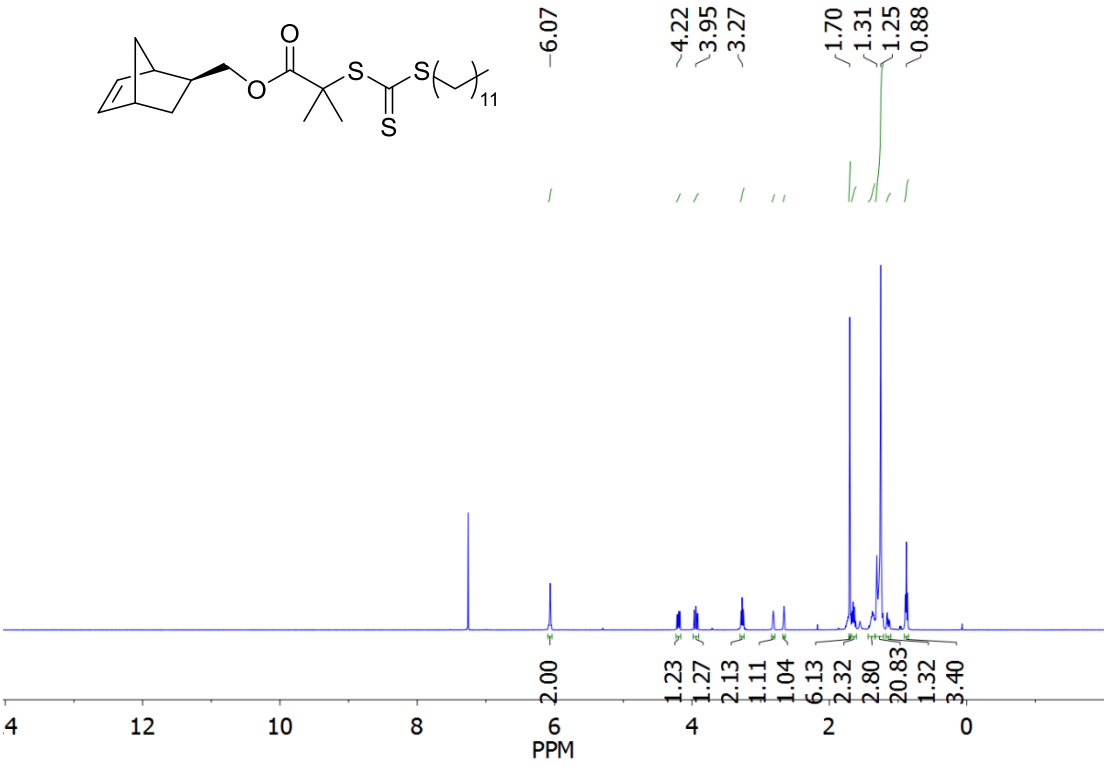

Figure 2S1. [1]H NMR spectrum of Compound **IV**.

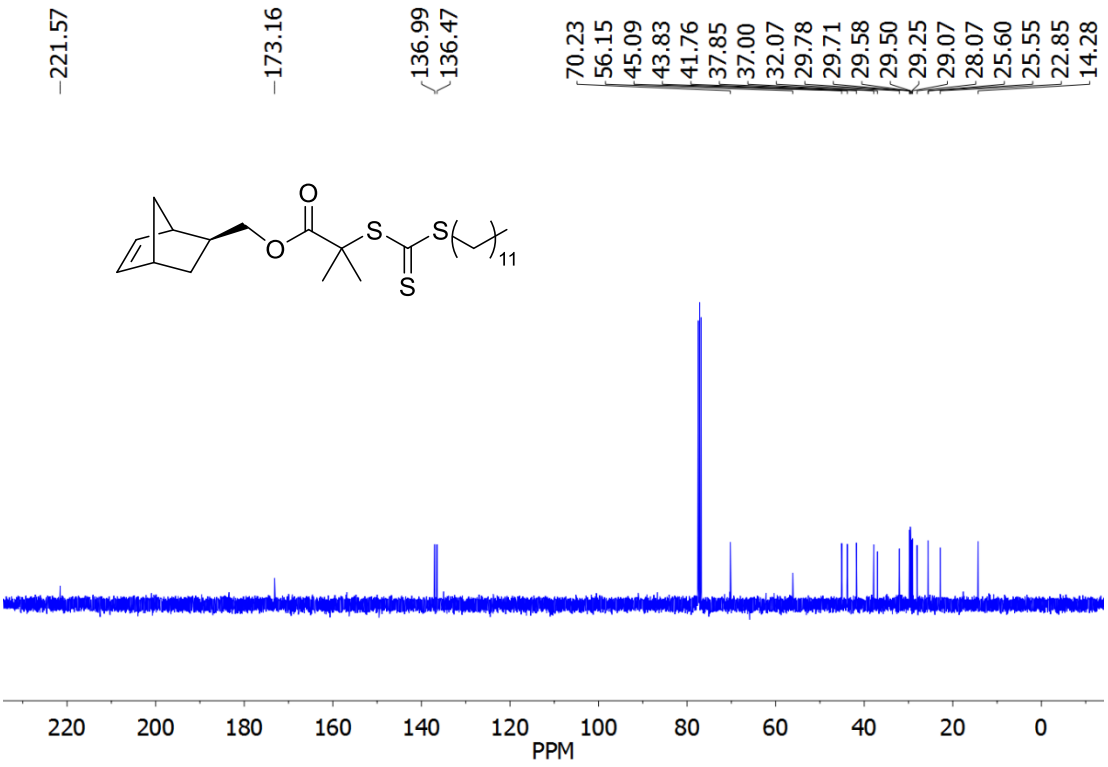

Figure 2S2. ^{13}C NMR spectrum of Compound **IV**.

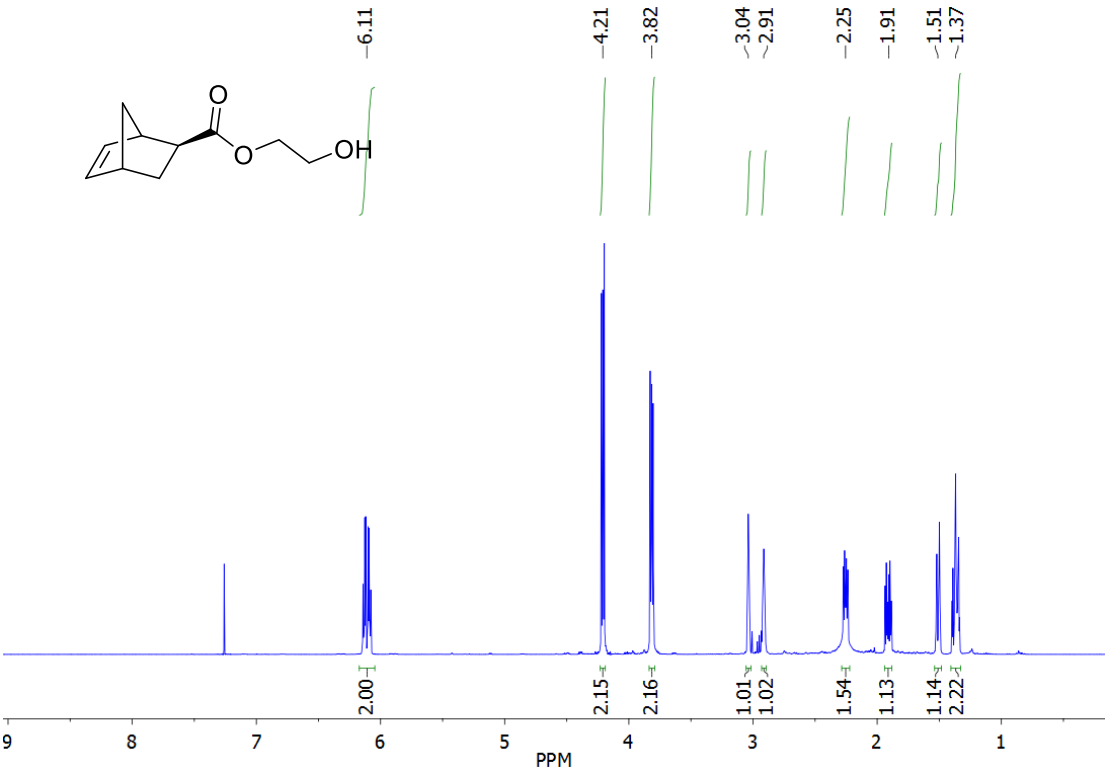

Figure 2S3. ^{1}H NMR spectrum of Compound V.

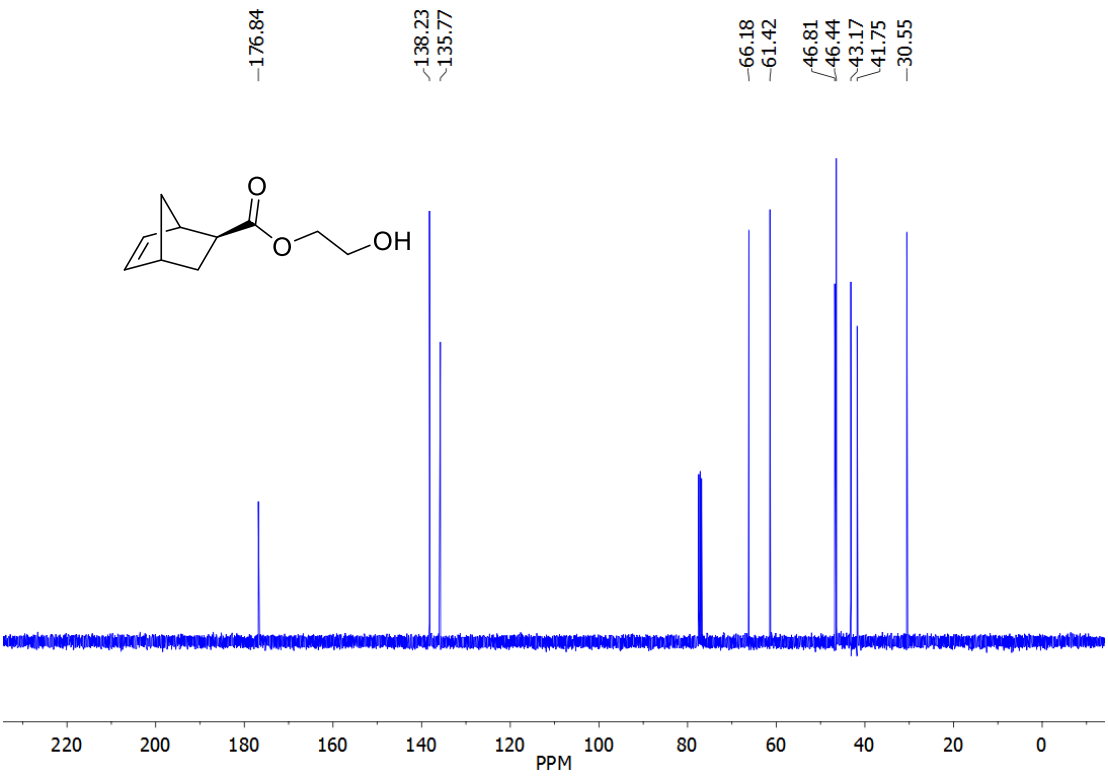

Figure 2S4. ^{13}C NMR spectrum of Compound **V**.

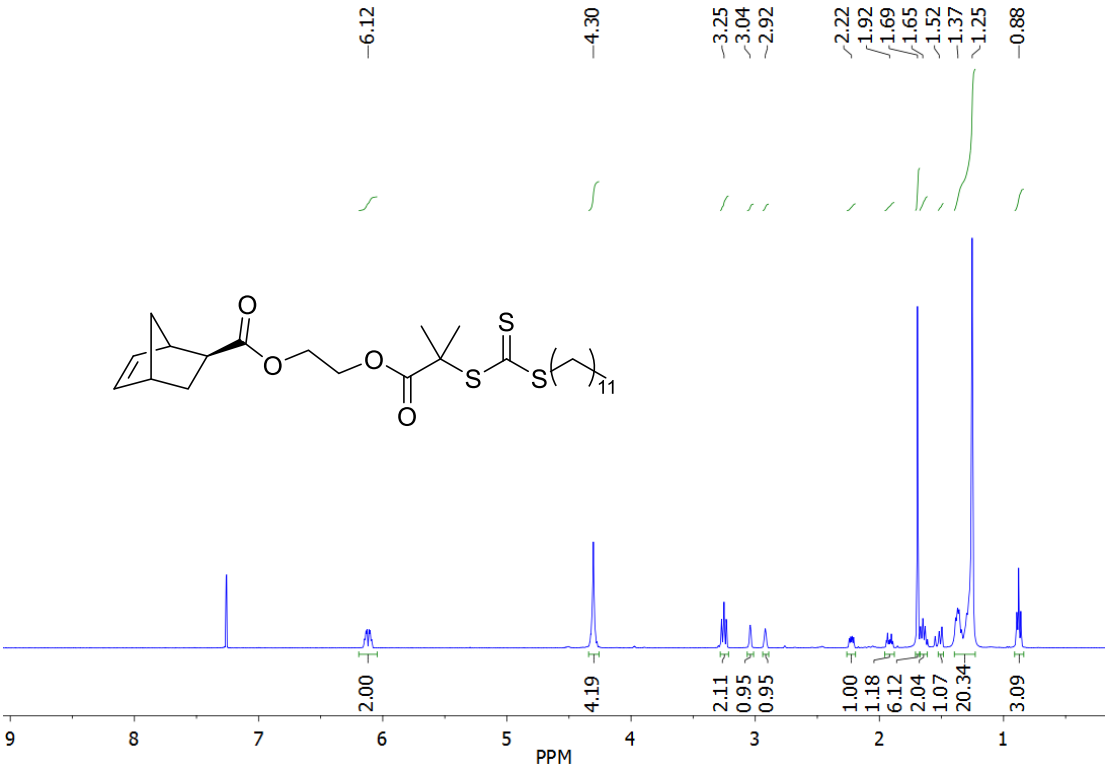

Figure 2S5. ^{1}H NMR spectrum of Compound **VI**.

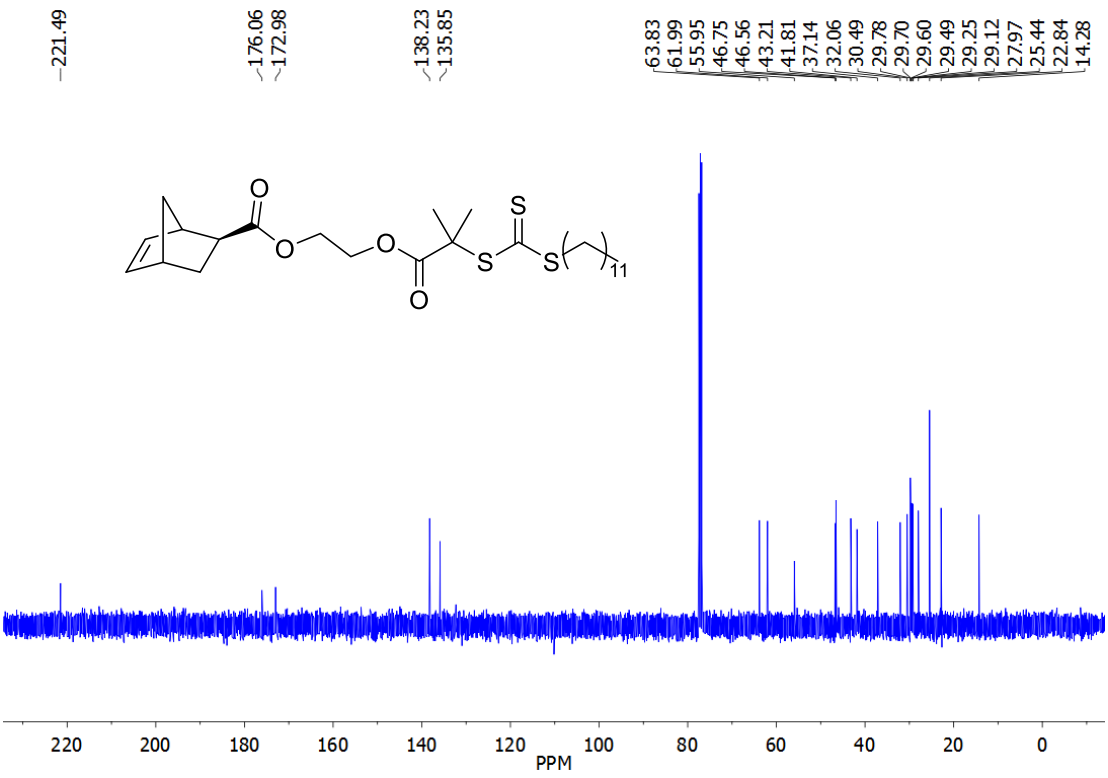

Figure 2S6. ^{13}C spectrum of Compound **VI**.

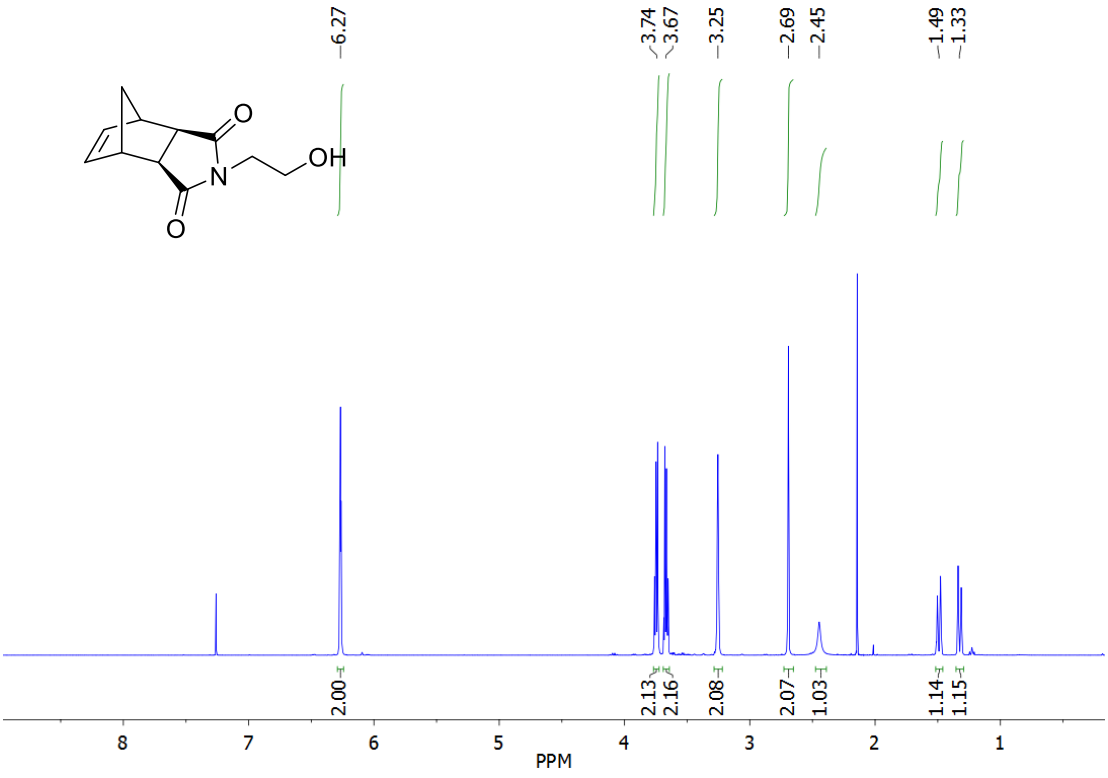

Figure 2S7. ^{1}H NMR spectrum of Compound **IX**.

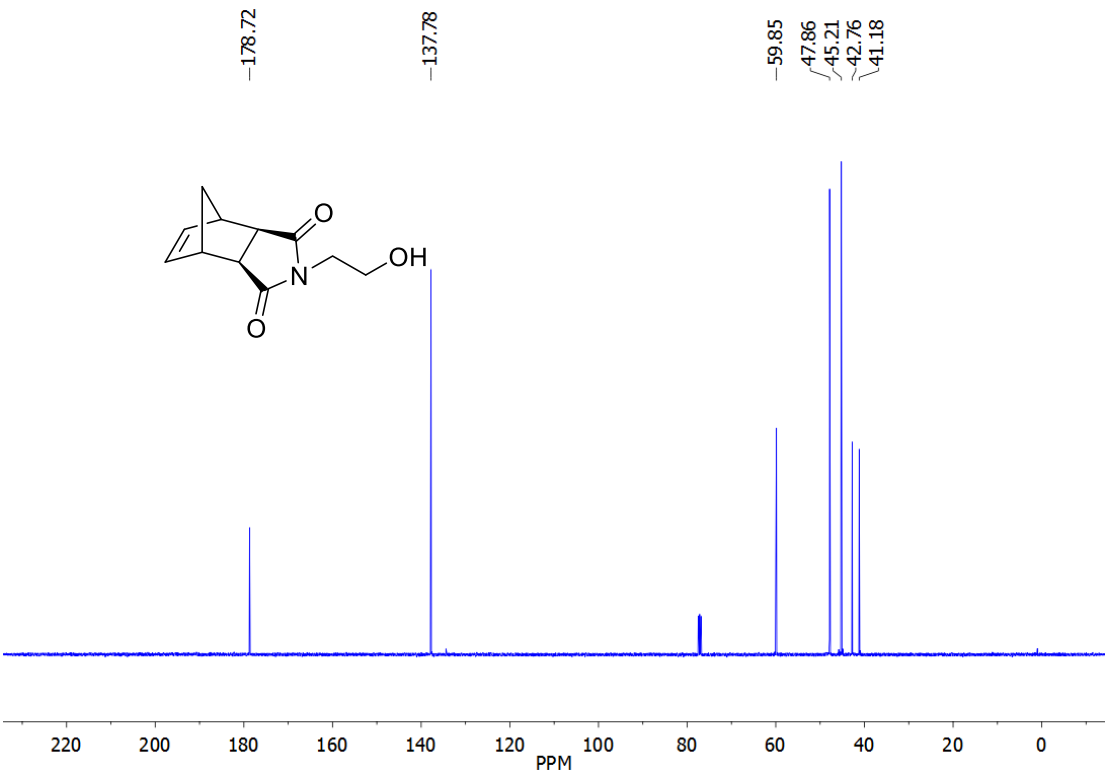

Figure 2S8. ^{13}C spectrum of Compound **IX**.

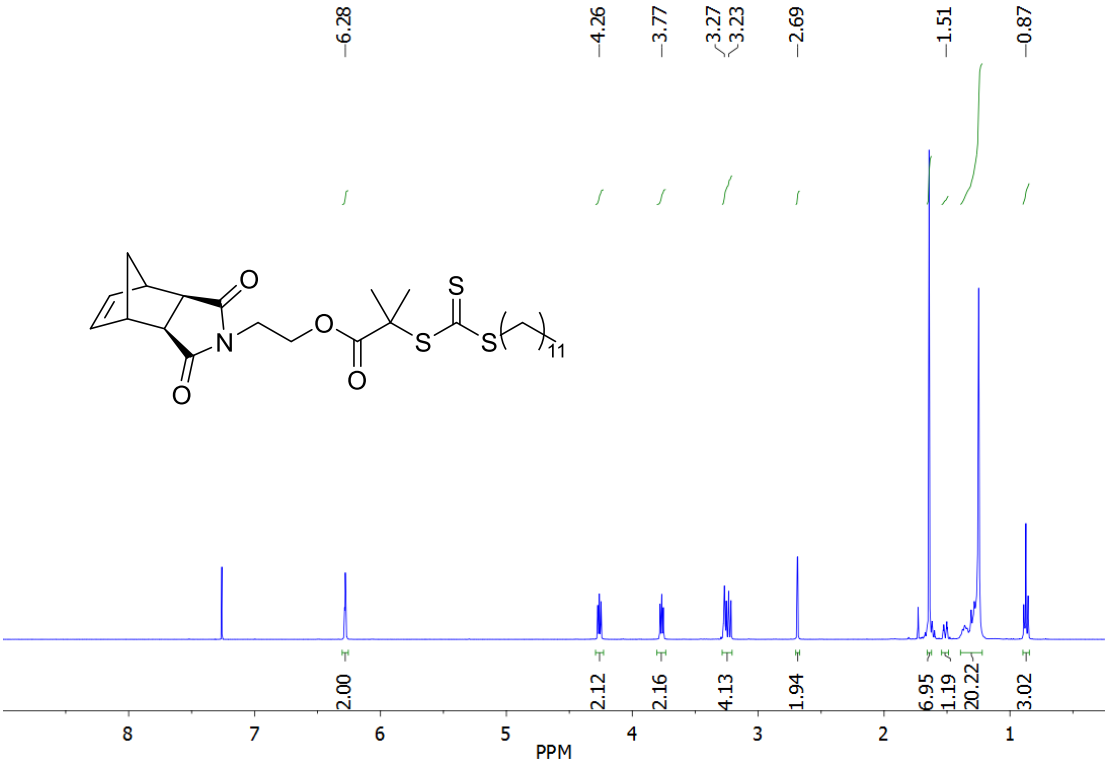

Figure 2S9. ^{1}H NMR spectrum of Compound **X**.

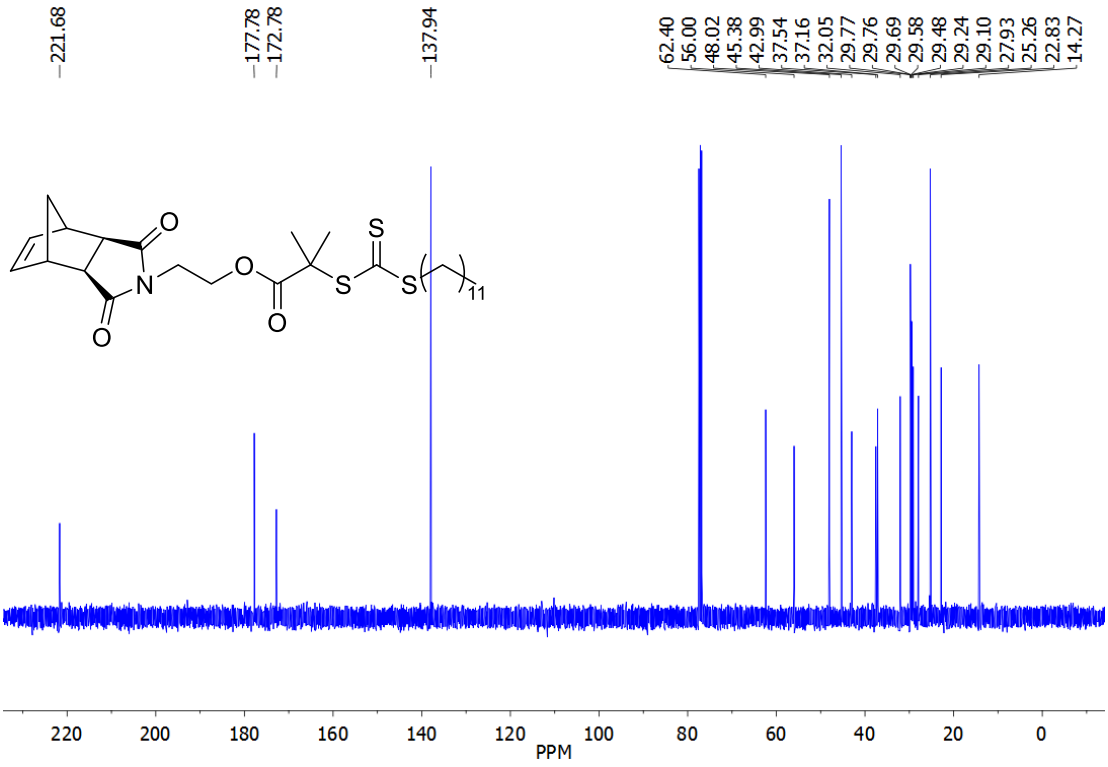

Figure 2S10. ^{13}C NMR spectrum of Compound **X**.

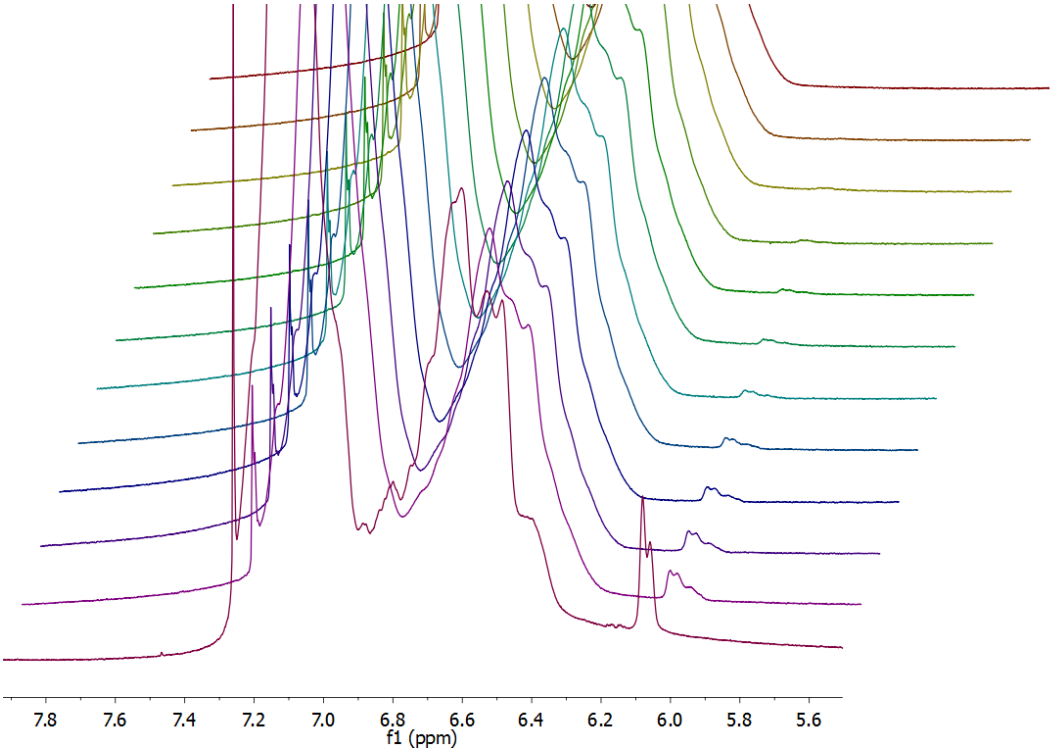

Figure 2S11. Representative spectral data for ^{1}H NMR kinetic experiment of the ROMP of **1S$_{3k}$**. As the polymerization proceeds, the norbornene olefin resonance at ~6 ppm decreases in intensity.

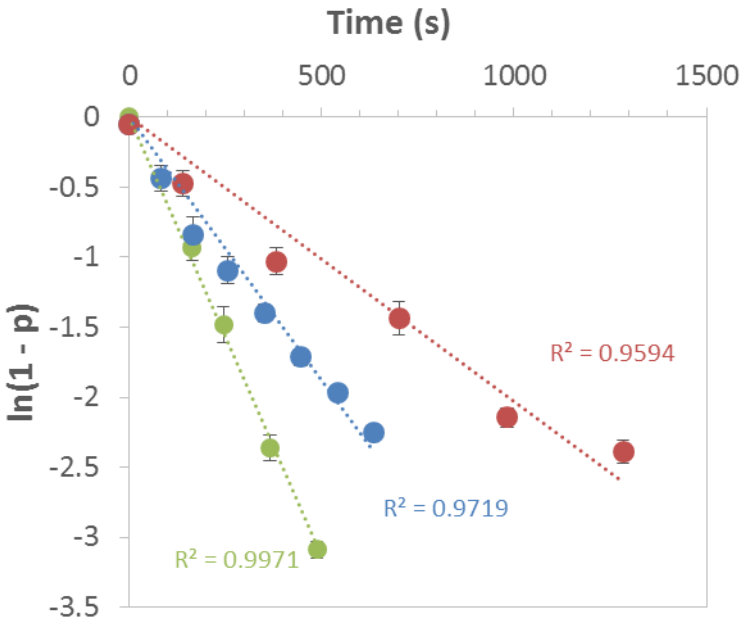

Figure 2S12. *In situ* NMR spectroscopic analysis of ROMP grafting-through of MMs **1-3S$_{3k}$**. Shown above are the log plots of **1S$_{3k}$** (green trace), **2S$_{3k}$** (blue trace), and **3S$_{3k}$** (red trace).

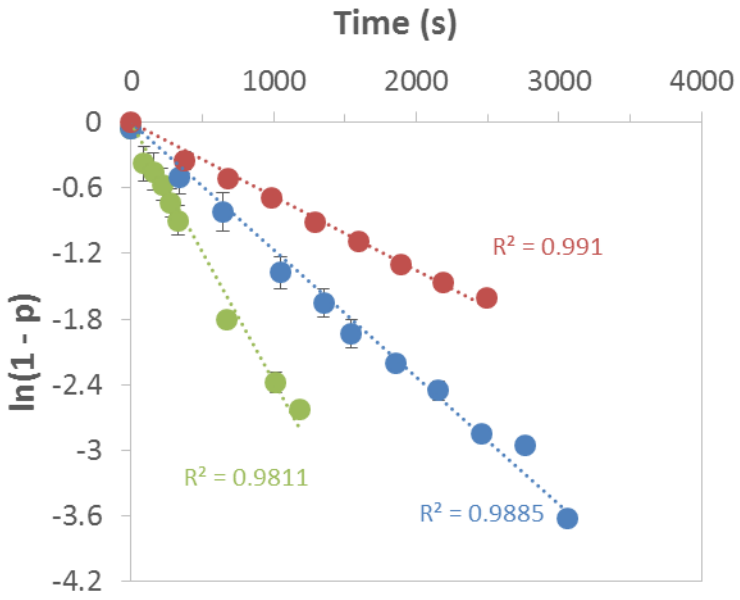

Figure 2S13. *In situ* NMR spectroscopic analysis of ROMP grafting-through of MMs **1-3S$_{5k}$**. Shown above are the log plots of **1S$_{5k}$** (green trace), **2S$_{5k}$** (blue trace), and **3S$_{5k}$** (red trace).

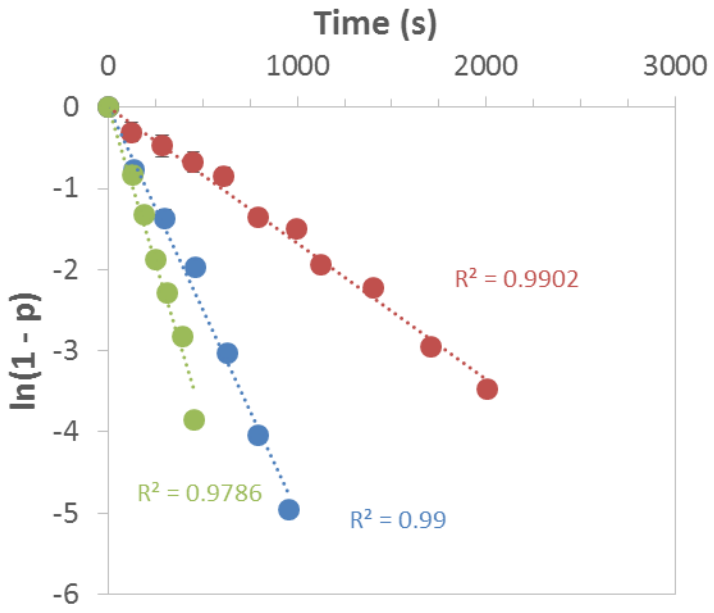

Figure 2S14. *In situ* NMR spectroscopic analysis of ROMP grafting-through of MMs **1-3L$_{4k}$**. Shown above are the log plots of **1L$_{4k}$** (green trace), **2L$_{4k}$** (blue trace), and **3L$_{4k}$** (red trace).

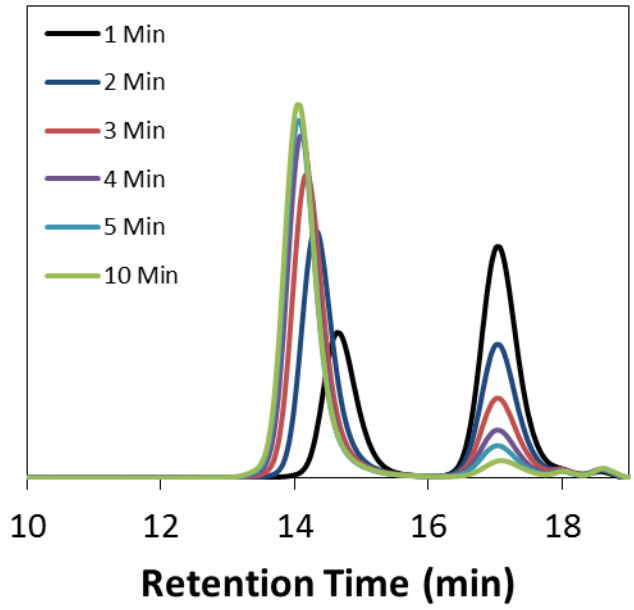

Figure 2S15. SEC kinetic analysis of the ROMP of **1S$_{3k}$**.

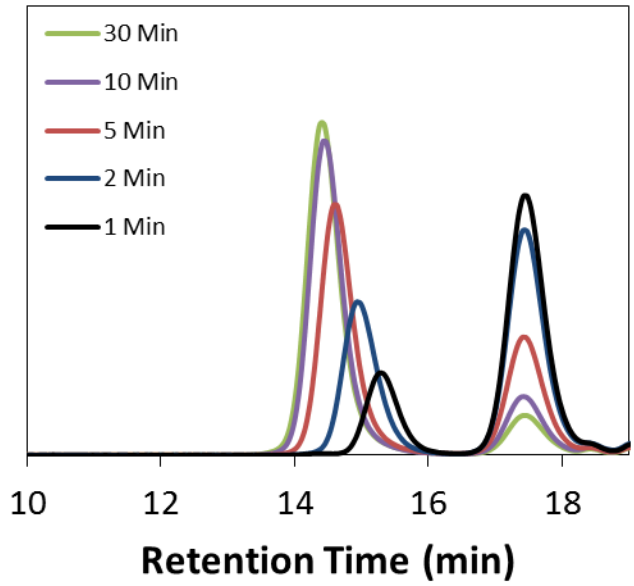

Figure 2S16. SEC kinetic analysis of the ROMP of **2S$_{3k}$**.

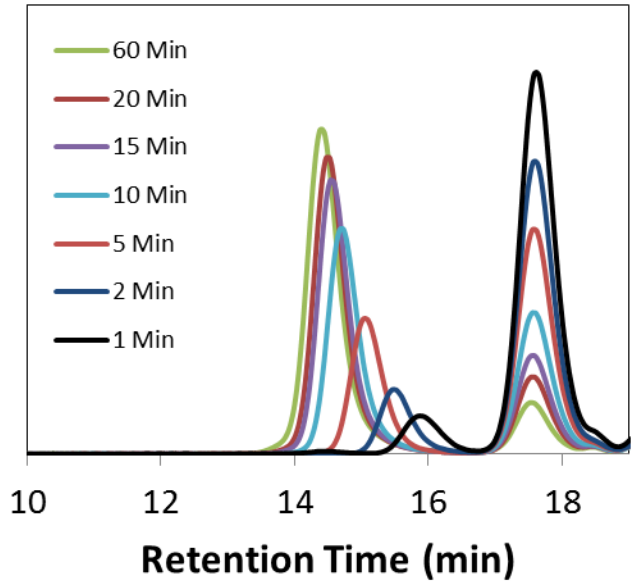

Figure 2S17. SEC kinetic analysis of the ROMP of **3S$_{3k}$**.

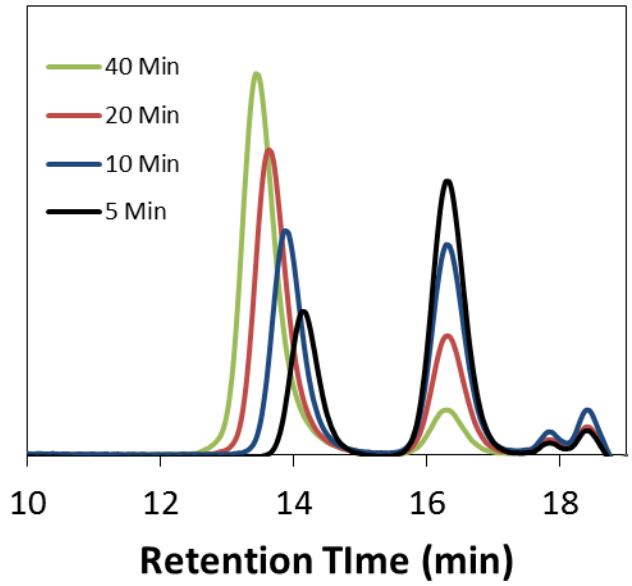

Figure 2S18. SEC kinetic analysis of the ROMP of **2S$_{5k}$**.

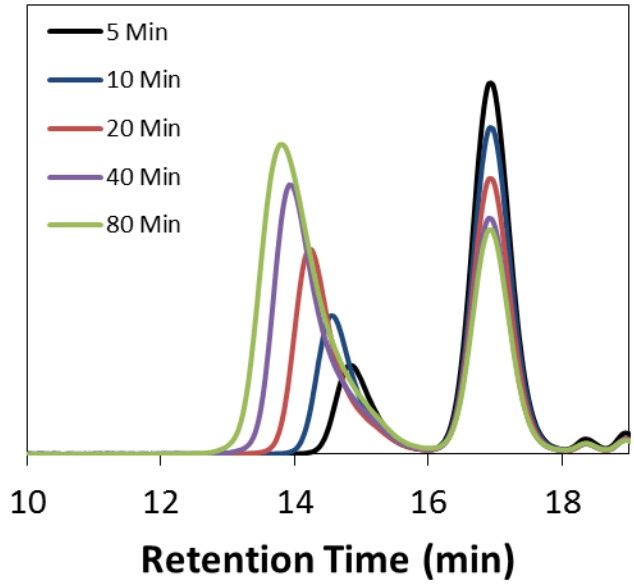

Figure 2S19. SEC kinetic analysis of the ROMP of **3S$_{5k}$**.

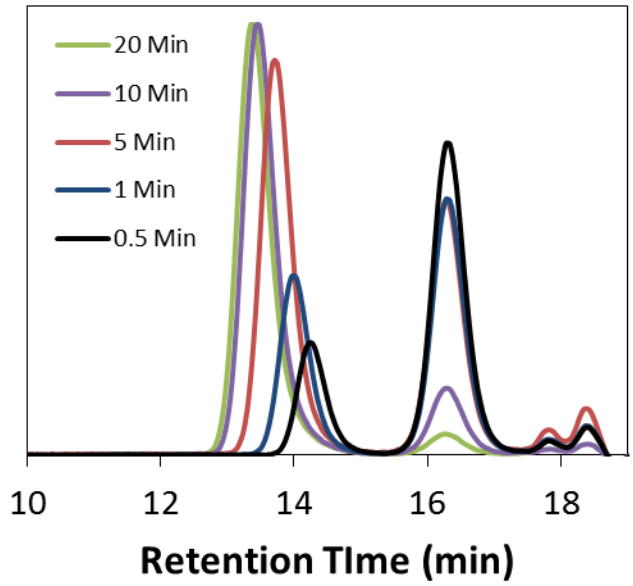

Figure 2S20. SEC kinetic analysis of the ROMP of **1L$_{4k}$**.

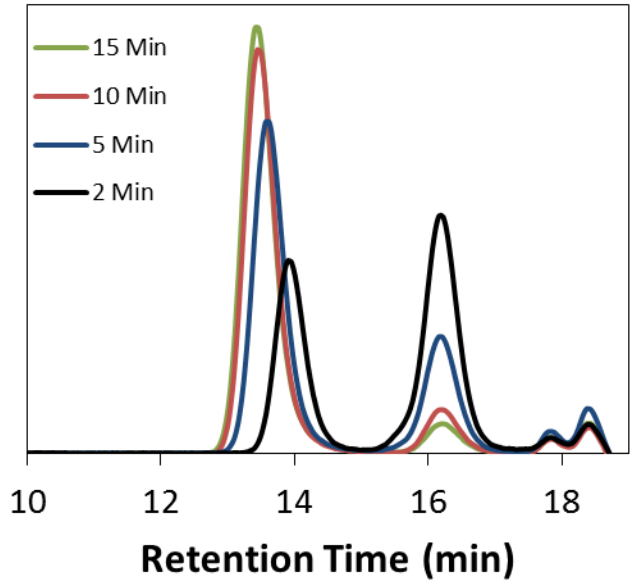

Figure 2S21. SEC kinetic analysis of the ROMP of **2L$_{4k}$**.

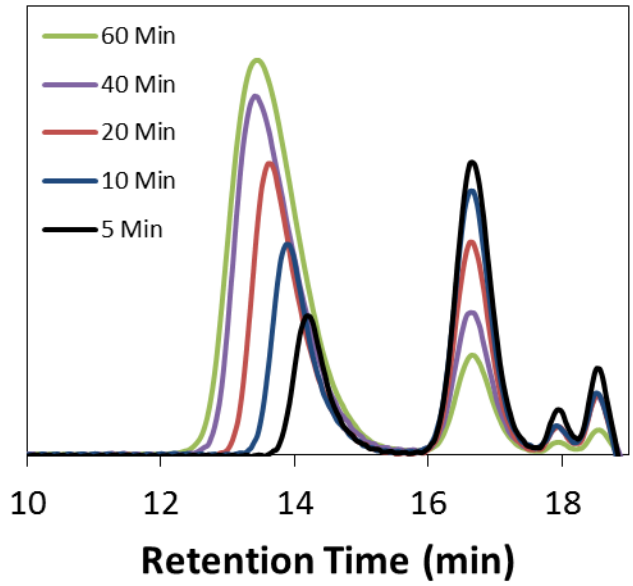

Figure 2S22. SEC kinetic analysis of the ROMP of **3L$_{4k}$**.

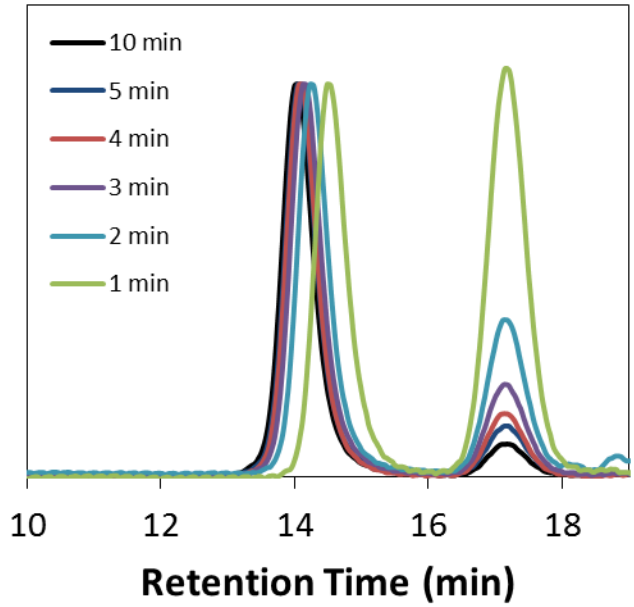

Figure 2S23: SEC kinetic analysis of the ROMP of **1S$_{3k}$** in THF

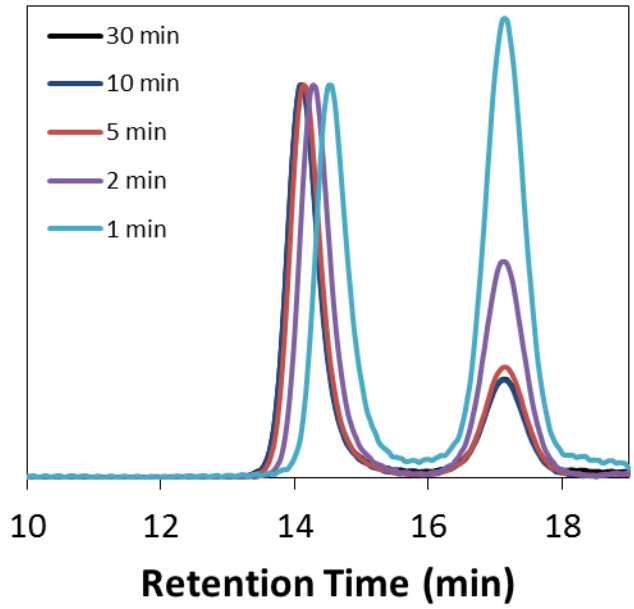

Figure 2S24: SEC kinetic analysis of the ROMP of **2S$_{3k}$** in THF

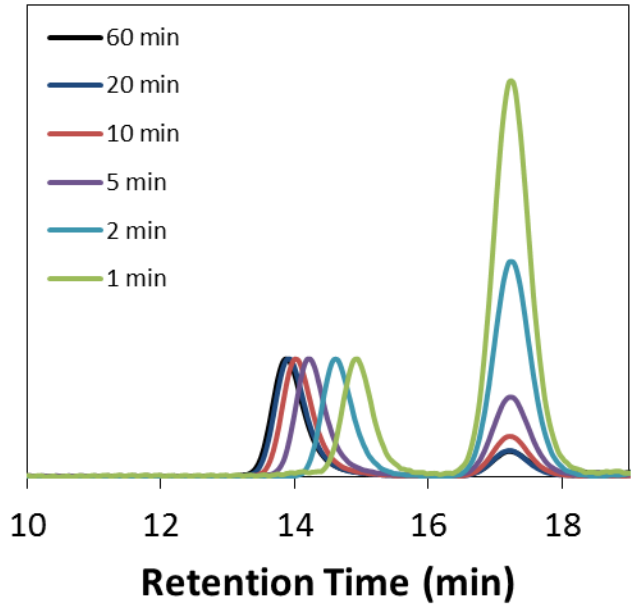

Figure 2S25: SEC kinetic analysis of the ROMP of **3S$_{3k}$** in THF

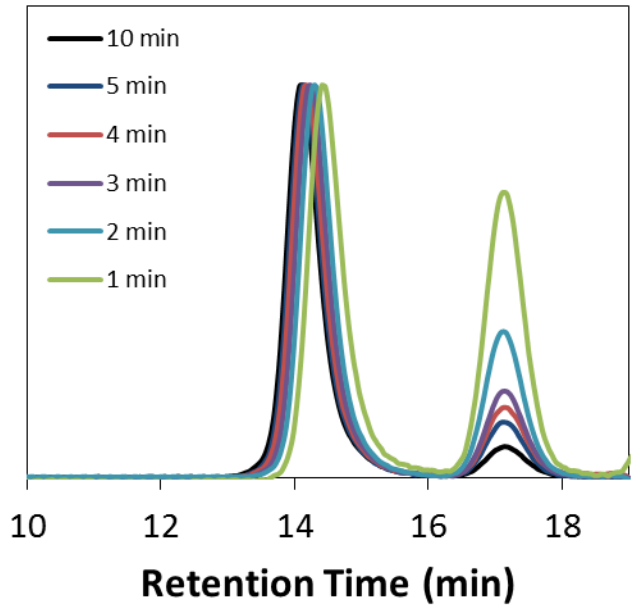

Figure 2S26: SEC kinetic analysis of the ROMP of $\mathbf{1S_{3k}}$ in DCM

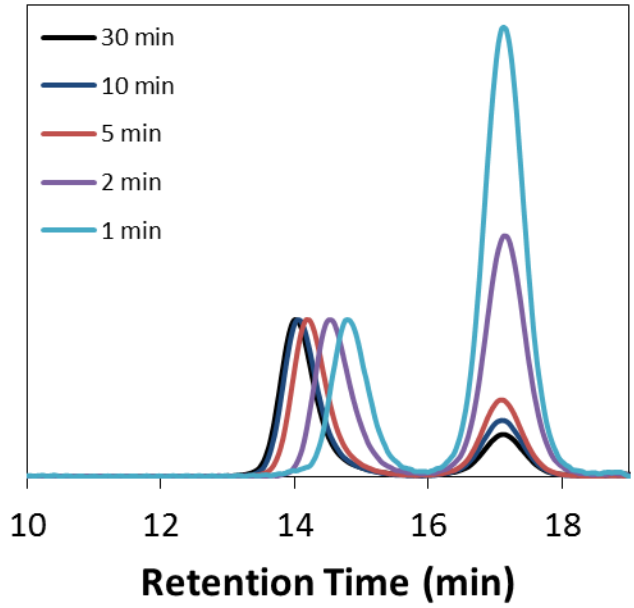

Figure 2S27: SEC kinetic analysis of the ROMP of $\mathbf{2S_{3k}}$ in DCM

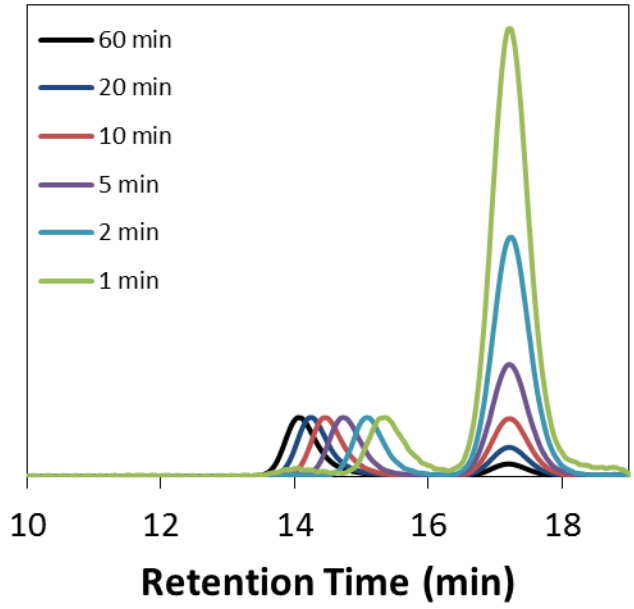

Figure 2S28: SEC kinetic analysis of the ROMP of $\mathbf{3S_{3k}}$ in DCM

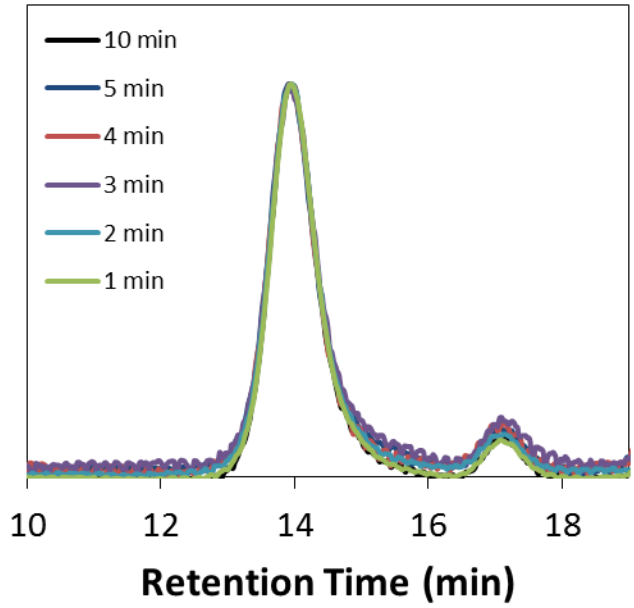

Figure 2S29: SEC kinetic analysis of the ROMP of $\mathbf{1S_{3k}}$ in $CDCl_3$ with 2eq TFA

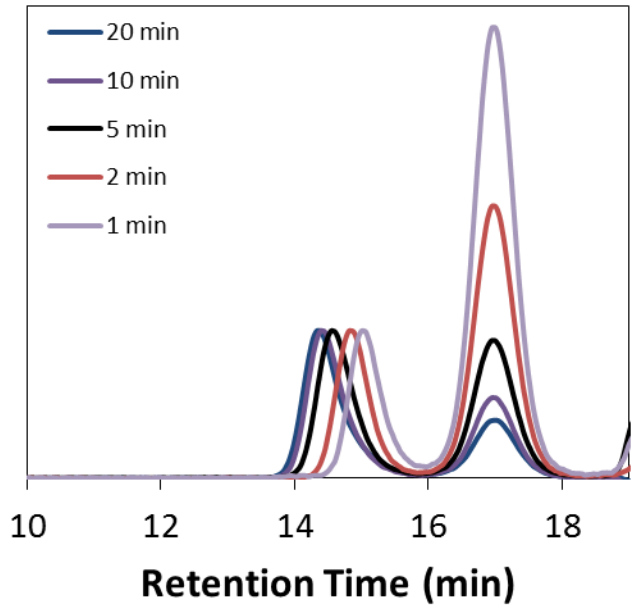

Figure 2S30: SEC kinetic analysis of the ROMP of $\mathbf{2S_{3k}}$ in $CDCl_3$ with 2eq TFA

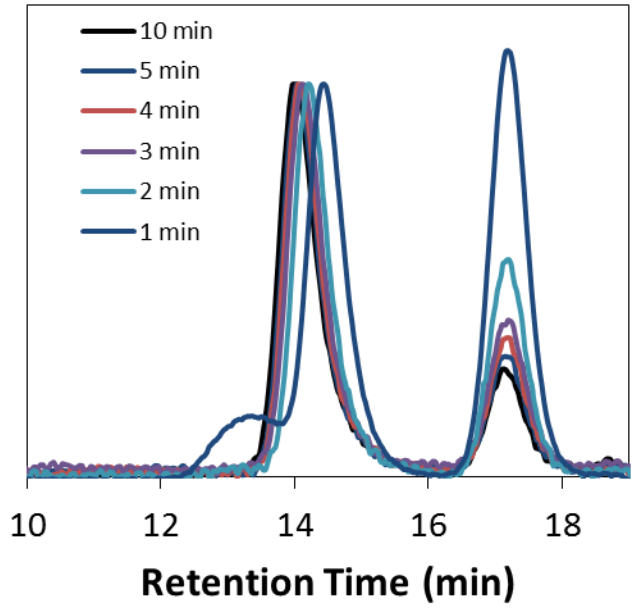

Figure 2S31: SEC kinetic analysis of the ROMP of $\mathbf{3S_{3k}}$ in $CDCl_3$ with 2eq TFA

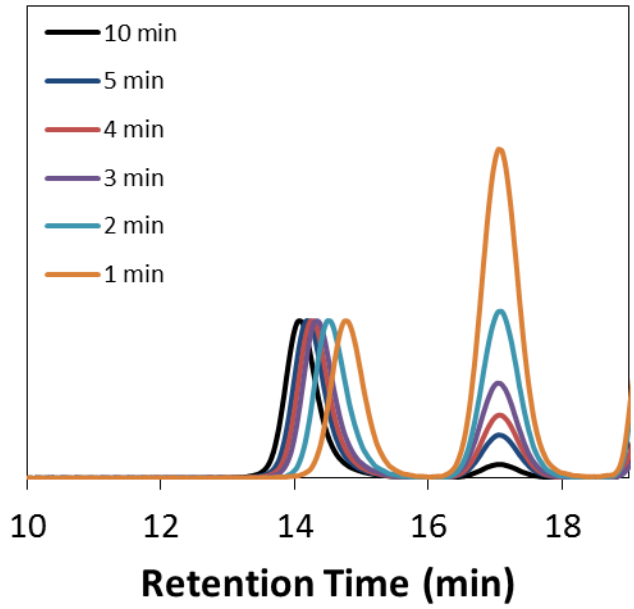

Figure 2S32: SEC kinetic analysis of the ROMP of **1S$_{3k}$** in $CDCl_3$ with 2eq TTIP

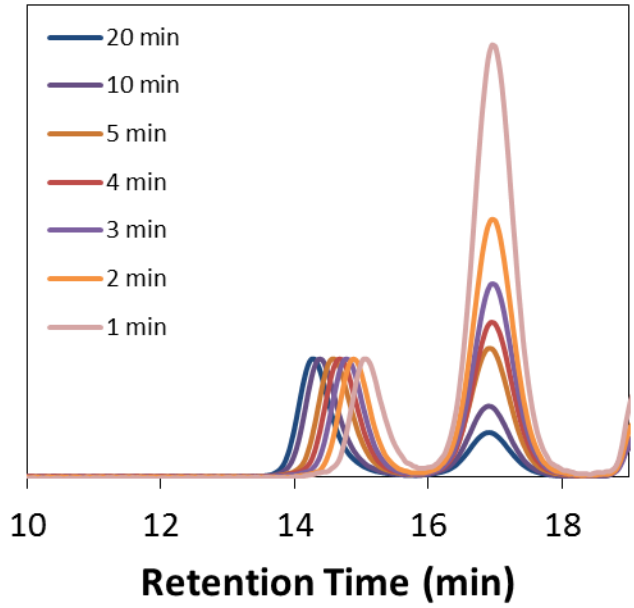

Figure 2S33: SEC kinetic analysis of the ROMP of **2S$_{3k}$** in $CDCl_3$ with 2eq TTIP

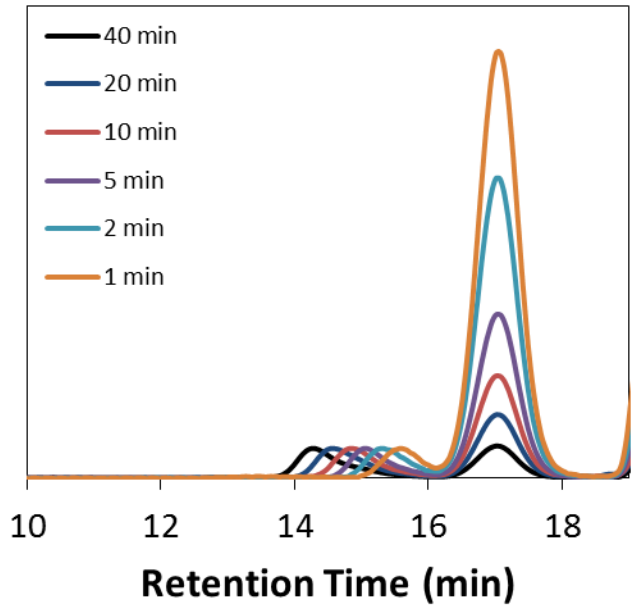

Figure 2S34: SEC kinetic analysis of the ROMP of $\mathbf{3S_{3k}}$ in $CDCl_3$ with 2eq TTIP

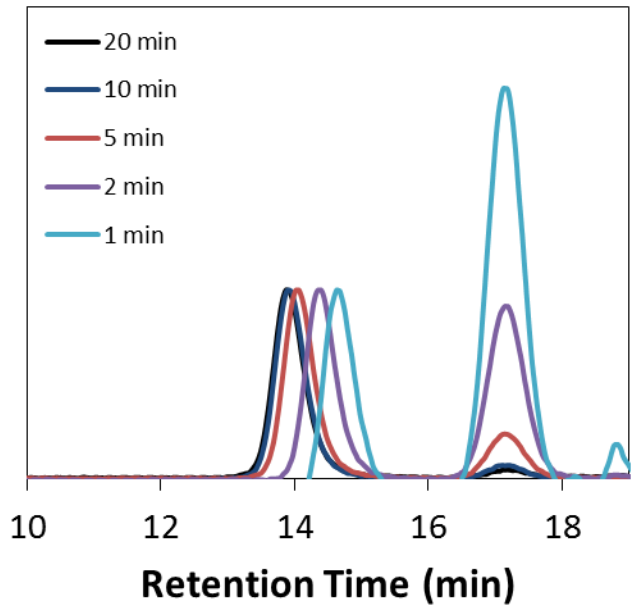

Figure 2S35: SEC kinetic analysis of the ROMP of $\mathbf{1S_{3k}}$ in $CDCl_3$ with 100eq TTIP

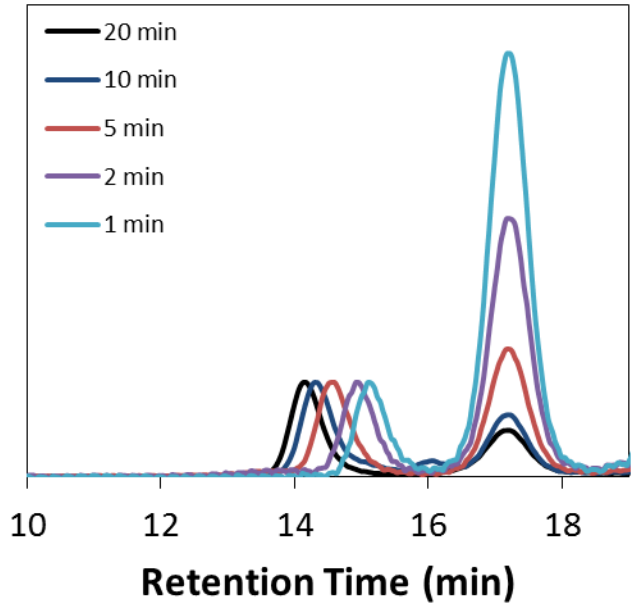

Figure 2S36: SEC kinetic analysis of the ROMP of **$2S_{3k}$** in $CDCl_3$ with 100eq TTIP

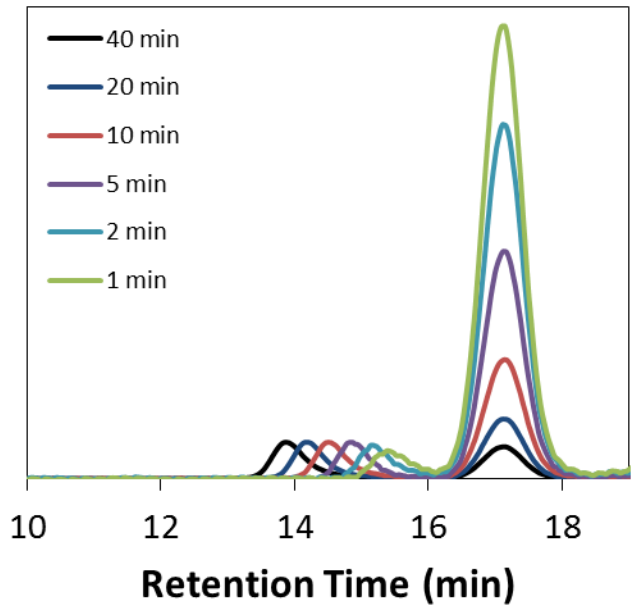

Figure 2S37: SEC kinetic analysis of the ROMP of **$3S_{3k}$** in $CDCl_3$ with 100eq TTIP

Table 2S2: Evaluation of solvents on ROMP of MMs **1-3S$_{3k}$**.

	Solvent k_p (10^{-3} L * mol^{-1} * s^{-1})[a]		
MM	$CDCl_3$	DCM	THF
1S$_{3k}$	8.0	8.2	7.6
2S$_{3k}$	3.6	4.0	4.0
3S$_{3k}$	1.6	2.2	2.2

[a]Determined from MM conversions using SEC.

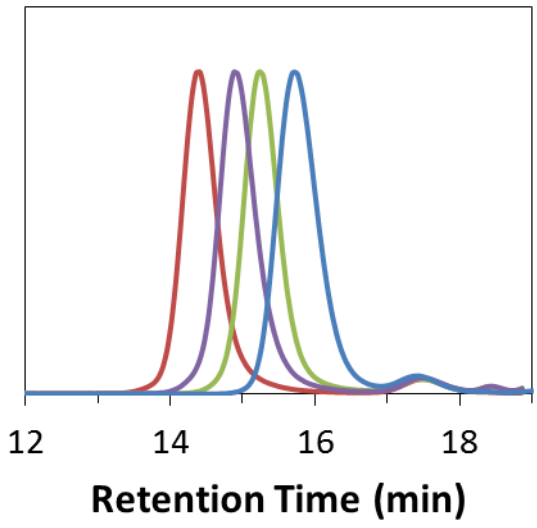

Figure 2S38. SEC traces of ROMP grafting-through of **1S$_{3k}$** using different initial [MM]/[**G3**] ratios ([MM]/[**G3**] values are: blue trace = 10; green trace = 25; purple trace = 50; red trace = 100). The peak at ~17.5 min in all traces corresponds to initiator-derived species that did not undergo grafting-through.

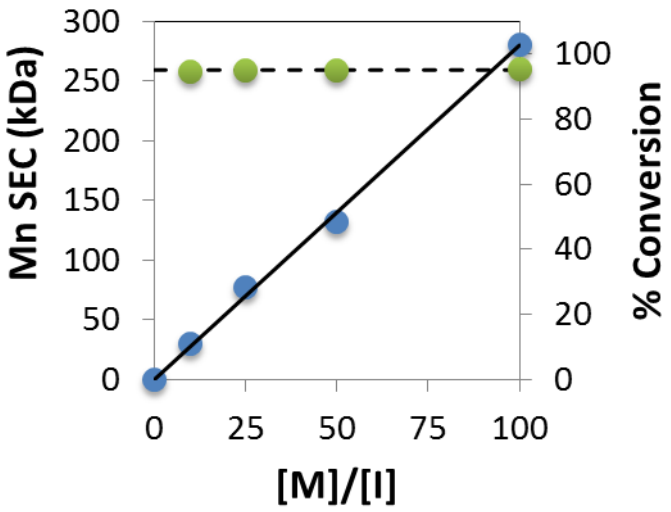

Figure 2S39. "Livingness" plot of ROMP grafting-through of **1S$_{3k}$** using different initial [M]/[I] ratios (blue circles), highlighting a maximum conversion of 95% for all trials (green circles). The residual 5% corresponds to initiator-derived, or "residual", MMs.

Theoretical Calculations:

All density functional theory calculations were performed using the Gaussian 09[4] suite of software. Geometries were optimized using the B3LYP functional. For nonmetal atoms, the 6-31G(d) basis set was used, and for Ru, the Lanl2dz basis set and pseudopotential were used. Using these optimized geometries, single-point energies and molecular orbitals were calculated with the M06 density functional and the 6-311+G(d,p) basis set for nonmetal atoms and the SDD basis set and pseudopotential for Ru. Geometry optimizations were performed in the gas phase, and single-point energies and molecular orbitals were calculated with the SMD implicit solvation model with toluene as a solvent.

Figure 2S40 shows the optimized structures for the non-chelated and chelated $(H_2IMes)(Cl)_2Ru$=MM alkylidenes with truncated models of macromonomers MM1, MM2, and MM3. For catalysts **1** and **2**, chelation is possible through binding of the Ru atom to either the O-sp^2 atom or the O-sp^3 atom in the ligand. In these cases, both chelated structures are shown. Catalyst **3** shows chelation through Ru-Osp^2 bond formation. The energies of each chelated species are given in Table 2S3. For each catalyst, the electronic energies, enthalpies, and Gibbs energies provided are relative to those of the nonchelated species. Figure 2S41 shows orbital density plots for the highest-occupied molecular orbitals for models of the three MMs along with the orbital energy of each HOMO.

Chelation of the Ru alkylidenes from the non-chelated isomers requires a rotation around a Ru=C-C-C dihedral. Figure 2S42 shows a relaxed B3LYP/[6-31G(d) + Lanl2dz] potential energy scan of that dihedral angle for catalyst 3. The chelation process is activated and involves a barrier of ca. 5 kcal/mol.

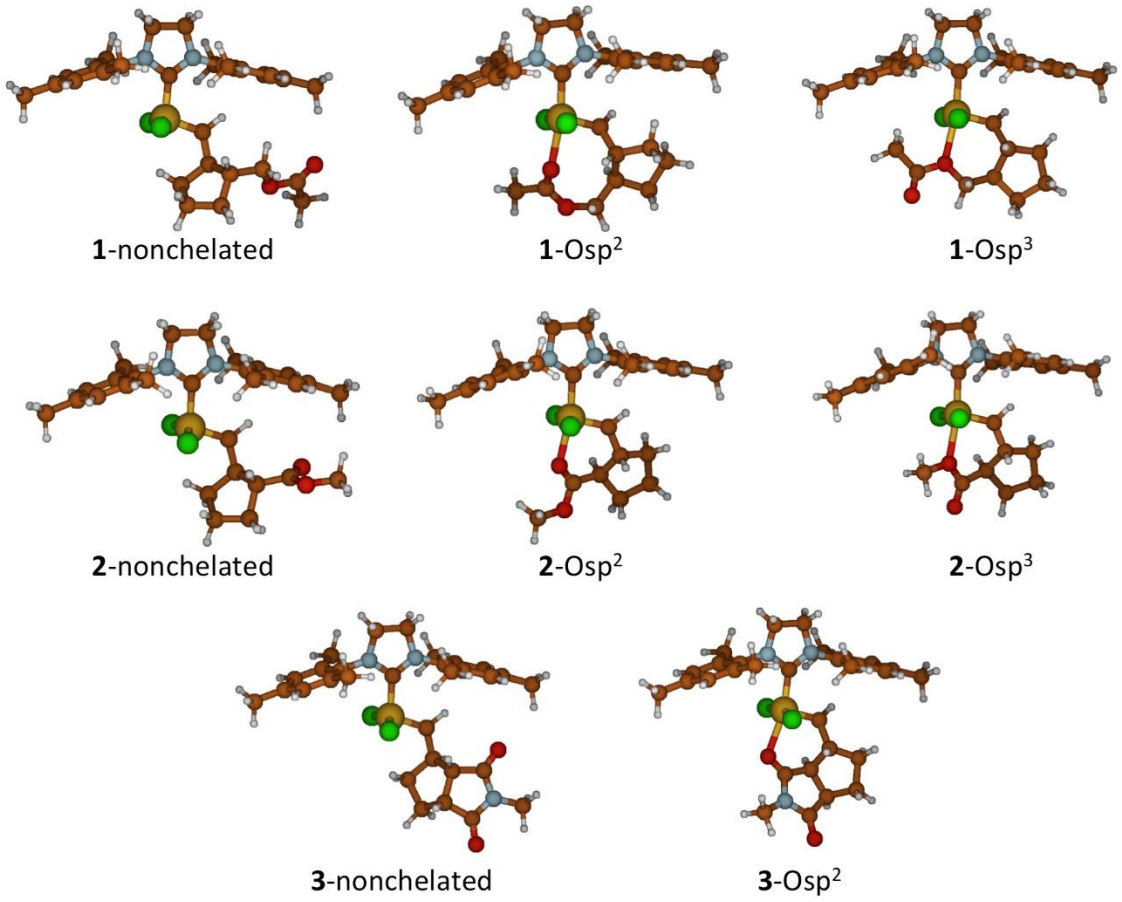

Figure 2S40. B3LYP/[6-31G(d) + Lanl2dz] optimized structures of Grubbs II catalysts in both nonchelated and chelated forms. Color code: Ru: gold, Cl: green, C: brown, N: blue, O: red, H: gray.

Table 2S3. Electronic energies, zero-point corrected electronic energies, enthalpies, and 298K Gibbs free energies (kcal/mol) of the chelated species shown in Figure 2.1. All energies were calculated using M06/[6-311+G(d,p) + SDD]/SMD(toluene)//B3LYP/[6-31G(d) + Lanl2dz] and are given relative to the nonchelated form of each catalyst.

	1-nonchelated	**1**-Osp^2	**1**-Osp^3
ε_0	0.0	-1.8	-5.9
ε_0+ZPE	0.0	-1.3	-5.6
ΔH	0.0	-1.6	-5.7
ΔG	0.0	0.1	-4.9
	2-nonchelated	**2**-Osp^2	**2**-Osp^3
ε_0	0.0	-4.2	-3.3
ε_0+ZPE	0.0	-4.0	-3.2
ΔH	0.0	-4.1	-3.3
ΔG	0.0	-3.8	-2.9
	3-nonchelated	**3**-Osp^2	
ε_0	0.0	-1.4	
ε_0+ZPE	0.0	-1.0	
ΔH	0.0	-1.2	
ΔG	0.0	0.1	

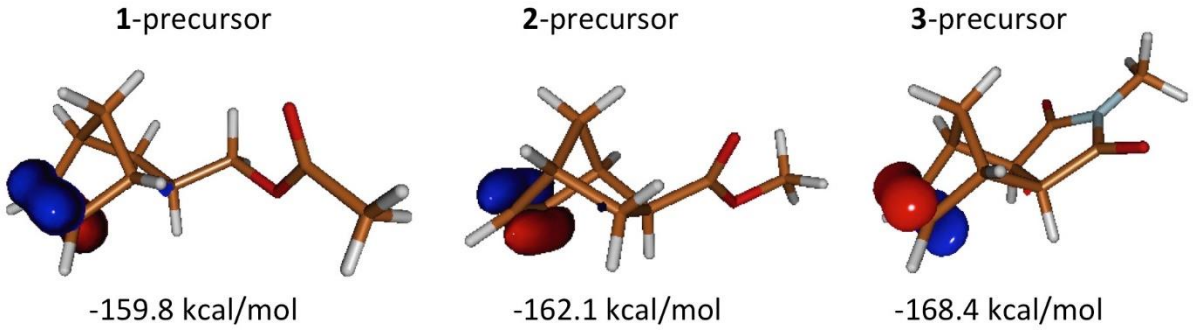

Figure 2S41. Highest-occupied molecular orbital density plots and HOMO energies for the precursors to complexes **1**, **2**, and **3**.

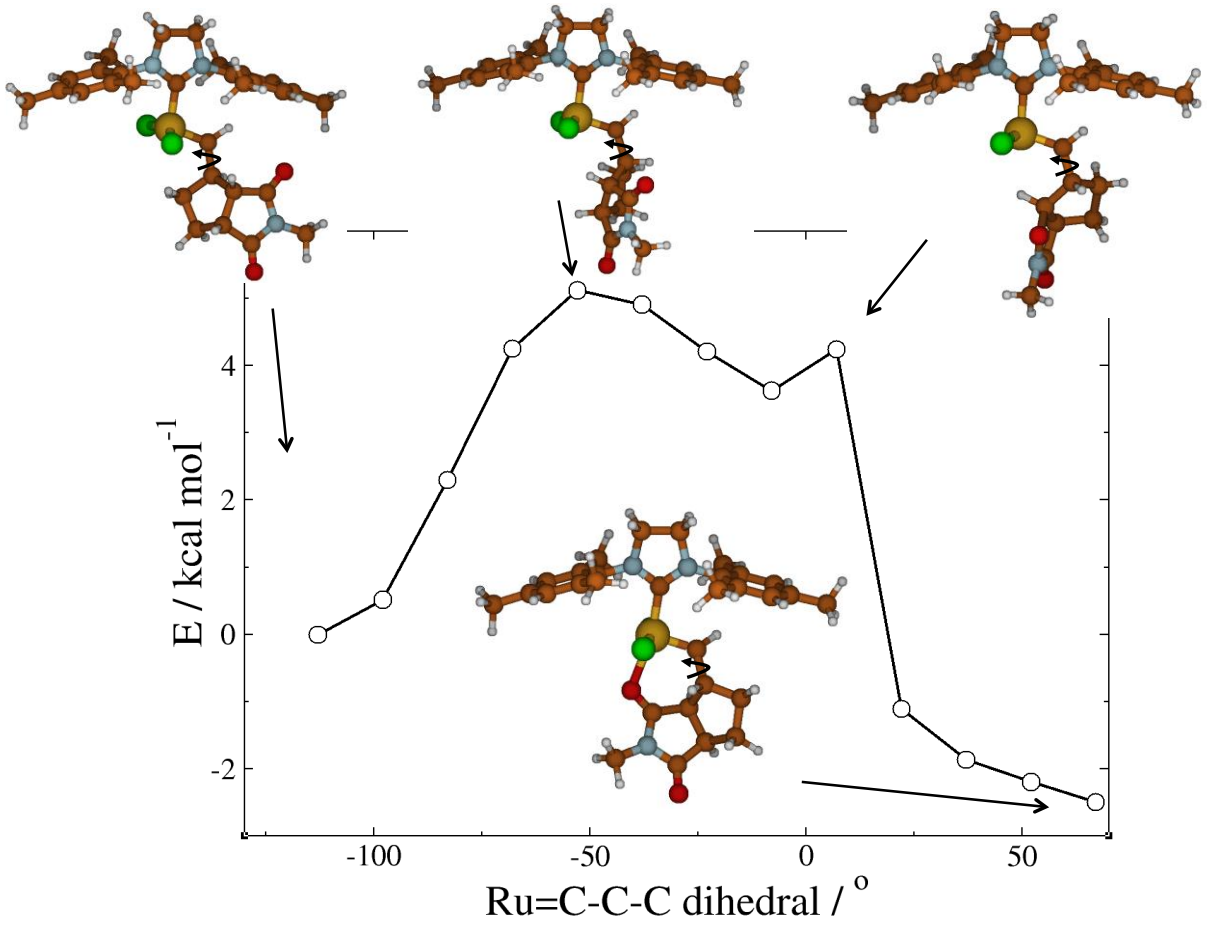

Figure 2S42. Potential energy scan of the Ru=C-C-C dihedral angle that results in the chelated isomer of Catalyst 3 from the non-chelated isomer.

References

1. Skey, J.; O'Reilly, R. K. *Chem. Commun.* **2008**, 4183.
2. Radzinski, S. C.; Foster, J. C.; Matson, J. B. *Macromol. Rapid Commun. DOI:10.1002/marc.201500672*
3. Radzinski, S. C.; Foster, J. C.; Matson, J. B. *Polym. Chem.* **2015**, *6*, 5643.
4. Gaussian 09, Revision **D.01**, Frisch, M. J.; Trucks, G. W.; Schlegel, H. B.; Scuseria, G. E.; Robb, M. A.; Cheeseman, J. R.; Scalmani, G.; Barone, V.; Mennucci, B.; Petersson, G. A.; Nakatsuji, H.; Caricato, M.; Li, X.; Hratchian, H. P.; Izmaylov, A. F.; Bloino, J.; Zheng, G.; Sonnenberg, J. L.; Hada, M.; Ehara, M.; Toyota, K.; Fukuda, R.; Hasegawa, J.; Ishida, M.; Nakajima, T.; Honda, Y.; Kitao, O.; Nakai, H.; Vreven, T.; Montgomery, J. A., Jr.; Peralta, J. E.; Ogliaro, F.; Bearpark, M.; Heyd, J. J.; Brothers, E.; Kudin, K. N.; Staroverov, V. N.; Kobayashi, R.; Normand, J.; Raghavachari, K.; Rendell, A.; Burant, J. C.; Iyengar, S. S.; Tomasi, J.; Cossi, M.; Rega, N.; Millam, J. M.; Klene, M.; Knox, J. E.; Cross, J. B.; Bakken, V.; Adamo, C.; Jaramillo, J.; Gomperts, R.; Stratmann, R. E.; Yazyev, O.; Austin, A. J.; Cammi, R.; Pomelli, C.; Ochterski, J. W.; Martin, R. L.; Morokuma, K.; Zakrzewski, V. G.; Voth, G. A.; Salvador, P.; Dannenberg, J. J.; Dapprich, S.; Daniels, A. D.; Farkas, Ö.; Foresman, J. B.; Ortiz, J. V.; Cioslowski, J.; Fox, D. J. Gaussian, Inc., Wallingford CT, 2009.

Chapter 3: Preparation of Bottlebrush Polymers via a One-Pot Ring-Opening Polymerization (ROP) and Ring-Opening Metathesis Polymerization (ROMP) Grafting-Through Strategy

3.1 Authors

S. C. Radzinski, J. C. Foster, and J. B. Matson

Department of Chemistry and Macromolecules Innovation Institute, Virginia Tech, Blacksburg, Virginia 24061, United States

3.2 Abstract

Bottlebrush polymers were synthesized using a tandem ring-opening polymerization (ROP) and ring-opening metathesis polymerization (ROMP) strategy. For the first time, ROP and ROMP were conducted sequentially in the same pot to yield well-defined bottlebrush polymers with molecular weights in excess of 10^6 Da. The first step of this process involved the synthesis of a polylactide macromonomer (MM) via ROP of D,L-lactide initiated by an alcohol-functionalized norbornene. ROMP grafting-through was then carried out in the same pot to produce the bottlebrush polymer. The applicability of this methodology was evaluated for different MM molecular weights and bottlebrush backbone degrees of polymerization. Size-exclusion chromatographic and ^{1}H NMR spectroscopic analyses confirmed excellent control over both polymerization steps. In addition, bottlebrush polymers were imaged using atomic force microscopy (AFM) and stain-free transmission electron microscopy (TEM) on graphene oxide.

3.3 Introduction

Bottlebrush polymers have received substantial research interest in recent years due to their unique topology and interesting mechanical and rheological properties, which arise from steric repulsion between neighboring polymeric side chains along a large macromolecular backbone.[1] These steric interactions cause the backbone polymer to adopt a chain-extended conformation, leading to a cylindrical, worm-like, or spherical morphology in solution.[2-4] In addition, the dense packing of polymer side chains along the bottlebrush polymer backbone hinders chain entanglement, which provides properties that are useful in applications such as sound-damping materials, rheological modifiers, and super-soft elastomers.[5-8]

Several methods are employed to synthesize bottlebrush polymers including grafting-from,[9-11] grafting-to,[12,13] transfer-to (the Z-group approach),[14-16] and grafting-through.[17-20] Grafting-from polymerization involves the synthesis of a polymeric backbone with many pendant initiating sites. The polymer side chains are then grown from the backbone in a separate reaction. The grafting-to strategy involves the separate synthesis of both the backbone polymer and side-chain polymers. The two species are then allowed to react to couple the side-chain polymers to the backbone, typically via click chemistry. The transfer-to approach is a hybrid between grafting-from and grafting-to in which a polymer backbone is synthesized with pendant chain transfer agents. During transfer-to polymerization, growing polymer chains propagate in solution and reattach to the backbone through a chain transfer event. While the methods above can produce high molecular weight (MW) polymers, they all suffer from imperfect grafting densities, meaning that not every repeat unit along the bottlebrush backbone is functionalized with a polymer side-chain. The grafting-through strategy, also known as the macromonomer approach, involves the use of a pre-formed polymer with a polymerizable chain end (the macromonomer).

The chain end can then be polymerized in a second step using various chemistries to form a bottlebrush polymer with theoretically complete grafting density.

The synthetic strategies that are most often employed to synthesize bottlebrush polymers by the grafting-through approach are reversible addition-fragmentation chain transfer (RAFT) polymerization, atom transfer radical polymerization (ATRP), ring-opening polymerization (ROP), and/or ring-opening metathesis polymerization (ROMP). Macromonomers (MMs) are typically synthesized using a controlled or living polymerization technique to ensure the polymers have low dispersities (Đ) and high chain end fidelity, the latter of which is essential for an effective grafting-through polymerization. Once isolated, macromonomers with one polymerizable chain end are subjected to a grafting-through reaction to form a bottlebrush polymer. Frequently, grafting-through polymerization is accomplished using ROMP with a fast-initiating olefin metathesis catalyst.[18,21,22] ROMP is ideal for this process due to its high functional group tolerance, fast reaction times, and living character, typically leading to the formation of bottlebrush polymers with controllable backbone and side-chain MWs by the grafting-through process.

The synthesis of bottlebrushes via grafting-through using one or more of the techniques listed above often requires purification of the MM prior to the bottlebrush formation step. MM purification usually consists of multiple precipitation steps that consume large amounts of solvent and can be especially tedious for polymers with low glass transition temperatures (e.g., polyacrylates), which typically do not precipitate well. Only a few reports describe bottlebrush polymers prepared using a one-pot strategy where purification is not needed between the two polymerization steps. Both Wooley and Novak have shown the viability of a one-pot grafting-from strategy using ROMP and ATRP in which a polynorbornene with pendant ATRP initiators

is first grown via ROMP followed by ATRP in the second step to grow the polymer side-chains.[23,24] This method produced bottlebrush polymers with high MWs but lower than complete grafting densities, as expected when using the grafting-from strategy. Wooley also reported a one-pot, two-step process using the grafting-through technique wherein macromonomers were first polymerized via RAFT, the reaction mixture was then cooled to quench the radical polymerization, and finally Grubbs' catalyst was added to form the bottlebrush polymer.[25] This process yielded well-defined bottlebrush polymers with complete grafting densities in a one-pot method, although it is limited to MMs derived from vinyl monomers that are sterically hindered and electron deficient to avoid unwanted chain transfer reactions during ROMP.[26] To expand the scope of bottlebrush polymers that can be prepared rapidly and efficiently, we envisioned a ROP-ROMP strategy to produce bottlebrush polymers using a one-pot, two-step technique. In this report, we explore the compatibility of the ROP and ROMP reactions to produce bottlebrush polymers with polylactide (PLA) side-chains. This work represents a new synthetic methodology to accomplish the facile, one-pot, tandem ROP and ROMP grafting-through polymerization of molecular brushes with controllable side-chain and backbone MWs.

3.4 Results and Discussion

The process of synthesizing a bottlebrush polymer in a one-pot, two-step sequence requires control of both the synthesis of the MM and the grafting-through process. In addition, the polymerization techniques employed must necessarily be orthogonal. ROP of lactones (e.g., lactide) is potentially compatible with ROMP, as the ROP reaction does not involve an olefin-containing monomer. Of the many catalysts capable of mediating ROP, we chose the recently reported DBU/benzoic acid co-catalyst system (DBU = 1,8-diazabicycloundec-7-ene) due to its ability to maintain high end group fidelity, produce low dispersity polymers, and enable a high

degree of control over the polymerization.[27,28] We therefore aimed to evaluate whether a one-pot ROP-ROMP bottlebrush polymer synthesis would be possible using this ROP catalyst system.

We first investigated the ROP reaction using a norbornene-containing alcohol initiator. ROP of D,L-lactide was conducted in CH_2Cl_2 in the presence of a DBU/benzoic acid co-catalyst, (Scheme 3.1). Molecular sieves were employed in the polymerizations to minimize adventitious water that could initiate polymerization, which would result in the formation of polymeric species lacking norbornene moieties on their chain termini. Polymerizations were conducted at rt with aliquots taken at various timepoints to monitor MW evolution.

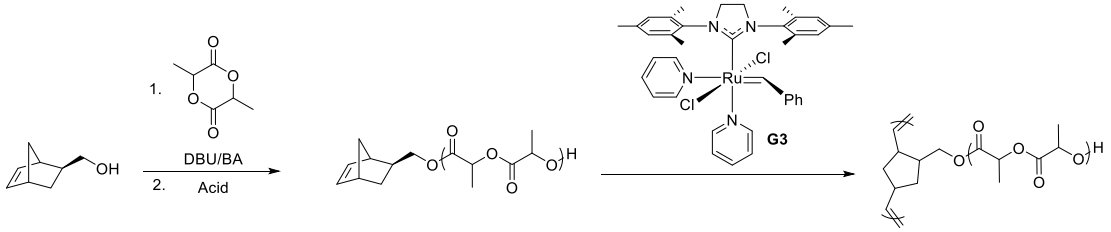

Scheme 3.1: One-pot synthesis of a bottlebrush polymer with PLA side chains.

Analysis of the resulting polymers by ^{1}H NMR spectroscopy and size exclusion chromatography (SEC) was conducted to assess polymerization kinetics and control of MW. The data revealed excellent control over the polymerization, evident in MW distributions with low Đ, good agreement between theoretical and experimental MWs, and high chain end fidelity (determined via end group analysis by ^{1}H NMR spectroscopy). Kinetic analysis showed first-order behavior (with respect to monomer) and a linear correlation between conversion and MW (**Figure 3.1**).

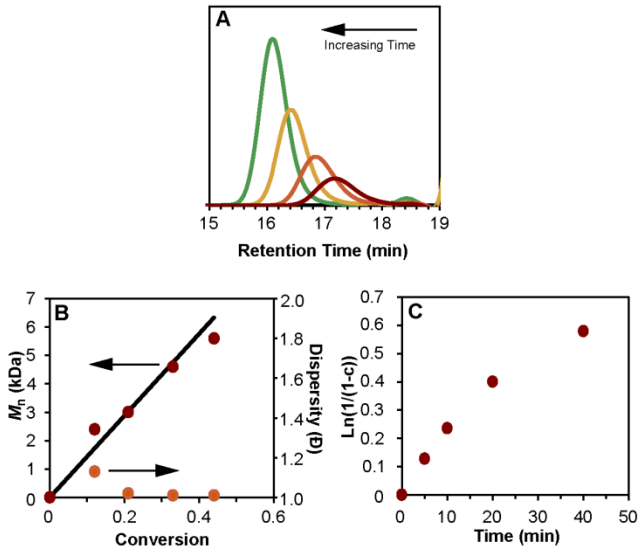

Figure 3.1: Kinetics of polymerization of D,L-lactide using a DBU/BA cocatalyst system. A) SEC traces (refractive index detector) showing decreasing retention time with increasing polymerization time. B) M_n and Đ versus conversion (solid line show theoretical M_n based on conversion as measured by ^{1}H NMR spectroscopy). C) Monomer consumption over time as measured by ^{1}H NMR spectroscopy. Polymerization conditions: [lactide]/[I]/[DBU]/[BA] = 100:1:0.7:0.3, CH_2Cl_2, rt. SEC was carried out in THF at 30 °C with RI and MALLS detectors.

The second step of our one-pot strategy toward bottlebrush polymers uses ROMP as the grafting-through polymerization technique with the highly active Grubbs' living initiator $(H_2IMes)(pyr)_2(Cl)_2Ru$=CHPh (**G3**). Although this catalyst generally exhibits excellent functional group tolerance, some strongly basic functional groups can adversely affect catalyst activity.[29] The ROP reaction mixture contains two functionalities that are potentially problematic for the catalyst: the alkoxide of the growing polymer chain and the tertiary amine of the DBU co-catalyst. Both species would need to be quenched with acid prior to the addition of **G3** to prevent catalyst deactivation. Fortunately, **G3** is typically stable in the presence of many acids; in fact, acetic acid has even been used as the solvent in olefin metathesis reactions.[30]

In order to determine whether addition of acid after the ROP step would fully quench the propagating alkoxide and the DBU catalyst, several different one-pot reactions were attempted (Scheme 3.1). In each, ROP was carried out, and then the polymerization was quenched with an acid. Next, **G3** initiator was added, and the ROMP reaction was allowed to proceed for 1 h. Polymerizations were then quenched with ethyl vinyl ether, and the reaction mixture was analyzed to determine % conversion to bottlebrush and bottlebrush MW. Several different acids were tested to determine which led to the highest conversion. When either acetic acid or benzoic acid was used, conversion to bottlebrush polymer was limited to < 30% (Table 3S1). This indicates that these acids are incapable of fully deactivating the DBU. When stronger acids were employed, tosic acid or trifluoroacetic acid (TFA), the conversions to bottlebrush polymer increased substantially. TFA showed slightly higher conversions to bottlebrush polymers and was chosen for the remainder of the experiments. When TFA was added just before addition of **G3**, conversion to bottlebrush polymer ranged from 80-85% with low Đ (1.07-1.20), indicating good control over ROMP grafting-through. ^{1}H NMR spectroscopy of the crude reaction mixture showed complete consumption of norbornene olefins after the ROMP step, indicating that the macromonomers had chain end functionalizations of approximately 85%. The remaining ~15% of the macromonomers that did not possess α-norbornyl functionality likely arose via initiation by adventitious water or a small degree of transesterification with other species during ROP. While higher conversions have been reported for the synthesis of PLA BB polymers,[31] these systems employed a two-pot procedure where MMs were purified prior to the grafting-through step.

The amount of TFA added after the ROP step was also found to be critical—enough TFA must be added to quantitatively terminate the ROP reaction and protonate the DBU co-catalyst. To

evaluate the effect of TFA concentration, several one-pot reactions were quenched with varying equivalents of TFA. In theory, a minimum of 2 equivalents (relative to initiator) would be required to fully protonate both the propagating alkoxide chain ends and the DBU co-catalyst. Indeed, using less than two equivalents of TFA relative to initiator led to low conversion to bottlebrush polymer, and MWs that were lower than expected (Table 3.1, entries 1 and 2). Addition of two equivalents of TFA was sufficient to achieve near-complete olefin conversion during ROMP (Table 3.1, entries 3-10).

Table 3.11: Summary of one-pot bottlebrush synthesis.

	ROP			**ROMP**				
Entry	M_n MM (Da)[a]	Đ[a]	Equiv. TFA	M:I	Theo. Mn BB (kDa)[b]	M_n BB (kDa)[a]	Đ BB[a]	Conversion[c]
1	4400	1.05	0.5	100	440	118	1.22	0.13
2	4000	1.02	1	100	400	204	1.25	0.51
3	4100	1.03	2	25	102	87.0	1.02	0.81
4	4100	1.03	2	50	205	196	1.08	0.81
5	4100	1.03	2	100	410	400	1.13	0.81
6	4100	1.03	2	200	820	600	1.34	0.77
7	5800	1.01	2	25	145	125	1.13	0.87
8	5900	1.01	2	50	295	280	1.07	0.84
9	5700	1.01	2	100	570	554	1.18	0.82
10	5600	1.02	2	200	1120	1030	1.50	0.80

[a]Measured by SEC using absolute MW determination by MALLS. [b]Expected molecular weight assuming full conversion at defined [M]/[I]. [c]Determined from SEC by comparing the relative integrations of BB and MM peaks.

To evaluate the scope of this technique, bottlebrush polymers with varying side-chain length and backbone degree of polymerization (DP) were synthesized using the one-pot approach. In each, ROP was performed first, targeting a MW of 4000 or 6000 Da for the PLA MM. Next, a specific amount of **G3** was added, targeting backbone DPs of 25, 50, 100, and 200. For the 4 kDa MMs, conversion of MM to BB ranged from 77 to 81%, with the highest conversions achieved for the

lowest targeted [MM]/[I] values (Table 3.1, entries 3-6). The observed decrease in conversion with increasing MM MW is consistent with other reports and results from increased steric hindrance around the propagating catalyst center when using larger MMs.[32,33] MWs remained close to the expected values across the series, and a maximum MW of 600 kDa was achieved when using the largest [MM]/[**G3**] ratio (Table 3.1, entry 6). These experiments were repeated with 6 kDa PLA MMs. For this series, the previously observed trend was conserved—conversions decreased slightly with increasing [MM]/[**G3**] ratios (Table 3.1, entries 7-10). As shown in Figure 3.2B, observed MWs were consistent with expected values based on the initial [MM]/[**G3**] ratio. Using this strategy, bottlebrush polymers with MWs in excess of 1 MDa were achieved (Table 3.1, entry 10).

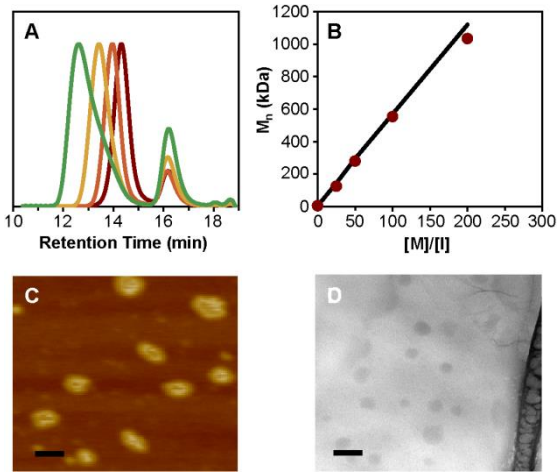

Figure 3.2: Evaluation of bottlebrush polymer synthesis and structure. A) SEC analysis of BB polymers with different [MM]/[**G3**] ratios, showing decreasing retention times as higher MWs are targeted (Table 3.1, entries 7-10). B) M_n vs the [MM]/[**G3]** ratio. The black line represents the expected M_n based on initial [MM]/[**G3**] ratios assuming 100 % conversion to BB (Table 3.1, entries 7-10). C) AFM image of a bottlebrush polymer sample (Table 3.1, entry 10) on freshly-cleaved mica. D) TEM image of the same bottlebrush polymer sample taken on graphene oxide without staining. Scale bars = 50 nm.

Atomic force microscopy (AFM) and transmission electron microscopy (TEM) were utilized to visualize the bottlebrush molecules. Samples for AFM were prepared by drop casting from a dilute solution (Table 3.1, Entry 10) in methanol onto freshly-cleaved mica. AFM analysis showed mostly globular objects of ca. 50-80 nm in diameter. This size scale is consistent with the theoretical maximum bottlebrush length of approximately 200 nm calculated assuming complete chain extension of the bottlebrush backbone. The observed globular structures likely arise from energetically unfavorable interactions between the bottlebrush sidechains and the substrate that cause the polymer to "pull away" from the surface.[34] TEM was conducted on lacy carbon grids that had been drop coated with a dilute polymer solution. Prior to drop-casting, the

grids were pretreated with graphene oxide using a literature procedure.[35] TEM imaging on graphene oxide avoids the need for staining. Images were similar to those obtained by AFM, confirming the existence of single bottlebrush molecules with an approximate diameter of 50 nm. Although few cylindrical structures were observed by these techniques, the polymers likely adopt a cylindrical conformation in solution. A conformation plot of M_w vs. radius of gyration, generated by SEC-MALLS, for bottlebrush polymer **10** gave a slope of 0.90, which is consistent for rod-like objects (Figure 3S6).[36]

3.5 Conclusions

In summary, ROP of lactide was successfully carried out to form macromonomers that could be directly polymerized via ROMP using the grafting-through strategy to form a bottlebrush polymer. Addition of TFA following the ROP step was necessary to achieve high conversions in the ROMP step. Good control over bottlebrush polymer MW and Đ was attained in most cases, with bottlebrush polymer molecular weights exceeding 1 MDa. Overall, this method allows for easy control over the side-chain and backbone MWs without purification between steps. This one step procedure allows for large bottlebrush polymers to be synthesized quickly. We expect that this and related strategies will prove to be useful as interest in bottlebrush polymers continues to grow.

Acknowledgements

This work was supported by the Army Research Office (W911NF-14-1-0322) and the American Chemical Society Petroleum Research Fund (54884-DNI7). We thank Materia for catalyst and Prof. Rachel O' Reilly (University of Warwick) for graphene oxide.

3.6 References

(1) Sheiko, S. S.; Sumerlin, B. S.; Matyjaszewski, K. *Prog. Polym. Sci.* **2008**, *33*, 759.

(2) Bolton, J.; Rzayev, J. *ACS Macro Lett.* **2012**, *1*, 15.

(3) Pesek, S. L.; Li, X.; Hammouda, B.; Hong, K.; Verduzco, R. *Macromolecules* **2013**, *46*, 6998.

(4) Lee, H.-i.; Pietrasik, J.; Sheiko, S. S.; Matyjaszewski, K. *Prog. Polym. Sci.* **2010**, *35*, 24.

(5) Pakula, T.; Zhang, Y.; Matyjaszewski, K.; Lee, H.-i.; Boerner, H.; Qin, S.; Berry, G. C. *Polymer* **2006**, *47*, 7198.

(6) Dalsin, S. J.; Hillmyer, M. A.; Bates, F. S. *ACS Macro Lett.* **2014**, *3*, 423.

(7) Dalsin, S. J.; Hillmyer, M. A.; Bates, F. S. *Macromolecules* **2015**, *48*, 4680.

(8) Cai, L.-H.; Kodger, T. E.; Guerra, R. E.; Pegoraro, A. F.; Rubinstein, M.; Weitz, D. A. *Adv. Mater.* **2015**, *27*, 5132.

(9) Beers, K. L.; Gaynor, S. G.; Matyjaszewski, K.; Sheiko, S. S.; Möller, M. *Macromolecules* **1998**, *31*, 9413.

(10) Sumerlin, B. S.; Neugebauer, D.; Matyjaszewski, K. *Macromolecules* **2005**, *38*, 702.

(11) Tsukahara, Y.; Tsutsumi, K.; Yamashita, Y.; Shimada, S. *Macromolecules* **1990**, *23*, 5201.

(12) Fredrickson, G. H. *Macromolecules* **1993**, *26*, 2825.

(13) Schappacher, M.; Deffieux, A. *Macromolecules* **2000**, *33*, 7371.

(14) Radzinski, S. C.; Foster, J. C.; Matson, J. B. *Polym. Chem.* **2015**, *6*, 5643.

(15) Barner, L.; Davis, T. P.; Stenzel, M. H.; Barner-Kowollik, C. *Macromol. Rapid Comm.* **2007**, *28*, 539.

(16) Stenzel, M. H.; Davis, T. P.; Fane, A. G. *J. Mater. Chem.* **2003**, *13*, 2090.

(17) Wintermantel, M.; Gerle, M.; Fischer, K.; Schmidt, M.; Wataoka, I.; Urakawa, H.; Kajiwara, K.; Tsukahara, Y. *Macromolecules* **1996**, *29*, 978.

(18) Xia, Y.; Kornfield, J. A.; Grubbs, R. H. *Macromolecules* **2009**, *42*, 3761.

(19) Teo, Y. C.; Xia, Y. *Macromolecules* **2015**, *48*, 5656.

(20) Jha, S.; Dutta, S.; Bowden, N. B. *Macromolecules* **2004**, *37*, 4365.

(21) Choi, T.-L.; Grubbs, R. H. *Angew. Chem.* **2003**, *115*, 1785.

(22) Love, J. A.; Morgan, J. P.; Trnka, T. M.; Grubbs, R. H. *Angew. Chem. Int. Ed.* **2002**, *41*, 4035.

(23) Cheng, C.; Khoshdel, E.; Wooley, K. L. *Nano Lett.* **2006**, *6*, 1741.

(24) Charvet, R.; Novak, B. M. *Macromolecules* **2004**, *37*, 8808.

(25) Li, A.; Ma, J.; Sun, G.; Li, Z.; Cho, S.; Clark, C.; Wooley, K. L. *J. Polym. Sci., Part A: Polym. Chem.* **2012**, *50*, 1681.

(26) Chatterjee, A. K.; Choi, T.-L.; Sanders, D. P.; Grubbs, R. H. *J. Am. Chem. Soc.* **2003**, *125*, 11360.

(27) Coady, D. J.; Fukushima, K.; Horn, H. W.; Rice, J. E.; Hedrick, J. L. *Chem. Commun.* **2011**, *47*, 3105.

(28) Dove, A. P. *ACS Macro Lett.* **2012**, *1*, 1409.

(29) Conrad, J. C.; Amoroso, D.; Czechura, P.; Yap, G. P. A.; Fogg, D. E. *Organometallics* **2003**, *22*, 3634.

(30) Adjiman, C. S.; Clarke, A. J.; Cooper, G.; Taylor, P. C. *Chem. Commun.* **2008**, 2806.

(31) Hu, M.; Xia, Y.; McKenna, G. B.; Kornfield, J. A.; Grubbs, R. H. *Macromolecules* **2011**, *44*, 6935.

(32) Morandi, G.; Mantovani, G.; Montembault, V.; Haddleton, D. M.; Fontaine, L. *New J. Chem.* **2007**, *31*, 1826.

(33) Cho, H. Y.; Krys, P.; Szcześniak, K.; Schroeder, H.; Park, S.; Jurga, S.; Buback, M.; Matyjaszewski, K. *Macromolecules* **2015**, *48*, 6385.

(34) Sun, F.; Sheiko, S. S.; Möller, M.; Beers, K.; Matyjaszewski, K. *The Journal of Physical Chemistry A* **2004**, *108*, 9682.

(35) Patterson, J. P.; Sanchez, A. M.; Petzetakis, N.; Smart, T. P.; Epps, I. I. I. T. H.; Portman, I.; Wilson, N. R.; O'Reilly, R. K. *Soft Matter* **2012**, *8*, 3322.

(36) Ishizu, K.; Tsubaki, K.; Mori, A.; Uchida, S. *Prog. Polym. Sci.* **2003**, *28*, 27.

3.7 Appendix

Materials

All reagents were obtained from commercial vendors and used as received unless otherwise stated. Monomer D,L-lactide was recrystallized from toluene. ROMP catalyst $(H_2IMes)(Cl)_2(PCy_3)Ru{=}CHPh$ (**G2**) was obtained as a generous gift from Materia, and $(H_2IMes)(pyr)_2(Cl)_2Ru{=}CHPh$ (**G3**) was prepared from **G2** according to literature procedures.[1,2] Dry solvents were obtained from a solvent purification system (MBraun).

Methods

NMR spectra were measured on Agilent 400 MHz or Bruker 500 MHz spectrometers. ^{1}H and ^{13}C NMR chemical shifts are reported in ppm relative to internal solvent resonances. Yields refer to chromatographically and spectroscopically pure compounds unless otherwise stated. Size exclusion chromatography (SEC) was carried out in THF at 1 mL min^{-1} at 30 °C on two Agilent PLgel 10 μm MIXED-B columns connected in series with a Wyatt Dawn Heleos 2 light scattering detector and a Wyatt Optilab Rex refractive index detector. No calibration standards were used, and dn/dc values were obtained by assuming 100% mass elution from the columns. Atomic force microscopy (AFM) was conducted using a Veeco BioScope II AFM in tapping mode in air at room temperature using Nano World Pointprobe-silicon SPM Sensor tips (spring constant = 7.4 N m^{-1} , resonance frequency = 160 kHz). Samples for AFM were drop cast from 0.01 wt. % solutions of bottlebrush polymer in MeOH onto freshly cleaved mica. After 5 minutes, the mica was placed onto a hot plate set at 80 °C until the MeOH evaporated. TEM samples were drop cast from 0.01 wt. % solutions of bottlebrush polymer in $CHCl_3$ onto lacey

carbon-coated copper 400 mesh TEM grids (Electron Microscopy Sciences) coated with graphene oxide.[3] Images were taken on a Philips EM420 TEM with a slow scan CCD camera.

Synthesis of *exo*-5-norbornene-2-carboxylic acid

The synthesis was adapted from a literature method.[4] Norbornene-5-carboxylic acid (*endo*/*exo* mixture) (1.00 g, 7.24 mmol) was dissolved in an aqueous solution of $NaHCO_3$ (0.669 g, 7.96 mmol, 10 mL of H_2O) in a round bottom flask (RBF) equipped with a stir bar. In a separate flask, I_2 (1.23 g, 4.85 mmol) and KI (1.32 g, 7.96 mmol) were dissolved in H_2O (20 mL). The I_2/KI solution was added dropwise via addition funnel to the flask containing the *endo*/*exo* norbornene acid**.** The addition was continued until the solution retained a dark brown color. The reaction mixture was then filtered and transferred to a separatory funnel. The aqueous solution was washed with Et_2O (5 x 30 mL) to remove the iodolactone formed by the *endo* isomer. The aqueous layer was decolorized using a 10% $Na_2S_2O_3$ solution and acidified to pH ~ 2 with 1N H_2SO_4. The product was extracted with Et_2O (4 x 30 mL), and the combined organic layers were dried over Na_2SO_4 and concentrated *in vacuo* to give the pure product as an off white solid (0.420 g, 42% yield). ^{1}H NMR ($CDCl_3$): δ 6.14 (m, 2H), 3.11 (s, 1H), 2.94 (s, 1H), 2.27 (m, 1H), 1.95 (m, 1H), 1.54 (d, 1H), 1.40 (m, 2H). ^{13}C NMR ($CDCl_3$): δ 182.77, 138.28, 135.85, 46.84, 46.54, 43.26, 41.81, 30.47.

Synthesis of *exo*-5-norbornene-2-methanol

Lithium aluminum hydride (1.00 g, 26 mmol) was added under nitrogen to a 250 mL RBF. The RBF was then placed into an ice bath. Dry THF (40 mL) was added dropwise into the flask, followed by a solution of *exo* -5-norbornene-2-carboxylic acid (3.00 g, 21 mmol) dissolved in dry THF (10 mL). The flask was then placed into an oil bath, and the reaction mixture was

refluxed for 12 h. Next, the reaction mixture was cooled in an ice bath, then 1 mL of water was added dropwise to the flask, followed by 1 mL of 10% sodium hydroxide solution and finally 3 mL of water. The flask was allowed to warm to room temperature and diluted with diethyl ether (200 mL). The solids were removed by filtering through Celite, and the filtrate was washed with brine and dried over sodium sulfate. The solvent was removed to afford the product as a colorless oil (2.56 g, 94% yield) ^{1}H NMR ($CDCl_3$): δ 6.08 (m, 2H), 3.70 (m, 1H), 3.54 (m, 1H), 2.82 (s, 1H), 2.74 (s, 1H), 1.64 (m, 1H), 1.30 (m, 3H), 1.12 (m, 1H). ^{13}C NMR ($CDCl_3$): δ 136.91, 136.57, 67.65, 45.08, 43.38, 41.99, 41.63, 29.64.

Representative One-Pot ROP-ROMP Polymerization Procedure

To a flame dried Schlenk flask was added D,L-lactide (500 mg, 3.47 mmol) and activated 3 Å molecular sieves followed by dry DCM (5 mL). To another flame dried Schlenk flask was added *exo*-5-norbornene-2-methanol (43.1 mg, 0.35 mmol), DBU (44.8 mg, 0.29 mmol), benzoic acid (6.36 mg, 0.052 mmol), and activated 3 Å molecular sieves followed by dry DCM (1 mL). Next, 100 uL of the initiator/catalyst solution was removed by N_2-purged syringe and injected into the monomer solution to initiate the polymerization. After 20 min, acid was added to terminate the ROP reaction. After approximately 1 min, **G3** was added from a stock solution in dry DCM, and the reaction mixture was allowed to stir for 1 h. Ethyl vinyl ether was then added to quench the ROMP reaction, allowing the reaction mixture to stir for 30 min. The reaction mixture was precipitated into cold MeOH to yield a white solid.

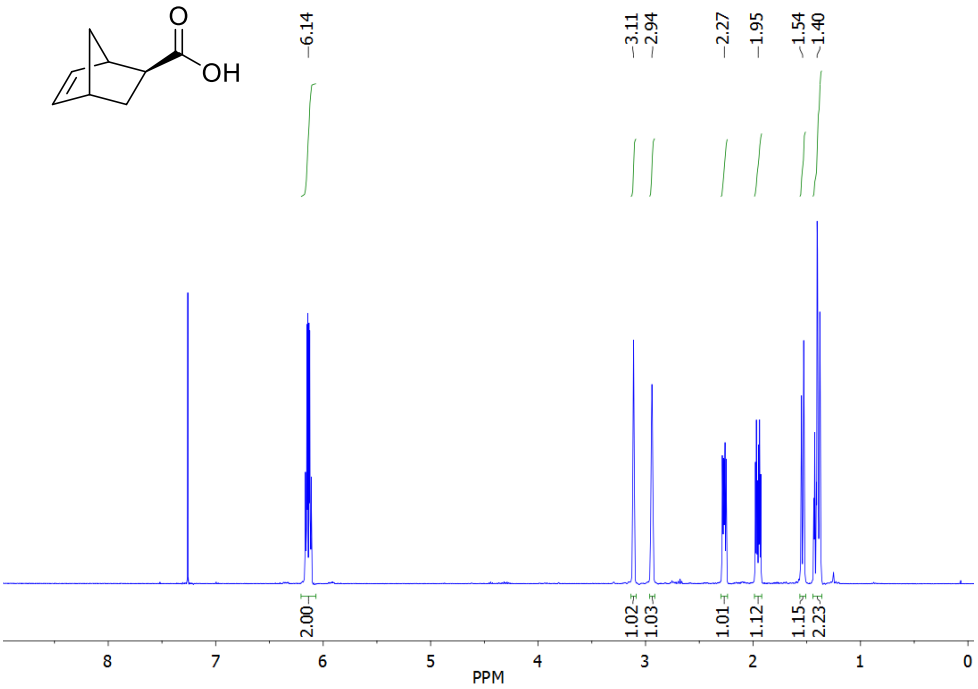

Figure 3S1: [1]H NMR spectrum of *exo*-5-norbornene-2-carboxylic acid.

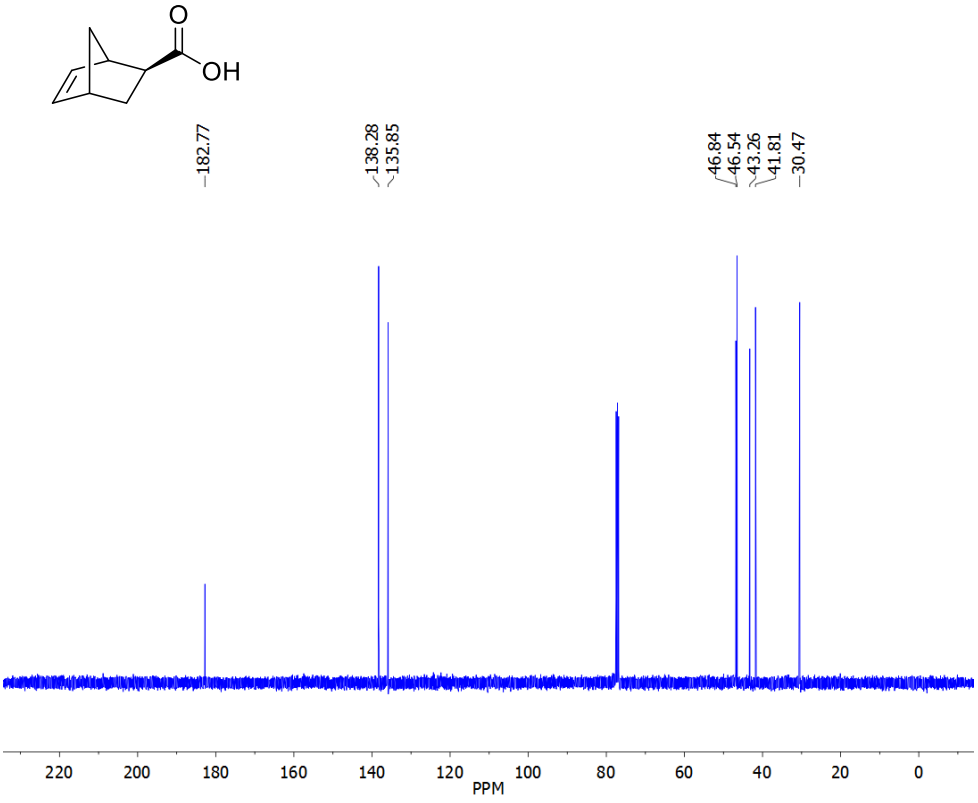

Figure 3S2: [13]C NMR spectrum of *exo*-5-norbornene-2-carboxylic acid.

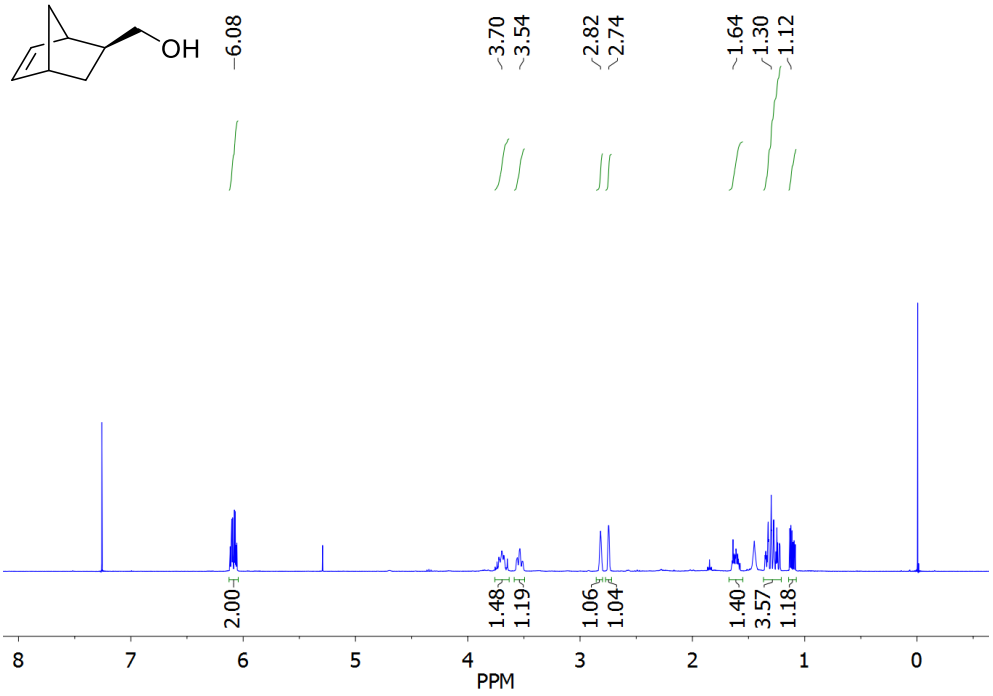

Figure 3S3: [1]H NMR spectrum of *exo*-5-norbornene-2-methanol.

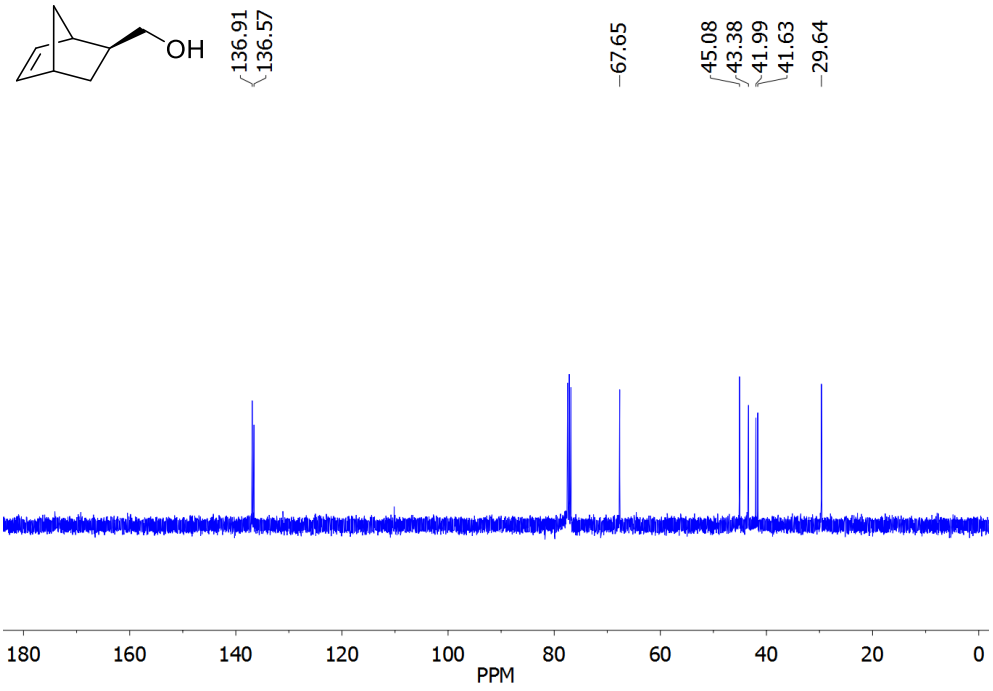

Figure 3S4: [13]C NMR spectrum of *exo*-5-norbornene-2-methanol.

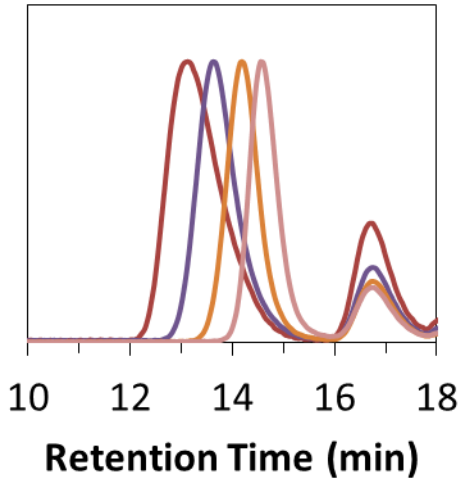

Figure 3S5: SEC traces of bottlebrush polymers showing decreasing retention times as higher molecular weights are targeted (Table 3.1, entries 3-6).

Table 3S1: Evaluation of acids tested to terminate the ROP.

	ROP				**ROMP**			
Entry	Acid	Acid Equiv.[a]	M_n MM[b]	Đ[b]	Theo. M_n BB (kDa)[c]	M_n BB (KDa)[b]	Đ BB[b]	Conversion[d]
1	Acetic acid	2	3000	1.03	300	51	1.30	0.13
2	Benzoic acid	2	3890	1.02	389	91	1.35	0.30
3	Tosic acid	2	4000	1.01	400	280	1.26	0.75
4	TFA	2	4100	1.03	410	400	1.13	0.81

[a]Equivalents relative to alcohol initiator. [b]Measured by SEC using absolute MW determination by light scattering. [c]Expected molecular weight assuming full conversion at [M]/[I] = 100:1. [d]Observed conversion to bottlebrush determined from SEC by comparing the relative integrations of BB and MM peaks.

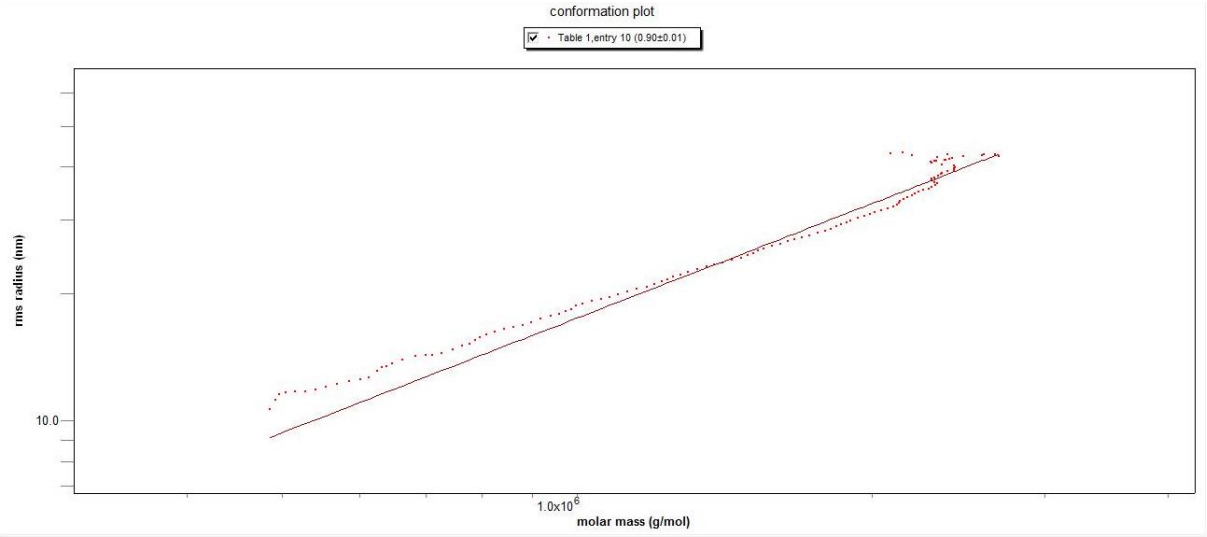

Figure 3S6: RMS Conformation plot of a bottlebrush polymer (Table 3.1, entry 10).

(1) Love, J. A.; Morgan, J. P.; Trnka, T. M.; Grubbs, R. H. *Angew. Chem. Int. Ed.* **2002**, *41*, 4035.

(2) Liu, J.; Gao, A. X.; Johnson, J. A. **2013**, e50874.

(3) Patterson, J. P.; Sanchez, A. M.; Petzetakis, N.; Smart, T. P.; Epps, I. I. I. T. H.; Portman, I.; Wilson, N. R.; O'Reilly, R. K. *Soft Matter* **2012**, *8*, 3322.

(4) Manning, D. D.; Strong, L. E.; Hu, X.; Beck, P. J.; Kiessling, L. L. *Tetrahedron* **1997**, *53*, 11937.

Section II: Synthesis of Bottlebrush Polymers using the Transfer-To Approach.

Chapter 4: Graft Polymer Synthesis by RAFT Transfer-to

4.1 Authors

Jeffrey C. Foster, Scott C. Radzinski, and John B. Matson

Department of Chemistry and Macromolecules Innovation Institute, Virginia Tech, Blacksburg, Virginia 24061, United States

S. C. Radzinski, J. C. Foster and J. B. Matson *J. Polym. Sci., Part A: Polym. Chem.* **2017**

4.2 Introduction

Polymer chemists have found that attaching polymers onto surfaces, nanoparticles, proteins, and even other polymers can enable a number of applications. By grafting polymers onto various substrates, the interface that separates the substrate from its external environment can be manipulated. Interfacial properties such as adhesion, wettability, chemical reactivity, and biocompatibility can be tuned through rational design of the grafted polymer layer. For example, polymers grafts are widely utilized to protect macroscopic substrates from UV damage and corrosion, alter their hydrophobicity, prevent interaction with cells and/or biomacromolecules, and imbue substrates with antibacterial properties.[1,2] Grafting of polymers onto nanoparticles is used widely to prevent nanoparticle aggregation, add bioactive components, and provide photonic properties.[3] Proteins are regularly grafted with polymer chains to increase their circulation half-life, modify their activity, and improve their stability to long-term storage.[4] Finally, grafting of polymers onto other polymers allows chemists to create complex polymer topologies, including star polymers and graft polymers (which may also be called comb, or bottlebrush polymers depending on grafting density).[5] It is clear that polymer grafting can have a dramatic effect on properties, regardless of the size of the underlying substrate. Throughout this

review, the term substrate will be used to refer broadly to the surface to which the polymer chains are attached during a graft polymerization. This could be, for example, a silicon wafer, a nanoparticle surface, or a soluble multifunctional initiator, biomacromolecule, or polymer bearing multiple initiating functionalities.

Despite the wide variety of applications for polymer grafting, only two or three different strategies are typically identified for attaching a polymer to a substrate. Grafting is typically achieved by either attaching pre-formed polymers to a substrate through the formation of a covalent bond (grafting-to) or by growing a polymer chain from an initiator or chain transfer agent (CTA) attached to a substrate (grafting-from).[6] If the substrate is another polymer, grafting can be carried out by stringing together pre-formed polymers via polymerization of an end group (grafting-through).[7,8] Each strategy has advantages and disadvantages. For example, when polymers are grown from a surface using the grafting-from technique, a high grafting density can be achieved, but some side reactions such as polymer-polymer coupling may occur. In contrast, grafting-through can provide "perfect" grafting densities with few structural defects under optimized conditions.[9]

We have recently begun studying a fourth grafting strategy that is mechanistically distinct from the other three. Termed "transfer-to" by Sumerlin in a 2011 review paper in the context of protein grafting, this synthetic strategy relies on a chain transfer reaction to attach actively growing polymer chains onto a substrate.[10] Transfer-to can be thought of as a hybrid between the grafting-from and grafting-to approaches, but it has its own limitations and advantages compared with the other grafting methods. It has been used to graft polymers onto surfaces, nanoparticles, proteins and other polymers, primarily using reversible addition–fragmentation chain transfer (RAFT) polymerization. In many reports in which transfer-to has been used, the grafting strategy

is incorrectly identified as grafting-from; in others it is correctly recognized but referred to by another name (often the Z-group or Z-star approach). While most reports concerning transfer-to pertain to its use in grafting polymerization via RAFT, this strategy is not limited to RAFT polymerization. Therefore, we recommend use of the term transfer-to rather than Z-group approach in order to more broadly identify this synthetic strategy. This review will focus on the use of transfer-to polymerization to prepare graft polymers in view of our current understanding of its advantages and shortcomings. In addition, previous work in the field of transfer-to graft polymerization from protein, nanoparticle, and macroscopic substrates will be identified and reviewed.

4.3 Reversible-Deactivation Radical Polymerization

The development of reversible-deactivation radical polymerization (RDRP) techniques reinvigorated the field of radical polymerization by facilitating the preparation of precisely-defined polymers of targeted size and narrow molecular weight distribution.[11] Nitroxide-mediated polymerization was the first RDRP to be developed,[12,13] followed by atom-transfer radical polymerization (ATRP)[14] and RAFT polymerization.[15] Prior to the advent of RDRPs, the synthesis of complex polymer topologies was non-trivial, often requiring intricate apparatuses and stringent reaction conditions. However, using RDRP, complex topologies are routinely prepared using a broad selection of functional monomers and reaction conditions. These topologies include multiblock copolymers,[16-18] hyperbranched polymers,[19,20] star polymers (having one or more type of arms),[21] and graft copolymers.[22,23]

RAFT Polymerization

RAFT polymerization is perhaps the most versatile RDRP technique. Using RAFT, polymerization of a wide variety of vinyl monomers can be achieved by careful selection of the

CTA and reaction conditions. In addition, RAFT polymerization is tolerant to most functional groups including electrophilic functionalities such as aldehydes[24] and challenging nucleophiles like acyl hydrazides.[25] RAFT CTAs contain a thiocarbonyl-thio moiety, an R-group (leaving group) that forms a stable radical upon cleavage,[26] and a Z-group (stabilizing group) that modulates reactivity towards monomer-derived radicals.[27] Polymerization proceeds via degenerative chain transfer between a radical (initiator- or monomer-derived) and the CTA, effectively swapping the thiocarbonyl-thio functionality between polymer chains. The control afforded by RAFT polymerization arises from a rapid equilibrium of chains such that all chains are given an equal opportunity to grow. As shown in Figure 4.1, the structures of RAFT CTAs are variable, with numerous dithioester, trithiocarbonate, dithiocarbamate, and xanthate compounds reported. The capability of a certain CTA to effectively mediate the polymerization of a specific monomer is largely determined by its chemical structure (i.e., the R and Z groups used). For example, dithiobenzoate or trithiocarbonate CTAs are generally well suited for polymerizing more-activated monomers (MAMs) such as methyl methacrylate (MMA), methyl acrylate (MA), and styrene, while dithiocarbamates and xanthates are appropriate when polymerizing less-activated monomers (LAMs) such as vinyl acetate and n-vinyl pyrrolidone. The reader is referred to several excellent reviews on the mechanism and scope of RAFT polymerization for further discussion.[28-36]

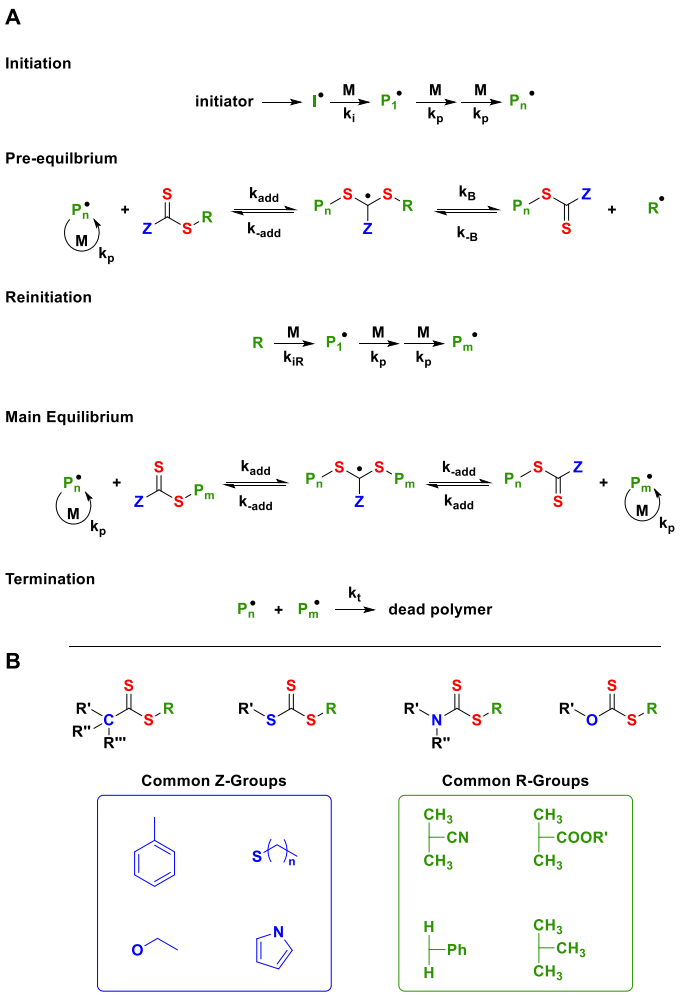

Figure 4.1. A) Mechanism of RAFT polymerization. Polymerization of vinyl monomers is mediated by degenerative chain transfer of radicals between dormant and active states. B) Typical structures of RAFT CTAs highlighting different thiocarbonyl-thio functionalities (dithioesters, trithiocarbonates, dithiocarbamates, and xanthates) and common Z- and R- groups. Reproduced from Ref. 28 with permission from The Royal Society of Chemistry.

4.4 Graft Polymerization Using RAFT

Polymer grafts can be grown from substrates using RAFT polymerization through either the grafting-from or transfer-to technique. The principal difference between RAFT grafting-from and transfer-to is the location of the polymer radical and thiocarbonyl-thio compound during

propagation. The direction of attachment of the CTA to the substrate regulates these mechanistic details, which determine types of imperfections and byproducts that can arise during polymerization. If the CTA is attached to the substrate via the R-group, then grafting-from is the operative mechanism (Figure 4.2). Conversely, if the CTA is anchored to the substrate through the Z-group, then transfer-to polymerization results.

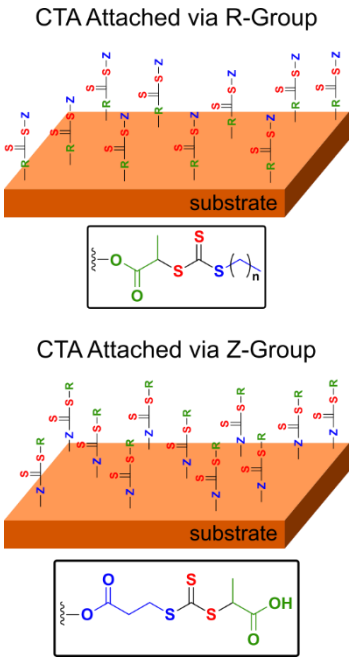

Figure 4.2. Attachment of the CTA to the substrate determines the mechanism of polymerization.

Grafting-From

Grafting-from is perhaps the most studied grafting methodology, largely because many CTA R-groups contain carboxylic acids or other reactive functionalities that facilitate derivatization. Indeed, many grafting reactions are likely conducted using the grafting-from strategy coincidentally instead of through rational design. When preparing graft polymers by grafting-from, the CTA is attached to the grafting surface or polymer backbone through its R-group (Figure 4.2). During polymerization, the CTA fragments, resulting in an R-group-derived radical

that remains tethered to the grafting surface and a thiocarbonyl-thio component that dissociates (Figure 4.3A). The surface bound radical can react with monomer to form polymer, with a CTA resulting in degenerative chain transfer, or with another surface bound radical. The latter case is a termination reaction that takes one of three forms: 1) disproportion to form two polymer chains that are bound to the substrate but no longer living; 2) coupling to form an intramolecular "loop"; or 3) coupling that results in the creation of an intermolecular cross-link. Intermolecular coupling reactions are most relevant for nano-scale grafting applications such as star/bottlebrush copolymers synthesis or grafting-from nanoparticles, and these side reactions contaminate the polymer sample with coupled byproducts much larger than the desired size.

In RAFT grafting-from there exists one more type of impurity that can form: unattached linear polymers. The dissociated thiocarbonyl-thio component acts like a "free" CTA in solution and can return to the substrate via chain-transfer with a surface-bound polymer radical. CTA in solution is also capable of reacting with radicals that are not bound to the grafting substrate, which come from initiator fragments or initiator-derived chains. This process results in the formation of linear polymer chains that are free in solution. These initiator-derived chains will always form to some extent, regardless of reaction conditions. Similar to traditional RAFT, initiator-derived chains in grafting-from undergo living polymerization to form linear polymer, but these solution-initiated polymers can never attach to the substrate during grafting-from. Because concentrations of linear polymers can be low under optimized conditions, this consideration is often overlooked, especially in the context of macroscopic surfaces where the linear polymer in solution can be easily washed away. However, these undesired side products become more important when making star or graft polymers by grafting-from, where linear polymer impurities are more challenging to remove from the star or graft polymer sample.

As with traditional RAFT polymerization, factors that limit the occurrence of termination—low radical concentration, high CTA concentration, high kp, high pressure, and low monomer conversion—can help to eliminate impurities that arise as the result of inter- or intramolecular radical reactions. However, linear polymer species will always form to some degree, as will imperfections in the polymer graft resulting from termination.

Grafting Density During Grafting-from

The density of polymers on the substrate is another important consideration when choosing a grafting strategy. The degree of chain extension of a polymeric graft is related to grafting density on the grafting substrate. At low grafting densities, the pendant polymer chains collapse, taking on a globular structure referred to as mushroom-like. In contrast, high grafting densities result in chain elongation, tight chain packing, and notable chain end effects as these are more likely to be found on the periphery of the polymer brush. Indeed, the properties of the resultant material often depend on the grafting density of the attached polymer chains. For example, the thickness of polymer films on macroscopic surfaces is directly related to the grafting density above a critical value, with higher grafting densities resulting in thicker films.[37] High grafting densities also inhibit the interaction/adhesion of biomacromolecules with surfaces.[38] Grafting density is also critically important for bottlebrush polymers, as their morphology (and properties) depend largely on the steric interactions between numerous pendant polymer chains. Deffieux and coworkers have demonstrated a dependence of the bottlebrush polymer persistence length on the grafting density using neutron scattering, with high grafting densities resulting in much larger persistence lengths for bottlebrush polymers with polystyrene grafts.[39] This phenomenon was also observed via dynamic mechanical analysis.[40]

The grafting density achieved during RAFT grafting-from depends on three factors: (1) the density of initiator/CTA moieties on the substrate; (2) the degree of termination that occurs during polymerization; and (3) the reinitiation efficiency of the polymerization (i.e., the ability of the R group to come off of the CTA and initiate polymerization). The first factor is determined by chemistry that is unrelated to the polymerization reaction and will not be discussed here. The second factor is termination reactions, which result in the loss of an active radical. If grafting density is taken to mean the density of polymer chains that are above a certain threshold MW (i.e., not oligomers), then termination reactions effectively reduce the grafting density of the polymer brush if they occur in the early stages of polymerization. The third factor, reinitiation efficiency, is another time dependent phenomenon that affects the grafting density of the polymer brush. At low conversions, some of the substrate-bound CTAs have not yet reacted with initiator fragments. Thus, grafting density is low early in the polymerization but rises quickly in an ideal RAFT polymerization. The re-initiation efficiency of a RAFT polymerization depends on several factors, most notably the selection of monomer and CTA. This will be discussed in further detail below.

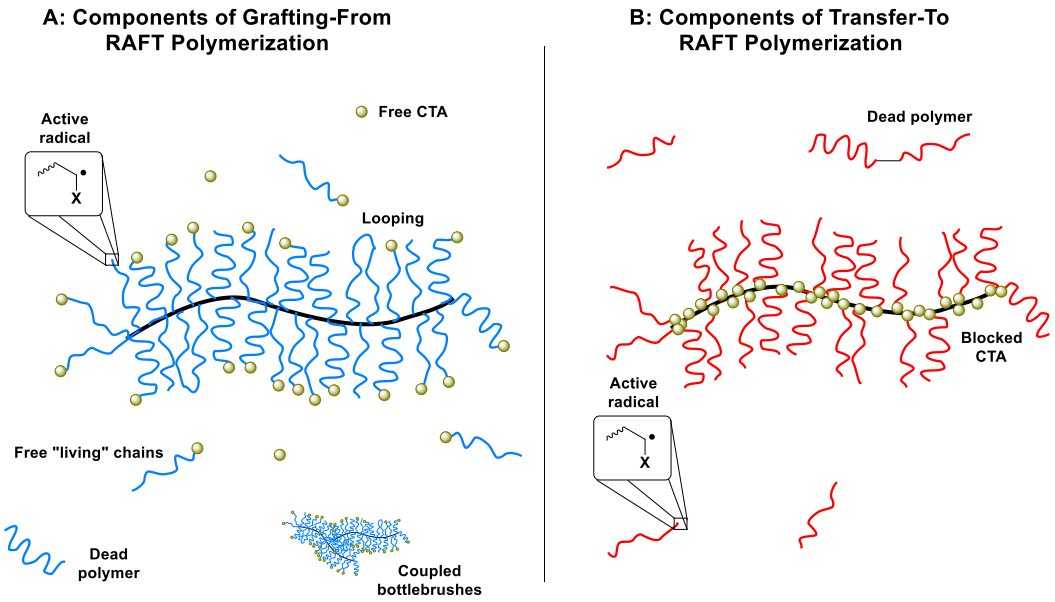

Figure 4.3. Comparison of the grafting-from and transfer-to methods of grafting.

Transfer-to

In contrast to grafting-from, when conducting RAFT transfer-to the CTA is attached to the substrate via the Z-group.[41] Z-groups with reactive functionalities are uncommon, contributing to far fewer studies using this grafting technique. Despite this fact, a number of groups have applied RAFT transfer-to to grow polymer brushes from a variety of substrates including macroscopic silicon surfaces,[42,43] silica particles,[44,45] solid support resins,[46,47] single-walled carbon nanotubes,48 and proteins.[49-51] Star polymers have been prepared from various initiating cores such as β-cyclodextrins[52] or hyperbranched polymers and dendrimers.[53-55] Polymers functionalized with pendant CTAs have mediated RAFT transfer-to polymerization to form bottlebrush polymers.[56-60]

Like traditional RAFT, transfer-to is initiated via thermal decomposition of the radical source. As in all RAFT reactions, this initiator-derived radical can add to monomer or CTA. A pre-equilibrium phase exists wherein initiator-derived radicals or short initiator-derived oligomers

add to CTAs, followed by fragmentation of the CTA R-groups. This continues until all CTA R-groups have been consumed and the reaction enters the main equilibrium.

During the main equilibrium of RAFT transfer-to, the substrate-bound thiocarbonyl-thio compounds fragment and active polymer radicals detach from the substrate (Figure 4.3B). The detached polymeric radicals are free to propagate away from the substrate. They can then return to the substrate via a chain-transfer reaction. Here, the graft polymers are in equilibrium with "free" linear propagating chains, allowing the polymer brush as a whole to grow in a controlled manner.[61] It is important to note that for RAFT transfer-to, active radicals are never present on substrate-bound polymer grafts and that propagation and termination always occur away from the substrate.

The difference in the location of polymer growth between grafting-from (from the surface) and transfer-to (free in solution) is important because it determines the types of impurities that form. Because the active radical is never tethered to the substrate in transfer-to, imperfections caused by intramolecular radical reactions (looping) do not arise. Moreover, intermolecular coupling is also absent. Termination through disproportionation also does not lead to impurities on the grafting surface. In short, transfer-to effectively eliminates side reactions that lead to defects on substrates in grafting-from polymerization.

Although termination reactions do not lead to loops, crosslinks, or short chains on a substrate when using RAFT transfer-to, termination reactions still occur, as in all RDRP reactions. Similar to traditional RAFT polymerization, linear polymer chains can undergo termination reactions. Dead polymer arises during transfer-to as the result of termination reactions between active radicals on these linear chains. These are, in fact, the only types of impurities that are present in transfer-to polymerization. The quantity of these linear impurities that arise as a result of

termination reactions can be kept low by employing conditions that limit termination, which we discuss further below. Dead polymer formation is unavoidable, however, and it becomes more prolific as the molecular weights of the polymer grafts increase due to steric interactions between these chains and the grafting surface. Therefore, under non-ideal conditions, large amounts of dead linear polymer can form in transfer-to graft polymerization.

Grafting Density During Transfer-to

Another important distinction between grafting-from and transfer-to polymerization is grafting density. For RAFT transfer-to, the grafting density of the graft polymer depends on the same primary factors as grafting-from—initial CTA density on the substrate, loss of chains to termination, and reinitiation efficiency. In addition to these considerations, grafting density in transfer-to is also affected by the steric shielding phenomenon. Grafting density during RAFT transfer-to will be discussed with respect to a number of considerations in the subsequent sections.

4.5 Considerations When Conducting RAFT Transfer-To

Similar to traditional RAFT polymerization, the conditions of the transfer-to polymerization reaction affect the polymer brushes that form. Factors affecting RAFT transfer-to have been studied by the groups of Vana,[62] Davis,[41] and Matson.[63] The length of the polymer grafts, their molecular weight distribution, the types and quantities of impurities (imperfections and/or byproducts) formed, and the grafting density of the graft polymer can all be manipulated by changing the CTA or monomer used, the reaction temperature, the substrate, or a number of other variables. These considerations will be discussed individually as they apply to RAFT transfer-to.

CTA Structure and Concentration

As with traditional RAFT polymerization, choosing an appropriate CTA is critical to achieving controlled polymerization. Poor CTA/monomer pairing can result in uncontrolled polymerization if addition to the thiocarbonyl-thio compound occurs significantly more slowly than propagation.[26,27] Therefore, rational selection of the appropriate CTA for the desired monomer is paramount. Much work has gone into studying the polymerization of common monomer classes (i.e., acrylates, methacrylates, styrenics, etc.) using a variety of CTAs, and several optimal combinations have been identified.[64] For example, methyl methacrylate (MMA) polymerization is well controlled by dithioester CTAs due to their high chain transfer coefficients.[28] In contrast, xanthate CTAs do not control MMA polymerization because the polymer radicals add more rapidly to monomer than they do to the xanthate CTAs, but xanthates are ideal CTAs for vinyl acetate and related LAMs. For traditional RAFT polymerization, poor control due to bad monomer/CTA pairing manifests as a broadening of the molecular weight distribution and, in most cases, deviation from expected molecular weights.[65]

For RAFT transfer-to, the choice of CTA has a variety of outcomes. Most importantly, the CTA in its "free" form (i.e., in traditional RAFT for linear polymer synthesis) must control polymerization of the monomer. If this is the case, then the substrate bound CTA is also expected to control polymerization. In other words, the guidelines for CTA R and Z group selection established for traditional RAFT polymerization translate well to transfer-to (Figure 4.4). For example, trithiocarbonate CTAs have been employed to mediate the polymerization of styrene to grow brush polymers from a variety of substrates.[52,55,57] Similarly, a xanthate CTA was found to control the polymerization of N-vinylcarbazole to form a star polymer,[53] and dithiocarbamate CTAs coupled to a poly(norbornene) backbone were used to prepare bottlebrush polymers with

poly(vinyl acetate) grafts.[66] However, CTAs that work only moderately well for traditional RAFT may not perform well in RAFT transfer-to. Fairly small deviations from ideal behavior are exasperated when conducting transfer-to, as low molecular weight byproducts or unconsumed CTAs are rarely detected in a traditional RAFT polymerization.

It is important to note that if the CTA does not control the polymerization of a given monomer during RAFT transfer-to polymerization, the desired polymer brush topology will not form. Initiation and propagation both occur away from the substrate when conducting transfer-to. In the case of a poor monomer/CTA pair in which the chain transfer efficiency is low, the vast majority of the polymer chains will not add to the substrate-bound CTAs, so few chains will be grafted to the substrate. Well controlled RAFT polymerization must therefore be verified by first conducting a solution polymerization using the chosen monomer/CTA pair.

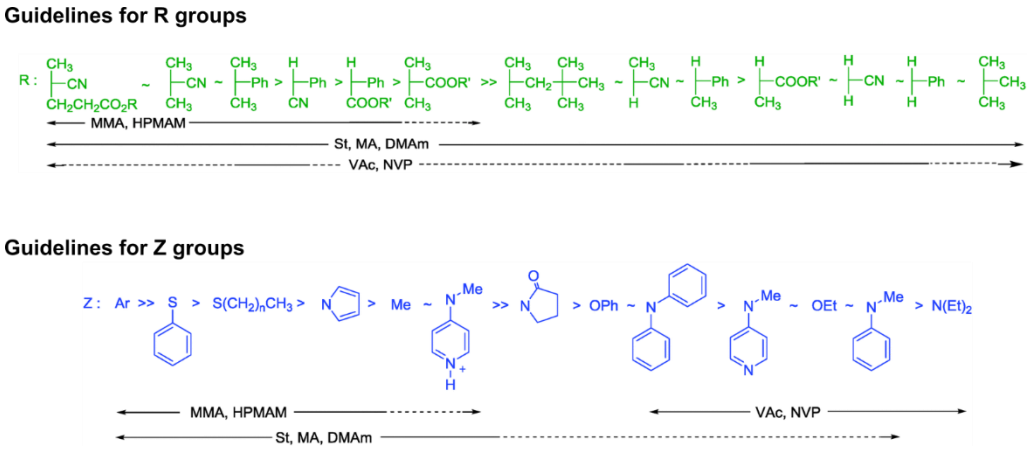

Figure 4.4. Guidelines for the selection of RAFT agent R and Z groups. Dashed lines indicate partial control over polymerization is achieved. For RAFT transfer-to, partial control is likely not sufficient to prepare well-defined graft polymers. Reproduced from Ref. 28 with permission from The Royal Society of Chemistry.

Effect on Termination

Termination reactions also become prevalent in RAFT transfer-to when a CTA does not adequately control the polymerization of a given monomer. Termination becomes more probable at high radical concentrations as is the case for polymerizations in which chain transfer between the active radical and the CTA occurs at a low rate relative to propagation. An example of this type of behavior would be the polymerization of styrene using a xanthate CTA.[67] Termination is particularly problematic for RAFT transfer-to due to the fact that termination reactions always occur away from the substrate. Termination between detached linear chains reduces the grafting density of the polymer brush and contaminates the sample with impurities that can sometimes be difficult to remove.

Effect on Polymerization Kinetics

Beyond controlled polymerization, the choice of CTA also affects the kinetics of the polymerization, with retardation and/or inhibition possible based on CTA and monomer structure. Retardation/inhibition typically originates from one of two sources: 1) unfavorable re-initiation by the leaving R-group (also referred to as poor re-initiation efficiency); or 2) slow fragmentation due to the stability of the adduct radical.[68] In traditional RAFT polymerization, this phenomenon is most typically observed in the polymerization of LAMs. Retardation/inhibition is also possible for RAFT transfer-to. For example, Vana and coworkers reported significant inhibition effects in the polymerization of vinyl acetate using a tetra-functional xanthate CTA with either a benzyl or a phenylethyl R-group.[69] Incubation times of ~10 h were observed for both R-groups, and this effect was attributed to the differences in radical stability of the R group relative to vinyl acetate.

Long incubation times in RAFT polymerization are related to poor re-initiation efficiencies. Re-initiation efficiency during RAFT transfer-to is a significant contributor to the structure of the resulting polymer brush. A common misconception of RDRPs is that all polymer chains begin growing immediately once the polymerization reaction is started. However, when conducting RAFT polymerization this is often not the case. Conditions for the polymerization need to be chosen such that the CTA is rapidly consumed during the initial stages. This will only be the case if the chosen CTA has a high chain transfer coefficient (C_{tr}) in the monomer being polymerized. C_{tr}, defined in equation 1, depends on the rate constant of chain transfer, k_{tr}, as well as the rate constant of propagation, k_p.

$$C_{tr} = \frac{k_{tr}}{k_p} \tag{1}$$

For RAFT polymerization, k_{tr} is given by the following expression:[70]

$$k_{tr} = k_{add} * \frac{k_{\beta}}{k_{-add} + k_{\beta}} \tag{2}$$

The rate constant k_{tr} is determined by the structure of the CTA; therefore, C_{tr} is determined by the CTA/monomer pair. If C_{tr} is low for a given monomer/CTA pair, then the CTA will not be consumed until the later stages of the reaction. It is therefore important to consider the consequences of slow pre-equilibration that could result from monomer/CTA pairs with low Ctr. C_{tr} is especially important for RAFT transfer-to due to its impact on grafting density. Boschmann et. al. showed the importance of re-initiation efficiency using ^{1}H NMR spectroscopy by studying the consumption of CTAs over the course of RAFT transfer-to polymerization in star polymer synthesis.[71] For the polymerization of styrene by a hexafunctional trithiocarbonate CTA with a benzyl R-group, complete re-initiation was not achieved until ~60% monomer conversion

(Figure 4.5). The poor re-initiation efficiency of this system manifested as a reduction in grafting density (less than the expected 6 arms per star polymer) and star polymer MWs lower than expected values. By changing to an ethylbenzyl R-group, re-initiation was complete at only ~10% monomer conversion, resulting in star polymers with grafting densities near their theoretical maxima. Many reports on star or bottlebrush synthesis by RAFT transfer-to have attributed observed deviations in star/bottlebrush MW from theoretical values to termination or steric effects without considering the impact of CTA structure on Ctr and its associated consequences. This work clearly shows that even though certain monomer/CTA pairs may work fairly well for traditional RAFT, C_{tr} is an important variable to consider when conducting RAFT transfer-to polymerization.

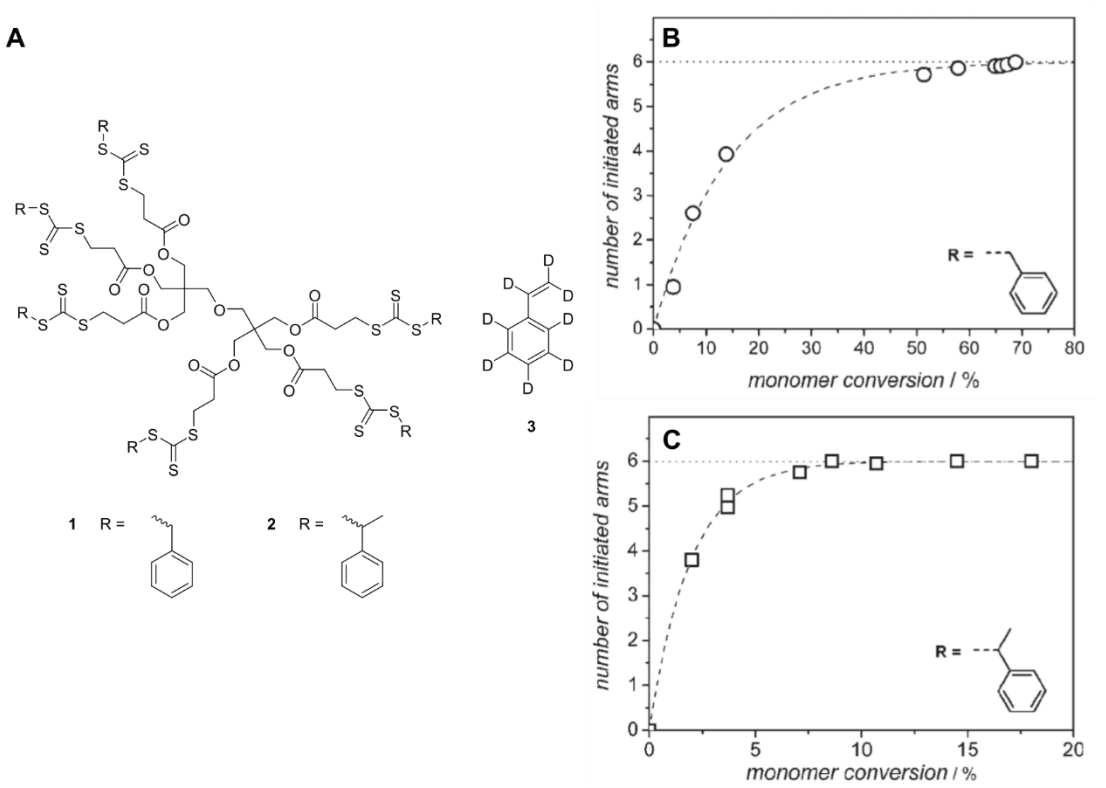

Figure 4.5. Effect of re-initiation efficiency on RAFT transfer-to. (A) Chemical structure of 6-arm star RAFT initiator in the polymerization of styrene-d8 with two different R groups. (B) Number of successfully initiated arms versus monomer conversion for R = benzyl. (C) Number of successfully initiated arms versus monomer conversion for R = phenylethyl. Reproduced from Ref. 71 with permission from Wiley Periodicals.

Finally, CTA concentration is important to consider when conducting RAFT transfer-to. In general, better control is achieved at high CTA concentration due to more rapid addition of active radicals to CTAs. High CTA concentrations lead to narrow molecular weight distributions and MWs that are close to theoretical values when conducting RAFT transfer-to.[52] In addition, high CTA concentrations minimize the amount of dead linear polymer impurities that form during transfer-to grafting reactions.[61,63]

The kp/kt Ratio

The ratio of the rate constant of propagation to the rate constant of termination, k_p/k_t, is an important factor to consider while performing RAFT transfer-to. Increasing this ratio leads to a reduced incidence of termination, meaning fewer dead polymers in solution and substrates with higher grafting densities. Several factors are important to consider that influence the k_p/k_t of the system, including monomer structure, solvent, temperature, and pressure.

Monomer Structure

The structure of the monomer utilized in a radical chain polymerization is the primary determinant of the k_p/k_t ratio. In general, acrylates and acrylamides possess high rate constants of propagation relative to termination, while styrene has a significantly lower k_p/k_t value.[72] Radzinski et. al. studied the effects of using different monomers during bottlebrush synthesis by RAFT transfer-to. Mediated by a polymeric dithiocarbamate CTA, the kinetics of RAFT polymerization of three different monomers—styrene, methyl acrylate (MA), and acryloyl morpholine (ACMO)—were investigated under identical conditions. Monomer choice had a large effect on the quantity of linear polymer impurities that formed during RAFT transfer-to polymerization, with high kp/kt monomers yielding the least amount of linear polymer even at high conversions (Table 4.1).[63]

Table 4.1. Effect of monomer on RAFT transfer-to polymerization.

Monomer	Mn (kDa)	Đ	%Dead	% Conv
Sty	97.0	1.08	21	29
MA	400	1.05	14	89
ACMO	740	1.04	11	82

All polymerizations were carried out at [Monomer] = 17 v/v% using the same polymeric CTA.

Solvent

The solvent choice for the polymerization has a direct effect on the kp/kt ratio in two ways: 1) propagation rate generally increases with solvent polarity, and 2) the equilibrium between the polymeric radicals and adduct radicals in the RAFT main equilibrium is biased towards the polymeric radical when more polar solvents are used due to decreased Ctr.[73] Both outcomes are expected to increase the MW of the polymer grafts and the quantity of dead linear polymer when conducting RAFT transfer-to.

Fröhlich used Monte Carlo simulations to investigate the use of good solvents vs theta solvents during RAFT transfer-to. It was determined that shielding effects (discussed in more detail below) were chain length dependent under good solvent conditions but became less pronounced when using a theta condition. Decreased shielding, i.e., the blocking of reactive CTA moieties by nearby polymer side-chains, was hypothesized to increase the contact probability of the active radical and the CTA, thereby increasing the rate of addition to CTA. These simulations were complemented by transfer-to experiments that yielded star polymers with smaller dispersity values in cyclohexane (a poor solvent) than those in toluene (a good solvent).[74]

Temperature

Temperature affects a variety of rates in RAFT polymerization. For thermally initiated polymerizations, increased temperatures cause faster initiator decomposition rates, leading to increased radical concentrations.75 Propagation and termination rates also increase with increasing temperature. In addition, some evidence suggests that fragmentation of the intermediate RAFT radical may be enhanced relative to addition to CTA at high temperatures.[76] Finally, thermal decomposition of the RAFT agent is also possible at high temperatures, leading to some loss of living character throughout the course of the polymerization.[77] Overall, high temperatures generally result in a broadening of the molecular weight distribution and a

deviation from expected MW. However, high temperature also reduces the duration of the polymerization. Therefore, a balance must be struck to achieve controlled polymerization in a reasonable time scale.

Further complexity is added by the shielding effect during RAFT transfer-to. Stenzel and coworkers evaluated the effect of polymerization temperature on star polymer synthesis using RAFT transfer-to.[52] At high CTA concentrations, a marked temperature dependence was observed, with higher temperatures leading to star polymers with MWs in good agreement between theoretical and experimental values. Dispersities of the star polymers did not vary substantially in this CTA concentration regime. In contrast, at low CTA concentrations, star polymer MW was not temperature-dependent, but dispersity values of the star polymers increased with increasing temperature. In addition to radical and chain exchange kinetics, the accessibility of the polymeric radical to the substrate-bound CTAs may also be influenced by temperature. It is therefore important to evaluate the effects of temperature on each system individually.

Pressure

Increasing the pressure in a RAFT polymerization will increase the rate of propagation while decreasing the rate of termination. These changes in rates are attributed to an increase in the rates of chemically controlled reactions whereas the rates of diffusion controlled reactions decrease.78 Pressures up to 2,500 bar have proven to be advantageous in traditional RAFT polymerization, enhancing both the rate and control of the polymerization. High pressures have also proven to be beneficial for transfer-to polymerization. Vana and coworkers evaluated the effect of pressure on star polymer synthesis via RAFT transfer-to polymerization. By employing high pressure (2,600 bar), the amount of dead polymer was reduced by a factor of 2.5 compared to polymerizations

run at atmospheric pressure.[79] This reduction in the amount of dead chains was attributed to an increase in the k_p/k_t ratio.

Shielding Effect/Core Size

The shielding effect is a phenomenon unique to the grafting-to and transfer-to methodologies. For RAFT transfer-to, this concept describes the interactions between large polymeric radicals and the CTAs on the grafting substrate. Steric interactions between these large objects have been observed in multiple systems.[52,56,57,80,81] Most often, high dead polymer quantities and low grafting densities result from a substantial shielding effect.

The shielding effect becomes more prominent when the polymer grafts are large, as is often the case when the RAFT transfer-to polymerization reaches high conversions. This has been observed both experimentally and in silico.[82] For example, Radzinski et al varied the initial [M]/[CTA] ratio utilized in RAFT transfer-to synthesis of a bottlebrush polymer with styrene as the monomer to evaluate the effect of side-chain MW. They observed a relationship between the amount of dead linear polymer that formed during the polymerizations and the initial [M]/[CTA] ratio utilized (Figure 4.6).[63] Because the length of the growing polymeric radicals is related to the [M]/[CTA] ratio, high [M]/[CTA] ratios promote dead polymer formation due to increased side-chain MW leading to greater steric shielding and therefore a greater incidence of termination.

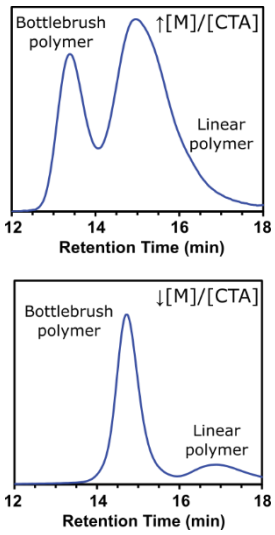

Figure 4.6. Effect of initial [M]/[CTA] ratio (top: 1000:1; bottom: 50:1) on bottlebrush polymer sample composition prepared via RAFT transfer-to using a polymeric dithiocarbamate CTA and styrene as the monomer. Reproduced from Ref. 63 with permission from The Royal Society of Chemistry.

Fröhlich et. al. have demonstrated in silico an exponential relationship between the length of the growing polymer graft, n, and the steric shielding factor, K, as shown in equation 3.82

$$K = A * n^{-0.45} \tag{3}$$

Here, A is a scaling constant and K is defined as:

$$K = \frac{k}{k_0} \tag{4}$$

where k is the rate constant of a bimolecular polymer-polymer reaction and k0 is the rate constant of a similar reaction that is not located at a polymer chain. K is small for high steric shielding and approaches unity in the absence of steric interactions.

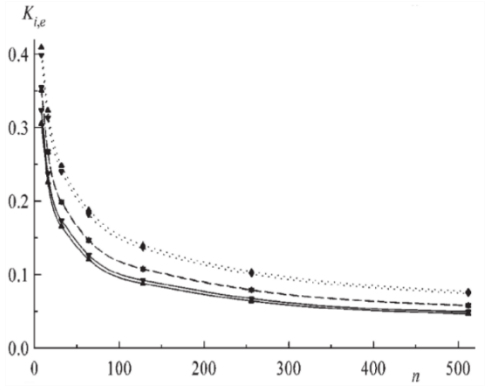

Figure 4.7. Shielding factors as functions of chain length n for polymers with different chain stiffnesses (K falls off faster for stiffer chains). Reproduced from Ref. 82 with permission from WILEY-VCH Verlag GmbH & Co.

The steric shielding factor decreases rapidly as chain length increases before asymptotically approaching zero. As the simulations in Figure 4.7 show, K approaches 0.1 with n ~100, indicating that the rate of addition of a growing polymer radical to a substrate-bound CTA is 10x slower than it would be in the absence of steric interactions. The principal outcome of this effect is an increased probability of termination with increasing polymer molecular weight. It should be noted that the shielding effect can be slightly reduced by increasing the distance between the CTA and the substrate. By expanding the tetrafunctional initiators in their computational model via the addition of non-relaxable segments between the core and the reactive CTA moieties, the researchers observed that the exponent relating the shielding factor and chain length was reduced to -0.43.82

Star-Star Coupling

The RAFT transfer-to mechanism involves the fragmentation of the RAFT adduct radical to yield an unattached polymer radical. Because the polymer racial is not attached to the substrate during propagation, star-star coupling reactions are not expected to occur. However, under certain conditions star-star coupling has been observed.80 Using a hexafunctional

trithiocarbonate CTA, Vana and coworkers synthesized methyl acrylate (MA), butyl acrylate (BA), and dodecyl acrylate (DA) star polymers using the RAFT transfer-to method. At low conversions, high molecular weight star polymers were produced with low dispersity values. However, as conversion increased, SEC analysis revealed high molecular weight byproducts (Figure 4.8A). The origin of these high MW impurities was attributed to star-star coupling that occurs through an intermolecular chain transfer reaction between the propagating radical and arms of the star (chain transfer-to polymer) (Figure 4.8B). This chain transfer event results in the creation of a radical on the arms of the star polymer that can add to a CTA attached to a different star polymer. Star-star coupling during RAFT transfer-to was modeled by kinetic (PREDICI) simulations, and this phenomenon was determined to be monomer dependent. Star-star coupling using RAFT transfer-to polymerization has only been observed with acrylates at high conversions, and this side reaction is generally easily prevented by avoiding conditions that promote chain transfer reactions to polymer.

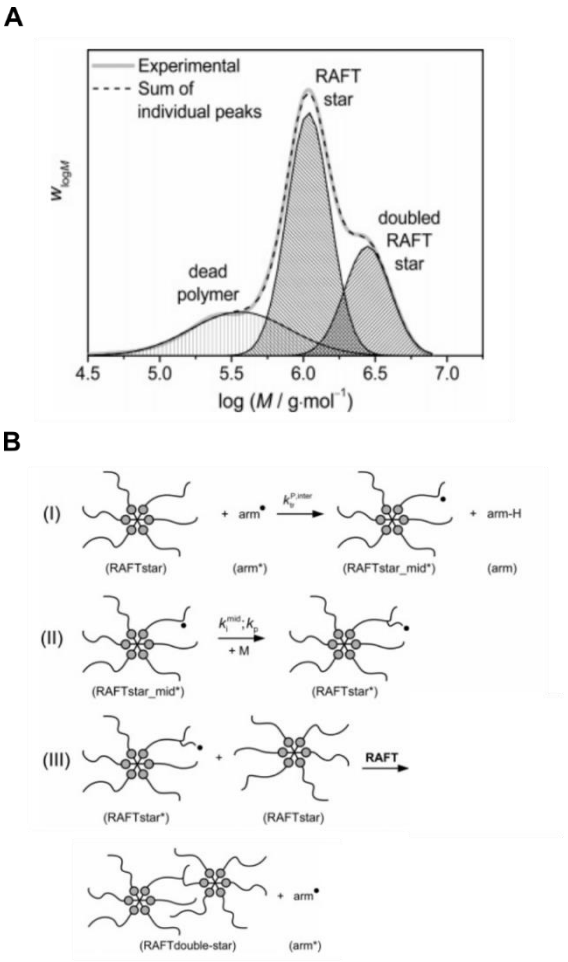

Figure 4.8. (A) Peak fitting of the SEC curve obtained from RAFT transfer-to polymerization of BA from a hexafunctional star polymer initiator. (B) The proposed mechanism for star-star coupling in RAFT transfer-to polymerization, which involves chain transfer-to polymer. Adapted with permission from Boschmann, D.; Vana, P. Macromolecules 2007, 40, 2683. Copyright 2007 American Chemical Society.

4.6 Conclusions

The transfer-to method in brush polymer synthesis is underutilized compared with other synthetic strategies for preparing brush polymers. In this review, we aimed to highlight both the advantages and shortcomings of this method compared with the more commonly used grafting-from method. We also showed how the transfer-to method can be optimized to provide brush

polymers with few imperfections and impurities. Several factors contributing to the structure and sample composition of graft polymers prepared by RAFT transfer-to were discussed, including CTA selection, monomer structure, and reaction conditions such as solvent, temperature, and pressure. To prepare high purity graft polymers using this method, conditions should be chosen that minimize termination and reduce steric shielding. In most cases this can be achieved by choosing RAFT agents have high C_{tr} in the monomer being polymerized, employing low initial [M]/[CTA] ratios, using non-polar solvents, and stopping the polymerization at low conversion. RAFT transfer-to is ideally suited for the functionalization of nano-scale substrates due to the fact that the transfer-to mechanism prevents formation of coupled byproducts except in rare cases. As such, we expect transfer-to to be particularly useful for nanoparticle and protein grafting and star or bottlebrush polymer synthesis. Due to the relative lack of CTAs that are amenable to conducting RAFT transfer-to, the development of a library of CTAs with functional Z-groups could expand the scope of this method.

Acknowledgments

We are grateful to the Army Research Office (W911NF-14-1-0322) and the American Chemical Society Petroleum Research Fund (54884-DNI7) for support of our work in this area.

4.7 References

(1) Kato, K.; Uchida, E.; Kang, E.-T.; Uyama, Y.; Ikada, Y. *Prog. Polym. Sci.* **2003**, *28*, 209.

(2) Siedenbiedel, F.; Tiller, J. C. *Polymers* **2012**, *4*, 46.

(3) Kango, S.; Kalia, S.; Celli, A.; Njuguna, J.; Habibi, Y.; Kumar, R. *Prog. Polym. Sci.* **2013**, *38*, 1232.

(4) Heredia, K. L.; Maynard, H. D. *Org. Biomol. Chem* **2007**, *5*, 45.

(5) Verduzco, R.; Li, X.; Pesek, S. L.; Stein, G. E. *Chem. Soc. Rev.* **2015**, *44*, 2405.

(6) Sheiko, S. S.; Sumerlin, B. S.; Matyjaszewski, K. *Prog. Polym. Sci.* **2008**, *33*, 759.

(7) Xia, Y.; Kornfield, J. A.; Grubbs, R. H. *Macromolecules* **2009**, *42,* 3761.

(8) Radzinski, S. C.; Foster, J. C.; Matson, J. B. *Macromol. Rapid Commun.* **2016**, *37*, 616.

(9) Radzinski, S. C.; Foster, J. C.; Chapleski, R. C.; Troya, D.; Matson, J. B. *J. Am. Chem. Soc.* **2016**, *138*, 6998.

(10) Sumerlin, B. S. *ACS Macro Lett.* **2012**, *1*, 141.

(11) Matyjaszewski, K.; Spanswick, *J. Mater. Today* **2005**, *8*, 26.

(12) Hawker, C. J.; Bosman, A. W.; Harth, E. *Chem. Rev.* **2001**, *101*, 3661.

(13) Moad, G.; Rizzardo, E.; Solomon, D. H. *Macromolecules* **1982**, *15*, 909.

(14) Matyjaszewski, K.; Xia, *J. Chem. Rev.* **2001**, *101*, 2921.

(15) Chiefari, J.; Chong, Y. K.; Ercole, F.; Krstina, J.; Jeffery, J.; Le, T. P. T.; Mayadunne, R. T. A.; Meijs, G. F.; Moad, C. L.; Moad, G.; Rizzardo, E.; Thang, S. H. *Macromolecules* **1998**, *31*, 5559.

(16) Gody, G.; Maschmeyer, T.; Zetterlund, P. B.; Perrier, S. *Nat. Commun.* **2013**, *4*, 2505.

(17) Chong, Y. K.; Le, T. P. T.; Moad, G.; Rizzardo, E.; Thang, S. H. *Macromolecules* **1999**, *32*, 2071.

(18) Mühlebach, A.; Gaynor, S. G.; Matyjaszewski, K. *Macromolecules* **1998**, *31*, 6046.

(19) Hawker, C. J.; Frechet, J. M. J.; Grubbs, R. B.; Dao, J. *J. Am. Chem. Soc.* **1995**, *117*, 10763.

(20) Gaynor, S. G.; Edelman, S.; Matyjaszewski, K. *Macromolecules* **1996**, *29*, 1079.

(21) Gao, H.; Ohno, S.; Matyjaszewski, K. *J. Am. Chem. Soc.* **2006**, *128*, 15111.

(22) Bolton, J.; Rzayev, J. *ACS Macro Lett.* **2012**, *1*, 15.

(23) Cheng, C.; Khoshdel, E.; Wooley, K. L. *Nano Lett.* **2006**, *6*, 1741.

(24) Foster, J. C.; Matson, J. B. *Macromolecules* **2014**, *47*, 5089.

(25) Hoff, E. A.; Abel, B. A.; Tretbar, C. A.; McCormick, C. L.; Patton, D. L. *Polym. Chem.* **2017**.

(26) Chong, Y. K.; Krstina, J.; Le, T. P. T.; Moad, G.; Postma, A.; Rizzardo, E.; Thang, S. H. *Macromolecules* **2003**, *36*, 2256.

(27) Chiefari, J.; Mayadunne, R. T. A.; Moad, C. L.; Moad, G.; Rizzardo, E.; Postma, A.; Thang, S. H. *Macromolecules* **2003**, *36*, 2273.

(28) Keddie, D. *J. Chem. Soc. Rev.* **2014**, *43*, 496.

(29) Chiefari, J.; Chong, Y. K.; Ercole, F.; Krstina, J.; Jeffery, J.; Le, T. P. T.; Mayadunne, R. T. A.; Meijs, G. F.; Moad, C. L.; Moad, G.; Rizzardo, E.; Thang, S. H. *Macromolecules* **1998**, *31*, 5559.

(30) Moad, G.; Rizzardo, E.; Thang, S. H. *Aust. J. Chem.* **2006**, *59*, 669.

(31) Moad, G.; Rizzardo, E.; Thang, S. H. *Aust. J. Chem*. **2009**, *62*, 1402.

(32) Moad, G.; Rizzardo, E.; Thang, S. H. *Aust. J. Chem*. **2012**, *65*, 985.

(33) Perrier, S.; Takolpuckdee, P. *J. Poly. Sci. Part A: Polym. Chem*. **2005**, *43*, 5347.

(34) Barner-Kowollik, C.; Davis, T. P.; Heuts, J. P. A.; Stenzel, M. H.; Vana, P.; Whittaker, M. *J. Poly. Sci. Part A: Polym. Chem.* **2003**, *41*, 365.

(35) Boyer, C.; Stenzel, M. H.; Davis, T. P. *J. Poly. Sci. Part A: Polym. Chem*. **2011**, *49*, 551.

(36) Barner-Kowollik, C.; Perrier, S. *J. Poly. Sci. Part A: Polym. Chem.* **2008**, *46*, 5715.

(37) Wu, T.; Efimenko, K.; Genzer, J. *J. Am. Chem. Soc.* **2002**, *124*, 9394.

(38) Norde, W.; Gage, D. *Langmuir* **2004**, *20*, 4162.

(39) Lecommandoux, S.; Chécot, F.; Borsali, R.; Schappacher, M.; Deffieux, A.; Brûlet, A.; Cotton, J. P. *Macromolecules* **2002**, *35*, 8878.

(40) Berry, G. C.; Kahle, S.; Ohno, S.; Matyjaszewski, K.; Pakula, T. *Polymer* **2008**, *49*, 3533.

(41) Barner-Kowollik, C.; Davis, T. P.; Stenzel, M. H. *Aust. J. Chem.* **2006**, *59*, 719.

(42) Peng, Q.; Lai, D. M. Y.; Kang, E. T.; Neoh, K. G. *Macromolecules* **2006**, *39*, 5577.

(43) Stenzel, M. H.; Zhang, L.; Huck, W. T. S. *Macromolecular Rapid Communications* **2006**, *27*, 1121.

(44) Zhao; Perrier, S. *Macromolecules* **2006**, *39*, 8603.

(45) Zhao, Y.; Perrier, S. *Macromolecular Symposia* **2007**, *248*, 94.

(46) Takolpuckdee, P.; Mars, C. A.; Perrier, S. *Org. Lett.* **2005**, *7*, 3449.

(47) Perrier, S.; Takolpuckdee, P.; Mars, C. A. *Macromolecules* **2005**, *38*, 6770.

(48) Wang, G.-J.; Huang, S.-Z.; Wang, Y.; Liu, L.; Qiu, J.; Li, Y. *Polymer* **2007**, *48*, 728.

(49) Liu, J.; Bulmus, V.; Herlambang, D. L.; Barner-Kowollik, C.; Stenzel, M. H.; Davis, T. P. *Angew. Chemie. Int. Ed.* **2007**, *46*, 3099.

(50) Boyer, C.; Bulmus, V.; Liu, J.; Davis, T. P.; Stenzel, M. H.; Barner-Kowollik, C. *J. Am. Chem. Soc.* **2007**, *129*, 7145.

(51) Boyer, C.; Bulmus, V.; Davis, T. P.; Ladmiral, V.; Liu, J.; Perrier, S. *Chem. Rev.* **2009**, *109*, 5402.

(52) Stenzel, M. H.; Davis, T. P. *J. Poly. Sci. Part A: Polym. Chem.* **2002**, *40*, 4498.

(53) Mori, H.; Ookuma, H.; Endo, T. *Macromol. Symp.* **2007**, 249-250, 406.

(54) Jesberger, M.; Barner, L.; Stenzel, M. H.; Malmström, E.; Davis, T. P.; Barner-Kowollik, C. *J. Poly. Sci. Part A: Polym. Chem.* **2003**, *41*, 3847.

(55) Shi, X.; Zhao, Y.; Gao, H.; Zhang, L.; Zhu, F.; Wu, Q. *Macromolecular Rapid Communications* **2012**, *33*, 374.

(56) Radzinski, S. C.; Foster, J. C.; Matson, J. B. *Polym. Chem.* **2015**, *6*, 5643.

(57) Hernández-Guerrero, M.; Davis, T. P.; Barner-Kowollik, C.; Stenzel, M. H. *Eur. Polym. J.* **2005**, *41*, 2264.

(58) Stenzel, M. H.; Davis, T. P.; Fane, A. G. *J. Mater. Chem.* **2003**, *13*, 2090.

(59) Fleet, R.; McLeary, J. B.; Grumel, V.; Weber, W. G.; Matahwa, H.; Sanderson, R. D. *Eur. Polym. J.* **2008**, *44*, 2899.

(60) Bernard, J.; Favier, A.; Davis, T. P.; Barner-Kowollik, C.; Stenzel, M. H. *Polymer* **2006**, *47*, 1073.

(61) Mayadunne, R. T. A.; Jeffery, J.; Moad, G.; Rizzardo, E. *Macromolecules* **2003**, *36*, 1505.

(62) Boschmann, D.; Mänz, M.; Fröhlich, M. G.; Zifferer, G.; Vana, P. In Controlled/Living Radical Polymerization: Progress in RAFT, DT, NMP & OMRP; *American Chemical Society:* **2009**; Vol. 1024, p 217.

(63) Radzinski, S. C.; Foster, J. C.; Lewis, S. E.; French, E. V.; Matson, J. B. *Polym. Chem.* **2017**, 10.1039/C6PY01982J.

(64) Moad, G.; Rizzardo, E.; Thang, S. H. *Polymer* **2008**, *49*, 1079.

(65) Rizzardo, E.; Chiefari, J.; Mayadunne, R. T. A.; Moad, G.; Thang, S. H. In Controlled/Living Radical Polymerization; American Chemical Society: **2000**; Vol. 768, p 278.

(66) Foster, J. C.; Radzinski, S. C.; Lewis, S. E.; Slutzker, M. B.; Matson, J. B. *Polymer* **2015**, *79*, 205.

(67) Destarac, M.; Brochon, C.; Catala, J.-M.; Wilczewska, A.; Zard, S. Z. *Macromol. Chem. Phys.* **2002**, *203*, 2281.

(68) Perrier, S.; Barner-Kowollik, C.; Quinn, J. F.; Vana, P.; Davis, T. P. *Macromolecules* **2002**, *35*, 8300.

(69) Boschmann, D.; Vana, P. *Polymer Bulletin* **2005**, *53*, 231.

(70) Moad, G.; Mayadunne Roshan, T. A.; Rizzardo, E.; Skidmore, M.; Thang San, H. In Advances in Controlled/Living Radical Polymerization; American Chemical Society: **2003**; Vol. 854, p 520.

(71) Boschmann, D.; Mänz, M.; Pöppler, A.-C.; Sörensen, N.; Vana, P. *J. Poly. Sci. Part A: Polym. Chem.* **2008**, *46*, 7280.

(72) Odian, G. Principles of Polymerization; 4th ed.; John Wiley & Sons, Inc.: New Jersey, 2004.

(73) Benaglia, M.; Rizzardo, E.; Alberti, A.; Guerra, M. *Macromolecules* **2005**, *38*, 3129.

(74) Fröhlich, M. G.; Nardai, M. M.; Förster, N.; Vana, P.; Zifferer, G. *Polymer* **2010**, *51*, 5122.

(75) Walling, C. *J. Poly. Sci.* **1954**, *14*, 214.

(76) Arita, T.; Buback, M.; Vana, P. *Macromolecules* **2005**, *38*, 7935.

(77) Xu, J.; He, J.; Fan, D.; Tang, W.; Yang, Y. *Macromolecules* **2006**, *39*, 3753.

(78) Arita, T.; Buback, M.; Janssen, O.; Vana, P. *Macromolecular Rapid Communications* **2004**, *25*, 1376.

(79) Boschmann, D.; Edam, R.; Schoenmakers, P. J.; Vana, P. *Polymer* **2008**, *49*, 5199.

(80) Boschmann, D.; Vana, P. *Macromolecules* **2007**, *40*, 2683.

(81) Darcos, V.; Dureault, A.; Taton, D.; Gnanou, Y.; Marchand, P.; Caminade, A.-M.; Majoral, J.-P.; Destarac, M.; Leising, F. *Chem. Commun*. **2004**, 2110.

(82) Fröhlich, M. G.; Vana, P.; Zifferer, G. Macromol. *Theory Simul* **2007**, *16*, 610.

Chapter 5: Synthesis of Bottlebrush Polymers via Transfer-To and Grafting-Through Approaches Using a RAFT Chain Transfer Agent with a ROMP-Active Z-Group

S. C. Radzinski, J. C. Foster and J. B. Matson, *Polym. Chem.*, **2015**, *6*, 5643- Published by The Royal Society of Chemistry.

5.1 Authors

Scott C. Radzinski, Jeffrey C. Foster, and John B. Matson.

Department of Chemistry and Macromolecules Innovation Institute, Virginia Tech, Blacksburg, Virginia 24061, United States

5.2 Abstract

A novel dithiocarbamate chain transfer agent (**CTA1**) with a directly polymerizable Z-group was synthesized for use in reversible addition-fragmentation chain transfer polymerization (RAFT). This CTA effectively mediated RAFT polymerization of styrenic and acrylic monomers with dispersities (Đ) < 1.08. Utilizing the polymerizable Z-group on the ω-chain end that is inherited from the RAFT process, bottlebrush polymers were synthesized via ring-opening metathesis polymerization (ROMP) in a grafting-through process. The effect of a number of parameters on the grafting process was studied, and optimized conditions yielded bottlebrush polymers of controllable molecular weights, narrow molecular weight distributions, and high conversions (> 90%). Bottlebrush polymers made by a transfer-to strategy were also synthesized from **CTA1**. In this case, ROMP was first carried out to produce poly(**CTA1**) (**PCTA1**), then RAFT was performed from the **PCTA1** backbone. This technique allows for the preparation of high molecular weight bottlebrush polymers without radical coupling between bottlebrush polymers. Lastly, regardless of the synthetic method, all bottlebrush polymers produced using **CTA1** are composed of polymeric side chains that are attached to the bottlebrush backbone through a labile dithiocarbamate linkage that can be cleaved in the presence of nucleophiles such as amines. The

unique combination of these capabilities allows for the study of bottlebrush polymer formation by both transfer-to and grafting-through strategies using a single agent.

5.3 Introduction

Over the past two decades, bottlebrush polymers have become an increasingly relevant polymer topology as a result of their well-defined structures, shape persistence, nanoscopic dimensions, and unique mechanical and rheological properties.[1] Bottlebrush polymers are comprised of polymeric side-chains grafted to a polymer backbone, and given sufficient grafting density, steric repulsion between polymeric neighbors causes the backbone to adopt a chain-extended conformation.[2,3] Consequently, cylindrical,[4,5] spherical,[6,7] or worm-like,[8] morphologies can be realized in single macromolecules by tuning polymer composition, grafting density, or side-chain molecular weight. Additionally, important polymeric properties, such as amphiphilicity or stimuli-responsiveness, can be extrapolated to bottlebrush systems by tuning the chemical composition of the polymeric side-chains.[9-11] In terms of mechanical properties, bottlebrush polymers differ from linear polymers primarily due to their inability to interact via chain entanglements—a phenomenon from which many of the physical properties of linear polymers arise. Therefore, bottlebrush polymers have garnered interest for use in applications such as rheology modifiers and super-soft elastomers.[12] Lastly, their size and shape-persistence makes bottlebrush polymers well suited for the *in vivo* delivery of therapeutic agents.[13]

Bottlebrush polymers can be prepared via one of four approaches: (1) the grafting-from strategy, whereby polymer side chains are grown from a polymeric backbone decorated with initiating functionalities; (2) the grafting-to methodology involving the attachment of pre-formed polymers to reactive sites on a polymer backbone; (3) the grafting-through or macromonomer (MM)

approach, in which polymers fitted with a polymerizable moiety are utilized as MMs in an subsequent polymerization; and, (4) the transfer-to strategy (sometimes called the RAFT Z-group approach). Transfer-to is a unique hybrid of the grafting-from and grafting-to strategies in which polymeric radicals detach from the bottlebrush backbone, propagate freely in solution, and return to the backbone through a chain-transfer reaction with a pendant CTA.[14] While the grafting-from, grafting-to, and transfer-to strategies yield macromolecules with a bottlebrush topology, the grafting process is hindered by steric interactions between adjacent polymer chains, resulting in low grafting densities.[15] However, despite this shortcoming, grafting-from (and to a greater extent transfer-to) can be employed to synthesize bottlebrush polymers with relatively higher molecular weights (on the order of $\geq 10^6$ Da) than are possible with grafting-through. In contrast, grafting-through results in "perfectly grafted" (i.e. the highest possible grafting density) bottlebrush polymers, as each repeat unit bears a polymeric side chain. In view of the high grafting density and synthetic versatility of the grafting-through technique, recent efforts have focused on its application.[11,16-31]

To prepare well-defined bottlebrush polymers via the grafting-through strategy, reversible-deactivation radical polymerization techniques such as atom transfer radical polymerization (ATRP) and reversible addition-fragmentation chain transfer polymerization (RAFT) are often employed.[1] Generally, semi-telechelic MMs of predefined MW and low dispersity (Đ) are synthesized via one of these techniques. In a second step, the resulting MMs are functionalized with a polymerizable moiety in a post polymerization reaction, and the MMs are subsequently polymerized using an additional polymerization method in the third and final step.[20,23] Alternatively, in a two-step method, MM synthesis can be conducted in the presence of an

initiator or chain-transfer agent (CTA) containing an orthogonal functionality.[17,21,22] For example, norbornene and derivatives thereof have been coupled to dithioester and trithiocarbonate CTAs.[19] In this case, RAFT was utilized to prepare the MM grafts, and ring-opening metathesis polymerization (ROMP) was employed in a subsequent grafting-through step. ROMP is particularly well suited for this purpose because of the high functional group tolerance and rapid propagation rate of several ruthenium-based olefin metathesis catalysts (Figure 5.1).[16] Bottlebrush polymers have been prepared via a combination of these two polymerization techniques in separate steps as described above, or more simply via a one-pot strategy wherein a ROMP catalyst is added to a terminated RAFT reaction mixture.[18]

Figure 5.1. ROMP catalysts used in this work.

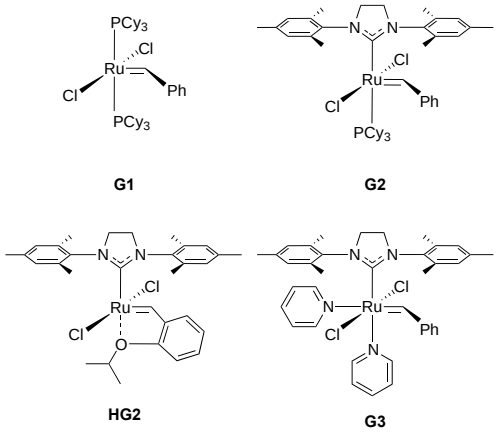

RAFT polymerization is mediated by a thiocarbonylthio-containing agent with an activating Z-group and a leaving group (R-group) that is comparable in radical stability to that of the monomer-derived radical. A number of R- and Z-groups have been utilized to gain control over the RAFT polymerization of a wide range of vinyl monomers.[32] However, to our knowledge, there exists no report in the literature on the incorporation of a directly polymerizable Z-group such as *exo*-norbornene imide into a RAFT agent (Scheme 5.1). We envisioned that such a CTA

(**CTA1**) could be employed in both RAFT transfer-to and ROMP grafting-through methodologies.

Scheme 5.1. Proposed CTA structure with directly polymerizable Z-group.

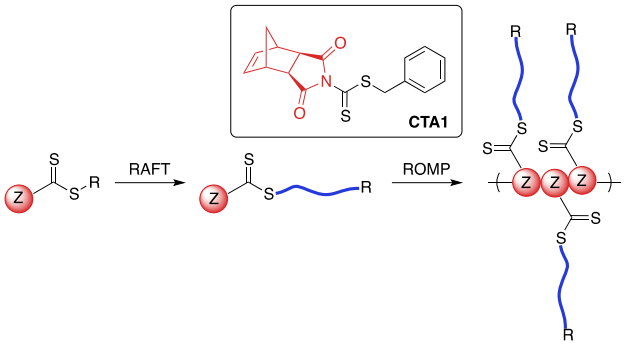

While directly polymerizable R-groups have been incorporated into RAFT CTAs,[18,19] a directly polymerizable Z-group would experience the benefits inherent in the Z-group, or transfer-to, approach.[33-36] Such benefits are a result of the RAFT mechanism when applied in a graft polymerization. During a RAFT transfer-to polymerization, growing polymer chains detach from the bottlebrush polymer backbone during propagation and then add back to the backbone through reaction with a pendant thiocarbonylthio group. Because the growing "arms" are free in solution, coupling between growing adjacent "arms" attached to the bottlebrush backbone does not occur. In addition, radical coupling between growing bottlebrush polymers cannot occur, as the propagating radical resides on the detached polymeric side chains. As a result, the transfer-to approach affords bottlebrush polymers with lower dispersities and higher possible conversions relative to conventional RAFT grafting-from using the R group approach.[36,37] An additional advantage of the incorporation of a directly polymerizable Z-group is the location of the thiocarbonylthio group in the bottlebrush polymer. In the case of bottlebrush polymers prepared from **CTA1**, the thiocarbonylthio group would link the polymeric arms to the backbone polymer, in contrast to systems using directly polymerizable R-groups, which leave the thiocarbonylthio

group on the bottlebrush surface. Given the wealth of literature concerning the post-polymerization removal of RAFT end groups,[38] we envisioned the possibility of thiocarbonylthio degradation-driven side chain dissociation. Herein, we investigate the efficacy of **CTA1** as a mediator of RAFT polymerization and the availability of the norbornene functionality for ROMP. Additionally, we evaluate the preparation of bottlebrush polymers via both transfer-to and grafting-through strategies. Finally, we explore side-chain cleavage by aminolysis to investigate side chain molecular weights and molecular weight distributions.

5.4 Materials and Methods

Materials. All reagents were obtained from commercial vendors and used as received unless otherwise stated. Styrene and *n*-butyl acrylate were passed through small columns of basic alumina prior to use. ROMP catalysts $(PCy_3)_2(Cl)_2Ru{=}CHPh$ (**G1**), $(H_2IMes)(Cl)_2(PCy_3)Ru{=}CHPh$ (**G2**) and $(H_2IMes)(Cl)_2(PCy_3)Ru{=}CH(2\text{-}OiPrPh)$ (**HG2**) were obtained as a generous gift from Materia. ROMP catalyst $(H_2IMes)(pyr)_2(Cl)_2Ru{=}CHPh$ (**G3**) was prepared from **G2** according to literature procedures.[39,40]

Methods. NMR spectra were measured on Agilent 400 MHz or Bruker 500 MHz spectrometers. ^1H and ^{13}C NMR chemical shifts are reported in ppm relative to internal solvent resonances. Yields refer to chromatographically and spectroscopically pure compounds unless otherwise stated. Size exclusion chromatography (SEC) was carried out in THF at 1 mL/min, 30°C on two Agilent PLgel 10 μm MIXED-B columns connected in series with a Wyatt Dawn Helios 2 light scattering detector and a Wyatt Optilab Rex refractive index detector. No calibration standards were used, and dn/dc values were obtained by assuming 100% mass elution from the columns.

Atomic force microscopy (AFM) was conducted using a Veeco BioScope II AFM in tapping mode in air at room temperature using Nano World Pointprobe-silicon SPM Sensor tips (spring constant = 7.4 N/m, resonance frequency = 160 kHz). Dynamic light scattering (DLS) was conducted using a Malvern Zetasizer Nano operating at 25 °C. Polymer solutions were prepared at 1 mg/mL and were filtered with a 0.25 μm filter prior to scanning. The calculations of the particle size distributions and distribution averages were conducted using CONTIN particle size distribution analysis routines. All measurements were made in triplicate and errors reflect standard deviations.

Synthesis of CTA1. KOH (0.60 g, 10.7 mmol) was ground to a fine powder with a mortar and pestle and placed in a 100 mL round bottom flask. To the flask was added *exo*-norbornene imide (1.33 g, 8.15 mmol) followed by 30 mL of DMF. This mixture was stirred for 5 min, followed by dropwise addition of CS_2 (2.46 mL, 40.8 mmol). The solution developed a deep red color. After an additional 3 h of stirring, benzyl bromide (4.84 mL, 40.8 mmol) was added dropwise, and the reaction mixture was stirred at rt for 12 h. The following day, the reaction mixture was diluted with diethyl ether (~50 mL) and washed with H_2O (3 x 150 mL) and brine. The organic layer was dried over Na_2SO_4, and the solvent was removed under reduced pressure. The crude product was purified on a silica gel column, eluting with 1:1 CH_2Cl_2/hexanes, to give 1.30 g of **CTA1** as a yellow solid (48% yield). ^{1}H NMR ($CDCl_3$): δ 1.57 (m, 2H), 2.82 (s, 2H), 3.39 (s, 2H), 4.50 (s, 2H), 6.33 (s, 2H), 7.35 (m, 5H). ^{13}C NMR ($CDCl_3$): δ 199.31, 173.75 138.29, 132.93, 129.34, 128.95, 128.26, 48.27, 46.47, 43.62, 43.22. HRMS (m/z): calculated 330.0617, found 330.0627.

Synthesis of Polystyrene MMs. A typical polymerization procedure of styrene is as follows: To an oven-dried Schlenk tube equipped with a magnetic stir bar was added **CTA1** (29.0 mg, 87.0 μmol), 2,2'-azobis(2-methylpropionitrile)(AIBN) (1.43 mg, 8.73 μmol), styrene (1 mL, 8.7 mmol), and 1 mL of THF. The reaction mixture was deoxygenated by three freeze-pump-thaw cycles. The Schlenk tube was then backfilled with N_2 and submerged in an oil bath maintained at 75 °C. Samples were removed periodically by N_2-purged syringe to monitor molecular weight evolution by SEC and conversion by ^{1}H NMR spectroscopy. The polymerization was quenched by submerging the tube into liquid N_2 and exposing the reaction mixture to air. The resulting polystyrene was purified via precipitation from MeOH (3x).

Synthesis of Poly(n-butyl Acrylate) (nBA) MMs. A typical polymerization procedure of nBA is as follows: To an oven-dried Schlenk tube equipped with a magnetic stir bar was added **CTA1** (46.0 mg, 140 μmol), 2,2'-azobis(2-methylpropionitrile)(AIBN) (2.29 mg, 14.0 μmol), nBA (2 mL, 14 mmol), and 2 mL of THF. The reaction mixture was deoxygenated by three freeze-pump-thaw cycles. The Schlenk tube was then backfilled with N_2 and submerged in an oil bath maintained at 60 °C. Samples were removed periodically by N_2-purged syringe to monitor molecular weight evolution by SEC and conversion by ^{1}H NMR spectroscopy. The polymerization was quenched by submerging the tube into liquid N_2 and exposing the reaction solution to air. The resulting poly(nBA) was purified via precipitation from hexanes (3x).

Synthesis of Poly(CTA1) (PCTA1). A typical polymerization procedure of **CTA1** is as follows: **CTA1** (109 mg, 329 μmol) was dissolved in 1.5 mL of anhydrous CH_2Cl_2 in a 1-dram vial. A solution of **G3** in anhydrous CH_2Cl_2 was prepared at 9.6 mg/mL in a second vial. 0.5 mL of this

G3 soln was added rapidly to the vial containing **CTA1**. The polymerization was quenched after 20 min by adding of 1-3 drops of ethyl vinyl ether. The polymer was isolated via precipitation from hexanes and dried under vacuum to yield 93 mg of pure polymer as an off-white powder (85% yield).

Synthesis of Poly(CTA1-*g*-styrene) by RAFT transfer-to. To an oven-dried Schlenk tube equipped with a magnetic stir bar was added poly(**CTA1**) (22.0 mg, 873 μmol, M_n = 25 100 g/mol), 2,2'-azobis(2-methylpropionitrile)(AIBN) (0.014 mg, 0.087 μmol), styrene (5 mL, 43 mmol), and 5 mL of THF. The reaction mixture was deoxygenated by three freeze-pump-thaw cycles. The Schlenk tube was then backfilled with N_2 and submerged in an oil bath maintained at 75 °C. Samples were removed periodically by N_2-purged syringe to monitor molecular weight evolution by SEC and conversion by ^{1}H NMR spectroscopy. The polymerization was quenched by submerging the tube into liquid N_2 and exposing the reaction solution to air. The resulting poly(**CTA1**-*g*-styrene) was purified via precipitation from MeOH.

Synthesis of Poly(CTA1-*g*-styrene) by RAFT grafting-through. A typical grafting-through polymerization procedure is as follows: To a vial containing **MM** in anhydrous CH_2Cl_2 was added rapidly a soln of **G3** in anhydrous CH_2Cl_2 to make a final polymer concentration of 100 mg/mL. The polymerization was stirred at rt. After 1 h, the polymerization was quenched by adding 1-3 drops of ethyl vinyl ether. The resulting bottlebrush polymer was isolated via precipitation from a MeOH/H_2O mixture and dried under vacuum.

Aminolysis of bottlebrush polymers. Bottlebrush polymer was dissolved in 0.3 mL of THF in a 1-dram vial equipped with a stir bar. To the vial was added 0.3 mL of a 40 w/v % soln of methylamine in H_2O. The reaction mixture was stirred at rt in air for 72 h to ensure complete thiol oxidation. A few drops of THF were added to dissolve the precipitated solids, and the resulting aminolyzed side chains were isolated via precipitation from MeOH and were dried under vacuum overnight.

5.5 Results and Discussion

CTA1 Synthesis. CTA1 was synthesized in one-pot starting from *exo*-norbornene imide (see Supporting Information for further details) as shown in Scheme 5.2. The reaction proceeds via the potassium hydroxide-assisted attack of the imide nitrogen on carbon disulfide, forming a dithiocarbamate salt. In the second step, the dithiocarbamate intermediate reacts with benzyl bromide in a substitution reaction to yield the desired product.

Scheme 5.2. One-pot synthesis of **CTA1**.

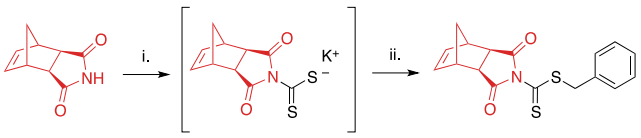

[a]Experimental conditions: (i) CS_2, KOH, DMF; (ii) benzyl bromide.

Column purification was required to remove unreacted starting materials, and isolated yields ranged from 35-48%. While this range is lower than reported values for the synthesis of other dithiocarbamates,[41,42] many such CTAs are derived from electron-rich secondary amines in contrast to the relatively electron-deficient imide employed in our study. This electron-deficiency results in the limited nucleophilicity of the imide nitrogen,[43] hindering its addition to

electrophiles such as CS_2. Longer reaction times or increased temperatures were not found to increase yields.

RAFT Polymerization. The success of a RAFT polymerization is tied to many factors, chief among which is the matching of monomer reactivity to that of the CTA.[44-48] More activated monomers (MAMs) (i.e., methacrylates, acrylates, styrenes) require electron deficient C=S bonds, such as those present in dithioester and trithiocarbonate RAFT agents, while less activated monomers (LAMs) (i.e., vinyl esters and amides) can only be polymerized in the presence of more electron rich thiocarbonyl-containing compounds such as xanthates. In fact, reaction of LAMs with dithiobenzoate or certain trithiocarbonate CTAs can result in complete inhibition of polymerization.[49] The use of *N*-pyrrolyl and *N*-phthalimidyl moieties as Z-groups in dithiocarbamate RAFT CTAs was first reported by Cheifari and coworkers.[50] These CTAs are suitable for controlling the polymerization of many MAMs.[47,51-53] Therefore, we envisioned that **CTA1** could be employed to mediate the polymerization of this class of vinyl monomers.

To evaluate our hypothesis, RAFT polymerizations of styrene and *n*-butyl acrylate (nBA) were carried out in the presence of **CTA1** (Scheme 5.3). The polymerizations were conducted in THF (1:1 v/v% THF/monomer) at 75 °C for styrene or 60 °C for nBA in the presence of 2,2'-azobis(isobutyronitrile) (AIBN). To maintain a high level of chain end fidelity, a [CTA]/[AIBN] ratio of 10:1 was chosen.[54] Kinetic analysis was performed by removing aliquots of the polymerization solution at various time points via N_2-purged syringe. The polymerizations were quenched by exposing the reaction mixture to air and submerging the reaction vessel into liquid N_2. Molecular weight (MW) and dispersity (Đ) were determined by size-exclusion

chromatography (SEC), and conversions were measured by ^{1}H NMR spectroscopy. **CTA1**-mediated RAFT polymerization of styrene and nBA yielded polymers of controllable molecular weights with narrow molecular weight distributions (Đ < 1.08). As previously reported for similar dithiocarbamate CTAs,[55] polymerization of methyl methacrylate was uncontrolled. On the opposite end of the monomer reactivity spectrum, polymerization of vinyl acetate was completely inhibited in the presence of **CTA1**.

Scheme 5.3. CTA1-mediated RAFT polymerization of styrene or nBA.

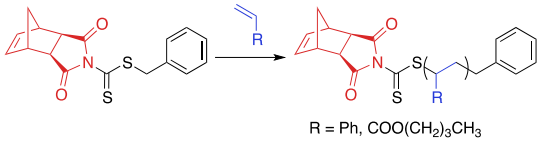

[a]Experimental conditions: AIBN, THF, 75 °C for styrene or 60 °C for nBA.

Kinetic analysis of **CTA1**-mediated polymerization of styrene and nBA is shown in Figure 5.2. Molecular weight distributions determined by SEC were monomodal with low Đ, indicative of a well-controlled polymerization and a high chain transfer efficiency of **CTA1** under the conditions investigated. Conversion increased linearly with time for nBA, and Đ decreased over the course of the reaction for both nBA and styrene. In the case of styrene, a non-linear relationship was observed in the semi-logarithmic plot (Figure 5.2C) and a maximum conversion of only 48% was obtained after 24 h, indicative of the occurrence of termination reactions during the polymerization. The polymerization was repeated under more dilute conditions (2:1 v/v% THF/styrene), resulting in a reduction of termination reactions and a higher terminal conversion (81% after 24 h). For both monomers, the linear relationship between MW and conversion corroborated the controlled nature of the polymerization (Figure 5.2D).

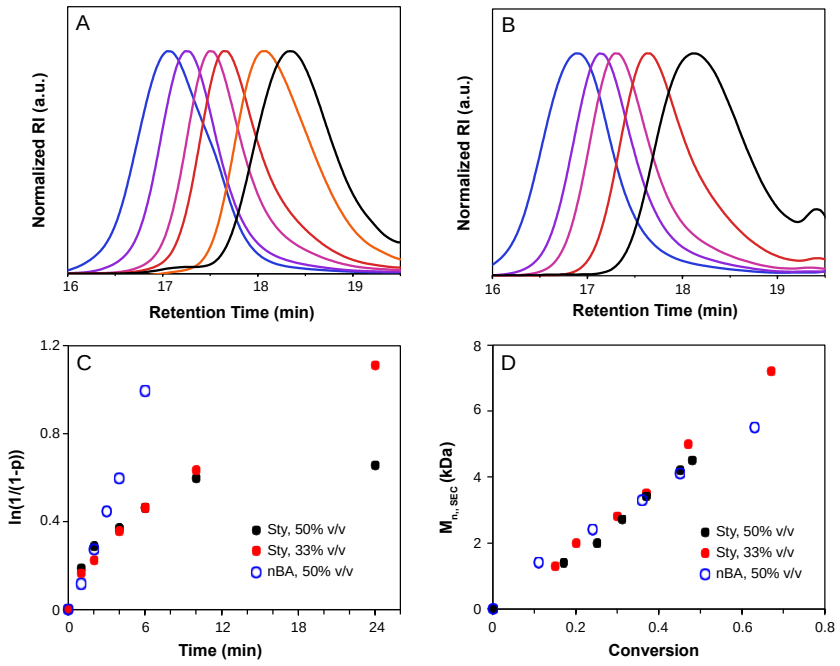

Figure 5.2. Kinetic analysis of **CTA1**-mediated RAFT polymerization. A and B) SEC traces show evolution of MW during the polymerizations of styrene (A) and nBA (B). C) ln(1/(1-p)) vs. time for the polymerization of styrene ([styrene]/[CTA]/[I] = 100:1:0.1, 50% v/v in THF, 75 °C, black circles; [styrene]/[CTA]/[I] = 100:1:0.1, 33% v/v in THF, 75 °C, red circles) and nBA ([nBA]/[CTA]/[I] = 100:1:0.1, 50% v/v in THF, 60 °C, blue open circles). D) M_n as a function of conversion for the polymerization of styrene and nBA.

Chain extension of a polymer prepared using **CTA1** was attempted to further validate its capability to mediate controlled RAFT polymerization. For the first block, poly(nBA) of MW = 6900 Da (Đ = 1.06) was synthesized using **CTA1**. This polymerization yielded a macroCTA with a dithiocarbamate at the ω-chain end. The poly(nBA) macroCTA was utilized in a second step to control the polymerization of styrene ([M]/[CTA]/[AIBN] = 1000:1:0.1), ultimately resulting in the formation of a block copolymer. After 4 h, the polymer had grown to 27.0 kDa as

measured by SEC (Đ = 1.05) (Figure 5S9). This measured MW agreed with the expected value of 26.6 kDa based on conversion as measured by ^{1}H NMR spectroscopy.

To prepare macromonomers for ROMP grafting-through, a series of polymers of differential MW were synthesized, and the isolated polymers were characterized by SEC and ^{1}H NMR spectroscopy (Figures 5S8 and 5S10). A summary of our analysis is provided in Table 5.1. The subscripts in the polymer name assignments refer to the degree of polymerization of the polystyrene component of the macromonomers. Polymers with relatively narrow molecular weight distributions were obtained. In addition, MWs measured by SEC were in good agreement with those calculated from conversion using ^{1}H NMR spectroscopy.

Table 5.1. Polystyrene MMs prepared by RAFT polymerization.

Polymer[a]	$M_{n\ (SEC)}$ (Da)	$M_{n\ (theo)}$[b] (Da)	Đ
MM_{29}	3,300	3,100	1.05
MM_{52}	5,700	6,000	1.02
MM_{113}	12,100	13,300	1.04

[a]Average degree of polymerization shown as a subscript calculated from SEC data using the formula DP = $(M_n\text{-}MW_{CTA})/MW_{styrene}$. [b]Determined by ^{1}H NMR spectroscopy using the formula $M_{n\ (theo)} = MW_{styrene} * ([styrene]/[CTA]) * \%\ conv$

An important outcome of **CTA1**-mediated RAFT polymerization is the preservation of the reactive norbornene olefin moiety on the ω-end of the resulting polymer chain, allowing for subsequent bottlebrush formation via ROMP grafting-through. The orthogonality of the norbornene olefin with reversible deactivation radical polymerization has been previously

shown.[56] The poor reactivity of the internal norbornene olefin in RAFT relative to the terminal, vinyl groups of acrylic monomers is attributed to their differences in electronics. ^{1}H NMR spectroscopic analysis of the pure MMs confirmed the preservation of the norbornene olefin, evident as a singlet at 6.2 ppm (Figure 5S8).

RAFT Transfer-To. There exist four methodologies for preparing bottlebrush polymers, and careful consideration is warranted to select the best strategy for a given system. For example, adoption of a grafting-through approach is appropriate when high grafting density is needed. However, bottlebrush formation via grafting-through is hindered by high MW macromonomers, limiting the use of this strategy to applications in which bottlebrushes with relatively short side chains are acceptable.[57] In contrast, the transfer-to technique allows for the synthesis of bottlebrush polymers with high MW side chains, but can potentially suffer from broad side chain dispersities and lower than "perfect" grafting densities due to termination reactions during the polymerization.[58]

Scheme 5.4. Preparation of bottlebrush polymers from **CTA1** by transfer-to or grafting-through.

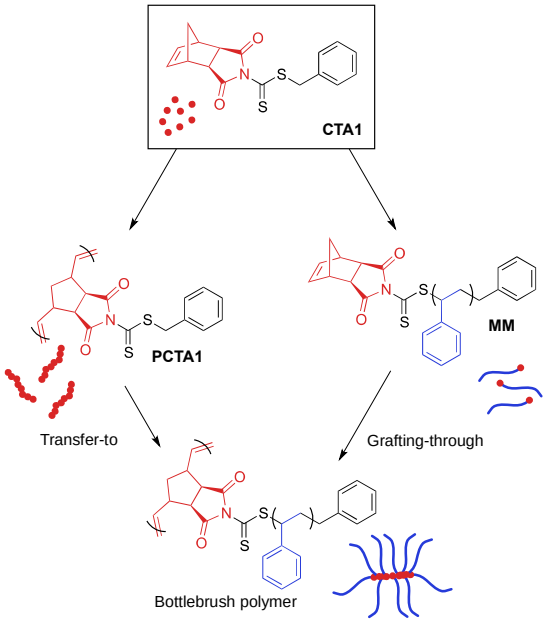

CTA1 can be utilized for both transfer-to and grafting-through strategies, creating a unique opportunity to evaluate the differences between these two techniques while using identical chemistry. To evaluate the ability of **CTA1** to control the growth of high MW side chains from a polymeric backbone by RAFT transfer-to, **CTA1** was first polymerized by ROMP (Scheme 5.4) using Grubbs' 3rd generation catalyst ($(H_2IMes)(Cl)_2(pyr)_2Ru$=CHPh) (**G3**) (50:1 [**CTA1**]/[**G3**]) to yield a poly(**CTA1**) (**PCTA1**) consisting of a poly(norbornene) backbone with a dithiocarbamate group on each repeat unit (Figures 5.3 and 5S7). Following our characterization of the resulting polymeric CTA, **PCTA1** was then subjected to RAFT polymerization conditions ([styrene]/[macroCTA]/[AIBN] = 50,000:1:0.1, THF, 75 °C), and the progress of the reaction was monitored by SEC. Molecular weight distributions of the growing bottlebrush polymer were monomodal, and the corresponding polymers exhibited successively shorter retention times, indicative of increasing MW (Figure 5.3). After 91 h, the polymer had grown from 25.1 kDa (for

PCTA1) to 1250 kDa, with Đ remaining low (< 1.02) throughout the course of the polymerization. A second peak in the SEC traces at ~15 min corresponds to dead polymer arising from termination reactions between detached polymeric radicals. This phenomenon is discussed in further detail below.

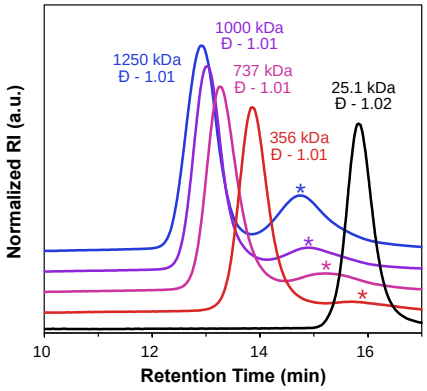

Figure 5.3. RAFT transfer-to mediated by **PCTA1** (black trace), sampled at 19 h (red trace), 42 h (magenta trace), 67 h (purple trace), and 91 h (blue trace). Starred peaks correspond to "dead" polymer. Baselines are shifted for clarity.

ROMP Grafting-Through. The presence of a strained, cyclic olefin at the ω-chain end of polymers prepared via RAFT using **CTA1** allows for the direct synthesis of bottlebrush polymers by ROMP. In order to prepare bottlebrush polymers by ROMP, polystyrene MMs were precipitated three times from THF into methanol to ensure the complete removal of styrene, which can participate in olefin metathesis in the presence of Ru catalysts.[59] The existence of residual styrene during ROMP has been shown to result in chain transfer and a broadening of the molecular weight distribution.[60] Therefore, MM purity was confirmed by monitoring the disappearance of styrene olefin peaks at 5.5 and 5.0 ppm by ^{1}H NMR spectroscopy between precipitations.

A series of Ru-based metathesis catalysts were evaluated for their efficacy towards the grafting-through polymerization of **CTA1**-derived polystyrene (**MM_{29}**)(Scheme 5.4). Toward this end, ROMP of **MM_{29}** was conducted in the presence of various ROMP catalysts at a [MM]/[catalyst] ratio of 50 : 1 (Figure 5S11). Grafting-through polymerizations initiated by Grubbs' 1st ((PCy_3)$_2$(Cl)$_2$Ru=CHPh) (**G1**) and 2nd generation ((H_2IMes)(Cl)$_2$(PCy_3)Ru=CHPh) (**G2**) catalysts showed poor conversion to the corresponding bottlebrush polymer after 1 h in CH_2Cl_2 (Table 5.2, entries 1 and 2, respectively). The Hoveyda-Grubbs' 2nd generation catalyst ((H_2IMes)(Cl)$_2$(PCy_3)Ru=CH(2-OiPrPh)) (**HG2**) effected higher conversion to bottlebrush polymer (78%); however, the resulting polymer had a broad molecular weight distribution (Đ = 1.50) (Table 5.2, entry 3). Grafting-through by the modified Grubbs' 2nd generation catalyst (**G3**) showed 91% conversion to bottlebrush polymer with Đ = 1.03 and a monomodal molecular weight distribution (Table 5.2, entry 5). Based on this analysis, **G3** was utilized for further experiments.

Table 5.2. Investigation of the effect of catalyst, MW, and MM concentration on conversion to bottlebrush.

entry	MM	MM $M_{n,SEC}$ (kDa)[a]	cat.	[MM]/[I]	[MM] (mg/mL)	%conv to BB[b]	BB $M_{n,theo}$ (kDa)[c]	BB $M_{n,SEC}$ (kDa)[a]	BB Đ[a]
1	**MM_{29}**	3.3	**G1**	50:1	100	8	13.2	21.1	1.11
2	**MM_{29}**	3.3	**G2**	50:1	100	16	26.4	353	1.48
3	**MM_{29}**	3.3	**HG2**	50:1	100	78	129	334	1.50
4	**MM_{29}**	3.3	**G3**	25:1	100	91	75.0	85.6	1.04
5	**MM_{29}**	3.3	**G3**	50:1	100	91	150	152	1.03
6	**MM_{29}**	3.3	**G3**	75:1	100	89	220	240	1.14
7	**MM_{29}**	3.3	**G3**	100:1	100	87	330	340	1.25
8	**MM_{29}**	3.3	**G3**	50:1	25	70	116	100	1.10
9	**MM_{29}**	3.3	**G3**	50:1	50	80	132	125	1.09
10	**MM_{52}**	5.6	**G3**	50:1	100	65	182	190	1.09
11	**MM_{113}**	12.1	**G3**	50:1	100	40	242	180	1.16

[a]Measured by SEC using absolute MW determination by light scattering. [b]Determined from SEC by comparing the integrations of BB and MM peaks. [c]Calculated using the formula % conv*([M]/[I])*$M_{n,\,MM}$. Polymerizations conducted for 1 h in CH_2Cl_2.

Macromonomer MW was found to influence ROMP grafting-through polymerization (Table 5.2, entries 5, 10-11, Figure 5S12). Comparing the grafting-through polymerization of three MMs of differing MW (3.3 KDa, 5.6 KDa, and 12 KDa) revealed an inverse correlation between MW and conversion. This observed dependence of conversion on MW is attributed to steric factors.[57]

The MW of the isolated bottlebrush polymer made from **MM$_{29}$** was 152 kDa, which is in good agreement with the expected molecular weight of 150 kDa. Despite lower conversions, polymerizations of **MM$_{52}$** and **MM$_{113}$** showed reasonable agreement between theoretical and observed M_n values and maintained fairly low dispersities.

To further confirm the livingness of grafting-through polymerization of **CTA1**-derived MMs, the [**MM$_{29}$**]/[**G3**] ratio was varied from 25:1 to 100:1 (Table 5.2, entries 4-7). The resulting bottlebrush polymers were monomodal and their SEC traces exhibited the expected inverse relationship between MW and retention time (Figure 5.4A). M_n values determined by SEC are in good agreement with theoretical MWs. A plot of M_n vs [M]/[I] showed the anticipated linear trend (Figure 5.4B).[61] Additionally, dispersity values were low, ranging from 1.04-1.25 throughout the series.

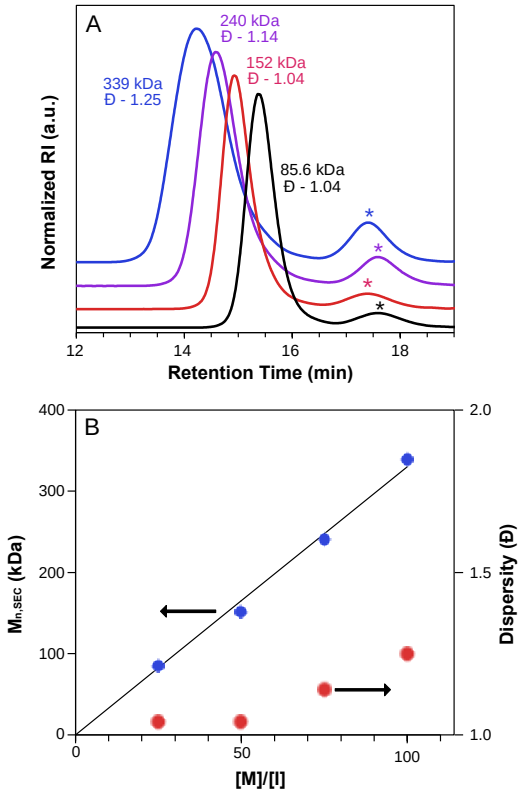

Figure 5.4. Assessment of the livingness of ROMP grafting-through of **MM$_{29}$**. A) SEC traces illustrating the increase in MW with increasing [MM]/[**G3**] ratio (black = [25]:[1], red = [50]:[1], purple = [75]:[1], blue = [100]:[1]). Starred peaks are assigned to residual MMs. Baselines are shifted for clarity. B) Plot of MW vs [M]/[I] ratio. The black line represents the theoretical MW for each [MM]/[**G3**].

Macromonomer concentration was shown to have a small but significant influence on the conversion to bottlebrush polymer (Table 5.2, entries 5, 8-9, Figure 5S13). Measured conversions varied from 70% to 80% to 91% for the evaluated concentration range (25 mg/mL to 100 mg/mL), with increasing concentration resulting in higher conversion to BB.

It is important to note that MM conversion could not be increased beyond 91%, even under optimized conditions. Given the wealth of literature regarding the dependence of RAFT chain-end fidelity on a number of factors including [M]/[I] and [CTA]/[I] ratios,[49] it can be hypothesized that the observed conversion limit of 91% originates from the existence of "non-living" chains, or those that do not possesses a thiocarbonylthio group on the ω-chain end, in the MM samples. It has been shown that ca. 8% of polymer chains prepared by RAFT polymerization under similar conditions are of this "non-living" type.[54,62] Polymers of this "non-living" variety do not possess a norbornene on the chain end and thus will not polymerize during ROMP grafting-through.

Aminolysis of Bottlebrush Polymers. The dithiocarbamate linkage is susceptible to reaction with nucleophiles such as amines.[38] Reaction of this functional group proceeds via an addition-elimination mechanism, resulting in detachment of polymeric side chains and their replacement by the nucleophile. The displaced side chains bear thiol groups at their ω-chain ends, which oxidize in air to form disulfide linkages between polymer chains.[38,63] Therefore, nucleophilic displacement initially yields a mixture of free side chains, side chain dimers, and the poly(norbornene) bottlebrush backbone. Over time, the remaining thiol-terminated polymers become quantitatively oxidized. Disulfide reduction is possible, but this process generally requires elevated temperatures and long reaction times.[64]

Scheme 5.5. Displacement of polymeric side chains by methylamine.

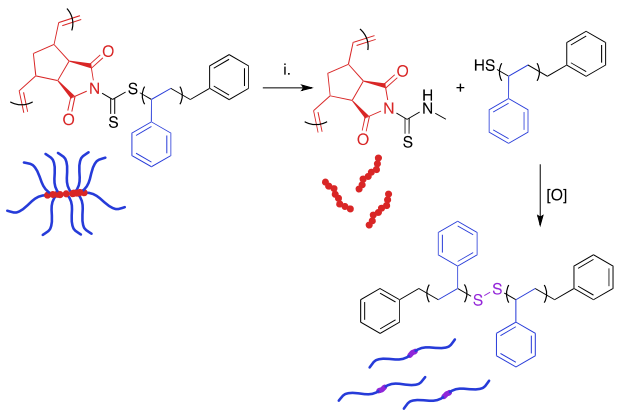

Experimental conditions: (i) CH_3NH_2, H_2O/THF.

Table 5.3. RAFT transfer-to mediated by **PCTA1** and subsequent aminolysis.

polymerization time (h)	$M_{n,\,SEC}$ (kDa)[a]	Đ[a]	$M_{n,\,sidechains\ theo}$ (kDa)[b]	$M_{n,\,sidechains\ SEC}$ (kDa)[a]	$Đ_{Aminolysis}$[a]
0	25.1	1.02	---	---	---
19	356	1.01	4.7	19.5	1.15
42	737	1.01	9.9	35.5	1.21
67	1000	1.01	13.2	47.4	1.23
91	1250	1.01	16.5	56.9	1.28

[a]Measured by SEC using absolute MW by light scattering. [b]Determined using the formula: $M_{n,sidechains} = M_{n,\,BB}/DP_{\mathbf{MCTA1}}$.

The presence of the dithiocarbamate moiety adjacent to the bottlebrush backbone allowed for the cleavage of the polystyrene side chains (Scheme 5.5). A series of bottlebrush polymers prepared by RAFT transfer-to were dissolved in THF and exposed to a 40% w/v solution of methylamine

in H_2O for 72 h. The resulting mixture of backbone and dimerized side chain polymers was separated from residual reactants via precipitation. SEC analysis of the aminolyzed bottlebrush polymers showed a clean shift of the molecular weight distribution to a longer retention time, indicating that the side chains had been quantitatively cleaved (Figure 5S14). Interestingly, the measured MWs of the dissociated side chains were higher than the expected values calculated by dividing the experimental BB MW by the DP of **PCTA1** (Table 5.3). We attribute this deviation to three independent phenomena. First, oxidation of ω-chain end thiols liberated during aminolysis resulted in disulfide bond formation, as has been previously reported.[63] This reaction doubles the observed molecular weight of the side chains. Second, increased steric crowding of the dithiocarbamate CTAs near the bottlebrush backbone by the attached polystyrene sidechains likely led to radical termination reactions between detached polymeric radicals during the transfer-to process, as has also been observed.[65,66] This side reaction not only yielded a significant amount of dead polymer, evident as a low MW peak in the SEC trace (Figure 5.3), but also likely resulted in lower than perfect grafting density and a higher than expected average side chain MW. Lastly, "dead" polymer arising during the RAFT polymerization is also incorporated into this sample. Although the concentration of "dead" polymer is surely eclipsed by the more abundant aminolyzed sidechains, these "dead" polymer chains could explain the observed broadening of the molecular weight distributions of the aminolyzed polymers relative to those of the bottlebrush polymers prior to aminolysis. While ultrahigh MW polymers can be obtained via RAFT transfer-to, the limitations of this methodology (i.e., limited control over grafting density) are made clear by this aminolysis experiment.

To further evaluate bottlebrush polymers prepared by the grafting-through approach, we subjected these polymers to aminolysis as well. ROMP of **MM$_{29}$** at a [MM]/[I] ratio of 50:1 was carried out to give a BB with degradable side chain linkages. A MW of 164 kDa was determined for the BB, with Đ = 1.07 (Figure 5.6). Aminolysis of the BB proceeded rapidly and quantitatively at rt in the presence of an excess of methylamine in THF/H_2O. SEC analysis of the precipitated reaction mixture revealed a narrow molecular weight distribution and a MW approximately double that of the starting MM (5400 Da, Đ = 1.01), as expected for polystyrene side chain disulfide dimers. Quantitative aminolysis was confirmed by the complete disappearance of the bottlebrush peak in the SEC trace. Additionally, DLS analysis of the cleaved bottlebrushes exhibited a shift in the size of the macromolecules from 11.8 ± 3.1 nm for the BB to 2.6 ± 0.4 nm for the dissociated side chain dimers (original **MM$_{29}$** = 2.0 ± 0.5 nm) (Figure 5S15).

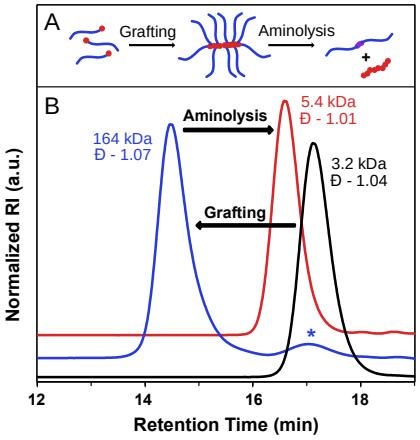

Figure 5.6. A) Graphical representation of grafting-through and aminolysis. B) BB synthesis by ROMP grafting-through (blue trace) from **MM$_{29}$** (black trace) and subsequent aminolysis with methylamine (red trace). The starred peak corresponds to residual MM. Baselines are shifted for clarity.

5.6 Conclusions

A novel RAFT CTA with a directly polymerizable Z-group was prepared in a one-pot synthesis from an *exo*-norbornene imide. **CTA1**-mediated RAFT polymerizations of styrene and nBA were conducted successfully, yielding polymers of controllable MW and low dispersity bearing a polymerizable norbornene moiety on the ω-chain end. We demonstrated that **CTA1** could be utilized effectively for transfer-to and grafting-through methodologies, with the former resulting in high MW bottlebrush polymers (1250 kDa). Polystyrene MMs prepared using **CTA1** were polymerized by ROMP via a grafting-through strategy. In general, ROMP polymerization of **CTA1**-derived MMs proceeded efficiently when catalyzed by Grubbs' 3rd generation catalyst, with conversions on the order of 70-90%. Macromonomer MW, concentration, and the [MM]/[catalyst] ratio of the polymerization were found to influence the conversion to BB. In general, an inverse relationship between MW of the MM and the conversion to BB was observed, with the smallest MM (3300 Da) resulting in the highest conversion. Increasing the MM concentration from 25 to 100 mg/mL also enhanced conversion, while increasing the [MM]/[**G3**] ratio from 25:1 to 100:1 resulted in decreased conversion and a broadening of the molecular weight distribution. Side chain scission via aminolysis was quantitative and revealed significant differences between the bottlebrush polymers prepared by the two different approaches. **CTA1** is unique in that it allows for the preparation of bottlebrush polymers utilizing functionality built into the chain-transfer agent. We expect **CTA1** will prove to be useful for the facile preparation of bottlebrush polymers possessing inherent side chain lability via the transfer-to or grafting-through approach.

Acknowledgements

This work was supported by the Virginia Tech Department of Chemistry. We also thank Oak-Ridge Associated Universities for partial support of this work (Powe Junior Faculty Enhancement Award).

5.7 References

(1) Sheiko, S. S.; Sumerlin, B. S.; Matyjaszewski, K. *Prog. Polym. Sci.* **2008**, *33*, 759.

(2) Grigoriadis, C.; Nese, A.; Matyjaszewski, K.; Pakula, T.; Butt, H.-J.; Floudas, G. *Macromol. Chem. Phys.* **2012**, *213*, 1311.

(3) Pietrasik, J.; Sumerlin, B. S.; Lee, H.-i.; Gil, R. R.; Matyjaszewski, K. *Polymer* **2007**, *48*, 496.

(4) Yuan, J.; Lu, Y.; Schacher, F.; Lunkenbein, T.; Weiss, S.; Schmalz, H.; Muller, A. H. E. *Chem. Mater.* **2009**, *21*, 4146.

(5) Bolton, J.; Rzayev, J. *ACS Macro Lett.* **2012**, *1*, 15.

(6) Pesek, S. L.; Li, X.; Hammouda, B.; Hong, K.; Verduzco, R. *Macromolecules* **2013**, *46*, 6998.

(7) Dalsin, S. J.; Hillmyer, M. A.; Bates, F. S. *ACS Macro Lett.* **2014**, *3*, 423.

(8) Wintermantel, M.; Gerle, M.; Fischer, K.; Schmidt, M.; Wataoka, I.; Urakawa, H.; Kajiwara, K.; Tsukahara, Y. *Macromolecules* **1996**, *29*, 978.

(9) Lee, H.-i.; Pietrasik, J.; Sheiko, S. S.; Matyjaszewski, K. *Prog. Polym. Sci.* **2010**, *35*, 24.

(10) Nese, A.; Li, Y.; Averick, S.; Kwak, Y.; Konkolewicz, D.; Sheiko, S. S.; Matyjaszewski, K. *ACS Macro Lett.* **2011**, *1*, 227.

(11) Li, Y.; Themistou, E.; Zou, J.; Das, B. P.; Tsianou, M.; Cheng, C. *ACS Macro Lett.* **2011**, *1*, 52.

(12) Matyjaszewski, K.; Tsarevsky, N. V. *Nat Chem* **2009**, *1*, 276.

(13) Johnson, J. A.; Lu, Y. Y.; Burts, A. O.; Lim, Y.-H.; Finn, M. G.; Koberstein, J. T.; Turro, N. J.; Tirrell, D. A.; Grubbs, R. H. *J. Am. Chem. Soc.* **2010**, *133*, 559.

(14) Sumerlin, B. S. *ACS Macro Lett.* **2011**, *1*, 141.

(15) Minko, S. In *Polymer Surfaces and Interfaces*; Stamm, M., Ed.; Springer Berlin Heidelberg: 2008, p 215.

(16) Bielawski, C. W.; Grubbs, R. H. *Angew. Chem.* **2000**, *112*, 3025.

(17) Hawker, C. J.; Mecerreyes, D.; Elce, E.; Dao, J.; Hedrick, J. L.; Barakat, I.; Dubois, P.; Jérôme, R.; Volksen, W. *Macromol. Chem. Phys.* **1997**, *198*, 155.

(18) Li, A.; Ma, J.; Sun, G.; Li, Z.; Cho, S.; Clark, C.; Wooley, K. L. *J. Polym. Sci., Part A: Polym. Chem.* **2012**, *50*, 1681.

(19) Li, Z.; Ma, J.; Cheng, C.; Zhang, K.; Wooley, K. L. *Macromolecules* **2010**, *43*, 1182.

(20) Masuda, E.; Kishiro, S.; Kitayama, T.; Hatada, K. *Polym J* **1991**, *23*, 847.

(21) Moughton, A. O.; Sagawa, T.; Gramlich, W. M.; Seo, M.; Lodge, T. P.; Hillmyer, M. A. *Polym. Chem.* **2013**, *4*, 166.

(22) Neugebauer, D.; Zhang, Y.; Pakula, T.; Sheiko, S. S.; Matyjaszewski, K. *Macromolecules* **2003**, *36*, 6746.

(23) Xia, Y.; Kornfield, J. A.; Grubbs, R. H. *Macromolecules* **2009**, *42*, 3761.

(24) Kim, K. O.; Choi, T.-L. *Macromolecules* **2013**, *46*, 5905.

(25) Kim, K. O.; Shin, S.; Kim, J.; Choi, T.-L. *Macromolecules* **2014**, *47*, 1351.

(26) Zou, J.; Jafr, G.; Themistou, E.; Yap, Y.; Wintrob, Z. A. P.; Alexandridis, P.; Ceacareanu, A. C.; Cheng, C. *Chem. Commun.* **2011**, *47*, 4493.

(27) Jha, S.; Dutta, S.; Bowden, N. B. *Macromolecules* **2004**, *37*, 4365.

(28) Engler, A. C.; Chan, J. M. W.; Fukushima, K.; Coady, D. J.; Yang, Y. Y.; Hedrick, J. L. *ACS Macro Lett.* **2013**, *2*, 332.

(29) Li, C.; Gunari, N.; Fischer, K.; Janshoff, A.; Schmidt, M. *Angew. Chem., Int. Ed.* **2004**, *43*, 1101.

(30) Nese, A.; Lebedeva, N. V.; Sherwood, G.; Averick, S.; Li, Y.; Gao, H.; Peteanu, L.; Sheiko, S. S.; Matyjaszewski, K. *Macromolecules* **2011**, *44*, 5905.

(31) Stenzel, M. H.; Zhang, L.; Huck, W. T. S. *Macromol. Rapid Commun.* **2006**, *27*, 1121.

(32) Moad, G.; Rizzardo, E.; Thang, S. H. *Polymer* **2008**, *49*, 1079.

(33) Tsujii, Y.; Ejaz, M.; Sato, K.; Goto, A.; Fukuda, T. *Macromolecules* **2001**, *34*, 8872.

(34) Stenzel, M. H.; Davis, T. P.; Fane, A. G. *J. Mater. Chem.* **2003**, *13*, 2090.

(35) Barner, L.; Davis, T. P.; Stenzel, M. H.; Barner-Kowollik, C. *Macromol. Rapid Commun.* **2007**, *28*, 539.

(36) Hernández-Guerrero, M.; Davis, T. P.; Barner-Kowollik, C.; Stenzel, M. H. *Eur. Polym. J.* **2005**, *41*, 2264.

(37) Barner-Kowollik, C.; Davis, T. P.; Heuts, J. P. A.; Stenzel, M. H.; Vana, P.; Whittaker, M. *J. Polym. Sci., Part A: Polym. Chem.* **2003**, *41*, 365.

(38) Willcock, H.; O'Reilly, R. K. *Polym. Chem.* **2010**, *1*, 149.

(39) Love, J. A.; Morgan, J. P.; Trnka, T. M.; Grubbs, R. H. *Angew. Chem., Int. Ed.* **2002**, *41*, 4035.

(40) Liu, J.; Gao, A. X.; Johnson, J. A. *J. Vis. Exp.* **2013**, e50874.

(41) Skey, J.; O'Reilly, R. K. *Chem. Commun.* **2008**, 4183.

(42) Azizi, N.; Aryanasab, F.; Saidi, M. R. *Org. Lett.* **2006**, *8*, 5275.

(43) Breugst, M.; Tokuyasu, T.; Mayr, H. *J. Org. Chem.* **2010**, *75*, 5250.

(44) Moad, G.; Rizzardo, E.; Thang, S. H. *Aust. J. Chem.* **2012**, *65*, 985.

(45) Moad, G.; Mayadunne Roshan, T. A.; Rizzardo, E.; Skidmore, M.; Thang San, H. In *Advances in Controlled/Living Radical Polymerization*; American Chemical Society: 2003; Vol. 854, p 520.

(46) Chiefari, J.; Chong, Y. K.; Ercole, F.; Krstina, J.; Jeffery, J.; Le, T. P. T.; Mayadunne, R. T. A.; Meijs, G. F.; Moad, C. L.; Moad, G.; Rizzardo, E.; Thang, S. H. *Macromolecules* **1998**, *31*, 5559.

(47) Moad, G.; Rizzardo, E.; Thang, S. H. *Aust. J. Chem.* **2006**, *59*, 669.

(48) Donovan, M. S.; Lowe, A. B.; Sumerlin, B. S.; McCormick, C. L. *Macromolecules* **2002**, *35*, 4123.

(49) Keddie, D. J. *Chem. Soc. Rev.* **2014**.

(50) Chiefari, J.; Chong, Y. K.; Ercole, F.; Krstina, J.; Jeffery, J.; Le, T. P. T.; Mayadunne, R. T. A.; Meijs, G. F.; Moad, C. L.; Moad, G.; Rizzardo, E.; Thang, S. H. *Macromolecules* **1998**, *31*, 5559.

(51) Mayadunne, R. T. A.; Rizzardo, E.; Chiefari, J.; Chong, Y. K.; Moad, G.; Thang, S. H. *Macromolecules* **1999**, *32*, 6977.

(52) Moad, G.; Chong, Y. K.; Postma, A.; Rizzardo, E.; Thang, S. H. *Polymer* **2005**, *46*, 8458.

(53) Zhou, D.; Zhu, X.; Zhu, J.; Yin, H. *J. Polym. Sci., Part A: Polym. Chem.* **2005**, *43*, 4849.

(54) Vandenbergh, J.; Junkers, T. *Macromolecules* **2014**.

(55) Keddie, D. J.; Moad, G.; Rizzardo, E.; Thang, S. H. *Macromolecules* **2012**, *45*, 5321.

(56) Dong, Z.-m.; Liu, X.-h.; Tang, X.-l.; Li, Y.-s. *Macromolecules* **2009**, *42*, 4596.

(57) Hilf, S.; Kilbinger, A. F. M. *Macromol. Rapid Commun.* **2007**, *28*, 1225.

(58) Beers, K. L.; Gaynor, S. G.; Matyjaszewski, K.; Sheiko, S. S.; Möller, M. *Macromolecules* **1998**, *31*, 9413.

(59) Chatterjee, A. K.; Choi, T.-L.; Sanders, D. P.; Grubbs, R. H. *J. Am. Chem. Soc.* **2003**, *125*, 11360.

(60) Crowe, W. E.; Mitchell, J. P.; Gibson, V. C.; Schrock, R. R. *Macromolecules* **1990**, *23*, 3534.

(61) Wagaman, M. W.; Grubbs, R. H. *Macromolecules* **1997**, *30*, 3978.

(62) Gody, G.; Maschmeyer, T.; Zetterlund, P. B.; Perrier, S. *Nat. Commun.* **2013**, *4*, 2505.

(63) Wang, Z.; He, J.; Tao, Y.; Yang, L.; Jiang, H.; Yang, Y. *Macromolecules* **2003**, *36*, 7446.

(64) Tsarevsky, N. V.; Matyjaszewski, K. *Macromolecules* **2005**, *38*, 3087.

(65) Zhao; Perrier, S. *Macromolecules* **2006**, *39*, 8603.

(66) Stenzel, M. H.; Davis, T. P. *J. Polym. Sci., Part A: Polym. Chem.* **2002**, *40*, 4498.

5.8 Appendix

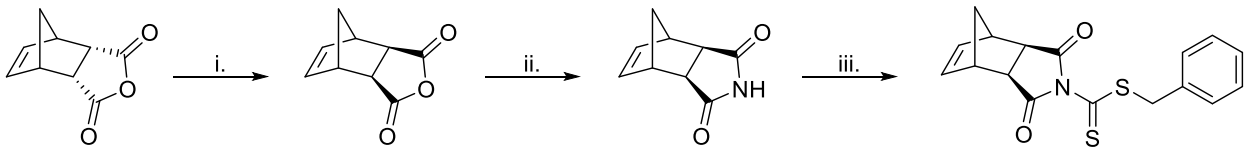

Scheme 5S1: Synthesis of **CTA1**. Experimental conditions: i. 1,2-dichlorobenzene at reflux; ii. urea, 135 °C; iii. KOH, CS_2, benzyl bromide, rt.

Synthesis of *cis*-5-norbornene-*exo*-2,3-dicarboxylic anhydride (1). A round-bottom flask was charged with *cis*-5-norbornene-*endo*-2,3-dicarboxylicanhydride (200 g). 200 mL 1,2-dicholorobenzene was added, a condenser was attached, and the reaction apparatus was immersed in an oil bath at 185 ºC for 2.5 h. Once cool, the flask was further cooled to 0 °C, and the precipitate was recovered by filtration and washed with hexanes. This crude product was recrystallized from benzene three times to yield 50.0 g pure *exo* product (25% yield). ^{1}H NMR ($CDCl_3$): δ 1.46 (d, 1H, J = 8 Hz), 1.66 (d, 1H, J = 8 Hz), 3.00 (s, 2H), 3.45 (s, 2H), 6.33 (s, 2H). ^{13}C NMR ($CDCl_3$): δ 171.69, 138.09, 48.90, 47.02, 44.26. HRMS: calculated 165.0552, found 165.0536 $[M+H]^+$.

Synthesis of *exo*-norbornene imide (2). A 100 mL round bottom flask was charged with **(1)** (4.02 g, 24.5 mmol) and urea (1.61 g, 26.8 mmol). The flask was fitted with a condenser. The reaction was conducted in the melt at 140 ˚C for 30 min. The reaction mixture was allowed to cool to rt. The crude product was purified by recrystallization from H_2O. The resulting white crystals were recovered via vacuum filtration and were dried under vacuum overnight to yield 2.84 g of pure product (71% yield). ^{1}H NMR ($CDCl_3$): δ 1.43 (d, 1H, J = 8 Hz), 1.51 (d, 1H, J =

8 Hz), 2.69 (s, 2H), 3.24 (s, 2H), 6.24 (s, 2H), 9.20 (bs, 1H). ^{13}C NMR ($CDCl_3$): δ 178.98, 137.80, 49.26, 45.16, 42.95. HRMS: calculated 162.0555, found 162.0546 $[M-H]^-$.

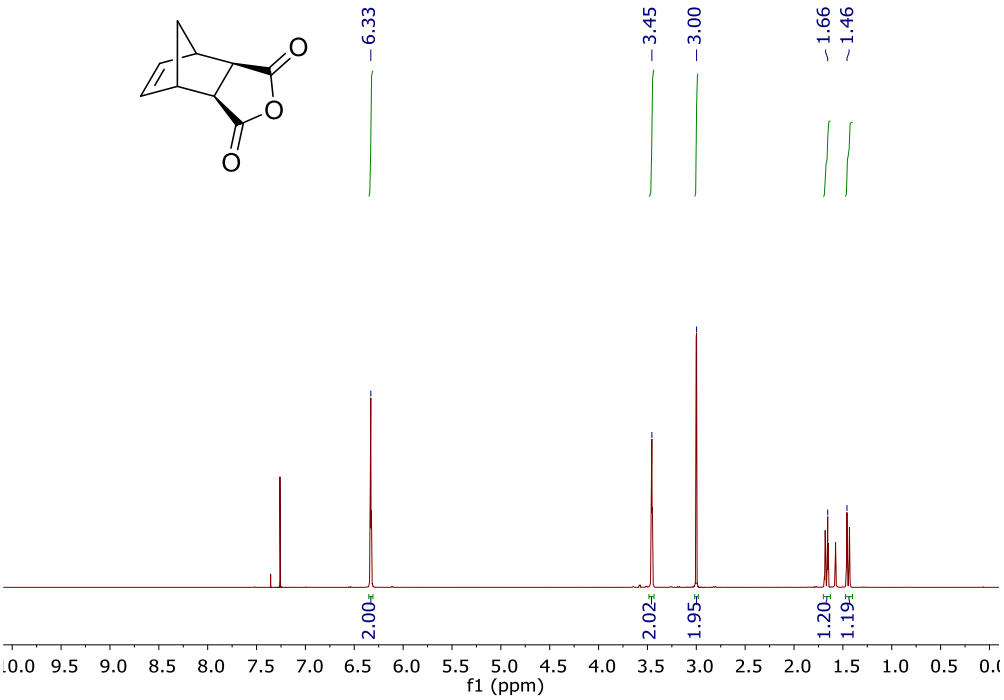

Figure 5S1: ^{1}H NMR of **(1)**

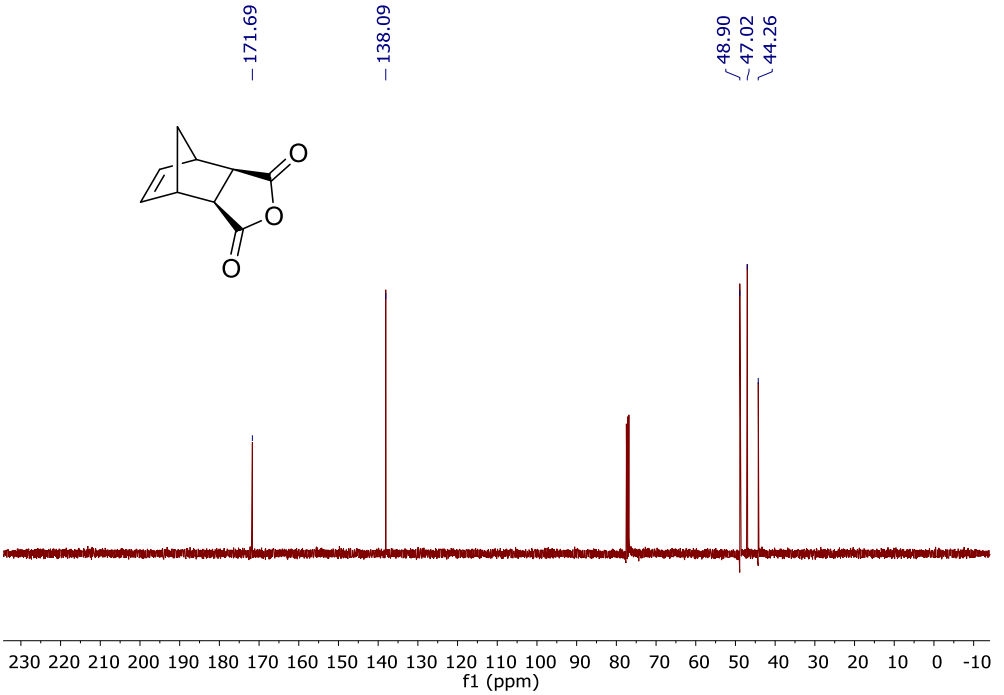

Figure 5S2: ^{13}C NMR of **(1)**

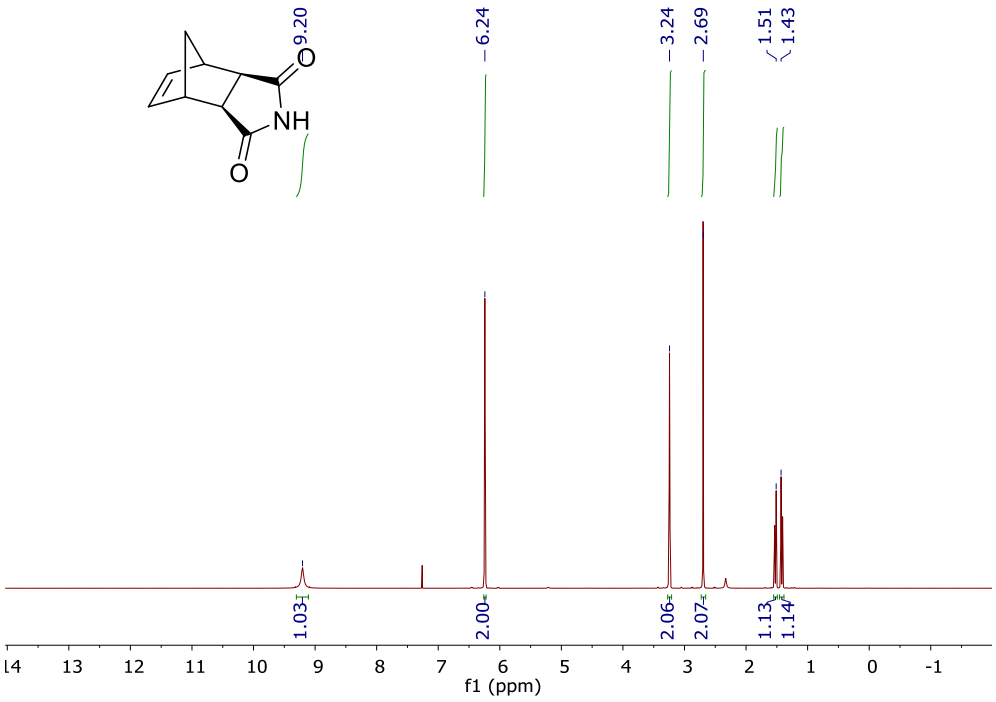

Figure 5S3: ^{1}H NMR of **(2)**

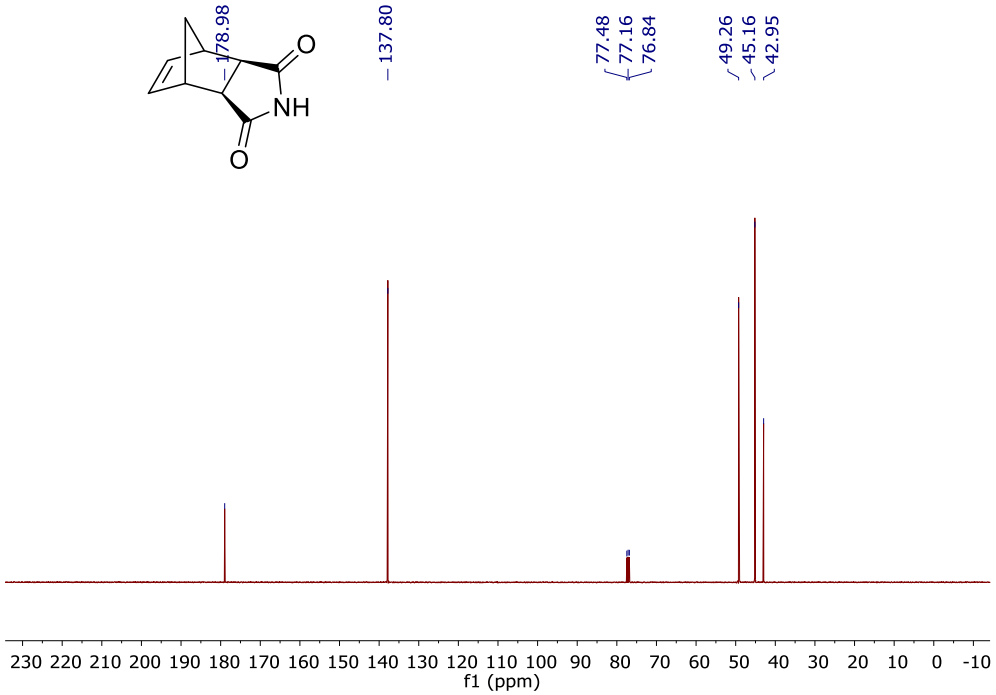

Figure 5S4: ^{13}C NMR of **(2)**

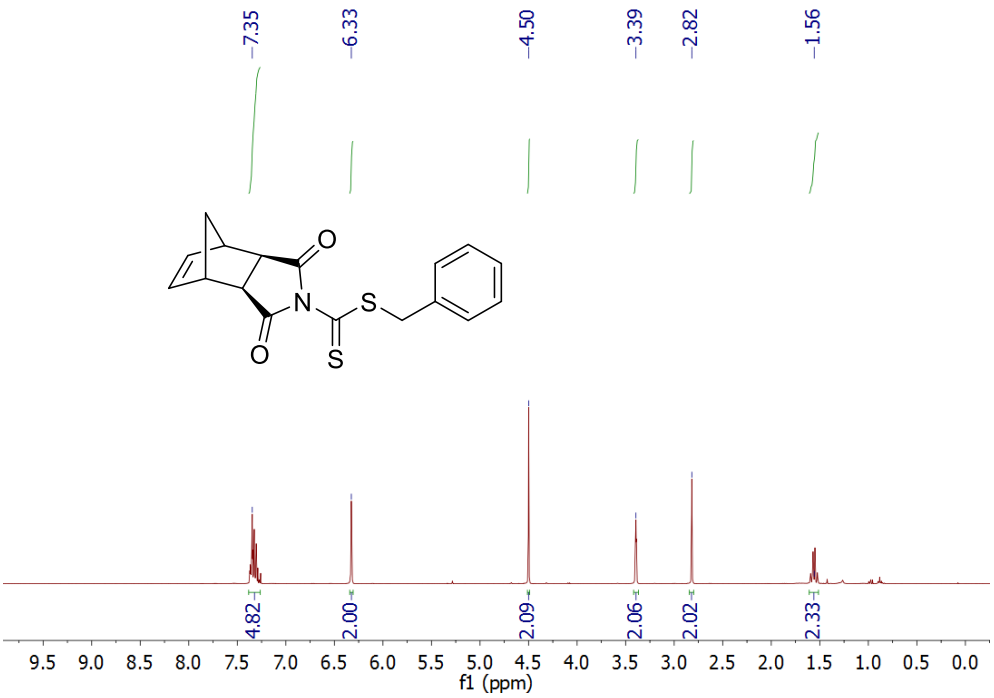

Figure 5S5: ^{1}H NMR of **CTA1**

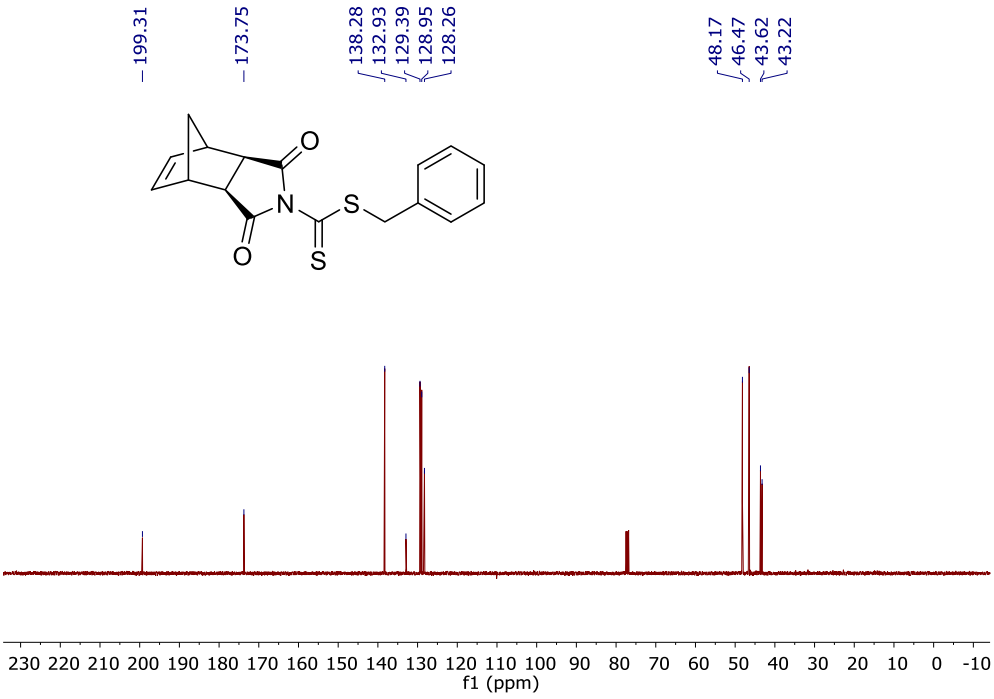

Figure 5S6: ^{13}C NMR of **CTA1**

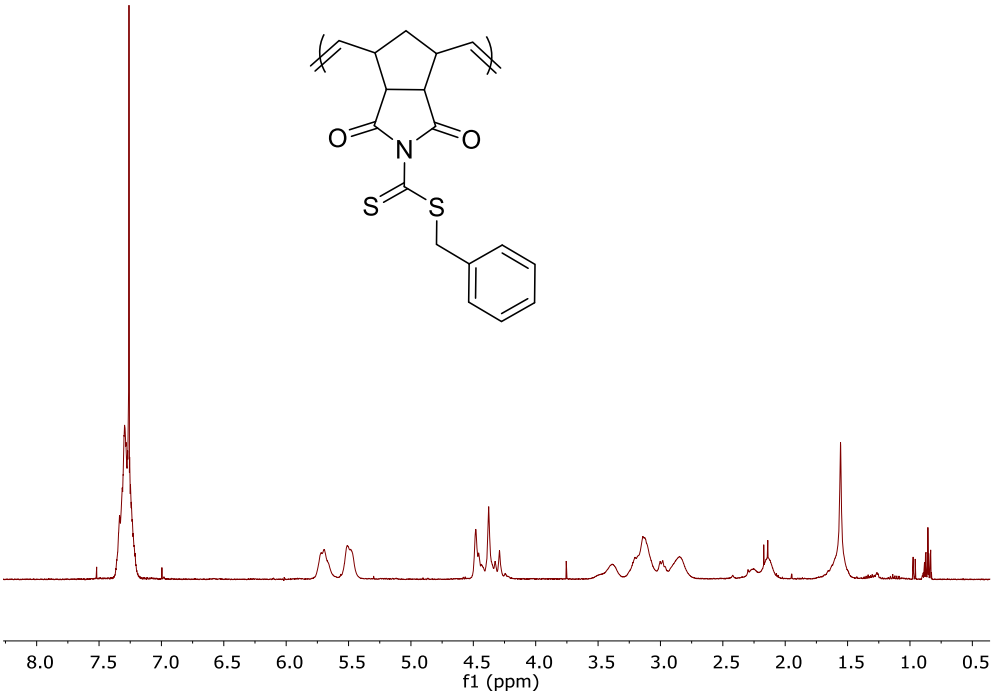

Figure 5S7: ^{1}H NMR of **poly(CTA1)**

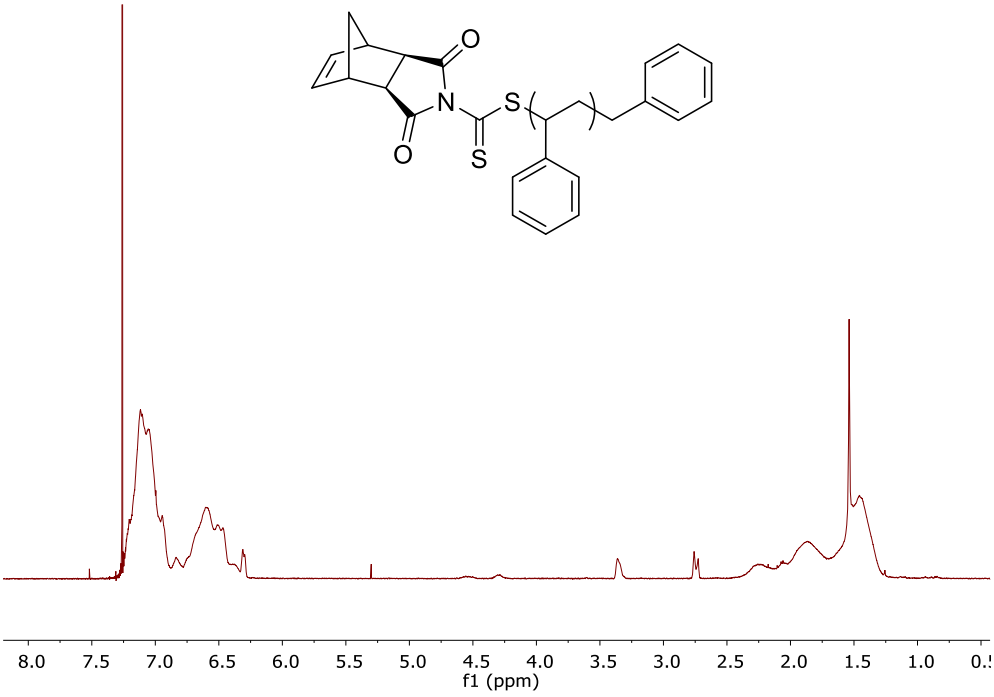

Figure 5S8: ^{1}H NMR of **MM$_{29}$**

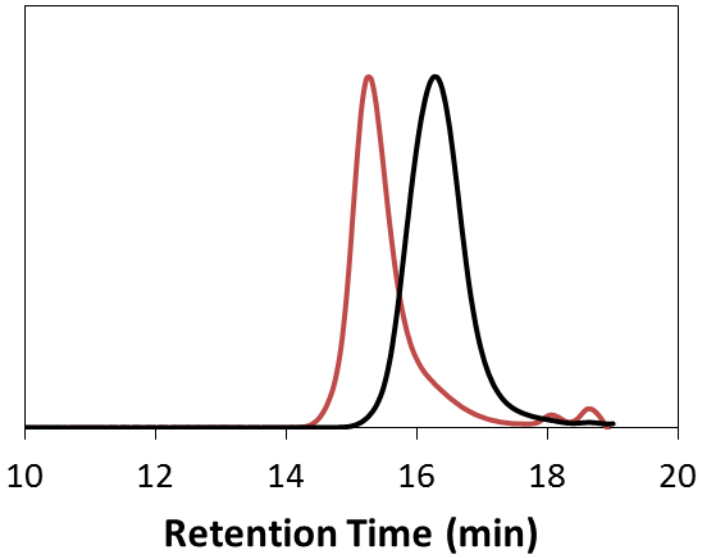

Figure 5S9: SEC traces of the RAFT chain extension with a PnBA Macro CTA (black line) with styrene to form a diblock copolymer (red line).

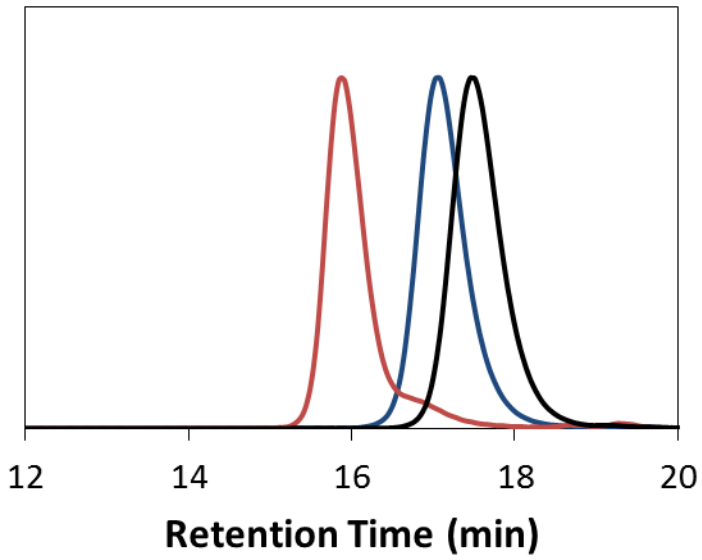

Figure 5S10: SEC traces of $\mathbf{MM_{29}}$ (black line), $\mathbf{MM_{52}}$ (blue line), and $\mathbf{MM_{113}}$ (red line).

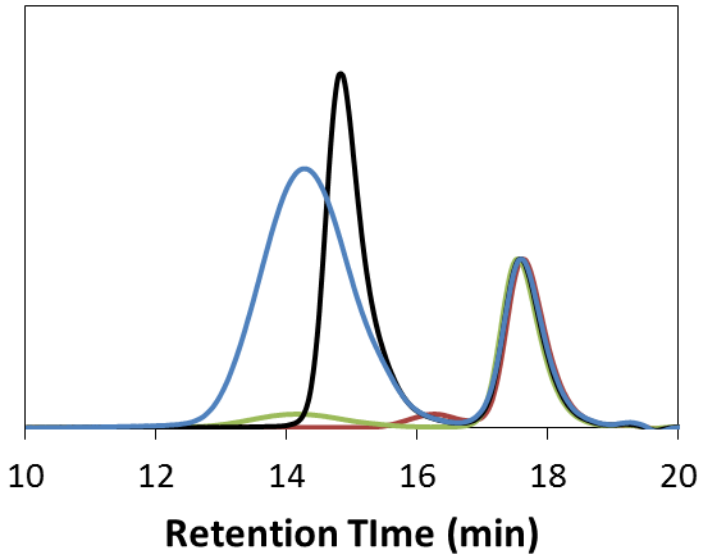

Figure 5S11: SEC traces of bottlebrush polymers prepared via grafting-through from $\mathbf{MM_{29}}$ using **G1** (red line), **G2** (green line), **G3** (black line), and **HG2** (blue line). Traces normalized to macromonomer peak height.

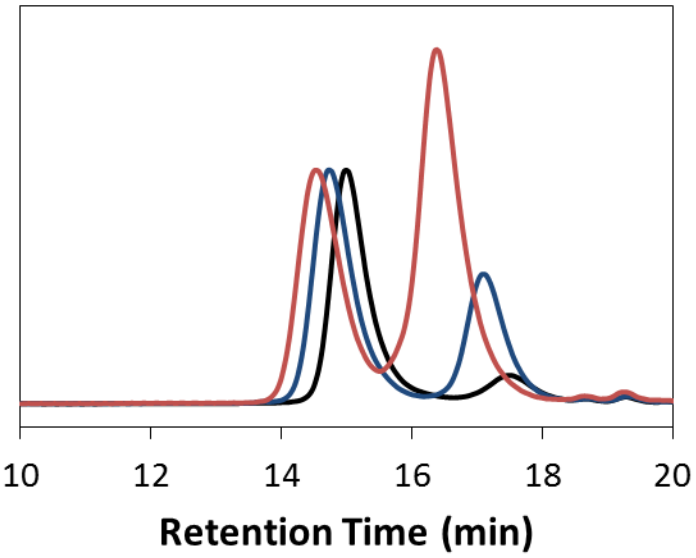

Figure 5S12: SEC traces of bottlebrush polymers prepared via grafting-through from $\mathbf{MM_{29}}$ (black line), $\mathbf{MM_{52}}$ (blue line), and $\mathbf{MM_{113}}$ (red line) using **G3**. Traces normalized to bottlebrush polymer peak height.

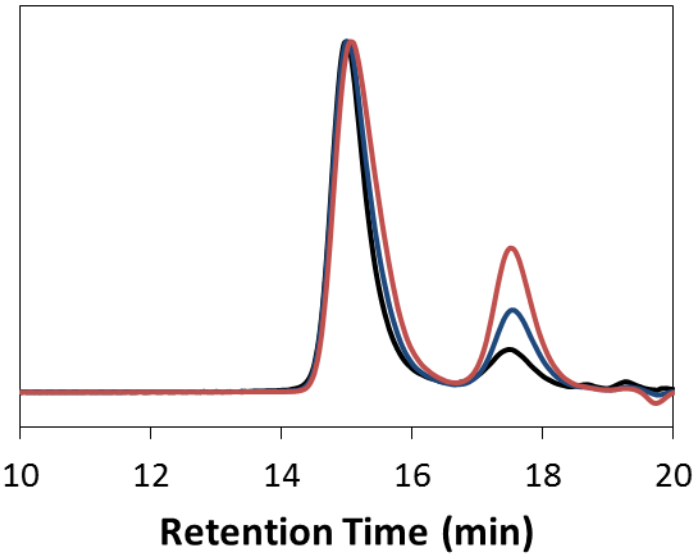

Figure 5S13: SEC traces of bottlebrush polymers prepared via grafting-through from **MM_{29}** at 100 mg/ml (black line), 50 mg/ml (blue line), and 25 mg/ml (red line). Traces normalized to bottlebrush polymer peak height.

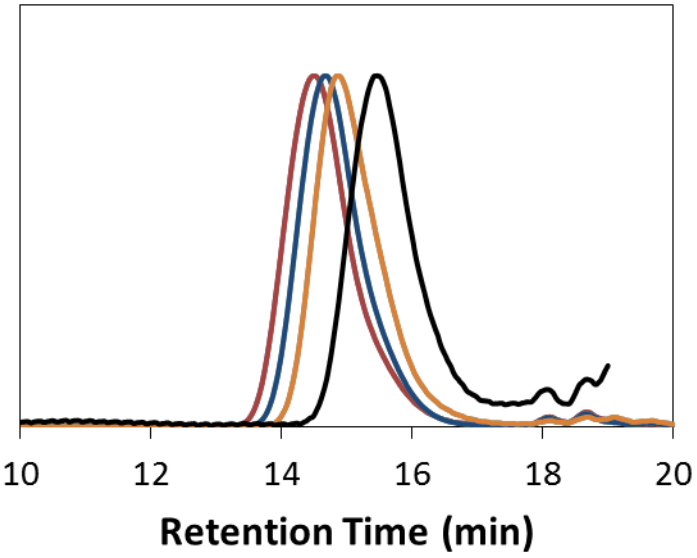

Figure 5S14: SEC traces of side chains aminolyzed from bottlebrush polymers prepared by transfer-to after 19 h (black line), 42 h (orange line), 67 h (blue line), and 91 h (red line).

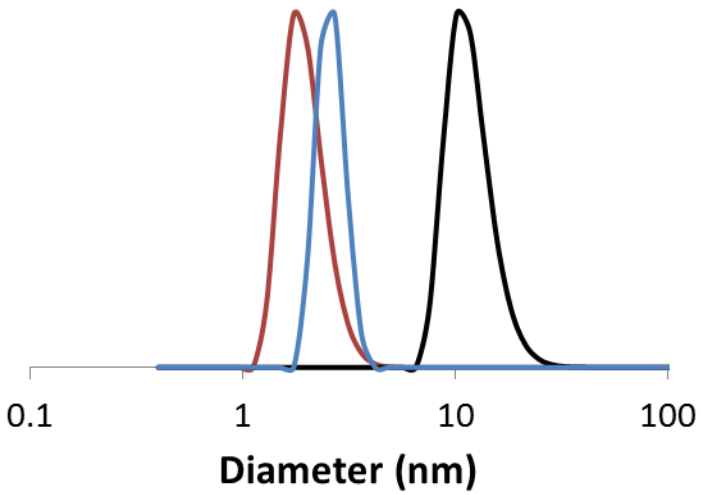

Figure 5S15: DLS traces of **MM_{29}** (red line), BB from **MM_{29}** (black line), and aminolysis product from the BB (blue line).

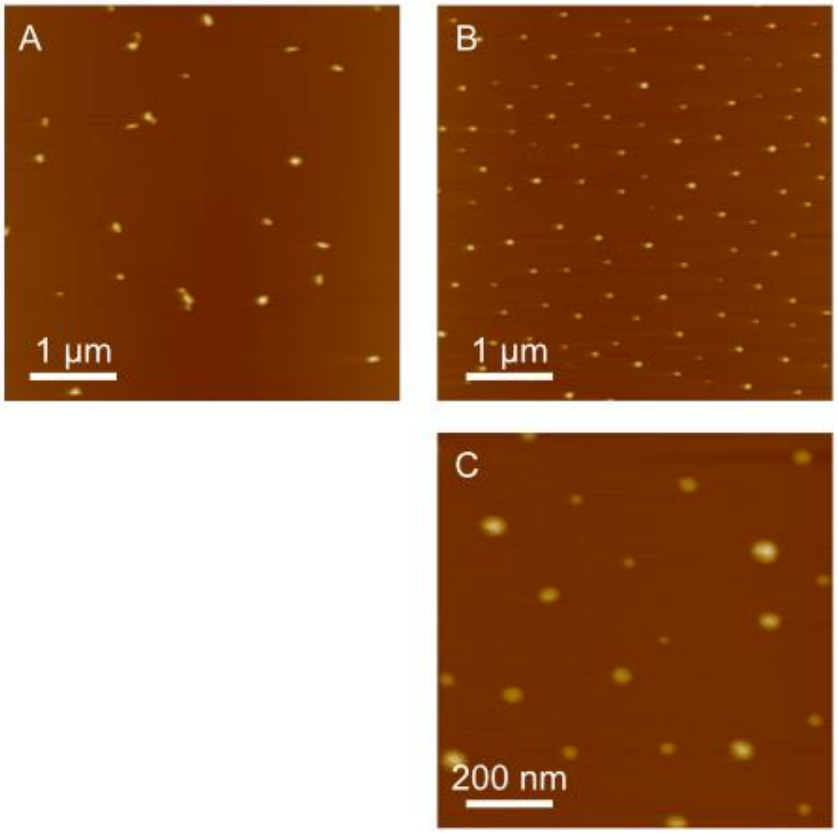

Figure 5S16: AFM height images of BB prepared from (A) transfer-to using **poly(CTA1),** (B) and (C) grafting-through using $\mathbf{MM_{29}}$ (Table 5.2 entry 5).

Chapter 6: Norbornene-Containing Dithiocarbamates for use in Reversible Addition–Fragmentation Chain Transfer (RAFT) Polymerization and Ring-Opening Metathesis Polymerization (ROMP)

Reprinted (adapted) with permission from Foster, J. C.; Radzinski, S. C.; Lewis, S. E.; Slutzker, M. B.; Matson, J. B. *Polymer*, **2015**, *79*, 205.

6.1 Authors

Jeffrey C. Foster, Scott C. Radzinski, Sally E. Lewis, Matthew B. Slutzker, and John B. Matson

Department of Chemistry and Macromolecules Innovation Institute, Virginia Tech, Blacksburg, Virginia 24061, United States

6.2 Abstract

Two new dithiocarbamate chain transfer agents (CTAs) with norbornene-containing Z-groups were prepared for use in reversible addition–fragmentation chain transfer (RAFT) polymerization. CTA **1b**, which contains an electron deficient norbornene imide Z-group, was found to effectively mediate RAFT polymerization of 2° more activated monomers (MAMs) but did not facilitate RAFT of 3° MAMs or less activated monomers (LAMs). In contrast, CTA **2**, derived from a norbornene amine, was well suited for the polymerization of LAMs, but did not control RAFT of MAMs. Poly(vinyl acetate) (PVAc), prepared by RAFT polymerization mediated by CTA **2,** possessed the expected CTA-derived α- and ω-end groups. Ring-opening metathesis polymerization (ROMP) of **2** was carried out, and full conversion to polymer was achieved within 20 min. Based on this result, ROMP grafting-through of a PVAc macromonomer derived from CTA **2** was carried out, resulting in the formation of a well-defined PVAc bottlebrush polymer with a narrow molecular weight distribution.

6.3 Introduction

Reversible deactivation radical polymerization (RDRP) techniques are versatile tools for the preparation of a variety of polymers with controlled molecular weights (MWs), narrow and symmetrical molecular weight distributions, and well-defined macromolecular architectures.[1-3] Examples of RDRPs include atom transfer radical polymerization (ATRP),[4,5] nitroxide-mediated radical polymerization (NMRP),[6] single electron transfer polymerization (SET-LRP),[7] and reversible addition–fragmentation chain transfer polymerization (RAFT).[8] In recent years, RAFT polymerization has been utilized extensively due its applicability to a wide range of monomers and reaction conditions. RAFT polymerization has been employed to functionalize biomolecules with stabilizing polymers,[9-12] mediate the formation of complex morphologies in suspension polymerizations,[13-16] prepare multiblock polymers containing up to 20 blocks,[17] and prepare advanced drug-releasing scaffolds,[18-21] among many other diverse applications.[22] RAFT polymerization has also been used to prepare macromonomers for use in bottlebrush synthesis,[23-25] a topic of interest to our group and others.

RAFT polymerization relies on reversible deactivation of the propagating or "active" radical species by a thiocarbonyl-thio-containing chain transfer agent (CTA).[26] Tremendous effort over the past two decades has been dedicated toward the design and synthesis of RAFT CTAs to improve their selectivity towards certain monomer types, to diversify the routes of their synthesis, to achieve specific built-in functionality that can be utilized in downstream processes, and to realize new classes of CTAs capable of mediating the polymerization of monomers across the radical stability spectrum (e.g., universal or switchable CTAs).[27] The structure of the dithio

compound [Z-C(S)-S-R] determines the types of monomers that can be polymerized by a given CTA. Specifically, the Z-group modulates the reactivity of the thiocarbonyl bond toward radicals, with more stable monomer radicals requiring more electron withdrawing Z-groups, in general.[28] The relative radical stability of the leaving R-group determines the partition coefficient for the monomer/CTA pair.[29] The partition coefficient is a term that describes the propensity of the CTA R-group to fragment with respect to the polymer radical. If the difference in relative radical stability between the R-group-derived radical and the polymer-derived radical is large, the polymerization can be either uncontrolled (if the polymer-derived radical is more stable) or inhibited (if the fragmented R-group radical is more stable). The rational selection of R and Z-groups allows chemists to design CTAs that mediate polymerization of a wide variety of monomer types.

Structural variation among RAFT CTAs allows for modulation of reactivity towards certain monomers as well as for tuning of non-RAFT specific parameters such as solubility, stability/lability (useful for aminolysis, as an example), and built-in functionality. Dithiobenzoate, trithiocarbonate, xanthate, and dithiocarbamate CTAs have been prepared from aryl Gringard, thiol, alcohol, and amine starting materials, respectively.[26,30,31] In the case of dithiocarbamate CTAs, the electron withdrawing ability of the nitrogen atom plays a critical role in the reactivity of the resulting CTA. More electron-deficient Z-groups such as those derived from amides, pyrrole, or imidazole effectively mediate the polymerization of the broad class of more-activated monomers (MAMs), while electron donating Z-groups allow for polymerization of less-activated monomers (LAMs).[32] We recently reported on the synthesis of a norbornene-imide-derived dithiocarbamate CTA with a benzyl R-group (CTA **1a**, Figure 6.1).[33] This novel

dithio compound was shown to effectively mediate the polymerization of styrene and *n*-butyl acrylate. In addition, the norbornene-containing Z-group was readily polymerized in the presence of a Ru-based metathesis catalyst, undergoing ring-opening metathesis polymerization (ROMP) to form a poly(CTA) with pendant chain transfer functionality on each repeat unit. This poly(CTA) was utilized subsequently in RAFT transfer-to polymerization to produce monodisperse bottlebrush polymers with molecular weights (MWs) in excess of 1 MDa. CTA **1a** was also utilized to prepare macromonomers for use in bottlebrush synthesis by the grafting-through approach.

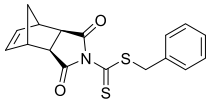

1a

Figure 6.1. CTA evaluated in our previous work.[33]

The norbornene-derived CTA previously reported by our group was incapable of mediating RAFT polymerization of the 3° MAM methyl methacrylate (MMA) or the LAM vinyl acetate (VAc). RAFT polymerization of 3° MAMs such as MMA requires a CTA with a deactivated, 3° R-group such as $–C(CH_3)_2CN$. Therefore, the poor control over the polymerization of MMA was attributed to the low partition coefficient of the benzyl R-group with respect to MMA. Polymerization of VAc in the presence of **1a** was completely inhibited, with no polymer product detected even after 48 h. Here, it was speculated that the electron withdrawing norbornene imide (**NI**) Z-group renders the C=S bond of the CTA derivative unreactive towards LAM radicals. To expand the scope of monomers that could be polymerized by norbornene-based CTAs, we sought to prepare new dithio compounds with different R- and Z-groups.

Based on our previous work, we hypothesized that replacing the benzyl R-group of **1a** with an R-group more suitable for the polymerization of MMA would yield a CTA suitable for mediating RAFT polymerization of methacrylate and methacrylamide monomers while still utilizing the ROMP-active norbornene-containing Z-group. We also envisioned a norbornene-derived CTA with a less active Z-group and a less stable homolytic leaving group (i.e., R = $–CH_2CN$) might facilitate the RAFT polymerization of LAMs such as VAc. In this contribution, we describe the synthesis and characterization of new dithiocarbamate CTAs with norbornene-containing Z-groups. In addition, we evaluate the ability of these novel CTAs to mediate RAFT polymerization of 5 different monomers—MMA, styrene, acryloylmorpholine (ACMO), methyl acrylate (MA), and VAc—encompassing common monomer types from 3° MAMs, 2° MAMs, and LAMs.

6.4 Materials and Methods

Materials

All reagents were obtained from commercial vendors and used as received unless otherwise stated. MMA, styrene, ACMO, MA, and VAc were passed through small columns of basic alumina prior to use. 2,2′-Azobis(2-methylpropionitrile) (AIBN) and 1,1′-azobis(cyclohexanecarbonitrile) (ACHN) were recrystallized from methanol prior to use. ROMP catalyst $(H_2IMes)(Cl)_2(PCy_3)Ru{=}CHPh$ (**G2**) was obtained as a generous gift from Materia. ROMP catalyst $(H_2IMes)(pyr)_2(Cl)_2Ru{=}CHPh$ (**G3**) was prepared from **G2** according to literature procedures.[34,35] exo-Norbornene imide (**NI**) was prepared according to a previous report.[33]

Methods

NMR spectra were measured on Agilent 400 MHz or Bruker 500 MHz spectrometers. ^{1}H and ^{13}C NMR chemical shifts are reported in ppm relative to internal solvent resonances. Yields refer to chromatographically and spectroscopically pure compounds unless otherwise stated. Size exclusion chromatography (SEC) was carried out in THF on two Agilent PLgel 10 μm MIXED-B columns connected in series with a Wyatt Dawn Helios 2 light scattering detector and a Wyatt Optilab Rex refractive index detector. No calibration standards were used, and dn/dc values were obtained by assuming 100% mass elution from the columns. High-resolution mass spectra were taken on an Agilent Technologies 6230 TOF LC/MS mass spectrometer. UV-Vis absorbance spectra were recorded on a Cary 5000 UV-Vis (Agilent) from 550 to 300 nm.

*Synthesis of CTA **1b***

KOH (0.360 g, 6.43 mmol) was ground to a fine powder with a mortar and pestle and placed in a 100 mL round bottom flask. To the flask was added **NI** (1.00 g, 6.13 mmol) followed by 15 mL of DMF. This mixture was stirred for 5 min, followed by dropwise addition of CS_2 (1.11 mL, 18.4 mmol). The solution developed a deep red color. After an additional 3 h of stirring, (1-bromoethyl)benzene (1.67 mL, 12.3 mmol) was added dropwise, and the reaction mixture was stirred at rt for 12 h. The reaction mixture was then diluted with CH_2Cl_2 (50 mL) and washed with H_2O (3 × 150 mL) and brine. The organic layer was dried over Na_2SO_4, and the solvent was removed by rotary evaporation. The crude product was purified on a silica gel column, eluting with 1:1 CH_2Cl_2/hexanes, to give 0.59 g of **1b** as a yellow solid (28% yield, 8:2 mixture of *S*-

and *N*-alkylated products that could not be separated via column chromatography). ^{1}H NMR ($CDCl_3$): δ 7.5-7.2 (m, 5H), 6.32 (t, 2H), 4.96 (q, 1H), 3.38 (s, 2H), 2.79 (s, 2H), 1.81 (d, 3H), 1.57 (m, 2H). ^{13}C NMR ($CDCl_3$) δ 198.63, 173.76, 139.61, 138.32, 128.93, 128.24, 127.90, 52.30, 48.20, 46.49, 43.24, 20.46. HRMS (m/z): calculated 344.0773, found 344.0757.

*Synthesis of Reduced Imide CTA **2***

A 3-necked round bottom flask was charged with $LiAlH_4$ (2.09 g, 55.2 mmol). The flask was placed in an ice bath. To the flask was slowly added 30 mL of dry THF under N_2 atmosphere. **NI** (3.00 g, 18.4 mmol) was dissolved in 70 mL of dry THF in a second flask. The imide solution was transferred to an addition funnel and was added dropwise to the $LiAlH_4$ slurry. After the addition was complete, the reaction mixture was allowed to warm to rt and then was heated at reflux for 12 h. To quench the reaction, the reaction mixture was placed in an ice bath, and 2 mL of H_2O was added slowly, followed by 2 mL NaOH solution (10% w/v in water) and then 6 mL H_2O. Upon warming to rt the solids became white. The quenched reaction mixture was diluted with diethyl ether (~200 mL) and filtered through celite. This solution was concentrated and washed with brine, dried over Na_2SO_4, and rotovapped. The resulting yellow oil norbornene amine (**NA**) was used in the next step without further purification.

NA was dissolved in 15 mL of EtOH in a round bottom flask. The flask was placed in an ice bath. To the flask was added CS_2 (1.23 mL, 20.3 mmol) followed by dropwise addition of 2.3 mL of 50 % wt/v aqueous KOH (1.1 equiv). The reaction mixture was allowed to warm to room temperature and was stirred for 12 h. The reaction mixture was then diluted with MeOH (~40 mL), dried over Na_2SO_4, and rotovapped. The residue was used in the next step without further purification.

The crude dithiocarbamate salt was dissolved in 40 mL of acetone in a round bottom flask. The flask was placed in an ice bath. To the flask was added bromoacetonitrile (1.40 mL, 20.1 mmol) dropwise. The reaction mixture was allowed to warm to room temperature and was stirred for 12 h. The reaction mixture was then rotovapped and the residue was dissolved in CH_2Cl_2. The CH_2Cl_2 solution was washed with H_2O and brine, dried over Na_2SO_4, and rotovapped. The crude product was purified on a silica gel column, eluting with 2:3 CH_2Cl_2/hexanes to give the pure product (**2**) as an off white powder (2.80 g, 61% yield). ^{1}H NMR ($CDCl_3$): δ 6.13 (q, 2H), 4.19 (s, 2H), 4.06 (m, 1H), 3.76 (m, 2H), 3.40 (m, 1H), 2.74 (d, 2H), 2.44 (m, 2H), 1.46 (d, 1H), 1.32 (d, 1H). ^{13}C NMR ($CDCl_3$): δ 187.20, 137.79, 137.20, 116.11, 60.41, 54.98, 47.69, 47.62, 45.36, 42.86, 42.20, 22.29. HRMS (m/z): calculated 251.0671, found 251.0671.

Representative RAFT Polymerization Procedure

A typical polymerization procedure is as follows: To an oven-dried Schlenk tube equipped with a magnetic stir bar was added CTA, azo initiator, monomer, and solvent (if applicable). The tube was deoxygenated by subjecting the contents to three freeze−pump−thaw cycles. The Schlenk tube was then backfilled with N_2 and submerged in an oil bath maintained at the appropriate temperature. Samples were removed periodically by N_2-purged syringe to monitor molecular weight evolution by SEC and conversion by ^{1}H NMR spectroscopy.

*Synthesis of poly(**2**)*

CTA **2** (50 mg) was dissolved in 1.5 mL of dry CH_2Cl_2 in a vial equipped with a stir bar. A 5.8 mg/mL solution of **G3** was prepared in a second vial by dissolving an amount of **G3** in dry CH_2Cl_2. 0.5 mL of this **G3** solution was added rapidly to the first vial. After 20 min, a few drops

of ethyl vinyl ether were added to terminate the polymerization, and the reaction mixture was stirred for an additional 5 min. The polymer was isolated via precipitation from hexanes.

Synthesis of PVAc Bottlebrush

Macromonomer **NA-PVAc** (40 mg) was dissolved in 0.3 mL of dry CH_2Cl_2 in a vial equipped with a stir bar. A 2.3 mg/mL solution of **G3** was prepared in a second vial by dissolving an amount of **G3** in dry CH_2Cl_2. 0.1 mL of of this **G3** solution was added rapidly to the first vial. After 60 min, a few drops of ethyl vinyl ether were added to terminate the polymerization, and the reaction mixture was stirred for an additional 5 min. The polymer was isolated via precipitation from diethyl ether.

6.5 Results and Discussion

R-Group Modification

To prepare **NI**-derived CTAs with various R-groups, we initially adopted a strategy that involved the *in situ* generation of a norbornene-imide dithiocarbamate intermediate that could be transformed into the desired CTA via addition of the appropriate alkyl-halide, as shown in Scheme 6.1. Similar to our previous report in which we obtained **1a** in moderate yields (30-40%) using a facile 1-pot procedure,[33] we attempted to synthesize additional norbornene-containing dithiocarbamates (**1a-1f**) by first dissolving the nucleophilic exo-norbornene imide (**NI**) in DMF, adding finely ground potassium hydroxide followed by dropwise addition of carbon disulfide (CS_2). Finally, the appropriate alkyl halide was added after a period of 1-2 h to form the desired product, which we would attempt to isolate using standard aqueous workup and/or column chromatography. Benzyl bromide (Table 6.1, entry **a**), (1-bromoethyl)benzene (**b**), *N*-(chloromethyl)phthalimide (**c**), 2-bromo-2-methylpropionic acid (**d**), ethyl α-bromoisobutyrate

(**e**), or 2-bromopropionic acid (**f**), was utilized to attempt to alkylate the intermediate in the final step. Of these, only **a** and **b** were found to yield the desired product in an appreciable quantity (see Table 6.1). Starting materials or *N*-alkylated byproducts were recovered from reactions with the other alkylating agents.

Scheme 6.1. Preparation of dithiocarbamate CTAs from **NI**.

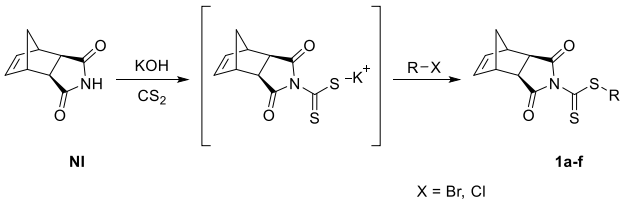

Table 6.1. Isolated yields from alkylation of **NI**-derived dithiocarbamate intermediate using various alkylating agents.

Entry	Alkylating Agent	Product	Isolated Yield
a	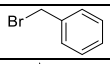	**1a**	40 %
b	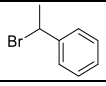	**1b**	28 %
c	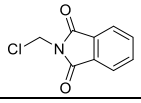	**1c**	< 1 %
d	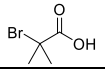	**1d**	--[a]
e	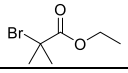	**1e**	--[a]
f	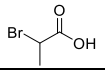	**1f**	--[a]

[a]Compounds not isolated from reaction mixtures.

To explain these results, a product analysis of the synthesis of **1a** was performed. ^{1}H NMR spectroscopy of a mixture of **NI**, KOH, and CS_2 that had been allowed to react in DMSO-d_6 revealed an important insight: the equilibrium between the deprotonated imide and the

dithiocarbamate intermediate depicted in Scheme 6.1 is strongly biased in favor of the reactants (K_{eq} = 0.024 by relative integration). We attribute this observation to both the poor nucleophilicity of the **NI** nitrogen and the instability of the dithiocarbamate salt, which may decompose via a zwitterionic intermediate formed through protonation of the N atom in a similar manner to related compounds.[36] After 2 h benzyl bromide was added, and the composition of the reaction mixture was re-evaluated after 12 h by ^{1}H NMR spectroscopy. By comparing integrations of the various benzyl methylene resonances, and knowing the identity of each of these species by matching against pure spectra of molecules isolated from the crude reaction mixture, it was determined that the *N*-alkylated norbornene imide was in fact the major product, with the desired dithiocarbamate (CTA **1a**) and a trithiocarbamate byproduct forming to a lesser extent (Scheme 6.2). Increasing the equivalents of CS_2 to attempt to drive the equilibrium toward the product had a negligible effect on the isolated yield.

Scheme 6.2. Product analysis of synthesis of CTA **1a**.

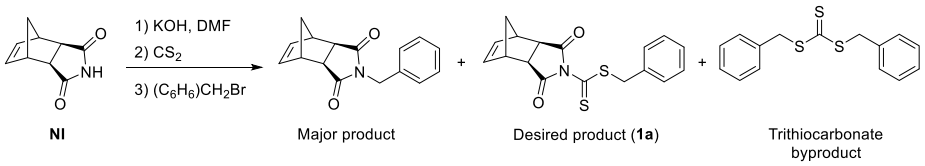

Given this analysis, it is not surprising that alkylating agents with carboxylic acid functionalities (**d** and **f**) could not be employed to synthesize dithiocarbamate CTAs with the **NI** Z-group. Alkylation using ethyl α-bromoisobutyrate (**e**, the ethyl ester of **c**) also proved fruitless, likely due to the fact that S_N2 at the α-carbon is sterically hindered and S_N1 using this particular alkyl bromide is unlikely due to the destabilization of the carbocation adjacent to the electron-withdrawing carbethoxy group. Neutralization of **d** with triethylamine prior to alkylation was

also attempted without success. Based on these observations, we speculate that the structures of CTAs with the norbornene imide Z-group may be limited to those prepared using alkylating agents that are sterically unhindered and do not contain acidic functionalities that may catalyze CTA decomposition (e.g., **a** or **b**). These limitations are at odds with the structural requirements of a good R-group for 3° MAMs.

We previously reported on the successful RAFT polymerization of styrene and *n*-butyl acrylate (2° MAMs) mediated by CTA **1a**. We therefore expected that CTA **1b** would effectively mediate RAFT polymerization of styrene, MA, and ACMO (2° MAMs). The polymerizations were carried out in THF at 50 v/v% at 60 ˚C for MA and ACMO and at 75 ˚C for styrene in the presence of 2,2′-azobis(2-methylpropionitrile) (AIBN) to provide initiating radicals by thermal decomposition. For each monomer type a [M] / [**1b**] / [AIBN] ratio of 100 : 1 : 0.1 was employed. Table 6.2 summarizes a series of polymers prepared by RAFT polymerization using CTA **1b**. In general, the polymers possessed low dispersities and MWs that were close to expected values. Kinetic analysis of these polymerizations revealed propagation rate profiles that were first order in monomer consumption (Figure 6.2A). As shown in Figure 6.2B, plots of number average molecular weight (M_n) (determined by size exclusion chromatography (SEC)) vs. conversion were linear, indicating well controlled polymerizations. SEC traces of aliquots taken at specific timepoints during kinetic analysis were generally narrow and monomodal (as in Figure 6.3). In general, polymerizations using CTA **1b** progressed more rapidly than those previously reported for CTA **1a**. We attribute this phenomenon to the relatively more stable homolytic leaving group of CTA **1b**, which likely accelerates consumption of the RAFT agent during the pre-equilibrium phase compared with CTA **1a**.[29] RAFT polymerization of MMA and

VAc were also attempted. As was the case with CTA **1a**, polymerization of MMA mediated by CTA **1b** was uncontrolled, while RAFT of VAc using this CTA was completely inhibited for > 48 h.

Table 6.2. Polymers prepared by RAFT polymerization using CTA **1b**.

Monomer	**% Conversion**[a]	**M_n (Da)**[b]	**$M_{n,\ expected}$ (Da)**[c]	**Đ**[b]
MMA	14	62,000	1,800	1.40
ACMO	99	15,000	17,500	1.09
MA	70	6,100	7,500	1.03
Styrene	40	4,400	5,200	1.01
VAc	0	--[d]	--[d]	--[d]

[a]Determined using ^{1}H NMR spectroscopy. [b]Measured by SEC-MALLS in THF at 30 °C. [c]Calculated based on monomer conversion measured by ^{1}H NMR spectroscopy. [d]No polymer was detected by SEC. Data represent the ultimate timepoint taken from kinetic analyses.

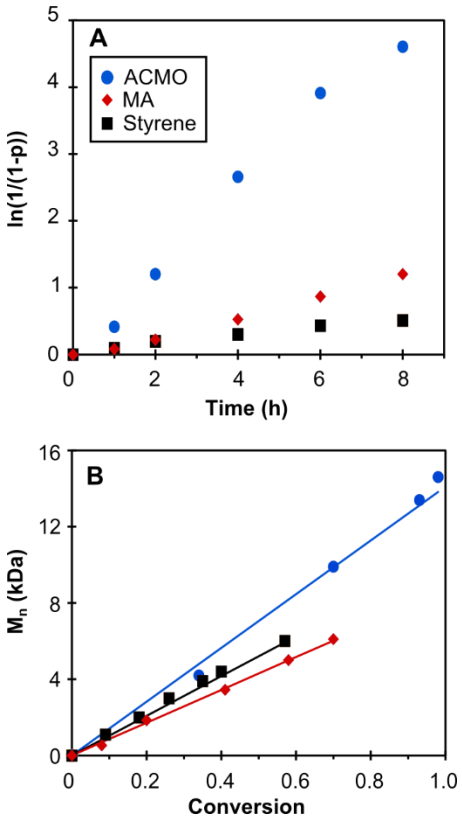

Figure 6.2. A) Kinetic analysis of RAFT polymerization of styrene (squares), MA (diamonds), and ACMO (spheres) using **1b**. B) Plot of M_n vs. conversion for the same polymerizations. The solid lines represent the theoretical M_n values calculated from conversions as determined by ^1H NMR spectroscopy.

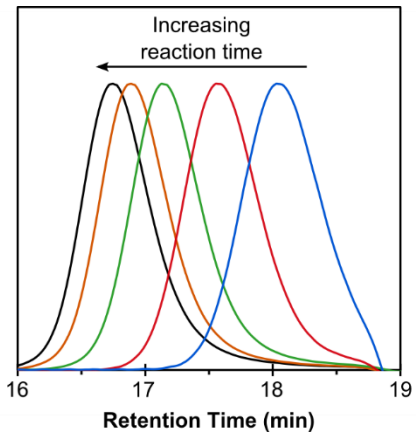

Figure 6.3. SEC traces of aliquots removed during the kinetic evaluation of the polymerization of styrene mediated by CTA **1b**.

Z-Group Modification

To access the class of LAMs, we pursued an alternative strategy in which **NI** was reduced to the corresponding secondary amine (Scheme 6.3)—a significantly more reactive nucleophile. The increased electron density of the nitrogen atom of the resulting dithiocarbamates is not desirable for mediation of the polymerization of MAMs; however, this change in electronics was expected to enable RAFT of LAMs such as VAc. The reduction of **NI** was accomplished using $LiAlH_4$,[37] giving norbornene amine (**NA**) in nearly quantitative yield. Treatment of this compound with CS_2 and aqueous KOH gave the dithiocarbamate potassium salt, which could be isolated from excess reagents. Alkylation was conducted in acetone at 0 ˚C using bromoacetonitrile. Using this strategy, a second generation norbornene-containing CTA(CTA **2**) was prepared in 3 steps from **NI** in 61% overall yield.

Scheme 6.3. Preparation of dithiocarbamate CTA, **2**, from **NA**.

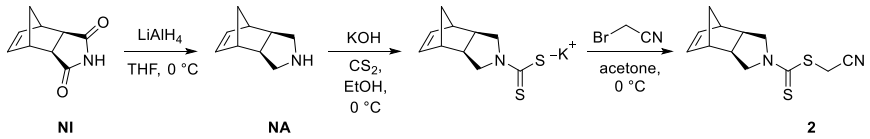

The dialkyl dithiocarbamate CTA **2** possesses an electron rich dialkyl amine Z-group. Typically, the electron-donating character of the N atom in dithiocarbamates renders the C=S bond less reactive toward radicals than CTAs that contain more electron-withdrawing Z-groups.[28] This has the effect of decreasing the chain transfer efficiency of the CTA, thereby increasing the active radical concentration. As a result, dialkyl dithiocarbamate CTAs tend to mediate the polymerization of LAMs effectively but lead to uncontrolled polymerization of MAMs. To assess the quality of the polymerization of various MAMs by RAFT using CTA **2**, reactions were conducted for 2 h using conditions similar to those employed when using CTA **1b**. Our evaluation is summarized in Table 6.3. SEC and ^{1}H NMR analysis of the crude reaction mixtures showed that RAFT polymerizations of MMA, MA, styrene, and ACMO were poorly controlled, giving polymers of moderate to broad dispersity with MWs significantly higher than expected. In addition, the anticipated CTA-derived polymer end groups were absent from the ^{1}H NMR spectrum of a purified poly(styrene) sample polymerized in the presence of CTA **2** (see Figure 6S8), supporting the expected low propensity of CTA **2** to react with MAM radicals. This result is further corroborated by comparing the UV-Vis absorption spectrum of CTA **2** to that of **1b** (Figure 6S10). The decreased λ_{max} of CTA **1b** relative to CTA **2** is consistent with increased electron density on C=S.[38]

Table 6.3. Polymers prepared by RAFT polymerization using CTA **2**.

Monomer	**% Conversion**[a]	**M_n (Da)**[b]	**$M_{n,\ expected}$ (Da)**[c]	**Đ**[b]
MMA	25	168,000	2,500	1.63
ACMO	> 99	61,800	14,000	2.05
MA	75	17,300	6,500	1.58
Styrene	16	37,600	1,700	1.31
VAc	48	6,600	4,100	1.43

[a]Determined using ^{1}H NMR spectroscopy. [b]Measured by SEC-MALLS in THF at 30 °C. [c]Calculated based on monomer conversion measured by ^{1}H NMR spectroscopy.

RAFT polymerization of VAc mediated by CTA **2** was more successful than the other monomers tested. The dialkyl amine Z-group has been shown to mediate (to a degree) RAFT polymerization of LAMs such as VAc.[32] The reduced reactivity of the C=S bond of alkyl dithiocarbamates and xanthates in particular promotes sufficient fragmentation of the CTA-polymer adduct, allowing for polymerization of LAMs to progress without retardation. VAc polymerizations using CTA **2** were conducted neat at 80 °C using 1,1′-azobis(cyclohexanecarbonitrile) (ACHN) as the radical source. As expected, the formation of polymer was observed when CTA **2** was used in the polymerization of VAc. However, the reaction exhibited a long incubation period of > 7 h, after which propagation proceeded rapidly. An isolated polymer prepared via RAFT of VAc mediated by CTA **2** was monomodal by SEC with an M_n that agreed with the expected value (Table 6.3). The relatively high Đ of this polymer likely resulted from two independent phenomena: (1) intermolecular termination by coupling (also supported by the higher than expected MW); and (2) the presence of a population of high MW species that typically form early in the polymerization of VAc.[39] ^{1}H NMR spectroscopy of the polymer sample showed the appropriate CTA-derived α- and ω-chain ends (Figure 6.4), and

end group analysis gave a MW value that was in relatively good agreement with those determined by SEC and monomer conversion (5,200 Da). Taken together, these data suggest that CTA **2** effectively mediates the polymerization of VAc.

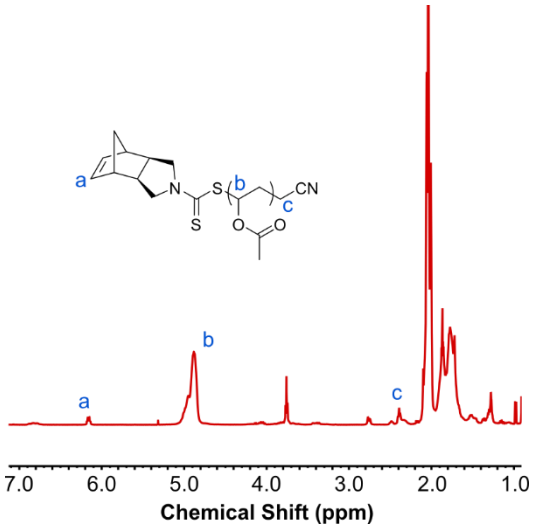

Figure 6.4. ^{1}H NMR spectrum of a PVAc MM prepared using CTA **2** highlighting the CTA-derived α- and ω-chain ends (protons a and c). Spectrum was taken in $CDCl_3$.

CTAs with norbornene Z-groups can be utilized in the synthesis of bottlebrush polymers by both the transfer-to and grafting-through approaches. Both strategies rely on ring-opening metathesis polymerization (ROMP) to generate the bottlebrush backbone. ROMP of CTA **2** was performed to prepare poly(**2**) as shown in Figures 6.5 and 6S9. Polymerizations by the modified 2nd generation Grubbs' catalyst (**G3**) at a [M]/[**G3**] ratio of 50 : 1 achieved quantitative conversion in < 20 min. The SEC trace of the resulting polymer (Mn = 12,700 Da) was monomodal with low Đ (1.01). ^{1}H NMR spectroscopy of the crude reaction mixture confirmed quantitative consumption of the olefin functionality, evidenced by the disappearance of the resonance at 6.13

ppm. A pair of new peaks between 5.2 and 5.6 ppm were assigned to the backbone olefins of poly(**2**).

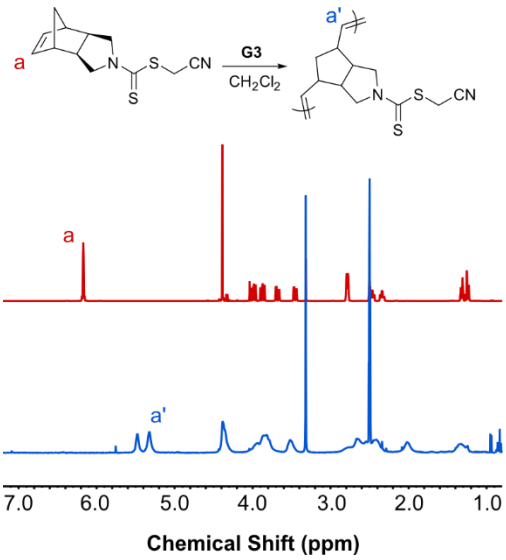

Figure 6.5. ^{1}H NMR spectra of **2** (top spectrum) and a crude spectrum of a polymer prepared via ROMP of **2** (bottom spectrum) highlighting the quantitative consumption of olefin protons. Spectra were taken in DMSO-d_6.

Scheme 6.4. Preparation of PVAc bottlebrush by ROMP grafting-through.

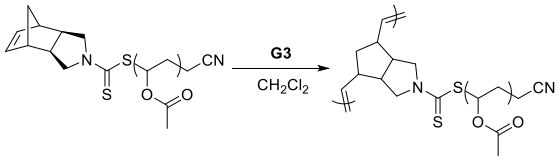

Based on this positive result, we considered whether ROMP grafting-through of PVAc prepared using **2** could be accomplished to form a bottlebrush polymer (as shown in Scheme 6.4). The

grafting-through technique involves the polymerization of a macromolecule functionalized with a polymerizable group on one chain end (macromonomer, MM). Bottlebrush polymers prepared using this method are considered to have perfect grafting density, as each repeat unit bears a pendant polymer side chain. Bottlebrush polymers possessing PVAc side chains have been synthesized previously via radical grafting-through using a vinyl-functionalized PVAc MM,[40] through a tandem ATRP/RAFT method by grafting-from,[41] and employing an all-RAFT method using the R-group (grafting-from) and Z-group (transfer-to) approaches.[42] These macromolecules are precursors to poly(vinyl alcohol) (PVOH)-based materials that have interesting industrial and biomedical applications.[43] In addition, branched PVOHs possess different physical properties than linear ones, such as decreased solution viscosity.[44]

As shown in Figure 6.4, the norbornene functionality of CTA **2** is retained on the ω-chain end after the polymerization of VAc. This ROMP-active moiety can be utilized to form a bottlebrush polymer via grafting-through. ROMP grafting-through was carried out at a [MM]/[**G3**] ratio of 25:1 using a PVAc MM prepared via RAFT polymerization mediated by CTA **2** (**NA-PVAc**)(M_n = 6,600 Da). The resulting bottlebrush polymer had a MW of 110 kDa with a narrow and symmetrical molecular weight distribution (Đ = 1.26). Full conversion of norbornene-functionalized MMs was confirmed by ^{1}H NMR spectroscopy. A second population of macromolecules centered on 17 min in the SEC trace in Figure 6.6 corresponds to residual PVAc MM that was not consumed during ROMP. These "dead chains" arise primarily from termination reactions during RAFT polymerization that leave the polymer chain without the desired ω-end group. The minimal fraction of residual polymer after ROMP grafting-through further supports

the capability of CTA **2** to control RAFT polymerization of VAc, as the majority of the macromonomers possess the norbornene ω-end group.

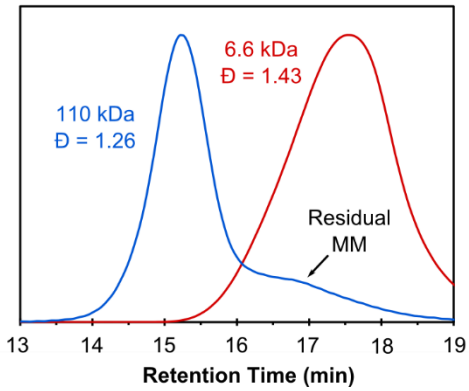

Figure 6.6. SEC traces of PVAc MM prepared using CTA **2** (**NA-PVAc**) (longer retention time) and a bottlebrush polymer prepared using this MM via ROMP grafting-through (shorter retention time).

6.6 Conclusions

In summary, we have prepared two new dithiocarbamate CTAs with Z-groups derived from **NI** and the corresponding reduced secondary amine. Based on the electronics of **NI**, it is apparent that only certain alkylating agents—sterically unhindered alkyl halides lacking acidic functionalities—can be employed to prepare CTAs derived from this Z-group. Nevertheless, CTA **1b** was prepared in moderate yields and was found to efficiently mediate RAFT polymerization of 2° MAMs—styrene, MA, and ACMO. Reduction of **NI** was conducted to reduce the electron withdrawing ability of the Z-group. Novel dithiocarbamate CTA **2** prepared from norbornene amine did not control the polymerization of 2° or 3° MAMs; however, it provided moderate control over the polymerization of VAc, yielding polymers with the appropriate CTA-derived end groups. ROMP of a PVAc MM prepared using CTA **2** was carried

out to give a bottlebrush polymer with PVAc side chains using the grafting-through technique. To the best of our knowledge, this work represents the first preparation of a bottlebrush polymer with PVAc side chains by the grafting-through method. We expect that this contribution will assist in the rational design of CTAs capable of mediating RAFT polymerization to form polymers functionalized with ROMP-active norbornene moieties.

Acknowledgements

This work was supported by the Army Research Office (W911NF-14-1-0322) and the American Chemical Society Petroleum Research Fund (54884-DNI7). We thank Materia for catalyst as well as Hannah Tecson and Kyle Moran for experimental assistance. We also thank Prof. Amanda J. Morris (Virginia Tech) for use of instruments.

6.7 References

(1) Matyjaszewski, K. *Macromolecules* **2012**, *45*, 4015.

(2) Moad, G.; Rizzardo, E.; Thang, S. H. *Aust. J. Chem.* **2012**, *65*, 985.

(3) Perrier, S.; Takolpuckdee, P. *J. Polym. Sci., Part A: Polym. Chem.* **2005**, *43*, 5347.

(4) Wang, J.-S.; Matyjaszewski, K. *Macromolecules* **1995**, *28*, 7901.

(5) Wang, J.-S.; Matyjaszewski, K. *J. Am. Chem. Soc.* **1995**, *117*, 5614.

(6) Sciannamea, V.; Jerome, R.; Detrembleur, C. *Chem. Rev.* **2008**, *108*, 1104.

(7) Zhang, N.; Samanta, S. R.; Rosen, B. M.; Percec, V. *Chem. Rev.* **2014**, *114*, 5848.

(8) Chiefari, J.; Chong, Y. K.; Ercole, F.; Krstina, J.; Jeffery, J.; Le, T. P. T.; Mayadunne, R. T. A.; Meijs, G. F.; Moad, C. L.; Moad, G.; Rizzardo, E.; Thang, S. H. *Macromolecules* **1998**, *31*, 5559.

(9) Vázquez-Dorbatt, V.; Tolstyka, Z. P.; Maynard, H. D. *Macromolecules* **2009**, *42*, 7650.

(10) Bulmus, V. *Polym. Chem.* **2011**, *2*, 1463.

(11) De, P.; Li, M.; Gondi, S. R.; Sumerlin, B. S. *J. Am. Chem. Soc.* **2008**, *130*, 11288.

(12) Sumerlin, B. S. *ACS Macro Lett.* **2012**, *1*, 141.

(13) Ratcliffe, L. P. D.; Ryan, A. J.; Armes, S. P. *Macromolecules* **2013**, *46*, 769.

(14) Warren, N. J.; Armes, S. P. *J. Am. Chem. Soc.* **2014**, *136*, 10174.

(15) Figg, C. A.; Simula, A.; Gebre, K. A.; Tucker, B. S.; Haddleton, D. M.; Sumerlin, B. S. *Chem. Sci.* **2015**, *6*, 1230.

(16) Kang, Y.; Pitto-Barry, A.; Maitland, A.; O'Reilly, R. K. *Polym. Chem.* **2015**, *6*, 4984.

(17) Gody, G.; Maschmeyer, T.; Zetterlund, P. B.; Perrier, S. *Nat. Commun.* **2013**, *4*, 2505.

(18) Foster, J. C.; Matson, J. B. *Macromolecules* **2014**, *47*, 5089.

(19) Zhang, L.; Liu, W.; Lin, L.; Chen, D.; Stenzel, M. H. *Biomacromolecules* **2008**, *9*, 3321.

(20) York, A. W.; Kirkland, S. E.; McCormick, C. L. *Adv. Drug. Deliv. Rev.* **2008**, *60*, 1018.

(21) Cerritelli, S.; Velluto, D.; Hubbell, J. A. *Biomacromolecules* **2007**, *8*, 1966.

(22) Moad, G.; Rizzardo, E.; Thang, S. H. *Chemistry – An Asian Journal* **2013**, *8*, 1634.

(23) Teo, Y. C.; Xia, Y. *Macromolecules* **2015**, *48*, 5656.

(24) Li, Z.; Zhang, K.; Ma, J.; Cheng, C.; Wooley, K. L. *J. Poly. Sci. Part A, Polym. Chem.* **2009**, *47*, 5557.

(25) Li, X.; ShamsiJazeyi, H.; Pesek, S. L.; Agrawal, A.; Hammouda, B.; Verduzco, R. *Soft Matter* **2014**, *10*, 2008.

(26) Moad, G.; Rizzardo, E.; Thang, S. H. *Polymer* **2008**, *49*, 1079.

(27) Hill, M. R.; Carmean, R. N.; Sumerlin, B. S. *Macromolecules* **2015**, *48*, 5459.

(28) Chiefari, J.; Mayadunne, R. T. A.; Moad, C. L.; Moad, G.; Rizzardo, E.; Postma, A.; Thang, S. H. *Macromolecules* **2003**, *36*, 2273.

(29) Chong, Y. K.; Krstina, J.; Le, T. P. T.; Moad, G.; Postma, A.; Rizzardo, E.; Thang, S. H. *Macromolecules* **2003**, *36*, 2256.

(30) Keddie, D. J.; Moad, G.; Rizzardo, E.; Thang, S. H. *Macromolecules* **2012**, *45*, 5321.

(31) Skey, J.; O'Reilly, R. K. *Chem. Commun.* **2008**, 4183.

(32) Mayadunne, R. T. A.; Rizzardo, E.; Chiefari, J.; Chong, Y. K.; Moad, G.; Thang, S. H. *Macromolecules* **1999**, *32*, 6977.

(33) Radzinski, S. C.; Foster, J. C.; Matson, J. B. *Polym. Chem.* **2015**, *6*, 5643.

(34) Love, J. A.; Morgan, J. P.; Trnka, T. M.; Grubbs, R. H. *Angew. Chem., Int. Ed.* **2002**, *41*, 4035.

(35) Liu, J.; Gao, A. X.; Johnson, J. A. *J. Vis. Exp.* **2013**, e50874.

(36) Humeres, E.; Debacher, N. A.; Sierra, M. M. d. S.; Franco, J. D.; Schutz, A. *J. Org. Chem.* **1998**, *63*, 1598.

(37) Van Vliet, L. D.; Ellis, T.; Foley, P. J.; Liu, L.; Pfeffer, F. M.; Russell, R. A.; Warrener, R. N.; Hollfelder, F.; Waring, M. J. *J. Med. Chem.* **2007**, *50*, 2326.

(38) McKenzie, T. G.; Fu, Q.; Wong, E. H. H.; Dunstan, D. E.; Qiao, G. G. *Macromolecules* **2015**, *48*, 3864.

(39) Stenzel, M. H.; Cummins, L.; Roberts, G. E.; Davis, T. P.; Vana, P.; Barner-Kowollik, C. *Macromol. Chem. Phys.* **2003**, *204*, 1160.

(40) Ohnaga, T.; Sato, T. *Polymer* **1996**, *37*, 3729.

(41) Nese, A.; Kwak, Y.; Nicolaÿ, R.; Barrett, M.; Sheiko, S. S.; Matyjaszewski, K. *Macromolecules* **2010**, *43*, 4016.

(42) Bernard, J.; Favier, A.; Davis, T. P.; Barner-Kowollik, C.; Stenzel, M. H. *Polymer* **2006**, *47*, 1073.

(43) Baker, M. I.; Walsh, S. P.; Schwartz, Z.; Boyan, B. D. *J. Biomed. Mater. Res. Part B Appl. Biomater.* **2012**, *100B*, 1451.

(44) Baudry, R.; Sherrington, D. C. *Macromolecules* **2006**, *39*, 5230.

6.8 Appendix

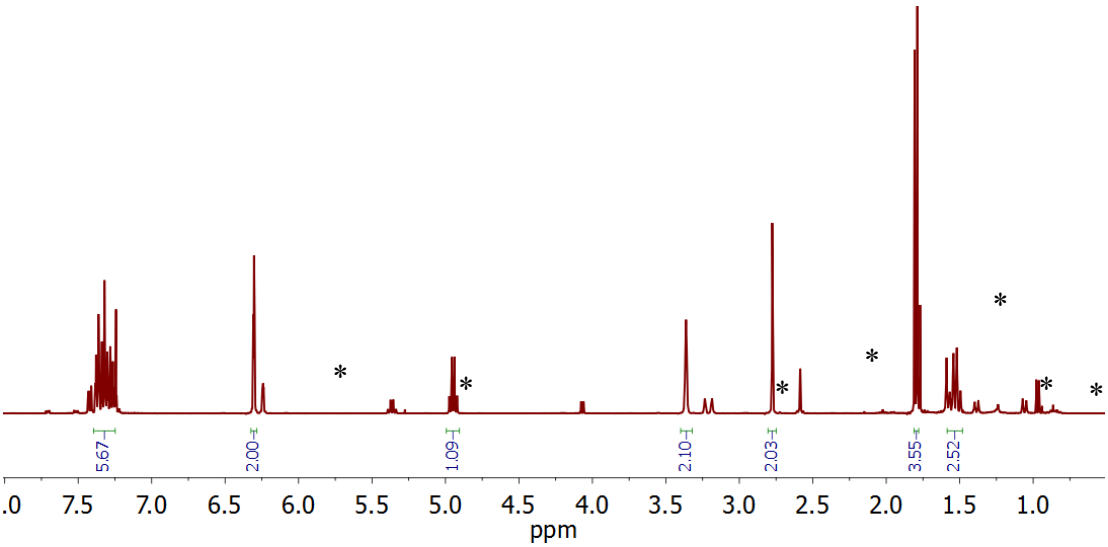

Figure 6S1. ^{1}H NMR spectrum of CTA **1b**. The starred peaks correspond to *N*-alkylated byproduct.

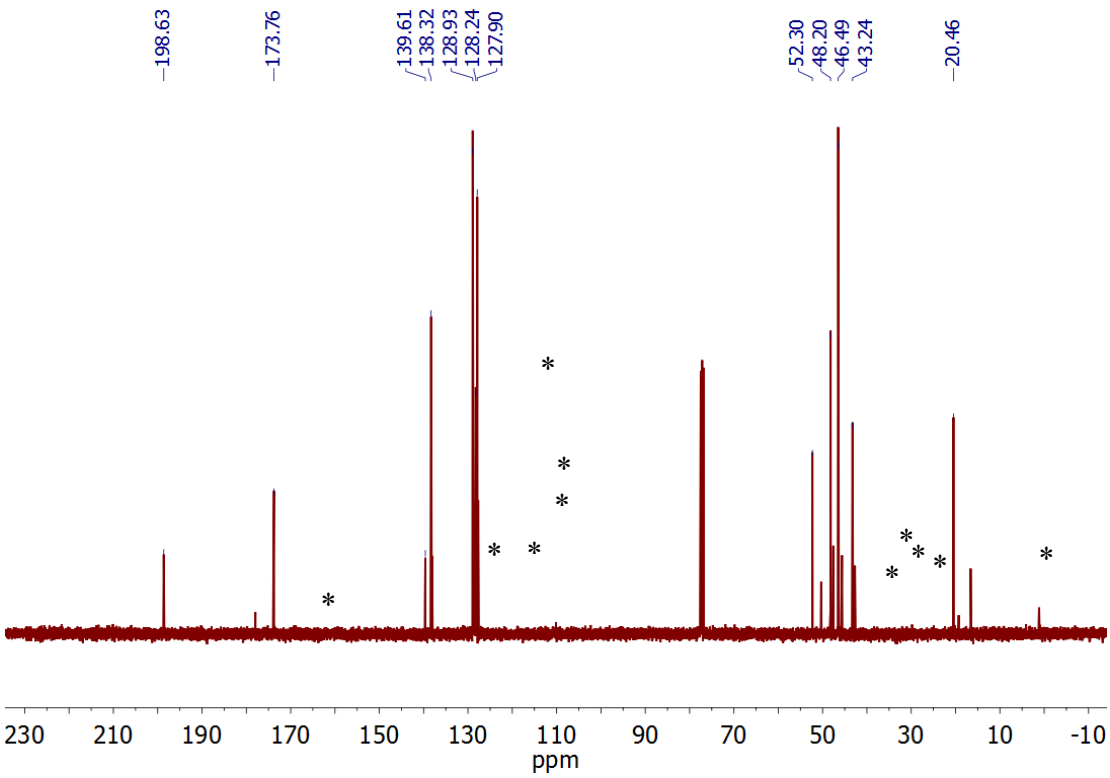

Figure 6S2. ^{13}C NMR spectrum of CTA **1b**. Starred peaks correspond to *N*-alkylated byproduct.

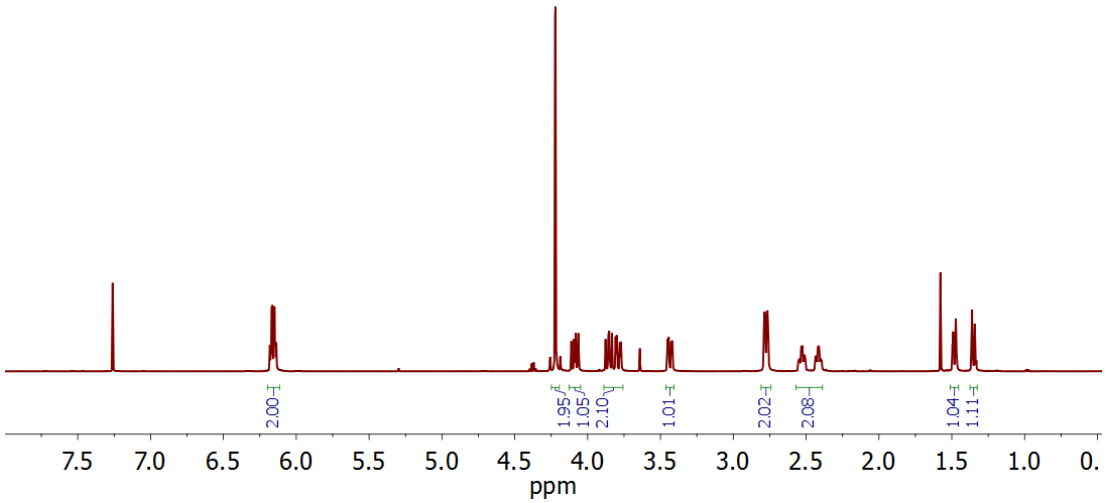

Figure 6S3. ^{1}H NMR spectrum of CTA **2**.

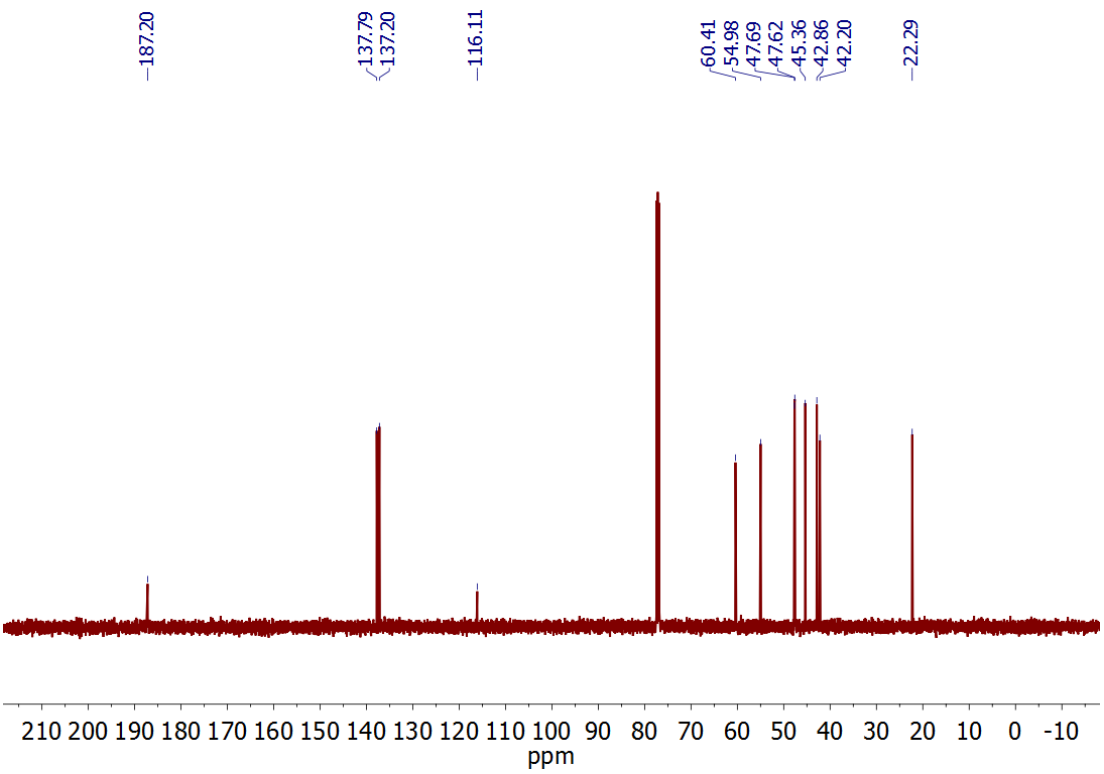

Figure 6S4. ^{13}C NMR spectrum of CTA **2**.

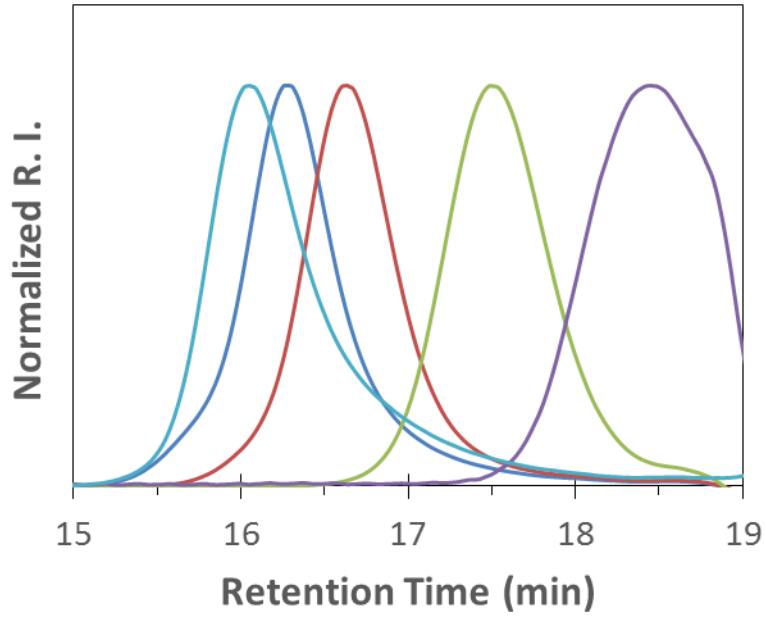

Figure 6S5. SEC traces of aliquots removed during the kinetic evaluation of the polymerization of MA mediated by CTA **1b**.

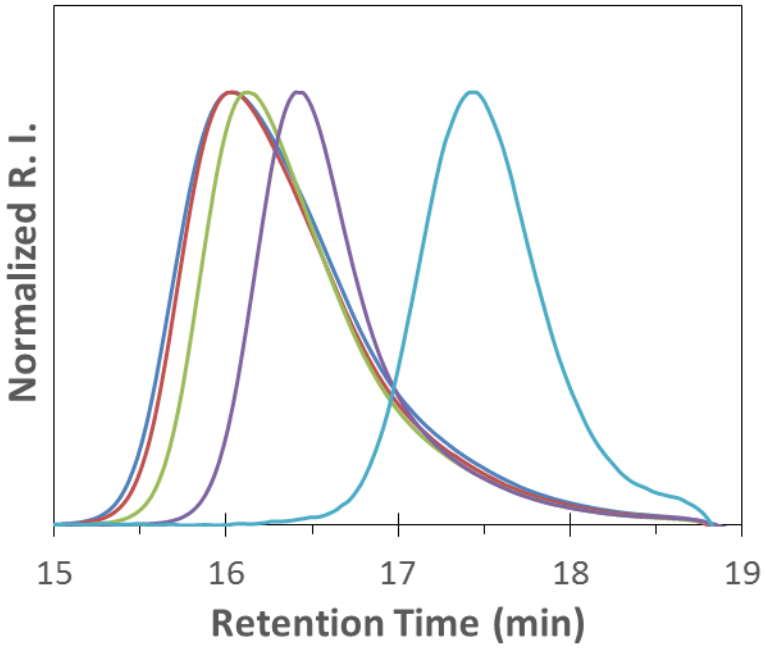

Figure 6S6. SEC traces of aliquots removed during the kinetic evaluation of the polymerization of ACMO mediated by CTA **1b**.

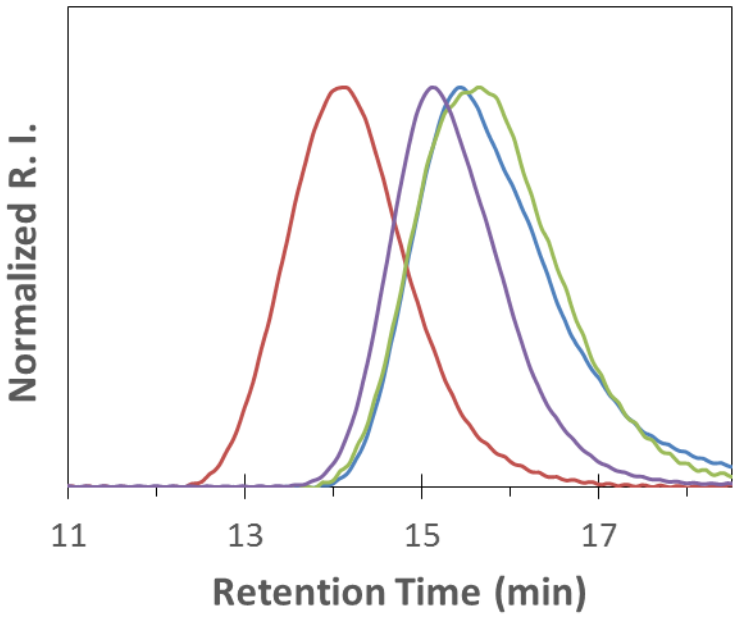

Figure 6S7. SEC traces of RAFT polymerizations of MMA (orange trace), ACMO (yellow trace), styrene (blue trace), and MA (grey trace) using CTA **2**.

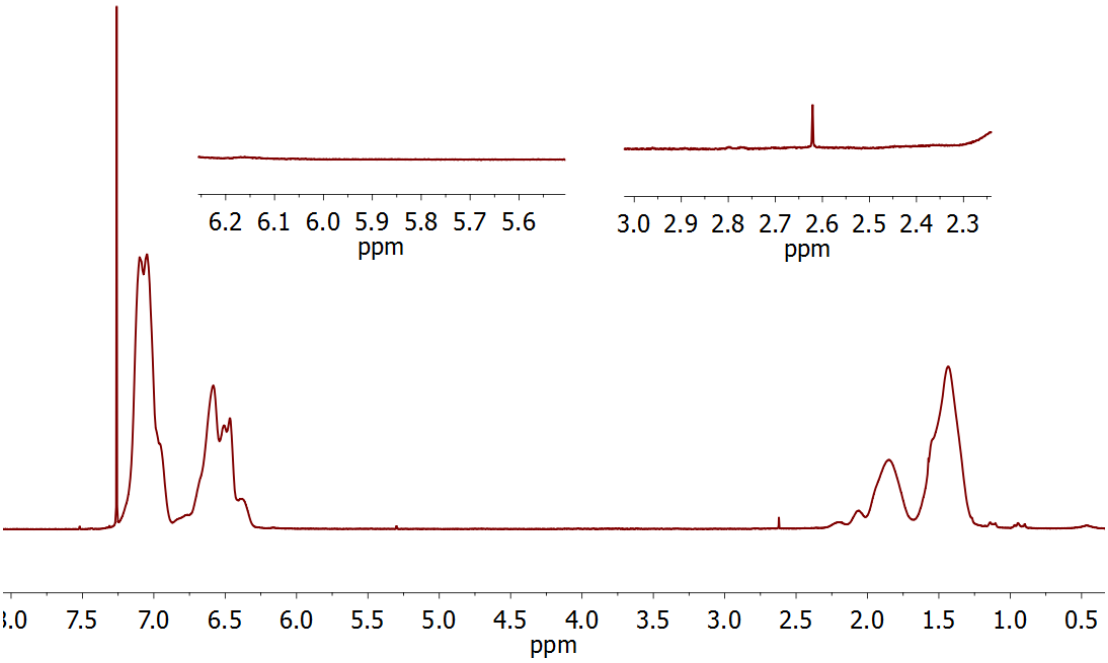

Figure 6S8. ^{1}H NMR spectrum of PS prepared using CTA **2** highlighting the absence of the expected CTA-derived end groups that should appear around 2.4 ppm and 6 ppm for the α and ω chain ends, respectively.

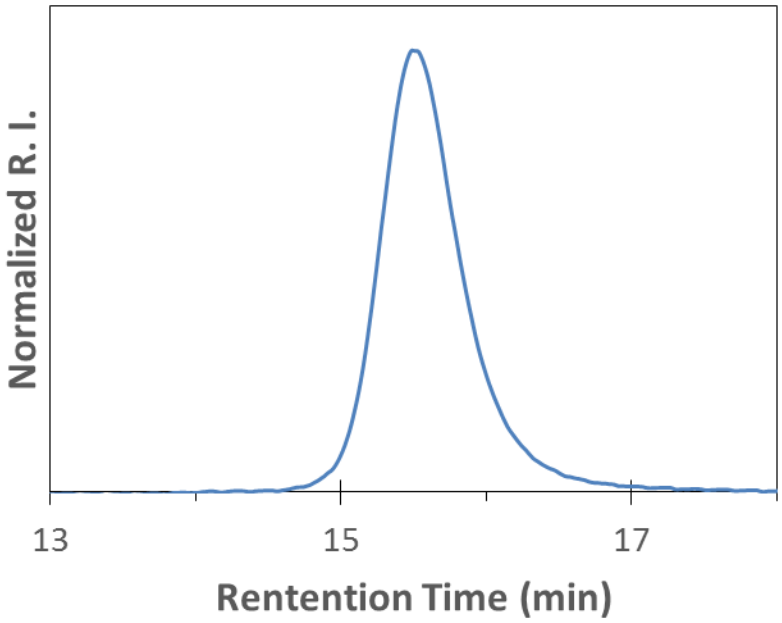

Figure 6S9. SEC trace of poly(**2**) prepared by ROMP of CTA **2**.

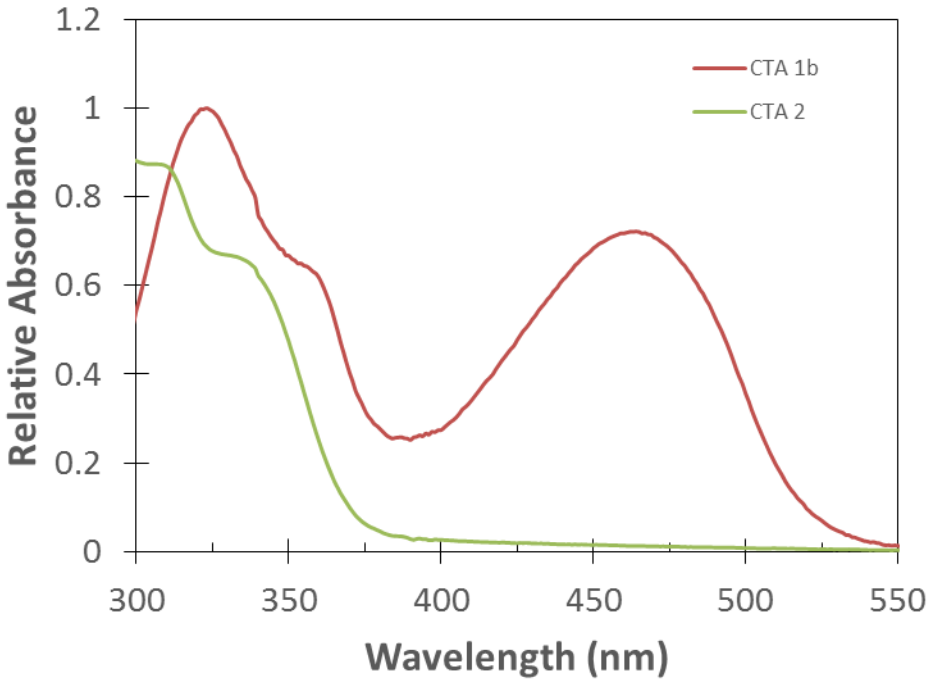

Figure 6S10. UV-Vis absorbance spectra of CTA **1b** (orange trace) and CTA **2** (grey trace) taken at 2 mg/mL in THF.

Chapter 7: Factors Affecting Bottlebrush Polymer Synthesis by the Transfer-to Method Using Reversible Addition–Fragmentation Chain Transfer (RAFT) Polymerization

S. C. Radzinski, J. C. Foster, S. E. Lewis, E. V. French and J. B. Matson, *Polym. Chem*., **2017**, Advance Article, DOI: 10.1039/C6PY01982J -Published by The Royal Society of Chemistry.

7.1 Authors

Scott C. Radzinski, Jeffrey C. Foster, Sally E. Lewis, Eric V. French, and John B. Matson

Department of Chemistry and Macromolecules Innovation Institute, Virginia Tech, Blacksburg, Virginia 24061, United States

7.2 Abstract

The transfer-to method is a unique way to prepare bottlebrush polymers by reversible addition-fragmentation chain transfer (RAFT) polymerization. This little-studied bottlebrush polymer synthesis strategy is distinct from the grafting-from, grafting-to, and grafting-through strategies and therefore may have specific advantages over these other synthetic approaches. Herein, we study the factors affecting the composition of bottlebrush polymer samples prepared by RAFT transfer-to, with particular emphasis on bottlebrush polymer molecular weight (MW) and dispersity (Đ) and the percentage of "dead" linear polymer as a function of initiator concentration, [M]/[CTA] ratio, backbone length, and monomer type. The lowest quantities of dead polymer were obtained under conditions that limited the MW of the bottlebrush polymer side-chains and that discouraged termination reactions. Under optimized conditions, high MW bottlebrush polymers were prepared with low dispersities and few dead polymer impurities.

7.3 Introduction

The unique properties of bottlebrush polymers have made this rich polymer topology a potential contributor in applications ranging from super-soft materials[1,2] to photonic crystals,[3,4] to drug delivery.[5,6] These properties arise from the densely grafted nature of bottlebrush polymers, which results in steric repulsion between polymeric side-chains that force the macromolecules to adopt a shape-persistent, chain-extended conformation.[7-10] In recent years, the field of bottlebrush polymer synthesis has advanced dramatically, with controlled polymerization techniques such as reversible addition–fragmentation chain transfer (RAFT)[11] polymerization and ring-opening metathesis polymerization (ROMP)[12] enabling precise control over the size and dispersity of the bottlebrush polymer backbone as well as the pendant polymeric side-chains.[13-19] However, despite this progress, the synthesis of high molecular weight (MW) bottlebrush polymers with controllable dimensions remains challenging.[20]

Bottlebrush polymers are prepared by one of four methods: grafting-to, grafting-from, grafting-through, or transfer-to. The polymers produced by these methods differ in their structures (i.e., grafting densities, imperfections, etc.) and sample compositions depending on the advantages and limitations of each method. For example, grafting-from allows for direct control over the synthesis of the polymer backbone, but the side-chains do not all match their theoretical MW due to undesirable side reactions. These include looping (intramolecular coupling) and brush-brush (intermolecular coupling) reactions that originate from the tethering of the propagating species to the bottlebrush polymer backbone.[21] These termination pathways yield imperfections, high MW impurities, and sometimes cross-linking in the resulting polymer samples. Despite these limitations, grafting-from is perhaps the most thoroughly studied bottlebrush polymer synthesis

technique. The transfer-to approach, while similar to grafting-from, has the potential to completely eliminate these bottlebrush polymer coupling and looping side reactions.[22]

Both grafting-from and transfer-to can be mediated by a polymeric RAFT chain transfer agent (CTA).[22-25] RAFT CTAs contain an R group, which is homolytically cleaved from the CTA to initiate chain-growth polymerization, and a Z group, which is immobile and regulates the reactivity of the CTA. The difference in the two strategies lies in the direction of CTA attachment to the polymer backbone. In RAFT grafting-from, the R group is attached to the polymer backbone, so growing radicals remain tethered to the bottlebrush polymer throughout the polymerization. In RAFT transfer-to, the CTA is attached through the Z-group (transfer-to is sometimes called the Z-group or Z-Star approach).[26,27] In this case, polymer-derived radicals do not remain tethered to the bottlebrush polymer backbone; instead, they detach and propagate freely in solution, eventually returning to a bottlebrush polymer via a chain-transfer reaction (Figure 7.1).[14,19] During polymerization, the detached linear chains are in equilibrium with the bottlebrush polymer side-chains; therefore, absent substantial termination, the MWs of these two populations are expected to be approximately equal.[28] Termination reactions between linear polymers lead to the formation of "dead" linear polymer but do not create loops or coupled bottlebrushes.

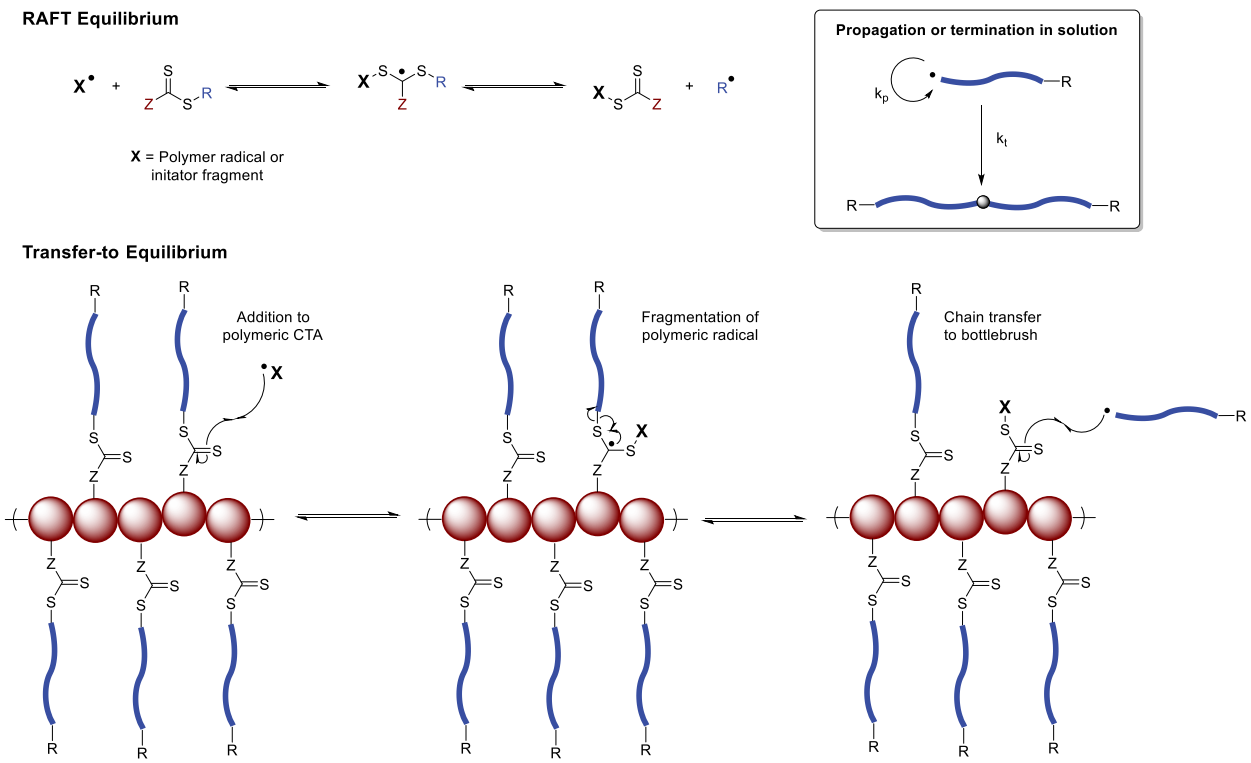

Figure 7.1. Illustration of idealized RAFT transfer-to equilibrium. The red spheres designate the bottlebrush polymer backbone repeat units, while the blue lines represent side-chains. The polymerization is mediated by polymeric RAFT CTAs, which fragment to yield polymeric radicals that grow freely in solution.

In our previous report on RAFT transfer-to polymerization, we observed the formation of a substantial fraction of dead polymer chains as the polymerizations progressed.[14] These dead polymers are sometimes difficult to separate from the bottlebrush polymers and could potentially affect the mechanical properties of the sample. In addition, loss of bottlebrush polymer side-chains to termination reactions results in a reduction in the grafting density of the bottlebrush polymer. Grafting density is difficult to measure directly due to the dynamic nature of RAFT transfer-to, but information about the grafting density can be inferred by inspecting the quantity of dead polymers that form during polymerization. Each dead polymer represents a chain that is

no longer attached to a bottlebrush polymer and therefore reduces the overall grafting density of the sample. In addition, the bottlebrush polymer grafting density can also be inferred by comparing the observed MWs of the bottlebrush polymers to expected values based on monomer conversion. In the absence of considerable termination, lower than expected bottlebrush polymer MWs most probably originate from the fact that they possess grafting densities less than 100%. Grafting density can also be approximated by isolating the bottlebrush polymer and cleaving the polymer side-chains from the bottlebrush polymer backbone and then dividing the observed bottlebrush polymer MW by the MW of the side-chains.

In this contribution, we sought to optimize the polymerization to achieve controlled bottlebrush polymer synthesis while decreasing the dead chain population without significantly extending its timescale. Toward this end, we investigate the effect of initiator concentration, initial [M]/[CTA] ratio, reaction time, bottlebrush polymer backbone DP, and monomer selection on the MW and dispersity (Đ) of the resulting bottlebrush polymers as well as the fraction of dead linear chains.

7.4 Experimental

Materials. All reagents were obtained from commercial vendors and used as received unless otherwise stated. Styrene, methyl acrylate (MA), and 4-acryloylmorpholine (ACMO) were passed through small columns of basic alumina prior to use. ROMP catalyst $(H_2IMes)(Cl)_2(PCy_3)Ru{=}CHPh$ (**G2**) was obtained as a generous gift from Materia. ROMP catalyst $(H_2IMes)(pyr)_2(Cl)_2Ru{=}CHPh$ (**G3**) was prepared from **G2** according to literature procedures.[29,30]

Methods. NMR spectra were measured on an Agilent 400 MHz spectrometer. ^{1}H and ^{13}C NMR chemical shifts are reported in ppm relative to internal solvent resonances. Size exclusion chromatography (SEC) was carried out in THF at 1 mL/min at 30°C on two Agilent PLgel 10

μm MIXED-B columns connected in series with a Wyatt Dawn Heleos 2 light scattering detector and a Wyatt Optilab Rex refractive index detector. No calibration standards were used, and dn/dc values were obtained by assuming 100% mass elution from the columns. **CTA1** was synthesized from previous literature reports.[14,31]

Typical synthesis of Poly(CTA1) (PCTA1). A typical polymerization procedure of **CTA1** is as follows: A solution of **G3** in anhydrous CH_2Cl_2 was prepared in a vial at 40X the desired concentration (0.02 to 0.001 equivalents with respect to monomer). A 100 μL aliquot of this **G3** solution was added rapidly to a vigorously stirring solution of **CTA1** (200 mg) in 3.9 mL of anhydrous CH_2Cl_2 in a 1 dram vial to make a final volume of 4 mL and a final monomer concentration of 50 mg/mL. The polymerization was quenched after 20 min by adding of 1-3 drops of ethyl vinyl ether. The polymer was isolated via precipitation from hexanes and dried under vacuum to yield the pure polymer as an off-white powder.

Typical synthesis of Poly(CTA1-*g*-polymer) by RAFT transfer-to. To an oven-dried Schlenk tube equipped with a magnetic stir bar was added **PCTA1** (2.88 mg, 0.18 mmol, M_n = 17,000 g/mol), styrene (1 mL, 8.73 mmol), and 5 mL of DMF. A stock solution of 2,2'-azobis(2-methylpropionitrile) (AIBN) was prepared by dissolving 2.9 mg in 10 mL of DMF. 100 μL of this stock solution was then added to the Schlenk tube. The reaction mixture was deoxygenated by three freeze-pump-thaw cycles. The Schlenk tube was then backfilled with N_2 and submerged in an oil bath maintained at 75 °C. Samples were removed periodically by N_2-purged syringe to monitor MW evolution by SEC and conversion by ^{1}H NMR spectroscopy. The polymerization was quenched by submerging the tube into liquid N_2 and exposing the reaction solution to air.

Peak Fitting. The relative weight fractions of bottlebrush polymer and dead linear polymer were determined via peak fitting of SEC RI data according to literature procedures.[32,33] These data are provided in the Supporting Information (Figures 7S1-7S13).

7.5 Results and Discussion

To study bottlebrush polymer synthesis by RAFT transfer-to polymerization, we first synthesized a dithiocarbamate CTA (**CTA1**) according to our previously reported procedure.[14] This CTA contains a norbornene-imide Z group and is suitable for mediating polymerization of acrylates, acrylamides, and styrene.[31] **CTA1** also contains a norbornene moiety that can be utilized in ROMP. Next, poly(CTA)s (PCTAs) were prepared via ROMP of **CTA1** initiated by Grubbs' 3rd generation catalyst, $(H_2IMes)(pyr)_2(Cl)_2Ru{=}CHPh$ (**G3**) as shown in Scheme 7.1. These polyCTAs were then utilized in various RAFT transfer-to polymerizations as discussed below.

Scheme 7.1. Idealized bottlebrush polymer synthesis by RAFT transfer-to polymerization.

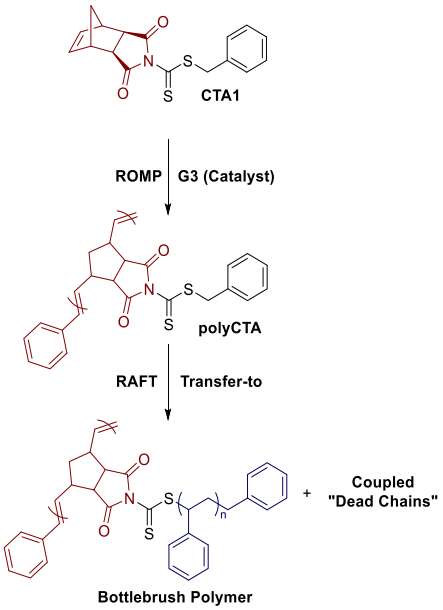

Effect of Radical Initiator Concentration

The amount of initiator utilized in a RAFT polymerization affects the polymerization kinetics and therefore the duration of the polymerization.[34] In addition, similar to conventional radical polymerization, the rate of termination is directly related to the concentration of actively propagating radicals.[35] Termination reactions during RAFT transfer-to result in dead linear polymer that cannot return to the bottlebrush polymer backbone. Therefore, limiting these termination events is critical to maintaining a low quantity of dead linear polymers. To test the effect of the [AIBN]/[CTA] ratio on RAFT transfer-to polymerizations, two experiments were performed with constant [M]/[CTA] ratio using a PCTA with a backbone degree of polymerization (DP) of 50, but with [AIBN]/[CTA] ratios of either 0.02 or 0.2 (Table 7.1, entries 1 and 2). The order of magnitude difference in AIBN concentration had an effect on the timescale of the polymerization and the amount of dead chains in solution. The polymerization with [AIBN]/[CTA] = 0.2 exhibited faster kinetics than the polymerization with less initiator (Figure 7S15). Size exclusion chromatographic (SEC) analysis of the 6 h time point of the polymerization with [AIBN]/[CTA] = 0.02 revealed a number average MW (M_n) of 114 kDa, while the the polymerization with [AIBN]/[CTA] = 0.2 reached a larger M_n of 293 kDa. We chose to evaluate the 6 h time points to relate data at low conversions with minimal influence from high viscosity or termination reactions. Based on the SEC traces in Figure 7.2, the bottlebrush polymer weight fraction was calculated for each time point by comparing the area under the curve of the bottlebrush polymer peak at lower retention time to that of the dead linear polymer peak at greater retention time using a peak-fitting algorithm.[32,33] The polymerization with a lower AIBN concentration possessed a dead chain fraction of 37%. In contrast, the polymerization with more AIBN had a significantly larger fraction of dead chains (57%). The

dispersity (Đ) of the bottlebrush polymer was unaffected by AIBN concentration as the bottlebrush polymer peak of both polymer samples was narrowly dispersed. Low bottlebrush polymer dispersity values are expected for RAFT transfer-to due to the absence of looping or bottlebrush polymer coupling reactions common in grafting-from.[26] Based on these results, a higher proportion of AIBN allows for faster polymerization and higher MWs at the cost of increased dead polymer. We chose to utilize the higher AIBN loading ([AIBN]/[CTA] = 0.2) in subsequent experiments to achieve reasonable polymerization timescales. We then aimed to reduce the fraction of dead chains by tuning other parameters of the reaction.

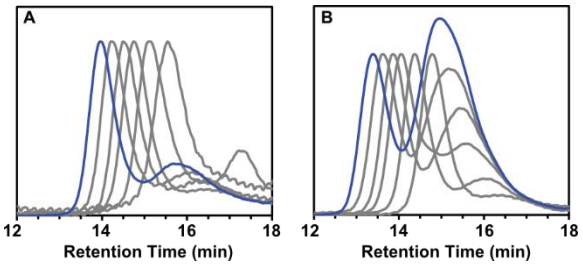

Figure 7.2. Effect of [AIBN]/[CTA] ratio on RAFT transfer-to polymerization (Table 7.1, entries 1 and 2), demonstrating that higher AIBN concentrations lead to a higher percentage of dead polymer. Shown above are SEC traces (refractive index detector) at various time points for (A) low AIBN loading (0.02 equiv with respect to CTA), (B) high AIBN loading (0.2 equiv with respect to CTA). The final time point for each run (blue lines) was taken after 24 h, while the gray traces represent the 1, 2, 4, 6, and 10 h time points. The bimodal distribution in most traces shows a high MW bottlebrush polymer peak at lower retention time and a lower MW peak at higher retention time representing dead linear polymer.

Table 7.1. Summary of polymers synthesized in this study.

Entry	Monomer	DP Backbone	[M]/[CTA]	[AIBN]/[CTA]	Mn (kDa)[a]	Đ[a]	%Dead[b]	% Conversion[c]
1	sty	50	1000	0.02	114	1.03	37	27
2	sty	50	1000	0.2	293	1.01	57	32
3	sty	50	750	0.2	260	1.02	43	44
4	sty	50	500	0.2	216	1.02	41	35
5	sty	50	100	0.2	103	1.04	28	40
6	sty	50	50	0.2	44.0	1.04	24	34
7	sty	100	50	0.2	97.0	1.08	21	29
8	sty	500	50	0.2	753	1.08	36	40
9	sty	750	50	0.2	1110	1.02	30	40
10	sty	1000	50	0.2	1150	1.07	40	33
11	MA	100	50	0.2	400	1.05	14	89
12	ACMO	100	50	0.2	740	1.04	11	82

[a]Measured by SEC using absolute MW determined by light scattering. [b]Determined using peak fitting of SEC RI data. [c]Calculated using relative integrations of monomer and polymer resonances using ^{1}H NMR spectroscopy. These data represent the 6 h time point for each polymerization. All polymerizations were carried out at [Monomer] = 17 v/v%.

Effect of Initial [M]/[CTA] Ratio

An additional factor that we expected to affect RAFT transfer-to polymerization was the initial [M]/[CTA] ratio. Typically, the initial [M]/[CTA] ratio used during RAFT determines the polymer MW.[34] For bottlebrush polymer synthesis by RAFT transfer-to, the MW of the bottlebrush polymer side-chains depends on the [M]/[CTA] ratio, as each repeat unit of the bottlebrush polymer backbone contains a pendant CTA. Holding the DP of **PCTA1** fixed at 50 and using an [AIBN]/[CTA] ratio of 0.2, the [M]/[CTA] ratio was varied between 1000 and 50 over a series of transfer-to polymerizations with styrene as the monomer (Table 7.1, entries 2-6 respectively). Aliquots were periodically taken from the reaction mixtures and analyzed by SEC (Figure 7.3). It should be noted that the conversions of the polymerizations as measured by ^{1}H

NMR spectroscopy varied slightly between experiments due to the different initial conditions employed in each. However, the bottlebrush polymer MWs and dead polymer fractions were less sensitive to conversion than they were to initial reaction conditions, so we chose to compare these parameters as a function of initial conditions for the 6 h time points.

Consistent with traditional RAFT polymerization, decreasing the [M]/[CTA] ratio resulted in lower MW bottlebrushes (293 kDa for [M]/[CTA] = 1000 to 44.0 kDa for [M]/[CTA] = 50). Given that the polymerizations used the same PCTA, this decrease in MW is a result of a decrease in the size of the side-chains. The initial [M]/[CTA] ratio had little effect on the conversion of the polymerizations after 6 h or the Đ values of the resulting bottlebrush polymers.

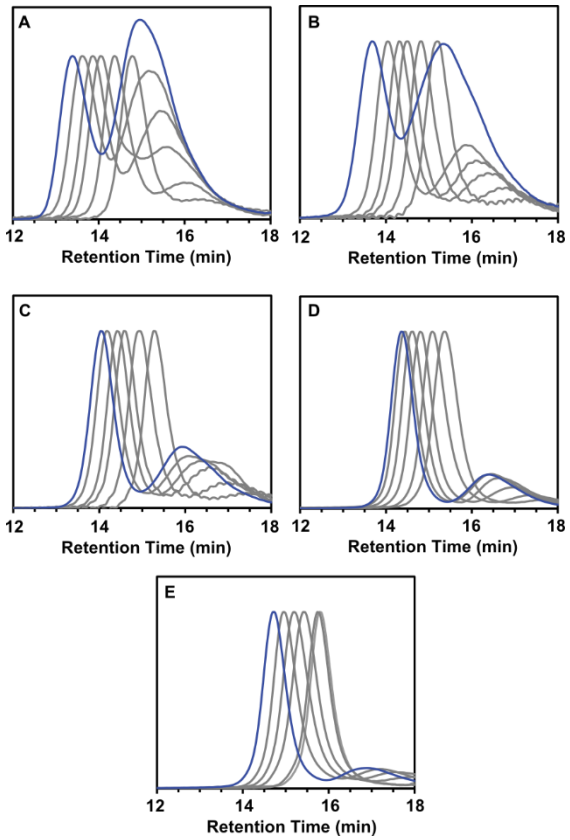

Figure 7.3. Effect of the [M]/[CTA] ratio on RAFT transfer-to polymerization (Table 7.1, entries 2-6), demonstrating that higher [M]/[CTA] ratios lead to higher percentages of dead polymer. Shown above are SEC traces (refractive index detector) at various time points for (A) [M]/[CTA] = 1000, (B) [M]/[CTA] = 750, (C) [M]/[CTA] = 500, (D) [M]/[CTA] = 100, and (E) [M]/[CTA] = 50. The final time point for each sample (blue lines) was taken after 24 h, while the gray traces represent the 1, 2, 4, 6, and 10 h time points. The peak at higher retention time in each trace corresponds to dead linear polymer.

Bottlebrush polymer weight fraction decreased over the course of the polymerizations, with higher [M]/[CTA] ratios yielding more dead polymer impurities (Figure 7S16). The effect of the [M]/[CTA] ratio was visualized by plotting bottlebrush polymer wt fraction as function of initial [M]/[CTA] ratio for the 6 h time points. As shown in Figure 7.4A, bottlebrush polymer weight

fraction decreased with increasing [M]/[CTA] ratios. Moreover, the weight fraction of bottlebrush polymer appeared to be negatively correlated with expected side-chain MW (Figure 7S17). We believe that these decreases in bottlebrush polymer weight fraction are likely due to steric factors. Large side-chains have a relatively greater entropic barrier against chain-transfer back to a bottlebrush polymer backbone compared with small chains.[36] Therefore, increasing the [M]/[CTA] ratio led to higher MW side-chains and larger bottlebrush polymers but also resulted a greater percentage of dead chains.

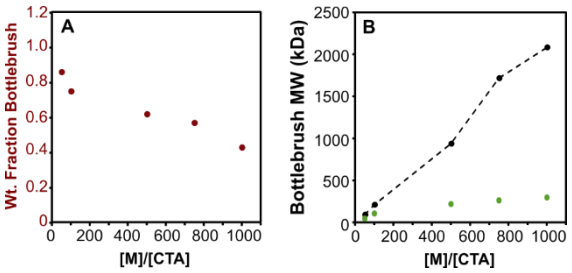

Figure 7.4. Evaluation of bottlebrush polymer weight fraction as a function of [M]/[CTA] ratio at 6 h (Table 7.1, entries 2-6). (A) Bottlebrush polymer weight fraction plotted as a function of [M]/[CTA] ratio. (B) MW of the bottlebrush polymers measured by SEC (green circles) compared to expected MW values calculated using monomer conversions as a function of [M]/[CTA] ratio (black circles).

Bottlebrush polymer MWs were compared to expected values that were calculated using monomer conversions obtained via ^{1}H NMR spectroscopy for the 6 h time points. As shown in Figure 7.4B, the observed bottlebrush polymer MWs were dramatically lower than expected. This deviation is most apparent at high [M]/[CTA] ratios. Star or bottlebrush polymers prepared by RAFT transfer-to polymerization often possess MWs that are much lower than expected;[37,38] however, the origin of this phenomenon is often attributed to inaccurate determination of MW. Plots of bottlebrush polymer MW vs conversion were linear for each [M]/[CTA] ratio utilized

(Figure 7S18); therefore, it is unlikely that the deviations between observed and expected MW values originate from chain-transfer or termination side reactions. Rather, the lower than expected bottlebrush polymer MW values most probably arise as the result of less than perfect grafting densities. For RAFT transfer-to polymerization mediated by **PCTA1**, the grafting density of the bottlebrush polymers likely decreases with increasing [M]/[CTA] ratio, which is consistent with the larger fraction of dead polymers observed at high [M]/[CTA] ratios.

Effect of PCTA Backbone Degree of Polymerization

Next, we investigated the effect of the initial backbone DP of the PCTAs on bottlebrush polymer MW, Đ, and dead polymer quantity. Several different PCTAs were synthesized via ROMP of **CTA1** with backbone DPs of 50, 100, 500, 750, and 1000 (Table 7S1). RAFT transfer-to polymerization was then performed using each of these PCTAs while keeping the [AIBN]/[CTA] ratio constant at 0.2 and the [M]/[CTA] ratio at 50 (Table 7.1, entries 6-10). Time points were taken from each polymerization and analyzed by SEC and ^{1}H NMR spectroscopy. Unsurprisingly, bottlebrush polymer MWs increased as a function of backbone DP, with Đ values remaining low regardless of initial conditions (Figure 7.5). The dead polymer fraction also appeared to increase as a function of backbone DP. For example, RAFT of styrene mediated by a DP = 50 PCTA after 6 h yielded a dead polymer fraction of 24% while the composition of the DP = 1000 sample was 40% dead polymer at a similar conversion. We did not expect a large increase in dead polymer fraction between these experiments due to the fact that the [M]/[CTA] ratio was held constant at 50 over the series. We observed that the polymerization solutions had become noticeably viscous after ~6 h for the DP = 500, 750, and 1000 samples despite the relatively dilute conditions utilized (17 v/v% monomer). Therefore, we speculate that the

observed increase in dead polymer percentage does not arise as a direct result of increasing the backbone DP, but rather due to increased solution viscosity for the higher DP PCTAs.

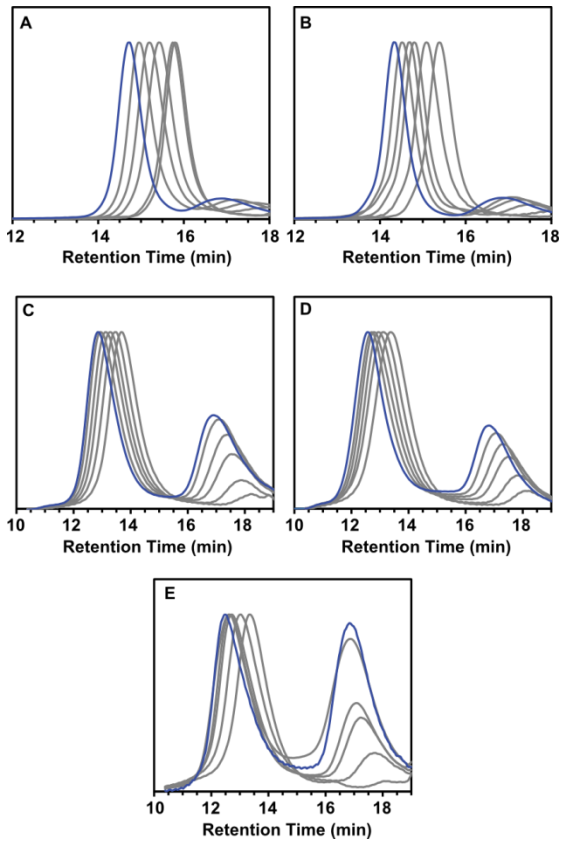

Figure 7.5. Effect of PCTA backbone DP on RAFT transfer-to polymerization (Table 7.1, entries 6-10, demonstrating that higher backbone DPs lead to higher percentages of dead polymer. Shown above are SEC traces (refractive index detector) at various time points for (A) DP = 50, (B) DP = 100, (C) DP = 500, (D) DP = 750, and (E) DP = 1000. The final time point for each sample (blue lines) was taken after 24 h, while the gray traces represent the 1, 2, 4, 6, and 10 h time points. The second population of chains in the traces at lower retention times corresponds to dead polymer.

The weight fraction of bottlebrush polymer decreased with increasing polymerization time, especially for higher DP PCTAs (Figure 7S19). The decrease in bottlebrush polymer wt fraction

observed at longer reaction times may also be the result of increased solution viscosity. An increase in viscosity during RAFT transfer-to polymerization would result in decreased chain transfer efficiency between the polymer radicals and the bottlebrush polymer backbone, leading to uncontrolled polymerization and/or termination of linear polymer chains. However, when comparing the 6 h time points, it appears that the weight fraction of bottlebrush polymer did not depend substantially on the DP of the PCTA backbone (Figure 7.6A).

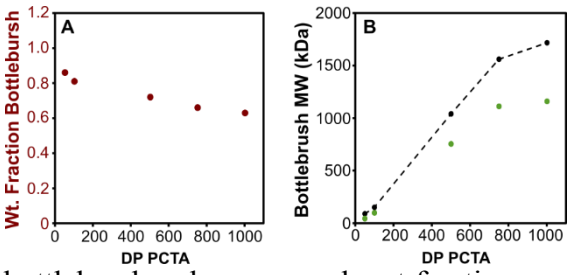

Figure 7.6. Evaluation of bottlebrush polymer sample wt fraction as a function of the DP of the PCTA at 6 h (Table 7.1, entries 6-10). (A) Bottlebrush polymer weight fraction plotted as a function of DP. (B) MW of the bottlebrush polymer measured by SEC (green circles) compared to an expected MW value calculated using monomer conversions as a function of PCTA DP (black circles).

The bottlebrush polymer MWs determined by SEC at the 6 h time points were compared against expected values (Figure 76B). In contrast to the experiments in which the [M]/[CTA] ratio was varied (Figure 74B), observed and expected MW values were in reasonably good agreement for this data set. Based on these data and the relatively high bottlebrush polymer wt fractions observed for the 6 h time points, we speculate that, in the absence of high viscosity, bottlebrush polymer grafting density does not depend extensively on the DP of the PCTA utilized.

Effect of Monomer Selection

In addition to the parameters above, the choice of vinyl monomer can have a significant influence on how the bottlebrush polymer forms during the transfer-to process. RAFT transfer-to polymerizations were performed on two different monomers—methyl acrylate (MA) and acryloylmorpholine (ACMO)—using **PCTA1** and similar polymerization conditions (Table 7.1, entries 11 and 12). The rate constants of propagation (k_p) of these monomers are at least an order of magnitude greater than styrene.[35] Given that the addition of a RAFT CTA to a polymerization reaction does not alter the concentration of radicals in solution, this trend in propagation rates is expected to hold regardless of the RAFT agent used or its concentration.[39] Therefore, polymerizations of MA and ACMO should experience fewer termination events than styrene, all other things being equal. Based on this knowledge, we hypothesized that transfer-to polymerization of MA or ACMO would provide bottlebrush polymers with high MW, high bottlebrush polymer purity, and a low quantity of dead polymer chains. Indeed, both of these transfer-to bottlebrush polymer syntheses reached near complete conversion in 6 h. The increase in k_p when using MA or ACMO relative to styrene allowed for the synthesis of large MW bottlebrush polymers (Figure 7.7) with high bottlebrush polymer weight fractions (Figure 7.8), implying high grafting density of the MA and ACMO bottlebrushes. Based on these results, it is clear that bottlebrush polymer synthesis by RAFT transfer-to using **PCTA1** is particularly well suited for polymerizing acrylate or acrylamide monomers.

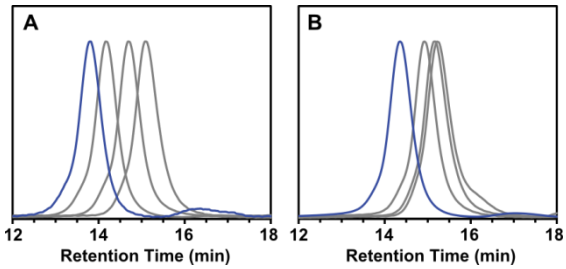

Figure 7.7 Effect of monomer on RAFT transfer-to polymerization (Table 7.1, entries 11 and 12). Shown above are SEC traces (refractive index detector) at various time points for RAFT transfer-to of (A) MA and (B) ACMO. The final time point for each sample (blue lines) was taken after 6 h, while the gray traces represent the 1, 2, and 4 h time points.

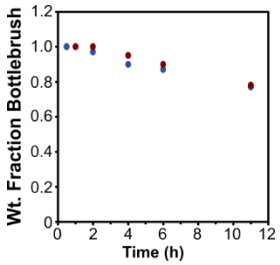

Figure 7.8. Change in bottlebrush polymer weight fraction over time for RAFT transfer-to polymerizations conducted with MA (blue circles) or ACMO (red circles).

7.6 Conclusions

The effect of radical initiator loading, [M]/[CTA] ratio, backbone DP, and monomer type were studied in RAFT transfer-to bottlebrush polymer synthesis with the goal of a polymerization that yielded high MW bottlebrush polymers of narrow dispersity with few dead linear chains. A low initial [M]/[CTA] ratio led to the formation of a bottlebrush polymer with few dead linear chains; however, this also restricted its MW. As the [M]/[CTA] ratio was increased, a greater fraction of dead linear chains was observed. The DP of the PCTA did not directly affect the population of dead linear chains; however, the use of large backbones resulted in high MW polymers but also noticeably viscous reaction mixtures, which eventually led to an increase in the amount of dead

linear polymer compared with lower DP PCTAs. The type of monomer had a dramatic effect on RAFT transfer-to polymerization. Compared with styrene, faster polymerizations and lower percentages of dead linear chains were generated when transfer-to polymerizations were carried out with MA or ACMO (high k_p monomers). Based on these results, we propose that for RAFT transfer-to polymerization, monomer choice and the initial [M]/[CTA] ratio are critically important considerations. High k_p monomers are expected to perform well due to reduced termination. The size of the side-chains determines the MW of the final bottlebrush polymer and the dead polymer fraction due to steric factors and likely affects the grafting density of the bottlebrush polymers as well. These insights may aid efforts toward fully realizing the potential of the transfer-to technique in bottlebrush polymer synthesis.

Acknowledgements

This work was supported by the Army Research Office (W911NF-14-1-0322) and the American Chemical Society Petroleum Research Fund (54884-DNI7). We thank Materia for catalyst.

7.7 References

(1) Pakula, T.; Zhang, Y.; Matyjaszewski, K.; Lee, H.-i.; Boerner, H.; Qin, S.; Berry, G. C. *Polymer* **2006**, *47*, 7198.

(2) Matyjaszewski, K.; Tsarevsky, N. V. *Nat Chem* **2009**, *1*, 276.

(3) Miyake, G. M.; Piunova, V. A.; Weitekamp, R. A.; Grubbs, R. H. *Angew. Chemie. Int. Ed.* **2012**, *51*, 11246.

(4) Sveinbjörnsson, B. R.; Weitekamp, R. A.; Miyake, G. M.; Xia, Y.; Atwater, H. A.; Grubbs, R. H. *PNAS* **2012**, *109*, 14332.

(5) Yu, Y.; Chen, C.-K.; Law, W.-C.; Mok, J.; Zou, J.; Prasad, P. N.; Cheng, C. *Mol. Pharm.* **2013**, *10*, 867.

(6) Johnson, J. A.; Lu, Y. Y.; Burts, A. O.; Lim, Y.-H.; Finn, M. G.; Koberstein, J. T.; Turro, N. J.; Tirrell, D. A.; Grubbs, R. H. *J. Am. Chem. Soc.* **2010**, *133*, 559.

(7) Grigoriadis, C.; Nese, A.; Matyjaszewski, K.; Pakula, T.; Butt, H.-J.; Floudas, G. *Macromol. Chem. Phys.* **2012**, *213*, 1311.

(8) Pietrasik, J.; Sumerlin, B. S.; Lee, H.-i.; Gil, R. R.; Matyjaszewski, K. *Polymer* **2007**, *48*, 496.

(9) Pesek, S. L.; Li, X.; Hammouda, B.; Hong, K.; Verduzco, R. *Macromolecules* **2013**, *46*, 6998.

(10) Sheiko, S. S.; Sumerlin, B. S.; Matyjaszewski, K. *Prog. Polym. Sci.* **2008**, *33*, 759.

(11) Moad, G.; Rizzardo, E.; Thang, S. H. *Acc. Chem. Res.* **2008**, *41*, 1133.

(12) Bielawski, C. W.; Grubbs, R. H. *Prog. Polym. Sci.* **2007**, *32*, 1.

(13) Xia, Y.; Kornfield, J. A.; Grubbs, R. H. *Macromolecules* **2009**, *42*, 3761.

(14) Radzinski, S. C.; Foster, J. C.; Matson, J. B. *Polym. Chem.* **2015**, *6*, 5643.

(15) N'Guyen, D. A.; Leroux, F.; Montembault, V.; Pascual, S.; Fontaine, L. *Polym. Chem.* **2016**, *7*, 1730.

(16) Bolton, J.; Rzayev, J. *ACS Macro Lett.* **2012**, *1*, 15.

(17) Li, Z.; Zhang, K.; Ma, J.; Cheng, C.; Wooley, K. L. *J. Poly. Sci. Part A: Polym. Chem.* **2009**, *47*, 5557.

(18) Dalsin, S. J.; Hillmyer, M. A.; Bates, F. S. *ACS Macro Lett.* **2014**, *3*, 423.

(19) Hernández-Guerrero, M.; Davis, T. P.; Barner-Kowollik, C.; Stenzel, M. H. *Eur. Polym. J.* **2005**, *41*, 2264.

(20) Radzinski, S. C.; Foster, J. C.; Chapleski, R. C.; Troya, D.; Matson, J. B. *J. Am. Chem. Soc.* **2016**, *138*, 6998.

(21) Sumerlin, B. S.; Neugebauer, D.; Matyjaszewski, K. *Macromolecules* **2005**, *38*, 702.

(22) Barner, L.; Davis, T. P.; Stenzel, M. H.; Barner-Kowollik, C. *Macromol. Rapid Commun.* **2007**, *28*, 539.

(23) Sumerlin, B. S. *ACS Macro Letters* **2012**, *1*, 141.

(24) Stenzel, M. H.; Zhang, L.; Huck, W. T. S. *Macromolecular Rapid Communications* **2006**, *27*, 1121.

(25) Stenzel, M. H.; Davis, T. P.; Fane, A. G. *J. Mater. Chem.* **2003**, *13*, 2090.

(26) Barner-Kowollik, C.; Davis, T. P.; Stenzel, M. H. *Aust. J. Chem.* **2006**, *59*, 719.

(27) Boschmann, D.; Mänz, M.; Fröhlich, M. G.; Zifferer, G.; Vana, P. In *Controlled/Living Radical Polymerization: Progress in RAFT, DT, NMP & OMRP*; American Chemical Society: 2009; Vol. 1024, p 217.

(28) Mayadunne, R. T. A.; Jeffery, J.; Moad, G.; Rizzardo, E. *Macromolecules* **2003**, *36*, 1505.

(29) Love, J. A.; Morgan, J. P.; Trnka, T. M.; Grubbs, R. H. *Angew. Chem., Int. Ed.* **2002**, *41*, 4035.

(30) Liu, J.; Gao, A. X.; Johnson, J. A. *J. Vis. Exp.* **2013**, e50874.

(31) Foster, J. C.; Radzinski, S. C.; Lewis, S. E.; Slutzker, M. B.; Matson, J. B. *Polymer* **2015**, *79*, 205.

(32) Arena, J. V.; Leu, T. M. *J. Chem. Ed.* **1999**, *76*, 867.

(33) Arena, J. V.; Mazzarella, C. R.; Gluodenis, R. J. *J. Chem. Ed.* **1994**, *71*, 483.

(34) Keddie, D. J. *Chem. Soc. Rev.* **2014**, *43*, 496.

(35) Odian, G. *Principles of Polymerization*; 4th ed.; John Wiley & Sons, Inc.: New Jersey, 2004.

(36) Fröhlich, M. G.; Vana, P.; Zifferer, G. *Macromol. Theory Simul* **2007**, *16*, 610.

(37) Boschmann, D.; Edam, R.; Schoenmakers, P. J.; Vana, P. *Polymer* **2008**, *49*, 5199.

(38) Jesberger, M.; Barner, L.; Stenzel, M. H.; Malmström, E.; Davis, T. P.; Barner-Kowollik, C. *J. Poly. Sci. Part A: Polym. Chem.* **2003**, *41*, 3847.

(39) Goto, A.; Sato, K.; Tsujii, Y.; Fukuda, T.; Moad, G.; Rizzardo, E.; Thang, S. H. *Macromolecules* **2001**, *34*, 402.

7.8 Appendix

Table 7S1: PCTA characterization data.

PCTA DP	NMR Conv.	Theo. M_n[a]	M_n (GPC)	Đ (GPC)
50	>99	16,500	17,000	1.09
100	>99	32,900	35,600	1.15
250	>99	82,300	-[b]	-[b]
500	>99	165,000	-[b]	-[b]
750	>99	247,000	-[b]	-[b]
1000	>99	329,000	-[b]	-[b]

[a]Based on M_n = (NMR Conv.)/100 * MW CTA*targeted DP [b]Polymer was not soluble in THF.

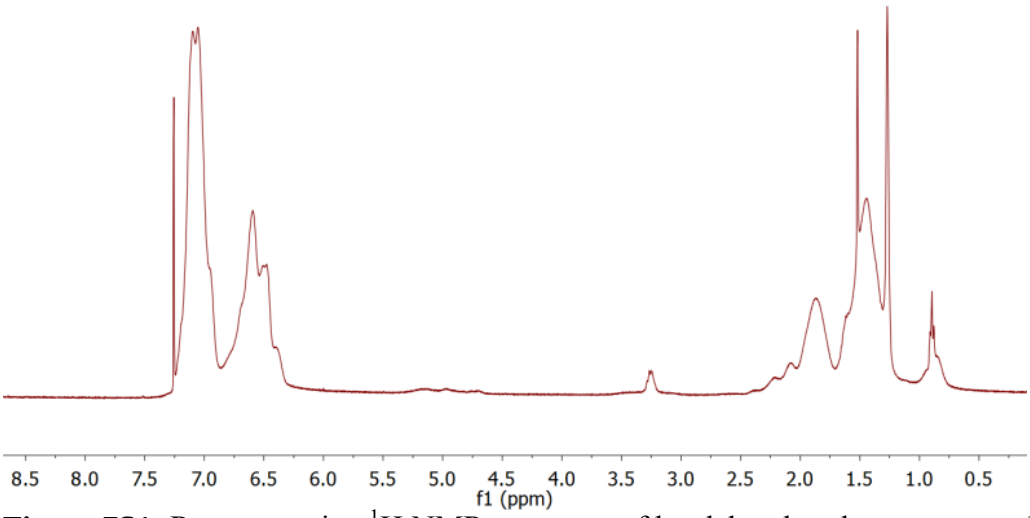

Figure 7S1: Representative ^{1}H NMR spectrum of bottlebrush polymer prepared using styrene as the monomer (Table 7.1, entry 2).

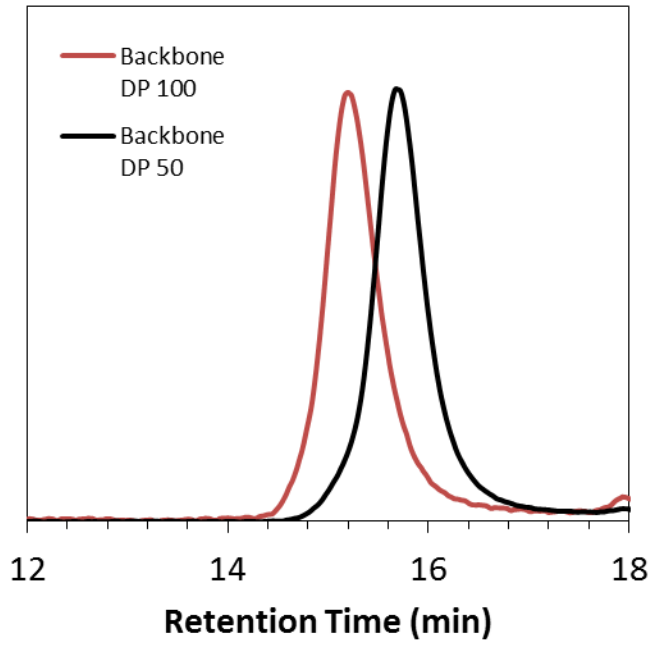

Figure 7S2: SEC traces of backbone PCTA with DP of 50 and 100.

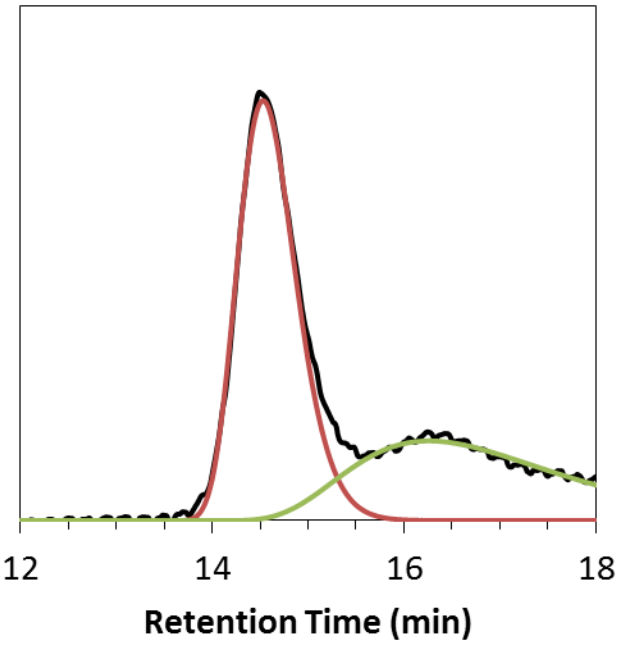

Figure 7S3: SEC trace and peak fit of bottlebrush polymer from Table 7.1, entry 1. The black trace is the raw RI signal obtained via SEC. Red and green traces represent fits of bottlebrush and linear polymer populations, respectively.

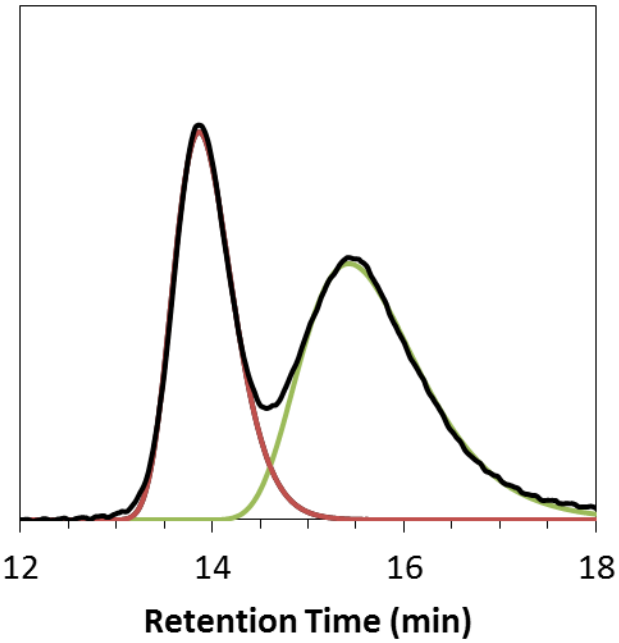

Figure 7S4: SEC trace and peak fit of bottlebrush polymer from Table 7.1, entry 2. The black trace is the raw RI signal obtained via SEC. Red and green traces represent fits of bottlebrush and linear polymer populations, respectively.

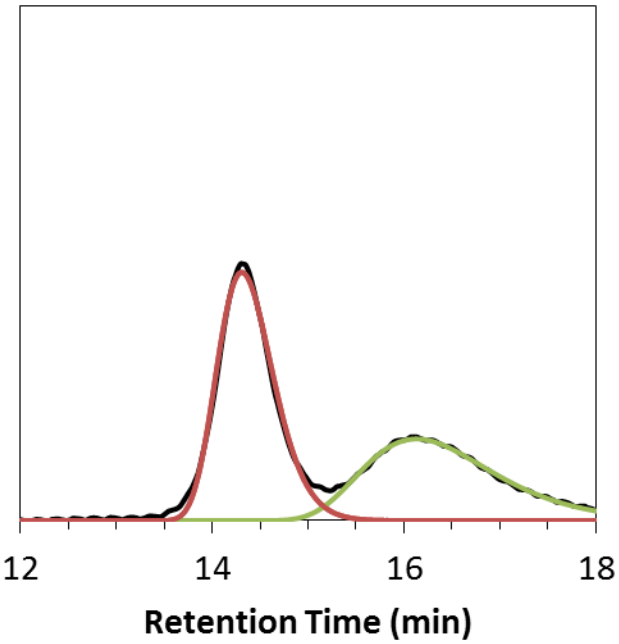

Figure 7S5: SEC trace and peak fit of bottlebrush polymer from Table 7.1, entry 3. The black trace is the raw RI signal obtained via SEC. Red and green traces represent fits of bottlebrush and linear polymer populations, respectively.

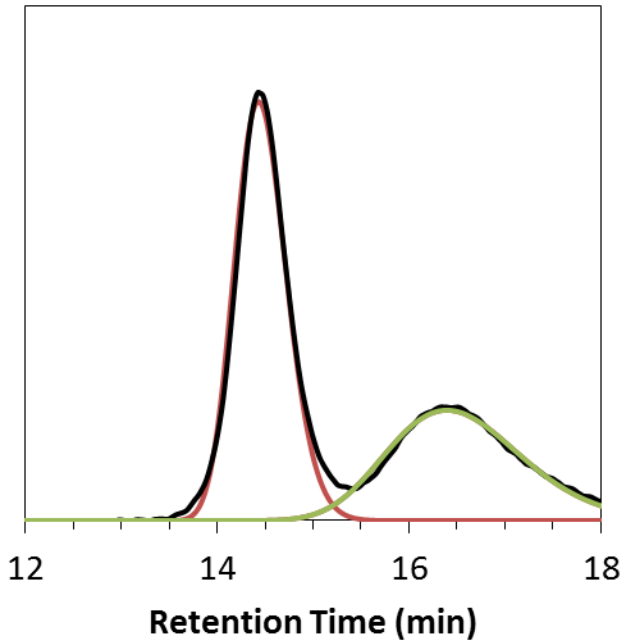

Figure 7S6: SEC trace and peak fit of bottlebrush polymer from Table 7.1, entry 4. The black trace is the raw RI signal obtained via SEC. Red and green traces represent fits of bottlebrush and linear polymer populations, respectively.

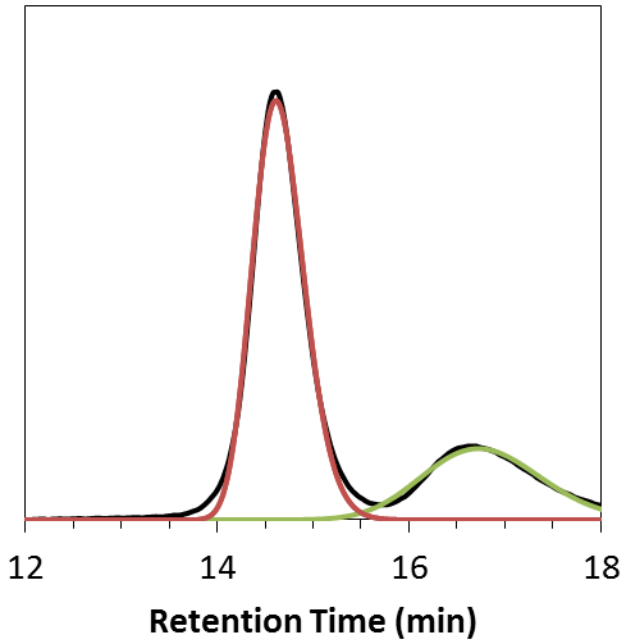

Figure 7S7: SEC trace and peak fit of bottlebrush polymer from Table 7.1, entry 5. The black trace is the raw RI signal obtained via SEC. Red and green traces represent fits of bottlebrush and linear polymer populations, respectively.

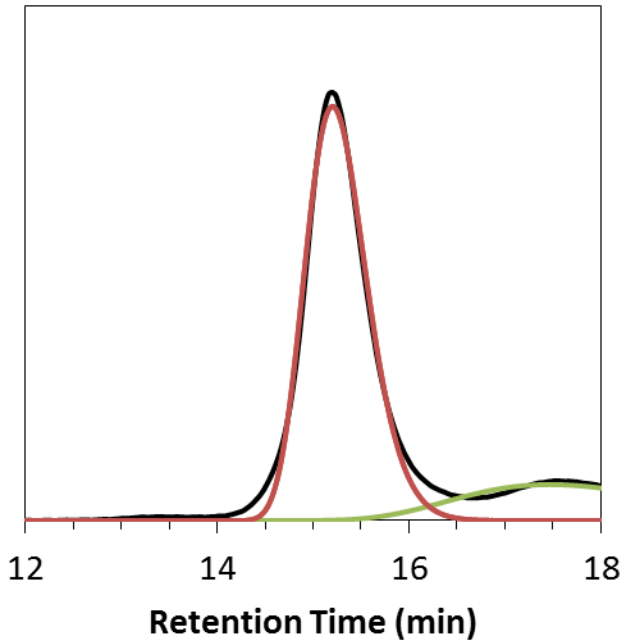

Figure 7S8: SEC trace and peak fit of bottlebrush polymer from Table 7.1, entry 6. The black trace is the raw RI signal obtained via SEC. Red and green traces represent fits of bottlebrush and linear polymer populations, respectively.

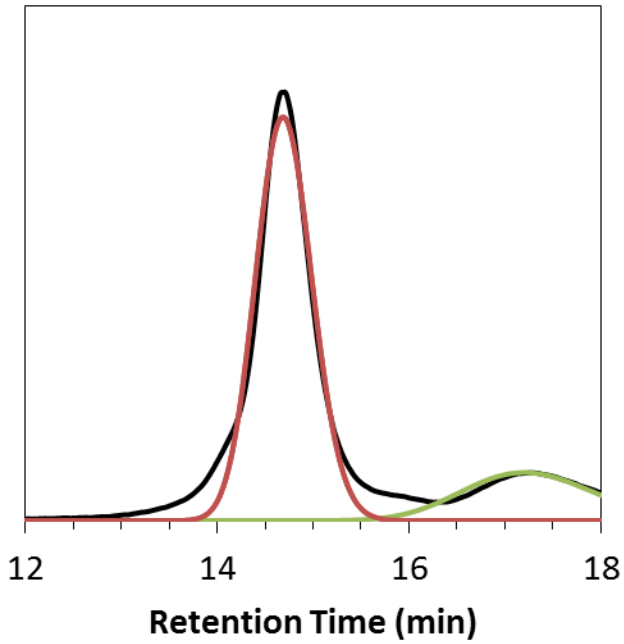

Figure 7S9: SEC trace and peak fit of bottlebrush polymer from Table 7.1, entry 7. The black trace is the raw RI signal obtained via SEC. Red and green traces represent fits of bottlebrush and linear polymer populations, respectively.

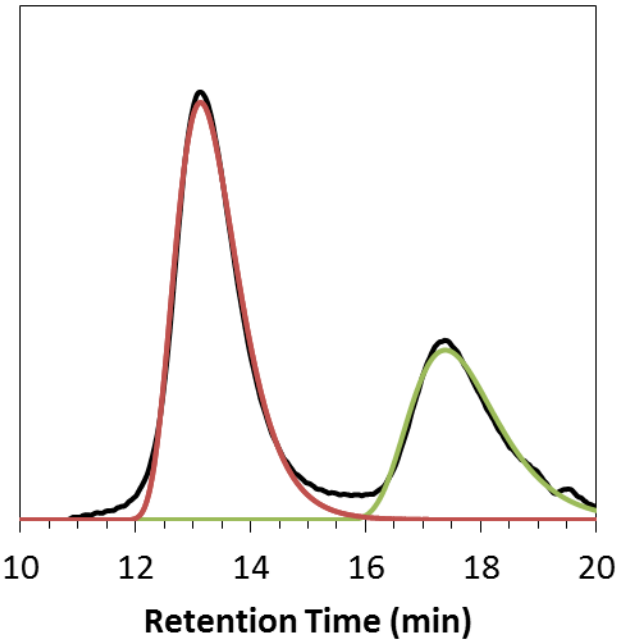

Figure 7S10: SEC trace and peak fit of bottlebrush polymer from Table 7.1, entry 8. The black trace is the raw RI signal obtained via SEC. Red and green traces represent fits of bottlebrush and linear polymer populations, respectively.

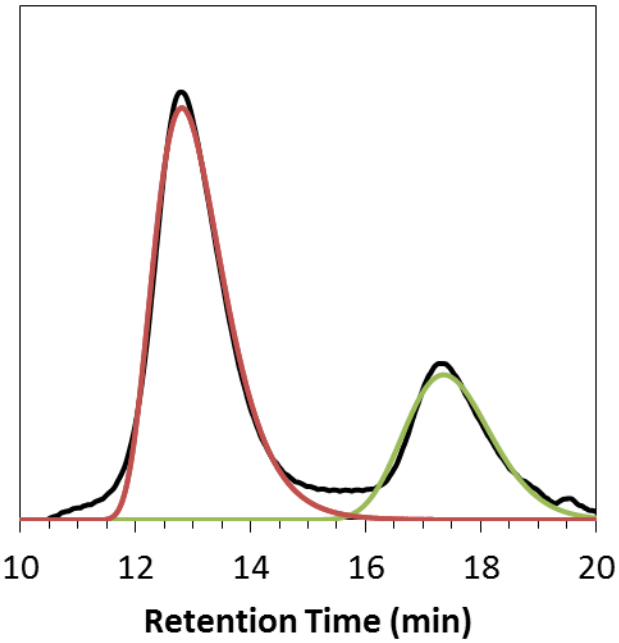

Figure 7S11: SEC trace and peak fit of bottlebrush polymer from Table 7.1, entry 9. The black trace is the raw RI signal obtained via SEC. Red and green traces represent fits of bottlebrush and linear polymer populations, respectively.

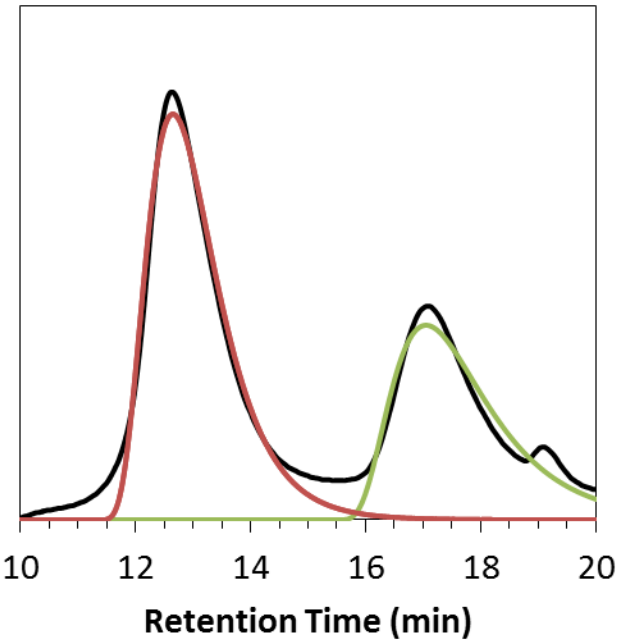

Figure 7S12: SEC trace and peak fit of bottlebrush polymer from Table 7.1, entry 10. The black trace is the raw RI signal obtained via SEC. Red and green traces represent fits of bottlebrush and linear polymer populations, respectively.

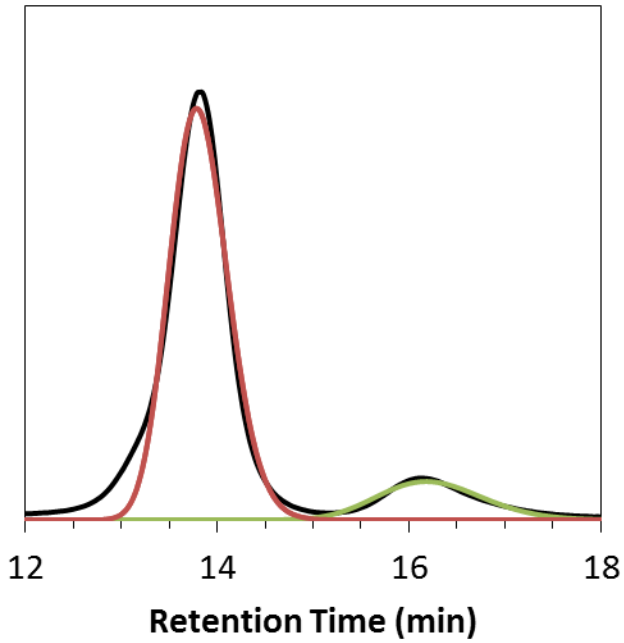

Figure 7S13: SEC trace and peak fit of bottlebrush polymer from Table 7.1, entry 11. The black trace is the raw RI signal obtained via SEC. Red and green traces represent fits of bottlebrush and linear polymer populations, respectively.

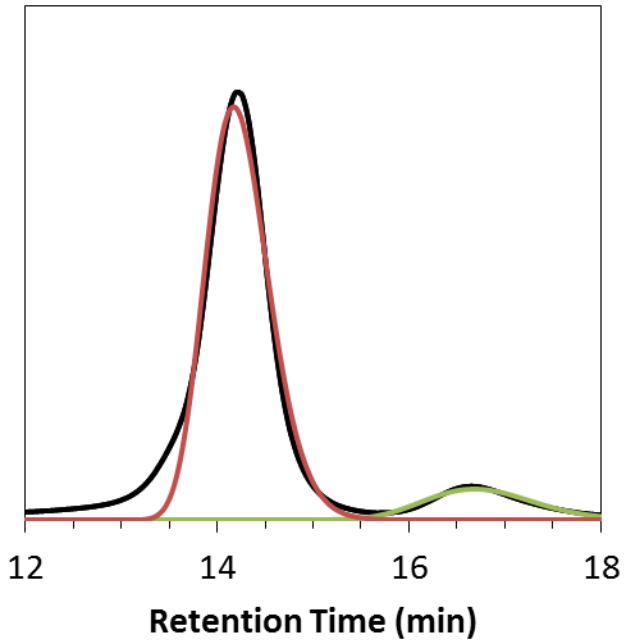

Figure 7S14: SEC trace and peak fit of bottlebrush polymer from Table 7.1, entry 12. The black trace is the raw RI signal obtained via SEC. Red and green traces represent fits of bottlebrush and linear polymer populations, respectively.

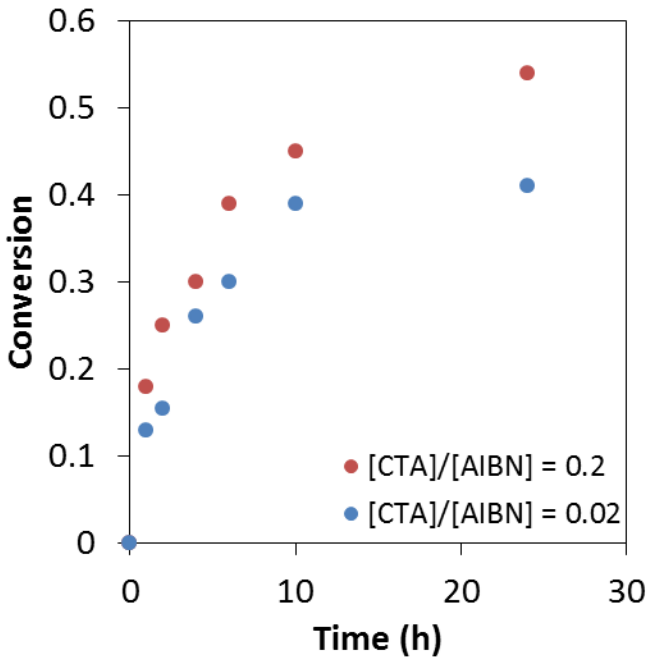

Figure 7S15. Kinetics of RAFT transfer-to polymerization of styrene with different amounts of radical initiator. Polymerizations were conducted at [M]/[CTA] = 1000 with different equivalents of AIBN relative to CTA.

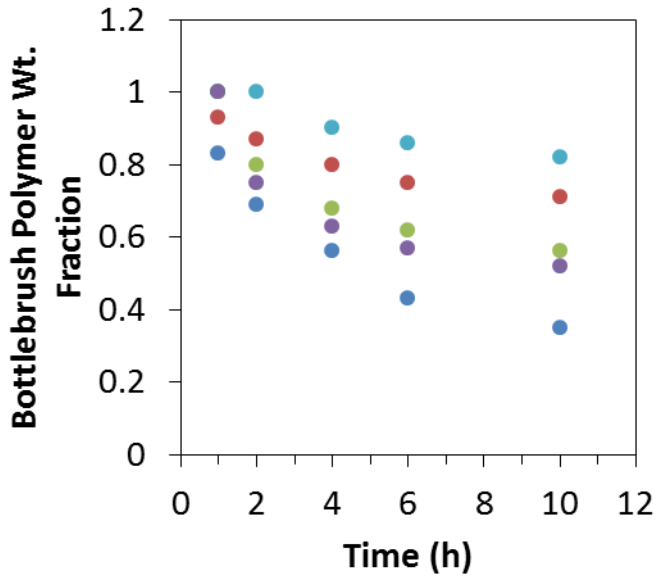

Figure 7S16. Change in bottlebrush weight fraction over time for polymerizations conducted with [M]/[CTA] = 1000 (dark blue circles), 750 (purple circles), 500 (green circles), 100 (red circles), and 50 (light blue circles).

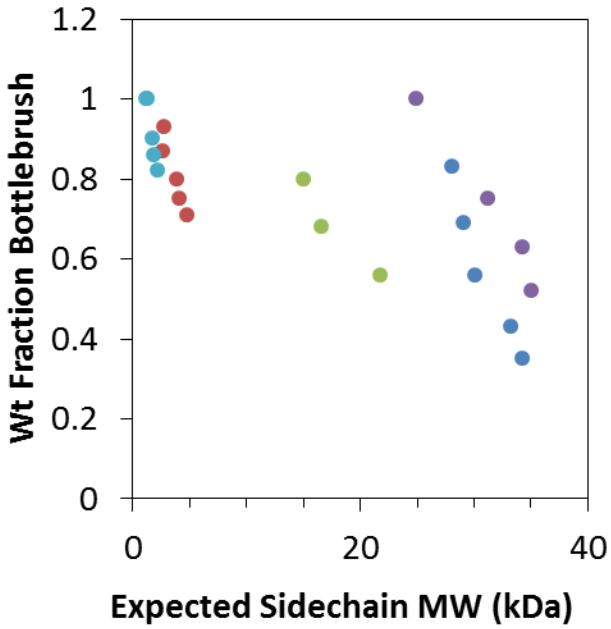

Figure 7S17. Relationship between expected sidechain molecular weight, calculated using the equation $MW_{sidechains} = conv * \frac{[M]}{[CTA]} * MW_{styrene}$, and the bottlebrush polymer sample composition based on area under the curves of the SEC traces at each time point for polymerizations conducted with [M]/[CTA] = 1000 (dark blue circles), 750 (purple circles), 500 (green circles), 100 (red circles), and 50 (light blue circles).

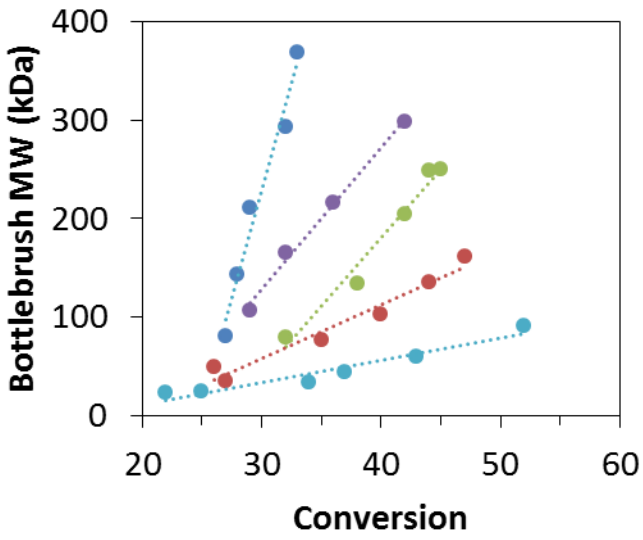

Figure 7S18. MW vs conversion for polymerizations conducted with conducted with [M]/[CTA] = 1000 (dark blue circles), 750 (purple circles), 500 (green circles), 100 (red circles), and 50 (light blue circles). Linear fit lines have been provided as a visual aid.

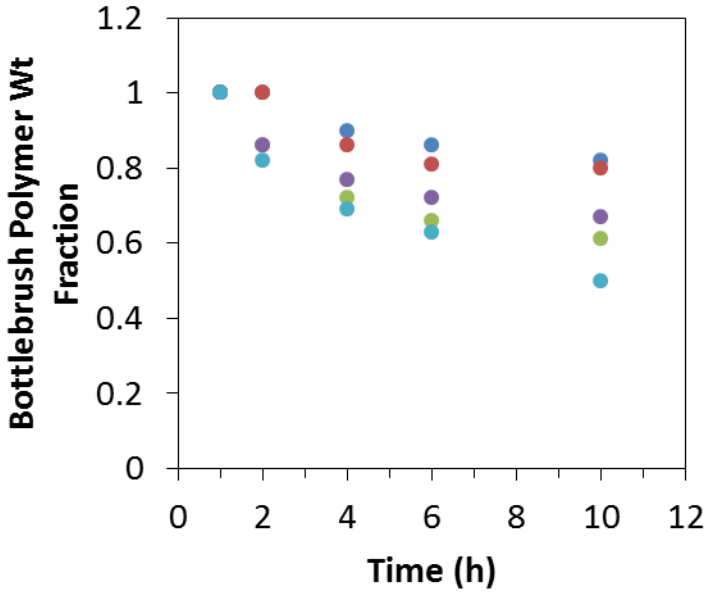

Figure 7S19. Change in bottlebrush polymer weight fraction over time for polymerizations conducted with PCTA DP = 50 (dark blue circles), 100 (purple circles), 500 (green circles), 750 (red circles), and 1000 (light blue circles).

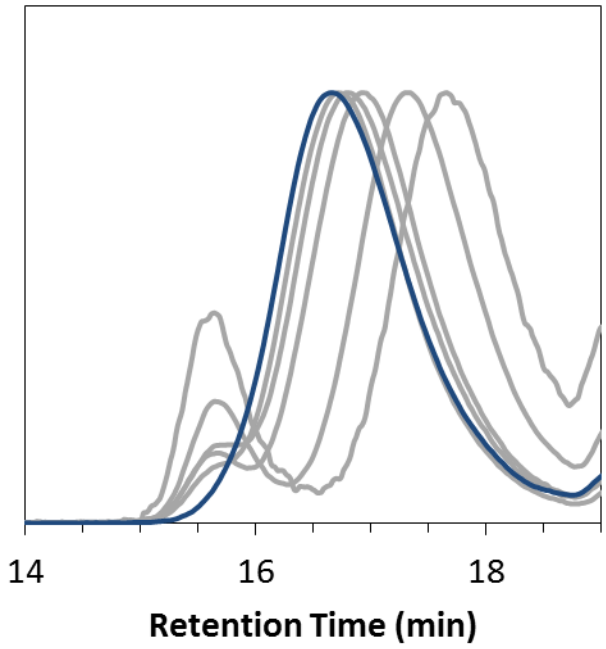

Figure 7S20. SEC traces of aminolyzied bottlebrush polymers from the polymerization denoted as Table 7.1, entry 6 at various time points. The final time point for each run (blue lines) was taken after 24 h. Aminolysis experiments were conducted by adding 0.5 mL of a 40 v/v% solution of methylene in H_2O to a solution of ~100 mg of bottlebrush polymer in 1 mL of THF for each time point. These mixtures were stirred for a minimum of 48 h under air to ensure complete oxidation of the ω-chain end thiols before the samples were analyzed by SEC.

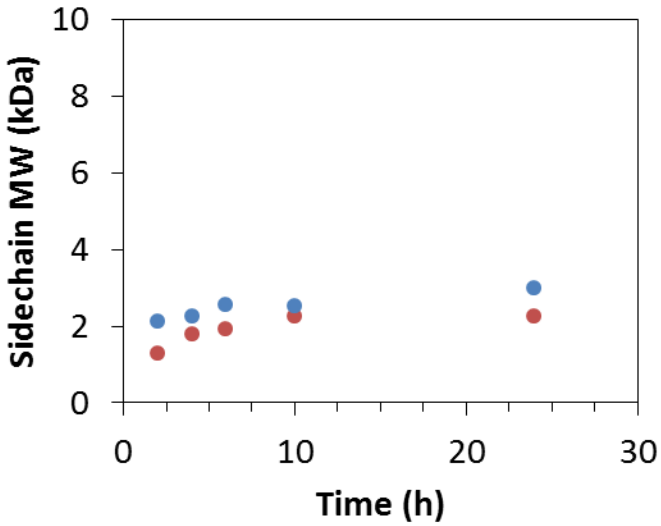

Figure 7S21. Comparison of bottlebrush polymer sidechain MWs calculated from monomer conversions obtained via ^{1}H NMR spectroscopy (red circles) and measured for cleaved sidechains (blue circles) for the polymerization with [M]/[CTA] = 50 and a backbone DP of 50. Sidechains MWs were calculated using the equation $MW_{sidechains} = conv * \frac{[M]}{[CTA]} * MW_{styrene}$.

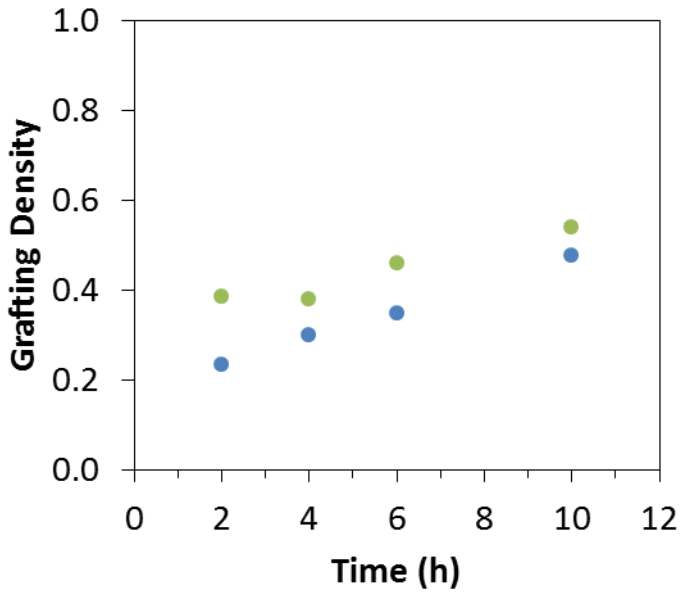

Figure 7S22. Comparison of bottlebrush polymer grafting density calculated by diving the observed MW of the bottlebrush polymer by sidechain MWs calculated from monomer conversions obtained via ^{1}H NMR spectroscopy (green circles) and measured for cleaved sidechains (blue circles) for the polymerization with [M]/[CTA] = 50 and a backbone DP of 50.

Chapter 8: Conclusions and Future Outlook

Chapter 2

Our kinetic analyses of ROMP grafting-through support our hypothesis that the anchor group has a large effect on polymerization kinetics and the ultimate MW of the bottlebrush polymer. The observed trend (k_p of anchor group 1 > 2 > 3) was conserved for polystyrene MMs of different MWs as well as for PLA MMs. Experimental and computational studies showed that this phenomenon likely originates from a combination of steric effects and differences in monomer electronic structure. Importantly, the >4 fold difference in the propagation rates between the three different anchor groups had a dramatic effect when targeting high bottlebrush backbone DPs. Given that the properties of these complex macromolecules depend on factors such as the backbone DP and the purity of the polymer sample, rational selection of the anchor group is a critical factor when designing synthetic strategies for preparing bottlebrush polymers. We expect that this anchor group effect may also be important for polymerization of other challenging monomers, such as those with peptides, sugars, dendrimers, or other bulky groups.

For future work, studying the effects of ROMP grafting-through allows for mechanistic insight in the ROMP process. This is due to the slowed propagation rates from using larger macromonomers, but the results can be extrapolated to many different systems. Using these systems different parameters may be studied on reasonable timescales. These include looking at an expansive list of solvents on ROMP grafting-through. Understanding how solvents affect the polymerization may give rise to a faster or more controlled synthesis. Along the same lines the effects of various additives on the polymerization will also give an idea to the mechanistic

understanding of this system. This chapter looked at two additives but there are many that have been used in the literature.

Additionally, understanding additional considerations for ROMP grafting-through may also be interesting. We have noticed in the lab that the choice of MM has a significant impact on the final bottlebrush synthesized. Above we have used styrene and PLA but one could think of many different types of MMs to use. When a methacrylate based MM is used, the polymerization is slow and will lead to low conversion meaning that a bottlebrush is hard to obtain. We have hypothesized on a few different factors that may lead to this result, which include: MM purity (vinyl monomer still in sample), disproportionated chain ends, and how the MM is in the solution (collapsed chains vs. chain extended). The first two can be answered through extensive purification and characterization of the MM. The last idea relates back to the solvent choice, is there a solvent that can be used to make methacrylate based MMs polymerize better.

Another project that arose from the information in Chapter 2 is mixing MMs with different anchor groups to synthesis bottlebrush polymers with interesting topologies of blocks. This can be accomplished my mixing a MM with anchor group 1 and another with anchor group 3. The MM with anchor group 1 should react faster than the one with anchor group 3 giving a one pot synthesis of a block type bottlebrush polymer.

Chapter 3

Ring opening polymerization of lactide was successfully carried out to form macromonomers that could be directly polymerized via ROMP using the grafting-through strategy to form a bottlebrush polymer in a one-pot two-step process. Addition of TFA following the ROP step was necessary to achieve high conversions in the ROMP step. Good control over bottlebrush polymer MW and Đ was attained in most cases, with bottlebrush polymer molecular weights exceeding 1

MDa. Overall, this method allows for easy control over the side-chain and backbone MWs without purification between steps. This one step procedure allows for large bottlebrush polymers to be synthesized quickly.

For future work, one could envision expanding the one-pot technique to other polymerization types. This work first started with a one pot ATRP-ROMP process but encountered a number on issues, such as the reagents in ATRP affecting the ROMP step. Various attempts to achieve a one-pot ATRP-ROMP process were attempted but with little success. It appeared that residual Cu catalyst, ligand, or both from the ATRP step affected the activity of the ROMP catalyst in the second step.

Chapter 5

A chain transfer agent was synthesized and shown to control RAFT polymerization of various monomers. We demonstrated that **CTA1** could be utilized effectively for transfer-to and grafting-through methodologies, with the former resulting in high MW bottlebrush polymers. Polystyrene MMs prepared using **CTA1** were polymerized by ROMP via a grafting-through strategy. In general, ROMP polymerization of **CTA1**-derived MMs proceeded efficiently when catalyzed by Grubbs' 3rd generation catalyst, with conversions on the order of 70-90%. Macromonomer MW, concentration, and the [MM]/[catalyst] ratio of the polymerization were found to influence the conversion to BB. In general, an inverse relationship between MW of the MM and the conversion to BB was observed, with the smallest MM (3300 Da) resulting in the highest conversion. Increasing the MM concentration from 25 to 100 mg/mL also enhanced conversion, while increasing the [MM]/[**G3**] ratio from 25:1 to 100:1 resulted in decreased conversion and a broadening of the molecular weight distribution. Side chain scission via aminolysis was quantitative and revealed significant differences between the bottlebrush

polymers prepared by the two different approaches. **CTA1** is unique in that it allows for the preparation of bottlebrush polymers utilizing functionality built into the chain-transfer agent. We expect **CTA1** will prove to be useful for the facile preparation of bottlebrush polymers possessing inherent side chain lability via the transfer-to or grafting-through approach.

Chapter 6

In summary, we have prepared two new dithiocarbamate CTAs with Z-groups derived from **NI** and the corresponding reduced secondary amine. Based on the electronics of **NI**, it is apparent that only certain alkylating agents—sterically unhindered alkyl halides lacking acidic functionalities—can be employed to prepare CTAs derived from this Z-group. Nevertheless, CTA **1b** was prepared in moderate yields and was found to efficiently mediate RAFT polymerization of 2° MAMs—styrene, MA, and ACMO. Reduction of **NI** was conducted to reduce the electron withdrawing ability of the Z-group. Novel dithiocarbamate CTA **2** prepared from norbornene amine did not control the polymerization of 2° or 3° MAMs; however, it provided moderate control over the polymerization of VAc, yielding polymers with the appropriate CTA-derived end groups. ROMP of a PVAc MM prepared using CTA **2** was carried out to give a bottlebrush polymer with PVAc side chains using the grafting-through technique. To the best of our knowledge, this work represents the first preparation of a bottlebrush polymer with PVAc side chains by the grafting-through method. We expect that this contribution will assist in the rational design of CTAs capable of mediating RAFT polymerization to form polymers functionalized with ROMP-active norbornene moieties.

Chapter 7

The effect of radical initiator loading, [M]/[CTA] ratio, backbone DP, and monomer type were studied in RAFT transfer-to bottlebrush polymer synthesis with the goal of a polymerization that yielded high MW bottlebrush polymers of narrow dispersity with few dead linear chains. A low initial [M]/[CTA] ratio led to the formation of a bottlebrush polymer with few dead linear chains; however, this also restricted its MW. As the [M]/[CTA] ratio was increased, a greater fraction of dead linear chains was observed. The DP of the PCTA did not directly affect the population of dead linear chains; however, the use of large backbones resulted in high MW polymers but also noticeably viscous reaction mixtures, which eventually led to an increase in the amount of dead linear polymer compared with lower DP PCTAs. The type of monomer had a dramatic effect on RAFT transfer-to polymerization. Compared with styrene, faster polymerizations and lower percentages of dead linear chains were generated when transfer-to polymerizations were carried out with MA or ACMO (high k_p monomers). Based on these results, we propose that for RAFT transfer-to polymerization, monomer choice and the initial [M]/[CTA] ratio are critically important considerations. High k_p monomers are expected to perform well due to reduced termination. The size of the side-chains determines the MW of the final bottlebrush polymer and the dead polymer fraction due to steric factors and likely affects the grafting density of the bottlebrush polymers as well. These insights may aid efforts toward fully realizing the potential of the transfer-to technique in bottlebrush polymer synthesis.

Future work regarding RAFT transfer-to involves the synthesis of more CTAs that are capable of performing this technique. To my knowledge no poly (methacrylate) bottlebrush, star, or brush polymer has been prepared using the transfer-to technique **(Figure 8.1**).

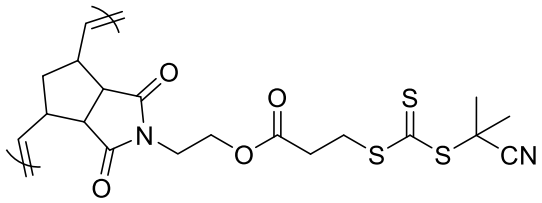

Figure 8.1: Potential backbone for transfer-to of methacrylates.

Synthesizing a CTA will fill some holes in this area as well as lead to a wider array of brushes that can be synthesized by this method. In addition, comparing BB polymers synthesized using grafting-from vs transfer-to will highlight key differences in the techniques and show where each technique has its advantages and disadvantages, this idea is discussed further in Chapter 9.

Chapter 9: Appendix

9.1 ROMP Grafting-Through Additives

Additives were tested on $1S_{3k}$ and $3S_{3k}$ during ROMP grafting-through. The polymerizations were set at 100:1 [MM]/[G3] in DCM at 100mg/ml with an equal molar additive to G3. Samples were taken at 20 min reaction time and run on the SEC, the results are summarized on table 9.1.

Table 9.1

Additive	1 Conv. (%)	2 Conv. (%)
None	94	52
Acetic Acid	93	51
H_3PO_4	95	55
TPPO	94	56
TTIP	90	52
Boric Acid	95	53
CuBr	52	47
CuI	9.5	56

No additive shows the anchor group 1 reached a higher conversion in 20 min than anchor group 3. During this study no additive showed an increase in conversion for 3, however two additives showed to decrease the conversion for anchor group 1, CuBr and CuI. It is to be noted for the above experiments were performed prior to the alumina everything before ROMP era in the lab, the data is to be something used as a starting point and not to be completely trusted.

9.2 Transfer-To Projects

The differences between grafting-from and transfer-to results in polymerizations with different impurities and results in similar yet different products, this idea is discussed in more detail in Chapter 4. Performing a direct comparison of the two methods would be interesting to highlight

when either should be used depending on different applications. The two schemes below were our initial attempt at this comparison.

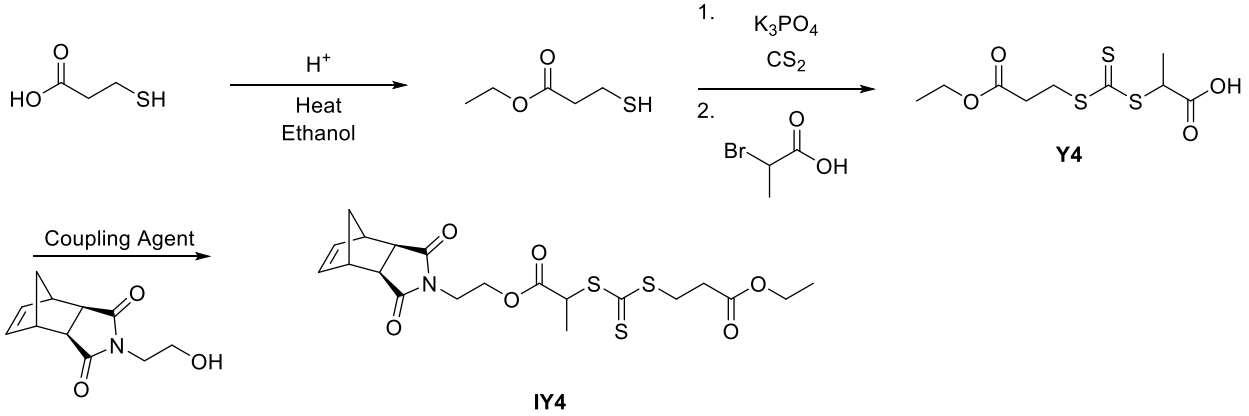

Scheme 9.1 CTA to be used for Grafting-from.

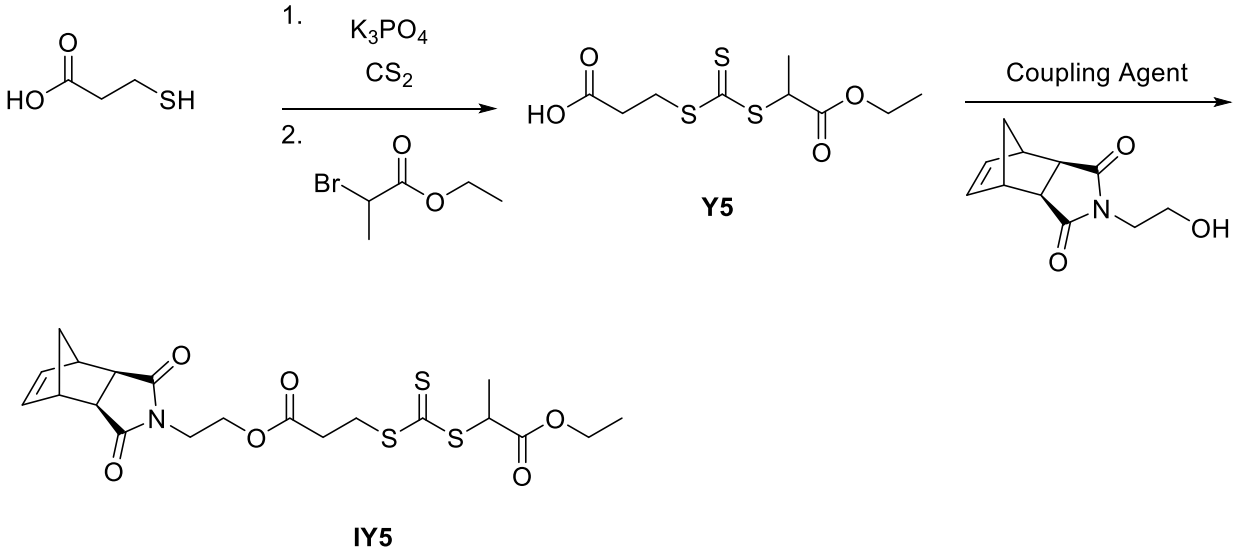

Scheme 9.2 CTA to be used for transfer-to.

Both IY4 and IY5 were synthesized in good yields and showed pure product. Both CTAs were polymerized under ROMP conditions to yield a polymer backbone. The backbone from IY4 can be used for grafting-from and the polymer from IY5 capable of performing transfer-to. When these backbones were subjected to bottlebrush synthesis conditions no bottlebrush polymers

were formed. We have theorized that residual ruthenium was in the polymer backbone sample causing issues in the RAFT step. We did not continue with this project but if the issues were cleared up regarding the bottlebrush synthesis step this should be an easy project to finish.